

NASA
TN
D-8176
c.1

NASA TECHNICAL NOTE



NASA TN D-8176

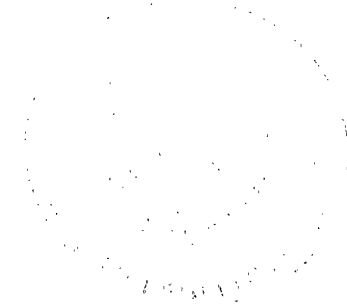
NASA TN D-8176

LOAN COPY: RETURN
FWL TECHNICAL LIBRARY
KIRTLAND AFB, N. I



SIMULATOR STUDY OF THE EFFECTIVENESS
OF AN AUTOMATIC CONTROL SYSTEM
DESIGNED TO IMPROVE THE HIGH-
ANGLE-OF-ATTACK CHARACTERISTICS
OF A FIGHTER AIRPLANE

*William P. Gilbert, Luat T. Nguyen,
and Roger W. Van Gunst*
*Langley Research Center
Hampton, Va. 23665*





0133789

1. Report No. NASA TN D-8176		2. Government Accession No.		3. Recipient's Catalog No.	
4. Title and Subtitle SIMULATOR STUDY OF THE EFFECTIVENESS OF AN AUTOMATIC CONTROL SYSTEM DESIGNED TO IMPROVE THE HIGH-ANGLE-OF-ATTACK CHARACTERISTICS OF A FIGHTER AIRPLANE				5. Report Date May 1976	
7. Author(s) William P. Gilbert, Luat T. Nguyen, and Roger W. Van Gunst				6. Performing Organization Code	
9. Performing Organization Name and Address NASA Langley Research Center Hampton, Va. 23665				8. Performing Organization Report No. L-10545	
12. Sponsoring Agency Name and Address National Aeronautics and Space Administration Washington, D.C. 20546				10. Work Unit No. 505-06-95-01	
15. Supplementary Notes				11. Contract or Grant No.	
16. Abstract <p>A piloted, fixed-base simulation has been conducted to study the effectiveness of some automatic control system features designed to improve the stability and control characteristics of fighter airplanes at high angles of attack. These features include an angle-of-attack limiter, a normal-acceleration limiter, an aileron-rudder interconnect, and a stability-axis yaw damper. The study was based on a current lightweight fighter prototype. The aerodynamic data used in the simulation were measured on a 0.15-scale model at low Reynolds number and low subsonic Mach number. The simulation was conducted on the Langley differential maneuvering simulator, and the evaluation involved representative combat maneuvering.</p> <p>Results of the investigation showed the fully augmented airplane to be quite stable and maneuverable throughout the operational angle-of-attack range. The angle-of-attack/normal-acceleration limiting feature of the pitch control system was found to be a necessity to avoid angle-of-attack excursions at high angles of attack. The aileron-rudder interconnect system was shown to be very effective in making the airplane departure resistant while the stability-axis yaw damper provided improved high-angle-of-attack roll performance with a minimum of sideslip excursions.</p>				13. Type of Report and Period Covered Technical Note	
17. Key Words (Suggested by Author(s)) Stall and poststall motion simulation Stability and control, fighter Automatic control Departure prevention Air combat maneuvering				14. Sponsoring Agency Code	
18. Distribution Statement Unclassified - Unlimited				Subject Category 08	
19. Security Classif. (of this report) Unclassified		20. Security Classif. (of this page) Unclassified		21. No. of Pages 155	
				22. Price* \$6.25	

SIMULATOR STUDY OF THE EFFECTIVENESS OF AN AUTOMATIC
CONTROL SYSTEM DESIGNED TO IMPROVE THE
HIGH-ANGLE-OF-ATTACK CHARACTERISTICS
OF A FIGHTER AIRPLANE

William P. Gilbert, Luat T. Nguyen, and Roger W. Van Gunst
Langley Research Center

SUMMARY

A piloted, fixed-base simulation has been conducted to study the effectiveness of some automatic control system features designed to improve the stability and control characteristics of fighter airplanes at high angles of attack. These features include an angle-of-attack limiter, a normal-acceleration limiter, an aileron-rudder interconnect, and a stability-axis yaw damper. The study was based on a current lightweight fighter prototype. The aerodynamic data used in the simulation were measured on a 0.15-scale model at low Reynolds number and low subsonic Mach number. The simulation was conducted on the Langley differential maneuvering simulator, and the evaluation involved representative combat maneuvering.

Results of the investigation showed the fully augmented airplane to be quite stable and maneuverable throughout the operational angle-of-attack range. The angle-of-attack/normal-acceleration limiting feature of the pitch control system was found to be a necessity to avoid angle-of-attack excursions at high angles of attack. The aileron-rudder interconnect system was shown to be very effective in making the airplane departure resistant, while the stability-axis yaw damper provided improved high-angle-of-attack roll performance with a minimum of sideslip excursions.

INTRODUCTION

High-performance fighter airplanes must be capable of effectively engaging in close-range, air-to-air combat involving vigorous maneuvering at high angles of attack near maximum lift. However, many current fighter configurations exhibit poor stability and control characteristics at high angles of attack, such as directional divergence ("nose slice"), reduced dihedral effect, low rudder effectiveness, and adverse aileron yaw. Such characteristics have caused a significant number of losses of airplanes and pilots as a result of inadvertent loss of control and spins encountered while maneuvering near maximum

lift. These losses continue to persist despite a considerable amount of stall/spin testing, use of artificial stall warning systems, and strong restrictions given in pilot handbooks. The continuing number of stall/spin accidents indicates the inadequacies of present approaches to stall/spin problems.

In recent years, the evolution of more sophisticated and reliable automatic control systems has created much interest in the development of automatic control concepts which produce a spin-resistant airplane. (See refs. 1 to 4, for example.) Recent fighter designs, such as the U.S. Air Force lightweight fighter prototypes, incorporate innovative advanced control systems in which several elements have been provided for flight at high angles of attack. The present investigation was conducted to evaluate the stability and control characteristics of the YF-16 design at high angles of attack, with particular emphasis on the effects of the control system on these characteristics. The study was conducted on the Langley differential maneuvering simulator and the piloting tasks were designed to determine the departure susceptibility of the configuration during hard maneuvering at high angles of attack. The objectives of the study were (1) to determine the controllability and departure resistance of the present configuration during 1g stalls and accelerated stalls, (2) to determine the departure susceptibility of the configuration during demanding air combat maneuvers, (3) to identify maneuvers or flight conditions which might overpower the departure-resistant characteristics provided by the control system, and (4) to identify the favorable characteristics of various elements of the control system at high angles of attack. The aerodynamic data used in the simulation were based on the results of low-speed, small-scale wind-tunnel tests of a 0.15-scale model of the configuration tested at Langley Research Center with no adjustments being made for either Reynolds number or Mach number effects.

SYMBOLS AND NOTATION

All aerodynamic data and flight motions are referenced to the body system of axes shown in figure 1 with the exception of lift, which is presented with respect to wind axes. The units for physical quantities used herein are presented in the International System of Units (SI) and U.S. Customary Units. The measurements and calculations were made in U.S. Customary Units. Conversion factors for the two systems are given in reference 5.

a_n normal acceleration, positive along negative Z body axis, g units

$a_{n,com}$ pilot-commanded normal acceleration, g units

a_y lateral acceleration, positive along positive Y body axis, g units

b	wing span, m (ft)
C_L	lift coefficient, $\frac{\text{Aerodynamic lift force}}{\bar{q}S}$
C_l	rolling-moment coefficient about X body axis, $\frac{\text{Aerodynamic rolling moment}}{\bar{q}Sb}$
$C_{l,t}$	total rolling-moment coefficient
C_m	pitching-moment coefficient about Y body axis, $\frac{\text{Aerodynamic pitching moment}}{\bar{q}S\bar{c}}$
$C_{m,1}$	pitching-moment coefficient data used to represent mild trim point at high angle of attack
$C_{m,2}$	pitching-moment coefficient data used to represent conventional high-angle-of-attack variation
$C_{m,t}$	total pitching-moment coefficient
C_n	yawing-moment coefficient about Z body axis, $\frac{\text{Aerodynamic yawing moment}}{\bar{q}Sb}$
$C_{n,t}$	total yawing-moment coefficient
C_X	X-axis force coefficient along positive X body axis, $\frac{\text{Aerodynamic X-axis force}}{\bar{q}S}$
$C_{X,t}$	total X-axis force coefficient
C_Y	Y-axis force coefficient along positive Y body axis, $\frac{\text{Aerodynamic Y-axis force}}{\bar{q}S}$
$C_{Y,t}$	total Y-axis force coefficient

C_Z	Z-axis force coefficient along positive Z body axis, $\frac{\text{Aerodynamic Z-axis force}}{\bar{q}S}$
$C_{Z,t}$	total Z-axis force coefficient
\bar{c}	wing mean aerodynamic chord, m (ft)
F_{lat}	pilot lateral stick force, positive for right roll, N (lb)
F_{long}	pilot longitudinal stick force, positive for positive normal acceleration, N (lb)
F'_{long}	F_{long} less mechanical preload force, N (lb)
F_{ped}	pilot pedal force, N (lb)
g	acceleration due to gravity, m/sec ² (ft/sec ²)
h	altitude, m (ft)
I_X, I_Y, I_Z	moments of inertia about X, Y, and Z body axes, kg-m ² (slug-ft ²)
I_{XZ}	product of inertia with respect to X and Z body axes, kg-m ² (slug-ft ²)
K	ARI rudder-aileron gain
M	Mach number
m	airplane mass, kg (slugs)
N_{Re}	Reynolds number based on \bar{c}
P_1	engine power command based on throttle position, percent of maximum power
P_2	engine power command to engine, percent of maximum power

P_3	engine power, percent of maximum power
p	airplane roll rate about X body axis, deg/sec or rad/sec
P_{com}	pilot-commanded roll rate, deg/sec
q	airplane pitch rate about Y body axis, deg/sec or rad/sec
\bar{q}	free-stream dynamic pressure, N/m^2 (lb/ft ²)
R	range, straight-line distance between subject and target airplanes, m (ft)
r	yaw rate about Z body axis, deg/sec or rad/sec
r_{stab}	approximate stability-axis yaw rate, $r - p\alpha$, rad/sec
S	wing area, m ² (ft ²)
s	Laplace variable, 1/sec
T	total instantaneous engine thrust, N (lb)
T_{idle}	idle thrust, N (lb)
T_{max}	maximum thrust, N (lb)
T_{mil}	military thrust, N (lb)
t	time, sec
$t_{1/2}$	time to damp to one-half amplitude, sec
u, v, w	components of airplane velocity along X , Y , and Z body axes, m/sec (ft/sec)
V	airplane resultant velocity, m/sec (ft/sec)

X, Y, Z	airplane body axes (see fig. 1)
X_I, Y_I, Z_I	orthogonal inertial axes
x_{cg}	center-of-gravity location, fraction of \bar{c}
$x_{cg,ref}$	reference center-of-gravity location for aerodynamic data, fraction of \bar{c}
α	angle of attack, deg
α_f	filtered α signal, deg
α_0	threshold value of angle of attack, deg
β	angle of sideslip, deg
γ	flight-path angle, deg
δ_a	aileron deflection, positive for left roll, deg
$\delta_{a,c}$	aileron deflection commanded by control system, deg
δ_D	differential horizontal tail deflection, positive for left roll, deg
δ_h	horizontal stabilator deflection, positive for airplane nose-down control, deg
δ_{lef}	leading-edge flap deflection, deg
δ_r	rudder deflection, positive for left yaw, deg
$\delta_{r,com}$	pilot-commanded rudder deflection, deg
δ_{sb}	speed-brake deflection, deg
ϵ	tracking error, angle between evaluation airplane X body axis and range vector \bar{R} (angle off), deg

θ, ϕ, ψ Euler angles, deg

τ_T engine thrust time constant, sec

$$C_{l_p} = \frac{\partial C_l}{\partial \frac{pb}{2V}} \quad C_{l_r} = \frac{\partial C_l}{\partial \frac{rb}{2V}} \quad C_{l_\beta} = \frac{\partial C_l}{\partial \beta} \quad C_{l_{\delta_a}} = \frac{\partial C_l}{\partial \delta_a}$$

$$C_{l_{\delta_r}} = \frac{\partial C_l}{\partial \delta_r} \quad C_{m_q} = \frac{\partial C_m}{\partial \frac{qc}{2V}} \quad C_{n_p} = \frac{\partial C_n}{\partial \frac{pb}{2V}} \quad C_{n_r} = \frac{\partial C_n}{\partial \frac{rb}{2V}}$$

$$C_{n_\beta} = \frac{\partial C_n}{\partial \beta} \quad C_{n_{\beta, \text{dyn}}} = C_{n_\beta} - \frac{I_Z}{I_X} C_{l_\beta} \sin \alpha \quad C_{n_{\delta_a}} = \frac{\partial C_n}{\partial \delta_a} \quad C_{n_{\delta_r}} = \frac{\partial C_n}{\partial \delta_r}$$

$$C_{X_q} = \frac{\partial C_X}{\partial \frac{qc}{2V}} \quad C_{Z_q} = \frac{\partial C_Z}{\partial \frac{qc}{2V}} \quad C_{Y_p} = \frac{\partial C_Y}{\partial \frac{pb}{2V}} \quad C_{Y_r} = \frac{\partial C_Y}{\partial \frac{rb}{2V}}$$

Subscripts:

$\delta_{i=j}$ deflection of control surface i to value j ; for example, $\Delta C_{l, \delta_h = -25^\circ}$ indicates increment of C_l produced by deflection of horizontal tail to $\delta_h = -25^\circ$

lef increment of variable produced by full retraction of leading-edge flaps; for example, $\Delta C_{m, \text{lef}}$ indicates increment in C_m produced by retraction of leading-edge flaps from 25° to 0°

sb increment in variable produced by deflection of speed brake

Abbreviations:

ACM air combat maneuvering

ARI aileron-rudder interconnect

rms root mean square

A dot over a symbol denotes a time derivative of the variable.

DESCRIPTION OF AIRPLANE

A three-view sketch of the YF-16 configuration is shown in figure 2, and the mass and geometric characteristics used in the simulation are listed in table I. The airplane control system is described in detail in appendix A. The primary deflections of the control surfaces used for the present configuration are symmetric deflection of the horizontal tail (stabilator) for pitch control, deflection of conventional wing-mounted ailerons and differential deflection of the horizontal stabilators for roll control, and rudder deflection for yaw control. Special features of the configuration include (1) the use of a normal-acceleration command longitudinal control system which provides static stability, normal-acceleration limiting, and angle-of-attack limiting, (2) the use of a wing leading-edge flap which is automatically deflected as a function of angle of attack and Mach number, (3) the use of a roll-rate command system in the roll axis, (4) the use of an aileron-rudder interconnect and a stability-axis yaw damper in the yaw axis, and (5) the use of a force-actuated (minimum displacement) side-stick controller and force-actuated rudder pedals. The simulations of the airplane engine characteristics and buffet characteristics are described in appendix B. All simulated flights were made for a center-of-gravity location of $0.35\bar{c}$.

DESCRIPTION OF SIMULATOR

The Langley differential maneuvering simulator (DMS) is a fixed-base simulator which has the capability of simultaneously simulating two airplanes as they maneuver with respect to one another, including a full, wide-angle visual display for each pilot. A sketch of the general arrangement of the DMS hardware and control console is shown in figure 3. Two 12.2-m (40 ft) diameter projection spheres each enclose a cockpit, an airplane-image projection system, and a sky-Earth-Sun projection system. A control console located between the spheres is used for interfacing the hardware and the computer and displays critical parameters for monitoring of the hardware operation. Each pilot is provided a projected image of his opponent's airplane, with the relative range and attitude of the target shown by use of a television system controlled by the computer program.

Cockpit and Associated Equipment

A photograph of one of the cockpits and the target visual display is shown in figure 4. A cockpit and an instrument display representative of current fighter aircraft equipment are used together with a fixed gunsight for tracking. Each cockpit was located to position the pilot's eyes near the center of the sphere, which resulted in a field of view representative of that obtained in current fighter airplanes. For the present study, a special modification was made to one cockpit to incorporate the side-stick controller as shown in

figure 5. The controller was placed in the same general location as the controller in the actual airplane; however, no special armrest was provided (as is the case in the actual airplane) other than the regular seat armrest which provided more of an elbow rest than a support for the forearm. The normal hydraulic control feel system was not employed for this simulation since the side-stick controller and rudder pedals were force sensitive with no deflection required to activate the controls. Although the cockpits are not provided with attitude motion, each cockpit incorporated a buffet system capable of providing programmable rms buffet accelerations as high as 0.5g with up to three primary structural frequencies simulated.

Visual Display

The visual display in each sphere consists of a target image projected onto a sky-Earth scene. The sky-Earth scene is generated by two point light sources projecting through two hemispherical transparencies, one transparency of blue sky and clouds and the other of terrain features; the scene provides a well-defined horizon band for reference purposes. No provision is made to simulate translational motions with respect to the sky-Earth scene (such as altitude variation); however, spatial attitude motions are simulated. A flashing light located in the cockpit behind the pilot is used as a cue when an altitude of less than 1524 m (5000 ft) is reached. The target-image generation system uses an airplane model mounted in a four-axis gimbal system and a television camera with a zoom lens to provide an image to the target projector within the sphere. The system can provide a simulated range between airplanes from 90 m (300 ft) to 13 700 m (45 000 ft) with a 10-to-1 brightness contrast between the target and the sky-Earth background at minimum range.

Additional special effects features of the DMS hardware include simulation of blackout at high normal accelerations (see appendix B), use of an inflatable anti-g garment for simulation of normal-acceleration loads, and use of sound cues to simulate wind, engine, and weapons noise as well as artificial warning systems. Additional details on the DMS facility are given in reference 6.

Computer Program and Equipment

The DMS is operated with real-time digital simulation techniques and a Control Data Corporation 6600 computer. The motions of the evaluation airplane were calculated by using equations of motion with a fixed-interval (1/32 sec) numerical integration technique. The equations used nonlinear aerodynamic data as functions of α and/or β in tabular form. These data were derived from results of low-speed static and dynamic (forced oscillation) force tests conducted at a Reynolds number of about 0.8×10^6 and a Mach number of about 0.1. The data included an angle-of-attack range from -10° to 90° and a side-

slip range from -40° to 40° . Effects of Mach number, Reynolds number, or aeroelasticity were not included in the mathematical model. Complete descriptions of the aerodynamic data and the equations of motion are given in appendix B.

DISCUSSION OF AERODYNAMIC CHARACTERISTICS

To provide a foundation for the analysis and interpretation of the simulation results which follow, the aerodynamic stability and control characteristics of the simulated airplane configuration are presented and discussed in this section. The reader is cautioned that an analysis of the characteristics of the basic airframe is not directly applicable to the complete configuration in view of the extensive control system augmentation employed in the airplane and the large effects that the control system produced at high angles of attack.

Longitudinal Characteristics

The longitudinal aerodynamic data are listed in tables II to VII and the representation of the characteristics in the simulation is discussed in appendix B. One unique characteristic of the present configuration is that it exhibits essentially neutral stability in pitch at the combat center-of-gravity position ($0.35\bar{c}$) at subsonic speeds, as shown in figure 6(a). The longitudinal control system (see appendix A) is equipped with angle-of-attack feedback to provide artificial pitch stability. The lift curve shown in figure 6(a) is relatively linear up to about $\alpha = 25^\circ$, with maximum lift occurring near $\alpha = 35^\circ$. Associated with the pitch stability augmentation system of the study configuration is an angle-of-attack/normal-acceleration limiting system which avoids overshoots in angle of attack; this system attempts to limit the angle of attack to below about $\alpha = 27^\circ$. A further discussion of the complete pitch control system is given in appendix A.

The results of wind-tunnel tests on models of the configuration at several Reynolds numbers (range from 0.8×10^6 to about 4.5×10^6) showed significantly different pitching-moment values above $\alpha = 40^\circ$. In particular, results from the Langley tunnel tests ($NR_e = 0.8 \times 10^6$) showed deep-stall trim points at high angles of attack above 50° , whereas the results from higher Reynolds number tests showed a reduction in stability but no deep-stall trim condition. To determine the relative significance of the trim point indicated by the low-speed tests, three pitching-moment curves were considered at $\beta = 0^\circ$ between $\alpha = 40^\circ$ and $\alpha = 70^\circ$ as shown in figure 6(b). The circular symbols represent the basic Langley data while the other two curves were faired in to represent a mild trim point (square symbols) more representative of the higher Reynolds number condition and a conventional curve (diamond symbols). The values of C_m used in the simulation were adjusted over the entire sideslip range between $\alpha = 40^\circ$ and $\alpha = 70^\circ$ by applying the differences between the various curves at $\beta = 0^\circ$. This procedure allowed the evaluation

of the effect of a particular C_m curve on recovery from poststall conditions. Another important aerodynamic characteristic exhibited by the configuration was the variation of C_m with β at high angles of attack as shown in figure 6(c). As can be seen, trim points were possible at large angles of sideslip because of nose-up C_m changes with increasing sideslip. This characteristic could have marked effects on poststall recovery motions which frequently involve large sideslip excursions.

Lateral-Directional Characteristics

Static lateral-directional stability. - The static lateral-directional stability characteristics of the basic configuration with scheduled leading-edge flap deflections are presented in figure 7(a) in terms of the static directional stability derivative $C_{n\beta}$, the effective dihedral derivative $C_{l\beta}$, and the dynamic directional stability parameter $C_{n\beta,dyn}$ as functions of angle of attack. The parameter $C_{n\beta,dyn}$, given by the expression

$$C_{n\beta,dyn} = C_{n\beta} - \frac{I_Z}{I_X} C_{l\beta} \sin \alpha$$

has been used in past investigations (refs. 7 and 8) as an indication of the existence of directional divergence (nose slice) at high angles of attack. Negative values of this parameter usually indicate the existence of a divergence. The data of figure 7(a) indicate that the configuration was statically stable (both directionally and laterally) for angles of attack up to 31° . Above $\alpha = 31^\circ$, $C_{n\beta}$ reached large unstable (negative) values. The parameter $C_{n\beta,dyn}$ remained positive for values of α up to 34° . These results show the configuration to be statically stable throughout the operational angle-of-attack range permitted by the longitudinal control system (limit of $\alpha = 27^\circ$). However, both directional and lateral stability decrease rapidly above $\alpha = 25^\circ$ and a directional divergence would be expected near $\alpha = 34^\circ$ if α is not limited.

The lateral-directional aerodynamic control characteristics for the configuration at $\beta = 0^\circ$ are shown in figure 7(b) in terms of moment increments caused by full control. The rudder effectiveness was high and essentially constant over the operational range of α . Roll control effectiveness of the ailerons and differential tails was good and well sustained up to the angle-of-attack limit with very little adverse yaw (compared with moments produced by the rudder) from either mode of roll control. These data indicate that the configuration should exhibit good lateral-directional control characteristics up to the angle-of-attack limit if proper coordination of roll and yaw controls is used to suppress the adverse yaw from roll control.

An aileron effectiveness parameter is often used to appraise the roll-control effectiveness at high angles of attack. This parameter is defined as

$$C_{n\beta} - C_{l\beta} \frac{C_{n\delta a}}{C_{l\delta a}}$$

for ailerons only, or by

$$C_{n\beta} - C_{l\beta} \left(\frac{C_{n\delta a} + KC_{n\delta r}}{C_{l\delta a} + KC_{l\delta r}} \right)$$

where K is the rudder-aileron gain for ailerons with an aileron-rudder interconnect. The variation of this parameter with angle of attack for the present configuration is presented in figure 7(c) for the combined aileron/differential tail alone and for these controls with an aileron-rudder interconnect. A negative value of this parameter is indicative of roll reversal; when a reversal is encountered, a right roll control input by the pilot will cause the airplane to roll to the left. Even without the interconnect, the parameter remained positive up to $\alpha = 31^\circ$. The interconnect provided a large positive increment between $\alpha = 15^\circ$ and $\alpha = 30^\circ$. This effect would be expected to show up as higher roll rates available in flight.

Dynamic lateral-directional stability. - A classical linearized lateral-directional stability analysis was made by using three-degree-of-freedom equations of motion and the aerodynamic data of appendix B. The calculations were made for the following four configurations:

- (1) Basic airplane (all augmentation systems active)
- (2) Basic airplane with aileron-rudder interconnect (ARI) inoperative
- (3) Basic airplane with stability-axis yaw damper deactivated
- (4) Basic airplane with ARI and stability-axis yaw damper deactivated

The ARI system caused the rudder to deflect in conjunction with roll control inputs so as to eliminate the adverse yaw due to these surfaces. The stability-axis yaw damper applied rudder deflections in response to an $r - p\alpha$ signal in order to reduce sideslip excursions during rolling maneuvers at high angles of attack. A detailed discussion of these systems is contained in appendix A.

The results of the dynamic stability calculations are presented in figure 8 in terms of the damping parameter $1/t_{1/2}$ and the period of oscillatory modes of motion. Positive values of $1/t_{1/2}$ indicate damped, or stable, modes. Data are shown for the classical Dutch roll, spiral, and roll modes of motion as functions of α for the four cases. The data show that the roll and spiral modes are stable for values of α up to 40° , where-

as the Dutch roll mode tends to become less stable as α is increased and is unstable above $\alpha \approx 32^\circ$. The stability-axis yaw damper has the effect of increasing the damping of the Dutch roll mode while decreasing its frequency. The ARI, on the other hand, had little effect on the Dutch roll frequency but slightly degraded the damping; this effect is caused by the roll damper signal feeding through the ARI to create, in effect, adverse yaw due to roll rate. It is noted that the Dutch roll modes of the four cases converge as α increases such that at $\alpha = 35^\circ$ they are essentially the same low-frequency unstable mode. This result indicates that the lateral-directional augmentation becomes ineffective above $\alpha = 30^\circ$, which is to be expected since in this region the Dutch roll stability characteristics are influenced mainly by the static stability parameters $C_{n\beta}$ and $C_{l\beta}$, which are not affected by either the stability-axis yaw damper or the ARI system.

Response to lateral-directional controls. - Maximum usable roll rates obtained in bank-to-bank reversals with full lateral controls (no rudder inputs) applied for the fully augmented airplane are shown in figure 9. The data were obtained during the piloted simulation study. The maneuver used involved starting from a low-angle-of-attack, level flight condition, banking into a turn, increasing the angle of attack rapidly to a desired value, then using maximum roll control input to reverse the bank angle and stabilize in a turn in the opposite direction. The decrease in maximum roll rate with increasing α is due to a combination of decreasing airspeed, reduced control effectiveness, and increasing adverse yaw due to roll rate as evidenced by the adverse β trace. Higher values of roll rate could have been obtained if complete 360° rolls were made; however, bank-to-bank maneuvers were chosen because they more accurately represent the roll response required during tactical situations.

The control system design of the present configuration produced responses due to rudder inputs which were considerably different from responses expected of conventional fighter airplanes at high angles of attack. Shown in figure 10 are time histories of the airplane response to step rudder inputs in level flights at $\alpha = 3^\circ$ and $\alpha = 18^\circ$. The resulting motions were steady sideslips with little rolling because the roll-rate command system counteracted any uncommanded roll rates. Thus, use of the rudder pedals alone is not effective for rolling and the pilot must use conventional lateral stick inputs to roll effectively, even at high angles of attack. It should be noted that this feature is desirable in that it eliminates the usual need for the pilot to make a transition from using lateral stick inputs at low values of α to using rudder pedal inputs at high values of α for roll control.

EVALUATION PROCEDURES

The results of the investigation were in the form of pilot comments and time-history records of airplane motions, controls, and tracking for the various maneuvers performed.

Most of the evaluations were performed with a research test pilot familiar with the air combat maneuvers used with current fighter airplanes; however, other research test pilots and contractor test pilots also flew the simulator. Linearized analyses of the dynamic stability characteristics of the combined airplane and control system were also made to aid in the interpretation of the results. Previous experience with the simulation of fighter stall/spin characteristics (see ref. 9) has shown that visual tracking tasks which require the pilot to divert his attention from the instrument panel are necessary to provide realism in studying the possibility of unintentional loss of control and spin entry. Furthermore, earlier studies (ref. 4) have shown that mild, well-defined maneuvers can produce misleading results inasmuch as a configuration that behaves fairly well in such mild maneuvers may be violently uncontrollable in the complex and pressing nature of high-g, air combat maneuvering (ACM). Finally, for purposes of evaluation in comparing the performance of several configurations, the tasks used must be repeatable. The following test procedures were implemented in order to account for the foregoing factors. In order to force the evaluation pilot to fly at high angles of attack, the target airplane was programmed to have the same thrust and performance characteristics as the evaluation airplane; however, the target had idealized high-angle-of-attack stability and control characteristics. The target airplane was flown by the evaluation pilot through a series of ACM tasks of varying levels of difficulty while the target motions were tape recorded for playback later to drive the target as the task for the evaluation airplane. In this manner, repeatable tasks ranging from simple tracking tasks to complex, high-g ACM tasks were developed for use in the evaluation.

The first phase of the study consisted of pilot familiarization and development of ACM tasks for the evaluation. The pilot performed simple air tasks requiring low g levels with no target airplane in order to determine and become familiar with the stability and control characteristics of the simulated airplane. The second phase of the study involved evaluation of the simulated airplane and its various control system features in the ACM tasks developed. Four tasks were chosen for use during the study: (1) a simple high-g pullup to maximum angle of attack in a turn followed by a maximum effort bank angle reversal near maximum angle of attack (called the roll performance task), (2) a 4g to 7g steady windup turn for steady tracking evaluation (called the steady tracking task), (3) a bank-to-bank task (or horizontal S) with gradually increasing angle of attack up to maximum α to evaluate rapid rolls and target acquisition (called the bank-to-bank task), and (4) a complex, vigorous ACM task (called the general ACM task) to evaluate the simulated airplane susceptibility to high-angle-of-attack handling qualities problems during aggressive maneuvering. These four tasks are described in more detail in the following paragraphs.

Roll Performance Task

The maneuver used to evaluate the rolling performance of the simulated airplane at high angles of attack was a high-g turn involving a maximum-effort bank-angle reversal near maximum angle of attack as sketched in figure 11. This task was executed by the pilot without reference to a target in order to allow the pilot to concentrate on the response of the airplane. The task was initiated at a Mach number of 0.8 and an altitude of 9144 m (30 000 ft). Upon initiation of a run, the pilot banked the airplane into a turn and rapidly loaded to maximum commanded normal acceleration in pitch. As the angle of attack approached 25° (airplane still pulling about 4g), the pilot used full roll control to reverse his turn direction and then reduced g loading. This maneuver allowed analysis of the airplane roll response near maximum angle of attack in terms of usable roll rate, sideslip generated, and bank-angle control. (The maximum α available on the present configuration is about 27° or 28° , as previously discussed.)

Steady Tracking Task

A steady windup turn was flown, with α of the target airplane increasing to an intermediate value and finally to near maximum α for the evaluation airplane in order to evaluate the tracking capability of the simulated airplane at high angles of attack. Initially, both airplanes were at an altitude of 9144 m (30 000 ft) at $M = 0.8$ with the subject airplane about 457 m (1500 ft) directly behind the target and at the same heading as the target. Upon initiation of the run, the target gradually established a banked attitude, slowly increased angle of attack producing a range of normal acceleration from 4g to 7g, decreased altitude, and finally decreased the Mach number to about 0.35. The pilot attempted to track the target as accurately as possible while staying at reasonably close range. At times the pilot would intentionally generate offset and then reacquire the target to study acquisition and settling time.

Maneuvering Tasks

Several general ACM tasks were generated by the evaluation pilot flying the target, and two of these were selected for evaluation. The first task, shown in figure 12, was a series of bank-to-bank maneuvers (or horizontal S's) at steadily increasing angles of attack. These maneuvers enabled the pilot to evaluate the ability to roll rapidly to acquire the target and stabilize while at high-g loadings. A second ACM task of a more general nature was developed in order to represent the complex and vigorous maneuvers encountered during air-to-air combat. As an aid in visualizing this task, the first half of the task is sketched in figure 13(a). The time history of the target motions is shown in figure 13(b). These tasks were considered to be very demanding and required the airplane

to have good handling characteristics at high angles of attack in order to achieve good tracking results and avoid loss of control.

Evaluation of Performance

In evaluating the simulated airplane with and without several of the special high-angle-of-attack control system features, numerous runs were made in each of the tasks for each configuration considered. The pilot was not normally informed of the control configuration or flight task prior to initiating a test run. This procedure minimized any tendency on the pilot's part to anticipate the problems or to be particularly cautious. In particular, during the performance of the recorded ACM tasks, the pilot tried to optimize his offensive position while obtaining as much tracking time as possible. Sufficient flights were made of the various configurations in the several tasks to insure that the pilot's "learning curve" was reasonably well established before drawing any conclusions on evaluation results. The present configuration required close attention to the learning factor as the pilot was required to adapt to both the side-stick controller and a new control system. On this basis, the performance of the simulated airplane in the tasks selected for discussion in this report is believed to be representative of the high-angle-of-attack handling qualities to be expected of the full-scale airplane (recognizing, however, the limitations imposed by the low Mach number and the low Reynolds number of the input aerodynamic data).

Evaluation of the performance of the several control system components was based on pilot comments, ability of the pilot to execute the task assigned, and analysis of time histories of airplane motions and tracking. In particular, close attention was given to the parameters α , β , ϕ , and ϵ and the pilot control inputs to determine (1) how well the task was executed, (2) the excursions experienced (for instance, in β), and (3) the workload of the pilot. The evaluation considered the effects of the control system features on the airplane handling qualities and tracking, including the aileron-rudder interconnect, the stability-axis yaw damper, both of the aforementioned combined, and the longitudinal angle-of-attack/normal-acceleration limiting system.

SIMULATION RESULTS FOR BASIC CONFIGURATION

In general the stability and control characteristics of the basic airplane (with normal control system) were good for the maneuvering tasks considered, within the angle-of-attack range allowed by the longitudinal control system, and caused no problems in the current simulation. These characteristics were studied in several stages, including (1) documentation of the stall, departure, and spin resistance characteristics of the configuration during simple air work, (2) performance of various piloting tasks, and (3) evaluation of the side-stick controller.

Stall, Departure, and Spin Resistance Characteristics

The first portion of the simulator investigation consisted of documenting the stall characteristics of the basic configuration with all elements of the control system. In this phase a particular effort was made to determine maneuvers which might lead to inadvertent loss of control and spin-entry conditions. For all of these simulated flights the C_m curve was modified above $\alpha = 40^\circ$ to be conventional ($C_{m,2}$ of fig. 6(b)) in order to avoid deep-stall characteristics which will be discussed later. All flights were started at $M = 0.6$ and $h = 6096$ m (20 000 ft). The initial maneuvers flown involved flying the airplane into a turn, increasing angle of attack to the maximum available, and then evaluating controllability. Figure 14 shows a rapid pullup to the maximum angle of attack followed by individual control applications. The horizontal stabilator had to be deflected only a few degrees to perform the initial pullup because of the neutral longitudinal stability of the configuration. Shortly after the airplane reached maximum α (about 27° to 28°), the speed dropped low enough to allow α to drift slightly above 30° , where the longitudinal control system automatically applied full nose-down elevator to stop the overshoot in α . As the airplane stabilized, full rudder was applied and held, followed by full aileron and fully crossed prospin controls. No tendency toward a departure or loss of control was observed.

Shown in figure 15 is a time history of an accelerated stall flown in a windup turn (5g to 6g stall) with full prospin controls applied (aileron with turn and rudder against) as the airplane reached $\alpha = 25^\circ$. The prospin controls were held for a prolonged time (about 25 sec) with no loss of control. As airspeed dropped very low ($M < 0.2$) near $t = 25$ sec, α began to overshoot to 30° and the pitch control system activated to stop the overshoot. Although α reached 40° , the control system reduced the angle of attack and control of the airplane was not lost.

In order to further evaluate the effectiveness of the control system to prevent inadvertent departures, three extreme maneuvers were flown during stall entry: (1) an inertially coupled entry, (2) an aerodynamically coupled entry, and (3) a vertical entry. Although these maneuvers may not be frequently encountered in air combat, they are possible and should therefore be considered for highly maneuverable fighter airplanes. Typical results obtained for these maneuvers are presented in figures 16 to 18.

The inertially coupled entry, shown starting after $t = 50$ sec in figure 16, was accomplished by pulling the airplane up rapidly in a windup turn near $t = 55$ sec and applying full roll control and full rudder when the airplane reached a high pitch rate. This maneuver produced a combination of high angular rates about all three body axes at high angles of attack, and the resultant inertial coupling forced the airplane through $\alpha = 30^\circ$, in spite of full nose-down elevator applied by the control system. Sideslip oscillations built up from the unstable Dutch roll, and a spin entry ensued. In the earlier portion of

the flight prior to $t = 50$ sec, the figure shows two attempts to depart the configuration by using crossed controls (ailerons with turn and rudder against) and both attempts were unsuccessful. However, as soon as the pilot reversed rudder and deflected it with the roll input (at $t = 57.5$ sec), the loss of control resulted. It was found that control-input timing was critical in obtaining such a coupled entry and that such entries could not be obtained consistently. Furthermore, no such situation was encountered in the ACM tasks to be discussed later. It must be noted, however, that this maneuver, however difficult to accomplish, is one which could lead to loss of control on the present configuration.

The aerodynamically coupled entry, shown in figure 17, was accomplished by pulling the airplane into a very low-speed, high-angle-of-attack condition in a turn and then reversing the bank angle. The bank-angle change translated angle of attack into sideslip (the low dynamic pressure reduced the effect of the stability-axis yaw damper), and a large increase in β resulted, followed by an increase in α due to aerodynamic pitchup at large sideslips (see fig. 6(c)). However, the resulting motion was easily recoverable for the variation of C_m with α used ($C_{m,2}$ of fig. 6(b)), even though the angle of attack exceeded 60° . A situation such as this could occur in air combat if the pilot attempted a rapid heading change at very low airspeeds.

The vertical stall entry (hammerhead stall), shown in figure 18, was accomplished by putting the airplane into a near vertical climb, allowing the airspeed to drop to near zero, and then pushing the nose over to cause a rapid increase in angle of attack which the pitch control system was unable to stop due to the low dynamic pressure and lack of control effectiveness. Near $t = 24$ sec, the angle of attack rose to nearly 90° with relatively small sideslip excursions, and the airplane was recovered without difficulty for the variation of C_m with α used ($C_{m,2}$ of fig. 6(b)).

In summary, the three foregoing maneuvers were the only ones discovered that could force the airplane above the angle-of-attack limit dictated by the pitch control system. An essential element in all three maneuvers was the relatively low airspeed which resulted in reduced control effectiveness available for the automatic control system. No attempt has been made to determine the possibility or character of developed spins following the poststall excursions because of lack of reliable aerodynamic representation at angles of attack above about 40° .

Performance in Tasks

An illustration of the performance of the basic airplane in the roll performance task is presented in figure 19 in time-history form. The pilot pulled about 7g in a windup turn and successfully executed a maximum-effort bank-angle reversal near maximum α . Sideslip excursion (adverse β) was small and steady (i.e., well damped), bank-angle con-

trol was positive, and a relatively high roll rate was obtained. The pilot commented that the airplane handled well, and the use of rudder pedals was not required to perform the maneuver.

Typical motions of the airplane during the tracking task with the target in a windup turn are shown in figure 20. Also included in the time history are the range between the two airplanes and the pilot tracking error ϵ . In this particular run, the pilot maintained a steady tracking effort with no intentional off-target time. The pilot tracking error was consistently small throughout the task until near the end when the target entered a near-vertical, spiraling-dive evasive maneuver. Sideslip excursions throughout the flight were minimal and control was good. The pilot rated the configuration as good with negligible deficiencies; no rudder inputs were felt to be necessary. The only adverse comments concerned the harmony between the pitch control force gradients and the angle-of-attack/normal-acceleration limiting schedule; this point will be discussed later.

Illustrations of the performance of the basic airplane in the two general maneuvering tasks, the bank-to-bank task and the general ACM task, are shown in figures 21(a) and 21(b). Figure 21(a) presents the results of a flight on the bank-to-bank tracking task. During the flight, the pilot tracked the target as closely as possible until the target executed a bank-angle change. The pilot then purposely lagged the target in order to study the task of acquiring and stabilizing the pipper (gunsight) on the target after each reversal. As shown by the time history, the pilot was able to accomplish this task with a minimum of control activity and sideslip excursions throughout the angle-of-attack range up to the maximum α available. The pilot rated the airplane from good, with negligible deficiencies, to fair, with minor but annoying deficiencies; the primary problem was one of stabilizing on the target after acquisition, probably due to the force-actuated side-stick controller. At any rate, the pilot had no difficulty in maintaining a good offensive position while keeping the target within a reasonably small angle-off position with no inadvertent departures. Again, the use of rudder pedals was not necessary during the maneuver.

The performance of the airplane in the general ACM task is illustrated in figure 21(b) in time-history form. In spite of the vigorous nature of the maneuvers involved, the pilot was able to maintain a good offensive position while accumulating some tracking time. It is also important to note the relatively small sideslip excursions experienced. The pilot commented that the configuration flew very well and gave him the ability and confidence to pull up and acquire the target almost at will. The pilot felt, in general, that the airplane was well damped and responsive; as shown by the α time history, the task covered the entire angle-of-attack range permitted by the limiting system. However, in certain instances (particularly at relatively high speeds), when the pilot attempted to get the nose up to acquire the target, the normal-acceleration limiting system slowed the rate

of rotation that could be obtained in pitch. This problem bothered the pilot somewhat (for example, note the α trace at $t = 75$ to 80 sec and $t = 125$ to 130 sec).

Overall, the basic airplane performed well in all of the tasks evaluated. No tendency toward loss of control was noted during any of the simulated flights. The pilot commented that the simulated airplane felt very safe and yet essentially unrestricted.

Evaluation of Side-Stick Controller

Since the side-stick controller used in the study configuration is unconventional, the pilot was requested to evaluate the suitability of the controller, to gather any data which might aid in the evaluation of the controller, and to determine the limitations of evaluating such a controller in fixed-base simulation.

The controller used by the pilot was a fixed (minimum displacement), force-actuated, side-stick controller located on the pilot's right-hand side near his right knee, as shown in figure 5. The controller was positioned to suit the primary evaluation pilot as much as possible; however, the position was not optimum (no canting or twisting of the controller was incorporated) and no special armrest was provided to aid the pilot in steadying his forearm. Instead, the pilot was required to rest his elbow on the cockpit seat armrest. This arrangement made it difficult for the pilot to make small precise control inputs. It should be noted that the side stick used on the actual airplane has a forearm rest, cant, and twist. A standard fighter grip was used, and the grip was rigidly mounted to a steel shaft connected to a very stiff force sensor which, in turn, was bolted to the cockpit floor.

It is important to emphasize the fact that the controller grip was rigid and did not move in response to pilot control. The forces exerted by the pilot in the lateral and longitudinal directions normal to the stick vertical axis were sensed by a force-sensing system which, in turn, actuated the control system. (See appendix A for a more detailed description.) Therefore, the only indication to the pilot (other than force) of a control input was the airplane response.

Evaluation of the controller was originally planned to be a natural consequence of the various tasks developed for the pilot, and a certain amount of information was provided by the tasks. However, it was recognized that an important factor would be to document control problems which may exist when the pilot is forced to twist around in his seat in order to view an opponent beside or behind him. Therefore, a special set of runs was made with pilots flying both simulated airplanes in one-on-one ACM, with the secondary airplane pressing the evaluation airplane from the rear.

During the ACM tasks, the evaluation pilot found that he was able to control the airplane satisfactorily with the side-stick controller, but the evaluations uncovered several annoying problems. The first problem noticed by the pilot was a need for a lighter roll-

force gradient for right roll than for left roll to account for the fact that a human pilot can normally pull laterally toward himself easier than he can push away. An asymmetric roll force gradient was developed which eliminated this problem as discussed in appendix A. Another recurring problem was that the pilot often encountered the aft force stop without realizing it, although a light mounted on the cockpit instrument panel was illuminated in this case. The same problem occurred to a lesser degree with lateral control. The pilot had no feel (no stick deflection stop) for when he was at maximum command or the amount by which he was exceeding the maximum. To demonstrate this problem as it occurred during one of the ACM tasks, time histories of the pilot force inputs are presented in figure 22. The maximum force values are denoted by dashed lines on the plots. It can be seen that the pilot often exceeded the maximum pitch command force and even attempted to modulate pitch control while exceeding the limit. Such modulation had no effect on the airplane response and therefore could appear to the pilot as improper airplane response. The problem was more evident in pitch than in roll control.

Evaluation of the controller in the one-on-one ACM runs provided additional data on the controller. Initially the pilot made inadvertent roll inputs while twisting and turning in the cockpit to keep his opponent in sight. However, in a relatively short time the pilot was able to adapt to the situation and avoid this problem by concentrating on keeping his arm properly aligned with the controller. Major questions remain as to the suitability of such a controller under high-g conditions, such as those associated with ACM. Such conditions could not be simulated in the present fixed-base simulator study because of the lack of g simulation. Another important factor is that, since the stick is mounted on the right side of the cockpit (as opposed to being in the center as a conventional stick), control would be very difficult if the pilot's right arm were injured and he were required to fly left-handed.

As a result of the obvious limitations of the current fixed-base simulation, it should be noted that the side-stick controller could not be fully evaluated under realistic ACM conditions. This evaluation remains to be accomplished during flight tests of the actual airplane.

EFFECTS OF SPECIAL CONTROL SYSTEM FEATURES

Once the performance of the basic airplane was established and the pilot was familiar with the characteristics, emphasis was placed on evaluating how the special control system features contributed to the good characteristics shown by the configuration at high angles of attack. This phase of the study determined the effects of the longitudinal angle-of-attack/normal-acceleration limiting system, the aileron-rudder interconnect system, and the stability-axis yaw-damper feature. Also included in this phase was an evaluation

of the three different variations of C_m with α in the poststall flight conditions shown in figure 6(b).

Effects of Angle-of-Attack/Normal-Acceleration Limiting System

As mentioned previously, the airplane configuration employs a sophisticated longitudinal control system which includes augmentation for static stability and for controlling the maximum load factor available at a given angle of attack. This latter feature also controls maximum angle of attack available. The angle-of-attack/normal-acceleration limiting system operates on the schedule shown in figure 23. Operationally, the system subtracts larger increments of a_n from the pilot's command ($a_{n,com}$) as the angle of attack is increased. At $\alpha = 27^\circ$, the pilot cannot command incremental positive normal accelerations above 1g. This feature tends to limit the maximum angle of attack available. As a backup to this feature, full nose-down elevator is applied by the control system to prevent angle-of-attack overshoot if α exceeds 30° . The system is described in detail in appendix A.

It should be noted that the angle-of-attack/normal-acceleration schedule shown in figure 23 has two distinct slopes above $\alpha = 15^\circ$. This feature is incorporated in order to provide an increasingly tight control of α as maximum α is approached.

The angle-of-attack/normal-acceleration limiting system was eliminated except for the overshoot-prevention feature and the pilot was asked to fly the airplane through the roll performance task shown in figure 19. The results of one such flight are presented in figure 24 and show that the airplane almost immediately exceeded the α limit, in spite of the full nose-down elevator above $\alpha = 30^\circ$, and the subsequent motion appeared to be an entry into a spin. The pilot recovered the airplane with some difficulty, and the recovery involved an additional inadvertent pitch departure. As previously noted, simulation of spin recovery in the present investigation was of questionable validity. This particular flight was made with the conventional variation of C_m with α ($C_{m,2}$) for $\alpha > 40^\circ$.

In view of the strong tendency toward high-angle-of-attack excursions without the angle-of-attack/normal-acceleration limiting feature, an effort was made to determine the effect of the three variations of C_m with α shown in figure 6(b) on the recovery motions in order to determine what problems a high-angle-of-attack trim point might cause. The maneuver employed for these evaluations was a simple high-g pullup in a windup turn; no adverse lateral-directional controls were applied. The flights were made without the angle-of-attack/normal-acceleration limiting schedule and without the overshoot-prevention system. The data of figures 25 to 27 illustrate the results obtained and show that all three cases resulted in a poststall gyration or spin-entry situation. In figure 25, the pilot was unable to recover from the strong high-angle-of-attack trim condition with elevator alone and finally reverted to the use of lateral and directional controls

to recover. Figure 26 shows that the pilot had considerably less difficulty with the weak trim point, although he did enter a slow, oscillatory spin. Recovery was effected with forward stick and rolling with the rotation in yaw. Recovery from the high-angle-of-attack excursion with the conventional variation of C_m with α (no trim point at high α) was relatively easy, as shown in figure 27. The pilot recovered with forward stick and some lateral-directional control inputs. The main point shown by the foregoing data is the increasing difficulty in recovering the airplane, without the angle-of-attack/normal-acceleration limiting system as a stronger high-angle-of-attack trim point was introduced. It should be emphasized that preceding results presented for the basic airplane, with the angle-of-attack/normal-acceleration limiting feature, indicate that a pilot would probably not have to contend with any poststall motions on this airplane with the basic control system unless he inadvertently executes one of the three low-speed maneuvers previously described. However, if a trim point exists at extreme angles of attack, it could cause significant delays in recovering from a poststall condition.

A limited effort was made to determine the sensitivity of the angle-of-attack/normal-acceleration limiting system to the particular angle-of-attack/normal-acceleration schedule variations used for the basic schedule. It was noted that any significant increase in the angle of attack for the second breakpoint led to a marginally safe airplane in that high-angle-of-attack excursions were possible in vigorous high-angle-of-attack maneuvers such as the roll performance task. On the other hand, it was noted that, by decreasing the lower schedule gradient and increasing the upper gradient (above $\alpha = 22.5^\circ$), the airplane became more responsive in pitch; that is, the pilot could rotate the airplane nose up more rapidly in ACM and could track slightly better. However, it was also obvious that modifications to the angle-of-attack/normal-acceleration limiting schedule would require corresponding modifications to the stick force characteristics before a satisfactory pitch response could be obtained. This degree of detail was beyond the scope of the current investigation.

Effects of Aileron-Rudder Interconnect and Stability-Axis Yaw Damper

Additional flights were made to establish the benefits the simulated airplane gained from the special lateral-directional control system features, including the aileron-rudder interconnect (ARI) and the stability-axis yaw damper. (These flights were made with the angle-of-attack/normal-acceleration limiter operative.) The ARI gain was scheduled with angle of attack (see appendix A) such that the amount of rudder commanded by the lateral stick increased with increasing angle of attack. The stability-axis yaw damper was implemented by feeding the directional control channel an approximation ($r - p\alpha$) of sideslip rate $\dot{\beta}$. (See appendix A.) The system tends to make the airplane roll about the stability axis, thereby minimizing β . Both control features require angle-of-attack information.

When the ARI system was disengaged from the lateral-directional control system, the airplane could be forced into a spin-entry condition by using crossed controls as shown in figure 28. As previously discussed, the basic airplane could not be departed by use of crossed controls with the ARI active, as shown in figure 14(b). Figure 28, however, shows a case in which the airplane, with the ARI system disengaged, overshot the $\alpha = 30^\circ$ boundary. The pitch control system attempted to stop the α buildup, and at this point, a pilot might have recovered with neutral lateral controls, but crossed controls were maintained and a spin entry ensued. This result shows that the ARI system is an important factor in the spin resistance of the airplane. The results of reference 4 also showed a similar effect of an ARI system.

An important aspect of fighter airplane handling qualities is the ability to maneuver safely and effectively at high angles of attack. This ability requires good roll performance throughout the operational angle-of-attack range. Both the ARI and the stability-axis yaw damper contributed significant improvements to the roll performance of the configuration at high angles of attack. The roll performance of the airplane was evaluated by documenting the maximum roll rate obtained, with full roll control, when the pilot attempted to reverse the airplane bank angle at a selected angle of attack while in an accelerated windup turn. This type of maneuver is typical of ACM and similar to the roll performance task. The results obtained on the simulated airplane are summarized in figure 29 which presents results for the basic airplane, the airplane without both features, and the airplane without each feature individually. As pointed out earlier, the roll performance of the basic airplane was excellent throughout the available angle-of-attack range. When both the ARI and the stability-axis damper were removed from the control system, the simulated airplane experienced (1) roll reversals above $\alpha = 25^\circ$, (2) a significant reduction in maximum roll rate available because of adverse yaw, and (3) markedly reduced lateral-directional damping. Figure 30 illustrates the performance of this configuration in the roll performance task and indicates the degraded handling qualities. When only the ARI was removed, the airplane exhibited less reduction in high-angle-of-attack roll rate and less adverse yaw; however, it showed relatively good damping at high α as evidenced by the β trace shown in figure 31. When only the stability-axis yaw damper was removed, the airplane maximum roll rate and adverse yaw were comparable to the basic airplane; however, the data of figure 32 show the marked reduction in high-angle-of-attack damping caused by removal of this feature. In summary, both features aided in reducing the adverse yaw and improving roll performance; the ARI provided the biggest single improvement in roll rate (by reducing adverse yaw), while the stability-axis damper provided primarily good lateral-directional damping at high α which resulted in reduced adverse yaw and improved roll performance. Both features would be expected to significantly reduce the pilot workload and increase confidence in the ACM environment.

As pointed out earlier, the tracking task was used primarily to evaluate the pilot's ability to track with the airplane at high angles of attack; this task therefore serves to highlight any problems evident in making precise control inputs. The simulated airplane was evaluated during the tracking task without both the ARI and the stability-axis yaw damper and without each feature individually. The results for each flight are presented in time-history form in figure 33. The solid line indicates the performance of the basic airplane, while the symbols represent the modified airplane. The basic airplane trace is the same flight for all comparisons and includes intentional inputs by the pilot to generate offset on the target and then reacquire it. When both features were removed from the control system, the overall tracking was noticeably degraded, as shown in figure 33(a). In this flight, the pilot did not intentionally generate any offset with the modified airplane. The β variations show that the pilot had more difficulty with β excursions and β oscillations during the task with the two control system features removed. These problems were reflected in bank-angle control problems and increased control activity. The pilot commented that he had considerable lateral-directional difficulty resulting in poor tracking at high angles of attack. The pilot stated that the configuration with neither of the subject control system features had very objectionable, but tolerable, deficiencies and that adequate performance required considerable pilot compensation.

When only the ARI was removed, considerable improvement was evident, as illustrated in figure 33(b). In this case the modified airplane still experienced larger β excursions than did the basic airplane, but the β oscillations evident in figure 33(a) were reduced, indicating improved damping due to the stability-axis yaw damper. Bank-angle problems were still evident and higher control activity in roll was present. Tracking was comparable with results for the basic airplane except for short periods at the beginning and the end of the flight. The pilot commented that the absence of the ARI made the airplane feel heavier in roll (apparent higher damping) and that it was difficult to make small corrections. The pilot also commented that the airplane without the ARI had minor, but annoying, deficiencies which required improvement.

A flight with only the stability-axis yaw damper removed, presented in figure 33(c), showed only small excursions in β , but β was considerably more oscillatory above $\alpha = 20^\circ$ with the damper removed, indicative of the loss of the damping provided by this feature. The tracking error ϵ is comparable with that of the basic airplane except for problems occurring near the end of the flight at higher angles of attack. The pilot sensed the loss in damping and commented that the airplane felt lighter in roll. This configuration was rated by the pilot to be about as difficult to handle as the configuration without the ARI, possibly a little more difficult due to the reduced damping. In general, the effects of the two control system features, as shown by the tracking task, correlate well with those effects shown in the roll performance task and in the linearized dynamic stability

analysis. That is, the ARI provides reduced adverse yaw and better roll response while the stability-axis yaw damper provides improved lateral-directional damping.

In order to further evaluate the effects of these two special control system features, the general ACM task described earlier was performed with and without the control features. Evaluation in such a task gives more insight into the effects of a given control system since the pilot has less time to compensate for stability and control deficiencies because the task requirements change rapidly. In general, the results obtained in this task further substantiated those obtained with the tasks previously described. In particular, removal of both systems (fig. 34(a)) resulted in a configuration which was prone to large sideslip excursions and oscillations. The tracking accuracy obtained was noticeably reduced as a result of these problems. The pilot commented that he was much less confident in the modified airplane since it exhibited general looseness and significant adverse yawing, which seemed to indicate an incipient nose slice, and was ineffective as a tracking platform. Attempting to maintain a good offensive position required considerably more attention than with the basic configuration. It is interesting to note here that the pilot rated this modified configuration lower in the ACM task than in the windup turn tracking as more problems became evident under the vigorous maneuvering conditions.

When only the ARI was removed, the modified configuration performed more like the basic airplane as shown in figure 34(b). However, the pilot was aware of β excursions and attempted to use his rudder pedals to correct them. Overall, the required control activity was increased to compensate for the adverse yaw, and the pilot managed to track about as well as with the basic configuration. Since the pilot did not notice the increased control activity as much in this ACM task as in the tracking task, he rated this modified configuration about the same as the basic airplane. It should be noted in this regard that the low-speed data for the present configuration indicate much less adverse yaw at high angles of attack than is the case for most current fighter airplanes.

When the stability-axis yaw damper was removed from the control system, the pilot's comments were much more unfavorable than when the ARI was removed. The results of a flight in this condition are presented in figure 34(c) and show significant oscillations in β , which are indicative of reduced damping. The reduced lateral-directional damping caused by the absence of the stability-axis yaw damper caused the pilot much more difficulty in this task than in the mild, windup turn tracking task. As a result, even though the pilot's tracking was comparable with that obtained with the basic airplane, the pilot rated this modified configuration the same as the airplane with neither special feature. Apparently, a pilot can compensate for a small amount of adverse yaw as long as lateral-directional damping is good, but he cannot adequately provide compensation for low damping in a rapidly changing maneuvering task. This result highlights the importance of evaluating airplanes not only in simple tracking tasks where time for compensa-

tion is available but also in vigorous, rapidly changing tasks where there is little time for pilot compensation of the airplane deficiencies.

INTERPRETATION OF RESULTS

Direct application of the present study results to the full-scale airplane is limited because of several study limitations. The present study was based on aerodynamic characteristics measured at low Mach number (test $M \cong 0.1$) and low Reynolds number ($N_{Re} = 0.8 \times 10^6$), and no adjustments were made for higher Reynolds number or Mach number. Past experience has established that variations in Mach number can have marked effects on aerodynamic stability and control characteristics for fighter airplanes. For example, results of reference 4 had to be modified for application to the full-scale airplane as flight tests indicated that the angle of attack for onset of adverse yaw due to differential tail deflection decreased with increasing Mach number above $M = 0.65$. It is therefore important that such effects as these be considered when systems are designed for actual airplanes. Furthermore, caution should be exercised in interpreting the simulation results obtained at angles of attack over 40° since some uncertainty exists as to the actual variation of C_m with α in the high-angle-of-attack regime for this configuration. However, relatively high confidence exists in the C_m data used below $\alpha = 40^\circ$. Finally, as has been noted earlier, the suitability of the side-stick controller used by this configuration could not be fully evaluated in the current simulation due to a lack of proper simulation of g forces in the cockpit. These limitations should be kept in mind in applying the following general study results.

The results of the present study have indicated that the control system for this prototype configuration causes the configuration to be very resistant to departure and spinning, as compared with current fighter airplanes. The use of such control systems allows the pilot to utilize the maximum maneuverability of an airplane without undue fear of control-induced departures and inadvertent spins; such systems, however, do not make the airplane spinproof. The implementation of these concepts on the present configuration and the airplane of reference 4 shows that the implementation of such control concepts is feasible within current control technology. The performance demonstrated in the simulation of this configuration is indicative of the fact that very good overall maneuverability and handling qualities for fighter airplanes can result from proper attention to high-angle-of-attack characteristics in airframe and control system design.

SUMMARY OF RESULTS

A piloted, fixed-base simulator investigation using a lightweight fighter prototype configuration has been conducted to evaluate the effectiveness of special automatic control

system features designed to enhance high-angle-of-attack maneuverability and handling qualities of fighter airplanes. The study used aerodynamic data based on tests of a 0.15-scale model at low Reynolds number (0.8×10^6) and low Mach number (approximately 0.1); therefore, the investigation cannot be considered a precise or complete representation of the full-scale airplane. The study produced the following results:

1. The basic configuration (with special control system features for high angle of attack) was highly maneuverable and was resistant to inadvertent departures or loss of control at high angles of attack and low values of Mach number.
2. The angle-of-attack/normal-acceleration limiting feature of the longitudinal control system was well tailored to permit maximum advantage to be taken of the good lateral-directional stability and control characteristics.
3. The aileron-rudder interconnect was found to significantly reduce adverse yaw at high angles of attack, which provided improved roll performance.
4. The stability-axis yaw damper also provided reduced adverse yaw and improved roll performance and, in addition, provided improvement in lateral-directional damping, which was quite apparent to the pilot at high angles of attack.
5. Whereas the absence of the stability-axis yaw damper proved to be only a nuisance to the pilot in the steady windup turn tracking task, its absence proved to be a severe handicap in the more vigorous and complex air-combat maneuvering tasks.
6. The basic configuration (with all special control features active) could not be forced to depart with conventional prospin controls (crossed controls), even in a highly accelerated stall entry.
7. The only maneuvers discovered which could overpower the angle-of-attack limiting system were low-speed maneuvers wherein the dynamic pressure was so low that control power was inadequate; these included (1) inertially coupled entries at high angles of attack, (2) aerodynamically coupled entries at high angles of attack and low speed, and (3) the classic vertical, or hammerhead, stall.
8. Use of an automatic control system designed to give good high-angle-of-attack handling characteristics and resistance to departure and spinning seemed to greatly improve the combat effectiveness of the simulated airplane.

Langley Research Center
National Aeronautics and Space Administration
Hampton, Va. 23665
March 11, 1976

APPENDIX A

DESCRIPTION OF CONTROL SYSTEM

Longitudinal

A block diagram of the longitudinal control system used in the simulation is presented in figure 35(a). The implementation was a fly-by-wire, command augmentation system whereby the pilot commanded normal acceleration through a minimum deflection, force-sensing side-stick controller. Washed-out pitch rate and filtered normal acceleration were fed back to give the desired response. A forward loop integration was used so that the steady-state acceleration response matched the commanded acceleration. The airplane was balanced to minimize trim drag, with the effect that it had essentially neutral static longitudinal stability at subsonic speeds; the desired static stability was provided artificially by the control system by means of angle-of-attack feedback.

The longitudinal control system also incorporated an angle-of-attack limiting system which functioned by using an α feedback to modify the pilot-commanded normal acceleration. The angle-of-attack feedback reduced the commanded normal-acceleration limit by 0.32g per degree between $\alpha = 15^\circ$ and 22.5° , and by 1.01g per degree above 22.5° . This feature resulted in an angle-of-attack limit in 1g flight of approximately 27° . The maximum allowable positive commanded normal acceleration is shown in figure 23. In addition, when α exceeded 30° , the system applied full nose-down control independent of pilot or feedback inputs. The reason for this feature was to inhibit the airplane from exceeding $\alpha = 30^\circ$ since the angle-of-attack sensor was limited to this value and, hence, no vital α information would be available to the control system at higher angles of attack. The stabilator actuator was modeled as a first-order lag of 0.05 sec with a rate limit of 60 deg/sec. The surface deflection limit was $\pm 25^\circ$.

The mathematical model used to simulate the activation of the leading-edge flap system is described in figure 35(b). The commanded flap deflection was scheduled with Mach number and angle of attack. Pitch rate was used to provide lead information. A schedule of the steady-state flap deflection is also indicated. The flap deflection varied linearly with α above a prescribed threshold value α_0 . The flap actuator was rate and position limited.

Lateral

The lateral control system is shown by the block diagram given in figure 35(c). The system incorporated a roll-rate command feature whereby the pilot commanded roll rates up to a maximum of 220 deg/sec through the force-sensing control stick. The schedule of roll-rate command as a function of force input was made asymmetric so that less force

APPENDIX A

was required to achieve a given roll rate to the right than to the left. Both the differential tail δ_D and the ailerons δ_a were deflected in response to the pilot's commands. The surface actuators were modeled as 0.05-sec first-order lags with rate limits of 60 deg/sec for the differential tail and 56 deg/sec for the ailerons. The surface deflection limits were $\pm 5^\circ$ and $\pm 20^\circ$ for the differential tail and the ailerons, respectively.

Directional

A block diagram of the directional control system used in the simulation is presented in figure 35(d). The pilot rudder input was computed directly from pedal force and was limited to $\pm 30^\circ$. Stability augmentation consisted of $r - p\alpha$ (r_{stab}) and a_Y feedbacks. The stability-axis yaw damper provided increased lateral-directional damping in addition to reducing sideslip during rolling maneuvers at high angles of attack. The lateral acceleration feedback provided increased directional stability, primarily at transonic and supersonic speeds, and therefore had little effect at subsonic speeds in the present investigation. The directional control system also incorporated an aileron-rudder interconnect (ARI) for improved coordination and roll performance. The ARI gain was scheduled as a linear function of angle of attack with a slope of 0.0375 per degree. Neither the stability augmentation system nor the ARI was authority limited. The rudder power actuator was modeled as a 0.05-sec first-order lag with a rate limit of 120 deg/sec. The total rudder travel was limited to $\pm 30^\circ$.

APPENDIX B

DESCRIPTION OF EQUATIONS AND DATA EMPLOYED IN SIMULATION SETUP

Equations of Motion

The equations used to describe the motions of the airplanes were nonlinear, six-degree-of-freedom, rigid-body equations referenced to a body-fixed axis system shown in figure 1 and are given as follows:

Forces:

$$\dot{u} = rv - qw - g \sin \theta + \frac{\bar{q}S}{m} C_{X,t} + \frac{T}{m}$$

$$\dot{v} = pw - ru + g \cos \theta \sin \phi + \frac{\bar{q}S}{m} C_{Y,t}$$

$$\dot{w} = qu - pv + g \cos \theta \cos \phi + \frac{\bar{q}S}{m} C_{Z,t}$$

Moments:

$$\dot{p} = \frac{I_Y - I_Z}{I_X} qr + \frac{I_{XZ}}{I_X} (\dot{r} + pq) + \frac{\bar{q}Sb}{I_X} C_{L,t}$$

$$\dot{q} = \frac{I_Z - I_X}{I_Y} pr + \frac{I_{XZ}}{I_Y} (r^2 - p^2) + \frac{\bar{q}S\bar{c}}{I_Y} C_{m,t}$$

$$\dot{r} = \frac{I_X - I_Y}{I_Z} pq + \frac{I_{XZ}}{I_Z} (\dot{p} - qr) + \frac{\bar{q}Sb}{I_Z} C_{n,t}$$

where the total aerodynamic coefficients $C_{X,t}$, $C_{Z,t}$, $C_{m,t}$, $C_{Y,t}$, $C_{n,t}$, and $C_{L,t}$ are defined in the next section. Euler angles were computed by using quaternions to allow continuity of attitude motions. Auxiliary equations included

$$\alpha = \tan^{-1} \left(\frac{w}{u} \right)$$

APPENDIX B

$$\beta = \sin^{-1} \left(\frac{v}{V} \right)$$

$$V = \sqrt{u^2 + v^2 + w^2}$$

$$a_n = \frac{qu - pv + g \cos \theta \cos \phi - \dot{w}}{g}$$

$$a_y = \frac{-pw + ru - g \cos \theta \sin \phi + \dot{v}}{g}$$

Aerodynamic Data

The aerodynamic data used in the simulation were derived from static and dynamic (forced oscillation) wind-tunnel force tests conducted with a 0.15-scale model of the present configuration in the Langley full-scale tunnel at low Reynolds number ($N_{Re} = 0.8 \times 10^6$) and low Mach number ($M \approx 0.1$). Special tests were made to measure such effects as the effects of horizontal tail position on pitch control power and on lateral-directional stability. The static aerodynamics were input in tabular form as functions of both angle of attack and sideslip over the ranges $-10^\circ \leq \alpha \leq 90^\circ$ and $-40^\circ \leq \beta \leq 40^\circ$.

The dynamic data were input in tabular form for $\beta = 0^\circ$ over the same α range. All aerodynamic coefficients are for $\delta_{lef} = 25^\circ$ unless otherwise indicated. Significant nonlinearities observed in the measured data were included. Total coefficient equations were used to sum the various aerodynamic contributions to a given force or moment coefficient as follows:

For the X-axis force coefficient

$$C_{X,t} = C_X(\alpha, \beta) + \Delta C_{X, sb}(\alpha) \left(\frac{\delta_{sb}}{60} \right) + \Delta C_{X, lef}(\alpha, \beta) \left(1 - \frac{\delta_{lef}}{25} \right) \\ + \frac{\bar{c}_q}{2V} \left[C_{X_q}(\alpha) + \Delta C_{X_q, lef}(\alpha) \left(1 - \frac{\delta_{lef}}{25} \right) \right] + \Delta C_{X, \delta_h}$$

where

$$\Delta C_{X, \delta_h} = \Delta C_{X, \delta_h = -10^\circ}(\alpha, \beta) + \left[\Delta C_{X, \delta_h = -25^\circ}(\alpha, \beta) - \Delta C_{X, \delta_h = -10^\circ}(\alpha, \beta) \right] \left(\frac{\delta_h + 10}{-15} \right) \\ (-25^\circ \leq \delta_h < -10^\circ)$$

APPENDIX B

$$\Delta C_{X, \delta_h} = \Delta C_{X, \delta_h = -10^\circ}(\alpha, \beta) \left(\frac{\delta_h}{-10} \right) \quad (-10^\circ \leq \delta_h < 0^\circ)$$

$$\Delta C_{X, \delta_h} = \Delta C_{X, \delta_h = 10^\circ}(\alpha, \beta) \left(\frac{\delta_h}{10} \right) \quad (0^\circ \leq \delta_h < 10^\circ)$$

and

$$\Delta C_{X, \delta_h} = \Delta C_{X, \delta_h = 10^\circ}(\alpha, \beta) + \left[\Delta C_{X, \delta_h = 25^\circ}(\alpha, \beta) - \Delta C_{X, \delta_h = 10^\circ}(\alpha, \beta) \right] \left(\frac{\delta_h - 10}{15} \right) \quad (10^\circ \leq \delta_h \leq 25^\circ)$$

For the Z-axis force coefficient

$$C_{Z, t} = C_Z(\alpha, \beta) + \Delta C_{Z, \delta_h} + \Delta C_{Z, sb}(\alpha) \left(\frac{\delta_{sb}}{60} \right) + \Delta C_{Z, lef}(\alpha, \beta) \left(1 - \frac{\delta_{lef}}{25} \right) \\ + \frac{\bar{c}_q}{2V} \left[C_{Zq}(\alpha) + \Delta C_{Zq, lef}(\alpha) \left(1 - \frac{\delta_{lef}}{25} \right) \right]$$

where

$$\Delta C_{Z, \delta_h} = \Delta C_{Z, \delta_h = -10^\circ}(\alpha, \beta) + \left[\Delta C_{Z, \delta_h = -25^\circ}(\alpha, \beta) - \Delta C_{Z, \delta_h = -10^\circ}(\alpha, \beta) \right] \left(\frac{\delta_h + 10}{-15} \right) \quad (-25^\circ \leq \delta_h < -10^\circ)$$

$$\Delta C_{Z, \delta_h} = \Delta C_{Z, \delta_h = -10^\circ}(\alpha, \beta) \left(\frac{\delta_h}{-10} \right) \quad (-10^\circ \leq \delta_h < 0^\circ)$$

$$\Delta C_{Z, \delta_h} = \Delta C_{Z, \delta_h = 10^\circ}(\alpha, \beta) \left(\frac{\delta_h}{10} \right) \quad (0^\circ \leq \delta_h < 10^\circ)$$

and

$$\Delta C_{Z, \delta_h} = \Delta C_{Z, \delta_h = 10^\circ}(\alpha, \beta) + \left[\Delta C_{Z, \delta_h = 25^\circ}(\alpha, \beta) - \Delta C_{Z, \delta_h = 10^\circ}(\alpha, \beta) \right] \left(\frac{\delta_h - 10}{15} \right) \quad (10^\circ \leq \delta_h \leq 25^\circ)$$

APPENDIX B

For the pitching-moment coefficient ($C_m(\alpha, \beta)$ selected to be C_m , $C_{m,1}$, or $C_{m,2}$ as desired)

$$C_{m,t} = C_m(\alpha, \beta) + C_{Z,t}(\mathbf{x}_{cg,ref} - \mathbf{x}_{cg}) + \Delta C_{m,\delta_h} + \Delta C_{m,lef}(\alpha, \beta) \left(1 - \frac{\delta_{lef}}{25}\right) \\ + \frac{\bar{c}_q}{2V} \left[C_{mq}(\alpha) + \Delta C_{mq,lef}(\alpha) \left(1 - \frac{\delta_{lef}}{25}\right) \right]$$

where

$$\Delta C_{m,\delta_h} = \Delta C_{m,\delta_h=-10^\circ}(\alpha, \beta) + \left[\Delta C_{m,\delta_h=-25^\circ}(\alpha, \beta) - \Delta C_{m,\delta_h=-10^\circ}(\alpha, \beta) \right] \left(\frac{\delta_h + 10}{-15} \right) \\ (-25^\circ \leq \delta_h < 10^\circ)$$

$$\Delta C_{m,\delta_h} = \Delta C_{m,\delta_h=-10^\circ}(\alpha, \beta) \left(\frac{\delta_h}{-10} \right) \quad (-10^\circ \leq \delta_h < 0^\circ)$$

$$\Delta C_{m,\delta_h} = \Delta C_{m,\delta_h=10^\circ}(\alpha, \beta) \left(\frac{\delta_h}{10} \right) \quad (0^\circ \leq \delta_h < 10^\circ)$$

and

$$\Delta C_{m,\delta_h} = \Delta C_{m,\delta_h=10^\circ}(\alpha, \beta) + \left[\Delta C_{m,\delta_h=25^\circ}(\alpha, \beta) - \Delta C_{m,\delta_h=10^\circ}(\alpha, \beta) \right] \left(\frac{\delta_h - 10}{15} \right) \\ (10^\circ \leq \delta_h \leq 25^\circ)$$

For the Y-axis force coefficient

$$C_{Y,t} = C_Y(\alpha, \beta) + \left[\Delta C_{Y,\delta_a=20^\circ}(\alpha, \beta) + \Delta C_{Y,\delta_a=20^\circ,lef}(\alpha, \beta) \left(1 - \frac{\delta_{lef}}{25}\right) \right] \left(\frac{\delta_a}{20} \right) \\ + \Delta C_{Y,\delta_D=5^\circ}(\alpha, \beta) \left(\frac{\delta_D}{5} \right) + \Delta C_{Y,\delta_r=30^\circ}(\alpha, \beta) \left(\frac{\delta_r}{30} \right) + \frac{b}{2V} \left\{ \left[C_{Y_r}(\alpha) \right. \right. \\ \left. \left. + \Delta C_{Y_r,lef}(\alpha) \left(1 - \frac{\delta_{lef}}{25}\right) \right] r + \left[C_{Y_p}(\alpha) + \Delta C_{Y_p,lef}(\alpha) \left(1 - \frac{\delta_{lef}}{25}\right) \right] p \right\}$$

APPENDIX B

For the yawing-moment coefficient

$$\begin{aligned}
 C_{n,t} = & C_n(\alpha, \beta) - C_{Y,t}(\mathbf{x}_{cg, ref} - \mathbf{x}_{cg}) \left(\frac{\bar{c}}{b} \right) + \Delta C_{n,lef}(\alpha, \beta) \left(1 - \frac{\delta_{1ef}}{25} \right) + \left[\Delta C_{n,\delta_a=20^\circ}(\alpha, \beta) \right. \\
 & + \Delta C_{n,\delta_a=20^\circ,lef}(\alpha, \beta) \left(1 - \frac{\delta_{1ef}}{25} \right) \left. \frac{\delta_a}{20} + \Delta C_{n,\delta_D=5^\circ}(\alpha, \beta) \left(\frac{\delta_D}{5} \right) + \Delta C_{n,\delta_r=30^\circ}(\alpha, \beta) \left(\frac{\delta_r}{30} \right) \right. \\
 & \left. + \Delta C_{n,\delta_h} + \frac{b}{2V} \left\{ \left[C_{n_r}(\alpha) + C_{n_r,lef}(\alpha) \left(1 - \frac{\delta_{1ef}}{25} \right) \right] r + \left[C_{n_p}(\alpha) + \Delta C_{n_p,lef}(\alpha) \left(1 - \frac{\delta_{1ef}}{25} \right) \right] p \right\} \right]
 \end{aligned}$$

where

$$\Delta C_{n,\delta_h} = \Delta C_{n,\delta_h=-25^\circ}(\alpha, \beta) \left(\frac{\delta_h}{-25} \right) \quad (-25^\circ \leq \delta_h < 0^\circ)$$

and

$$\Delta C_{n,\delta_h} = \Delta C_{n,\delta_h=25^\circ}(\alpha, \beta) \left(\frac{\delta_h}{25} \right) \quad (0^\circ \leq \delta_h \leq 25^\circ)$$

For the rolling-moment coefficient

$$\begin{aligned}
 C_{l,t} = & C_l(\alpha, \beta) + \Delta C_{l,lef}(\alpha, \beta) \left(1 - \frac{\delta_{1ef}}{25} \right) + \Delta C_{l,\delta_h} + \left[\Delta C_{l,\delta_a=20^\circ}(\alpha, \beta) \right. \\
 & + \Delta C_{l,\delta_a=20^\circ,lef}(\alpha, \beta) \left(1 - \frac{\delta_{1ef}}{25} \right) \left. \frac{\delta_a}{20} + \Delta C_{l,\delta_D=5^\circ}(\alpha, \beta) \left(\frac{\delta_D}{5} \right) + \Delta C_{l,\delta_r=30^\circ}(\alpha, \beta) \left(\frac{\delta_r}{30} \right) \right. \\
 & \left. + \frac{b}{2V} \left\{ \left[C_{l_r}(\alpha) + \Delta C_{l_r,lef}(\alpha) \left(1 - \frac{\delta_{1ef}}{25} \right) \right] r + \left[C_{l_p}(\alpha) + \Delta C_{l_p,lef}(\alpha) \left(1 - \frac{\delta_{1ef}}{25} \right) \right] p \right\} \right]
 \end{aligned}$$

where

$$\Delta C_{l,\delta_h} = \Delta C_{l,\delta_h=-25^\circ}(\alpha, \beta) \left(\frac{\delta_h}{-25} \right) \quad (-25^\circ \leq \delta_h < 0^\circ)$$

APPENDIX B

and

$$\Delta C_{l, \delta_h} = \Delta C_{l, \delta_h=25^\circ}(\alpha, \beta) \left(\frac{\delta_h}{25} \right) \quad (0^\circ \leq \delta_h \leq 25^\circ)$$

The aerodynamic coefficients contained in the preceding coefficient equations are presented in tables II to VII as functions of the indicated independent variables. The aerodynamic moment coefficients are referenced to a center-of-gravity location of $0.34\bar{c}$ and were corrected to the desired flight center-of-gravity position ($0.35\bar{c}$) in the coefficient equations.

Engine Simulation

The configuration was assumed to be powered by an afterburning turbofan jet engine. The thrust response to throttle inputs was computed by using the mathematical model indicated in figure 36(a). The response was modeled with a first-order lag which varied as shown in figure 36(c). The throttle command gearing is shown in figure 36(b). Presented in table VIII are thrust values for idle, military, and maximum thrust levels. The response of the engine to a step throttle command at $t = 0$ is shown in figure 36(d); the command was removed at $t = 6$ sec.

Buffet Characteristics

Aerodynamic buffeting of the airframe at high angles of attack was simulated by shaking the cockpit with a hydraulic mechanism. The buffet intensity and frequency content were controlled by the computer, with the buffet amplitude varying with angle of attack as shown in figure 37. The frequency content was controlled to represent the relative buffet amplitude contributions of the three primary structural modes of the airframe. The buffet levels employed represent moderate buffet and were derived from wind-tunnel tests of a 1/9-scale wind-tunnel model especially instrumented for this purpose. Buffet onset occurred near $\alpha = 15^\circ$, and the level of buffet increased fairly linearly thereafter with increasing angle of attack. The relatively high angle of attack for buffet onset made buffet onset a good angle-of-attack cue for the pilot.

Simulation of Blackout

Pilot blackout or "grayout" under sustained high values of normal acceleration was simulated by decreasing the brightness of the projected scene and the cockpit instruments as a function of the cumulative time spent at high load factors. At the same time, dimming of the target image was delayed relative to the scene in order to partially simulate tunnel vision for steady tracking maneuvers. This simulation of blackout provided a cue, in addi-

APPENDIX B

tion to the inflatable g-suit, of the extent of operation at high normal acceleration, and it penalized the pilot who flew at unrealistically high values of normal acceleration. The blackout representation assumed that a pilot will experience grayout if exposed to a value of normal acceleration greater than 5g and will tend to recover when returning to below this level. The algorithm used a direct relation between the logarithm of the load factor a_n and the logarithm of the time to blackout; the simulation used 300 sec to blackout at 5g and 10 sec to blackout at 9g, with simulated tunnel vision during the interim period.

REFERENCES

1. Chen, Robert T. N.; Newell, Fred D.; and Schelhorn, Arno E.: Development and Evaluation of an Automatic Departure Prevention System and Stall Inhibitor for Fighter Aircraft. AFFDL-TR-73-29, U.S. Air Force, Apr. 1973.
2. Lee, Robert E., Jr.; Sharp, Patrick S.; Winters, Charles P.; and Olsen, Richard W.: Evaluation of the F-111 Stall Inhibitor System/Landing Configuration Warning System/Adverse Yaw Compensation Modifications. FTC-TR-73-27, U.S. Air Force, July 1973. (Available from DDC as AD 913 532L.)
3. Gilbert, William P.; and Libbey, Charles E.: Investigation of an Automatic Spin-Prevention System for Fighter Airplanes. NASA TN D-6670, 1972.
4. Gilbert, William P.; Nguyen, Luat T.; and Van Gunst, Roger W.: Simulator Study of Applications of Automatic Departure- and Spin-Prevention Concepts to a Variable-Sweep Fighter Airplane. NASA TM X-2928, 1973.
5. Mechtly, E. A.: The International System of Units - Physical Constants and Conversion Factors (Second Revision). NASA SP-7012, 1973.
6. Ashworth, B. R.; and Kahlbaum, William M., Jr.: Description and Performance of the Langley Differential Maneuvering Simulator. NASA TN D-7304, 1973.
7. Moul, Martin T.; and Paulson, John W.: Dynamic Lateral Behavior of High-Performance Aircraft. NACA RM L58E16, 1958.
8. Greer, H. Douglas: Summary of Directional Divergence Characteristics of Several High-Performance Aircraft Configurations. NASA TN D-6993, 1972.
9. Moore, Frederick L.; Anglin, Ernie L.; Adams, Mary S.; Deal, Perry L.; and Person, Lee H., Jr.: Utilization of a Fixed-Base Simulator To Study the Stall and Spin Characteristics of Fighter Airplanes. NASA TN D-6117, 1971.

TABLE I. - MASS AND DIMENSIONAL CHARACTERISTICS USED IN SIMULATION

Weight, N (lb)	73 480 (16 519)
Moments of inertia, kg-m ² (slug-ft ²):	
I _X	12 662 (9339)
I _Y	53 147 (39 199)
I _Z	63 035 (46 492)
I _{XZ}	179 (132)
Wing dimensions:	
Span, m (ft)	8.84 (29.0)
Area, m ² (ft ²)	26.0 (280)
Mean aerodynamic chord, m (ft)	3.335 (10.94)
Surface deflection limits:	
Horizontal tail -	
Symmetric (δ_h), deg	±25
Differential (δ_D), deg	±5 per surface
Ailerons (flaperons), deg	±20
Rudder, deg	±30

TABLE II. - X-AXIS FORCE COEFFICIENT DATA USED IN SIMULATION

[All data are for $\delta_{1ef} = 25^\circ$ unless otherwise indicated](a) C_X

ALPHA	BETA												
	-40.0	-30.0	-20.0	-15.0	-10.0	-5.0	0.0	+5.0	+10.0	+15.0	+20.0	+30.0	+40.0
-10.0	-.09690	-.09460	-.09240	-.09130	-.09860	+.09920	-.09610	-.09720	-.09280	-.08970	-.08860	-.08630	-.08400
-5.0	-.07840	-.07940	-.08050	-.08100	-.08640	-.09220	-.09410	-.09050	-.08490	-.07520	-.07110	-.06290	-.05460
0.0	-.06410	-.06170	-.05930	-.05820	-.06600	-.06370	-.06650	-.06460	-.06200	-.05360	-.05470	-.05690	-.05920
+5.0	.00830	-.00370	-.01570	-.02170	-.01980	-.01760	-.02960	-.01850	-.01760	-.01460	-.00970	.00020	.01020
+10.0	-.00830	.00120	.01070	.01540	.01440	.01900	.02210	.02500	.02540	.02670	.02250	.01420	.00590
+15.0	.06440	.05920	.05400	.05140	.06400	.07070	.08280	.08280	.07580	.06840	.05380	.02460	-.00450
+20.0	.02550	.05850	.09160	.10810	.12030	.12470	.12190	.12980	.12370	.11310	.09920	.07140	.04370
+25.0	.13600	.13360	.13130	.13010	.13370	.13590	.13480	.14300	.14300	.13250	.12560	.11180	.09810
+30.0	.10460	.11240	.12020	.12400	.13470	.14490	.14600	.14980	.13510	.13200	.12560	.11280	.10010
+35.0	.13340	.11480	.13560	.12640	.13160	.14810	.15360	.14160	.12230	.11660	.11120	.12300	.12810
+40.0	.14440	.14020	.13000	.12210	.12650	.14320	.14540	.13770	.12870	.11500	.12180	.14370	.14520
+45.0	.13240	.13400	.12350	.11820	.12240	.13650	.13860	.12460	.12300	.11810	.11660	.12820	.12700
+50.0	.12550	.11690	.11200	.11150	.11260	.12550	.13110	.12020	.11130	.10960	.11230	.11860	.12140
+55.0	.12590	.11410	.11650	.11490	.11140	.11970	.12610	.11780	.10730	.11180	.11790	.10790	.12220
+60.0	.12200	.11530	.10700	.11310	.11180	.12160	.12920	.12600	.11070	.10920	.10240	.10730	.11520
+70.0	.10670	.09690	.08230	.08480	.07560	.08790	.08650	.08050	.07270	.07810	.08020	.08850	.09760
+80.0	.10750	.09440	.09080	.08630	.07830	.07940	.07720	.07600	.07500	.08430	.08840	.08950	.10460
+90.0	.12630	.10460	.09920	.09280	.08290	.08400	.08490	.08100	.08180	.09100	.09440	.09640	.11700

TABLE II.- Continued

(b) $\Delta C_{X, \delta_h} = -25^\circ$

		BETA											
ALPHA	-40.0	-30.0	-20.0	-15.0	-10.0	-5.0	0.0	+5.0	+10.0	+15.0	+20.0	+30.0	+40.0
-10.0	-.05600	-.05990	-.06370	-.06560	-.06190	-.06660	-.06570	-.06700	-.07140	-.07500	-.06960	-.05910	-.04850
-5.0	-.05860	-.05690	-.05510	-.05430	-.06130	-.06040	-.05810	-.05950	-.06150	-.06340	-.06410	-.06550	-.06700
0.0	-.05350	-.05490	-.05540	-.05700	-.05280	-.05320	-.04520	-.05140	-.05360	-.06050	-.05620	-.04760	-.03890
+5.0	-.06010	-.05850	-.05380	-.05600	-.05900	-.06130	-.04830	-.05630	-.05020	-.05660	-.05230	-.04360	-.03500
+10.0	-.01710	-.02990	-.04270	-.04910	-.05220	-.04980	-.05150	-.05750	-.05570	-.05660	-.05620	-.05540	-.05470
+15.0	-.05080	-.04840	-.04600	-.04480	-.05310	-.04410	-.05280	-.05500	-.05350	-.05840	-.05020	-.03400	-.01780
+20.0	.03680	.00140	-.03410	-.05180	-.04180	-.03510	-.02860	-.04110	-.04610	-.05380	-.04310	-.02180	-.00060
+25.0	-.00870	-.01810	-.02760	-.03230	-.03150	-.02660	-.02080	-.03180	-.04350	-.03990	-.03350	-.02090	-.00830
+30.0	.03020	.01010	-.01000	-.01990	-.01960	-.01600	-.00800	-.01980	-.03100	-.02060	-.03020	-.04930	-.06850
+35.0	.09850	.07300	.00810	-.03480	-.00340	-.00470	-.00260	-.00430	.00150	.00600	.00270	-.02730	-.05040
+40.0	-.01660	.02320	.02110	.01550	.01410	.00970	.01290	.02420	.02270	.02020	.00940	.02100	-.02360
+45.0	.01510	.01770	.03550	.03900	.03320	.02240	.02820	.03980	.03520	.02690	.03320	.02140	.02110
+50.0	.03590	.03360	.04620	.05000	.04690	.03790	.04120	.05220	.05500	.04290	.03360	.02900	.03660
+55.0	.03680	.04170	.04220	.05210	.05690	.05420	.06040	.04900	.06260	.03650	.02750	.03790	.03470
+60.0	.04110	.04640	.05530	.04760	.05550	.05150	.05710	.06120	.05790	.04220	.03680	.04230	.02770
+70.0	.05850	.06440	.07120	.06240	.07160	.06180	.06700	.07140	.07340	.05770	.06090	.05870	.06070
+80.0	.07380	.08430	.07610	.07420	.07300	.07250	.07770	.07610	.07560	.06540	.06450	.07180	.06670
+90.0	.07290	.08650	.08100	.08240	.08330	.07940	.07960	.08430	.08610	.07340	.07220	.08040	.06670

TABLE II. - Continued

(c) $\Delta C_X, \delta_h = -10^\circ$

		BETA												
ALPHA		-40.0	-30.0	-20.0	-15.0	-10.0	-5.0	0.0	+5.0	+10.0	+15.0	+20.0	+30.0	+40.0
-10.0		-.01490	-.01660	-.01810	-.01880	-.01380	-.01440	-.00990	-.01510	-.01240	-.01060	-.01410	-.02130	-.02840
-5.0		-.00250	-.00830	-.01400	-.01690	-.01550	-.01390	-.01780	-.01450	-.01080	-.01560	-.01620	-.01750	-.01900
0.0		-.02520	-.01900	-.01280	-.00960	-.01120	-.01650	-.01160	-.01160	.00040	-.01580	-.00250	.02420	.05090
+5.0		-.05190	-.03300	-.01410	-.00470	-.01440	-.01810	-.00650	-.01260	-.01310	-.00270	-.00500	-.00960	-.01430
+10.0		-.01450	-.01340	-.01220	-.01150	-.00560	-.00940	-.01060	-.01050	-.00380	-.00190	-.00260	-.00420	-.00580
+15.0		-.05250	-.03120	-.00990	.00080	-.01130	-.00020	-.00010	-.00440	-.01250	-.00190	-.00410	-.00850	-.01300
+20.0		.04640	.02410	.00160	-.00950	-.00830	-.00060	.00150	-.00430	-.00080	-.00420	-.00610	-.00980	-.01360
+25.0		.02010	.01240	.00460	.00080	.00120	.00470	.00600	-.00110	-.00480	-.00590	.00230	.01860	.03490
+30.0		-.00230	.00270	.00760	.01020	.00800	.01000	.01490	.00640	-.00030	.00690	.00430	-.00190	-.00630
+35.0		.05560	.05540	.01590	.01570	.01330	.01600	.01460	.01310	.01640	.02360	.02320	-.00060	-.01760
+40.0		-.01450	.02270	.02060	.01970	.02460	.02360	.03460	.03430	.03020	.03480	.01820	.03090	-.00560
+45.0		.01020	.01340	.02400	.03030	.02980	.01740	.02930	.03870	.03070	.03250	.03310	.02480	.02640
+50.0		.02310	.01700	.02770	.02740	.03180	.02510	.02630	.03330	.03640	.03610	.02840	.02570	.03390
+55.0		.01870	.01910	.01480	.02290	.02580	.02650	.02880	.01880	.02960	.02130	.01430	.02760	.02710
+60.0		.01490	.01880	.02070	.01540	.01760	.01500	.02360	.01830	.02010	.01300	.02860	.03040	.01600
+70.0		.02550	.02980	.03290	.02740	.03100	.02050	.03030	.02440	.03160	.03180	.03340	.03200	.03620
+80.0		.03680	.03530	.03480	.03660	.03670	.03380	.03900	.03970	.04080	.03870	.03900	.04000	.03840
+90.0		.03790	.03990	.04060	.04450	.04220	.04000	.03830	.04390	.04410	.04160	.04350	.04590	.04540

TABLE II. - Continued

(d) $\Delta C_X, \delta_h=10^\circ$

		BETA												
ALPHA		-40.0	-30.0	-20.0	-15.0	-10.0	- 5.0	0.0	+ 5.0	+10.0	+15.0	+20.0	+30.0	+40.0
-10.0	.01270	.00450	-.00350	-.00750	-.00320	-.00590	-.00720	-.00790	-.02710	-.00420	-.00200	.00230	.00660	
- 5.0	.00500	-.00020	-.00530	-.00790	-.01010	-.01010	-.00980	-.00900	-.00640	-.00930	-.00730	-.00330	.00060	
0.0	-.00340	-.00630	-.00920	-.01060	-.00460	-.01420	-.00760	-.01250	-.00510	-.00900	-.00840	-.00740	-.00630	
+ 5.0	-.06200	-.04140	-.02070	-.01040	-.01200	-.01810	-.00650	-.01110	-.00080	-.00850	-.01230	-.01990	-.02770	
+10.0	-.02890	-.02350	-.01810	-.01540	-.01500	-.01300	-.00820	-.01430	-.01620	-.01550	-.01680	-.01960	-.02230	
+15.0	-.03980	-.02940	-.01900	-.01380	-.01040	-.01940	-.02620	-.01840	-.02030	-.01480	-.01840	-.02580	-.03320	
+20.0	.02480	.03220	-.02340	-.03170	-.02600	-.02720	-.02550	-.03080	-.02520	-.02720	-.02370	-.01670	-.00990	
+25.0	-.01830	-.02260	-.02700	-.02910	-.03120	-.03460	-.03500	-.04020	-.03710	-.03890	-.03640	-.03150	-.02660	
+30.0	-.03110	-.02990	-.02870	-.02800	-.03450	-.03870	-.03580	-.03990	-.03150	-.03830	-.04210	-.04960	-.05720	
+35.0	.02330	.01770	-.02740	-.03030	-.03310	-.03350	-.03560	-.02960	-.02250	-.02220	-.02150	-.04330	-.05820	
+40.0	-.05020	-.02520	-.02540	-.02530	-.02510	-.03030	-.02500	-.02130	-.02650	-.01870	-.02390	-.01660	-.04880	
+45.0	-.03380	-.03160	-.02460	-.02450	-.02860	-.03510	-.02910	-.02260	-.02580	-.02060	-.01820	-.02170	-.02570	
+50.0	-.02670	-.02730	-.01750	-.02170	-.01800	-.02750	-.02100	-.01520	-.01480	-.01400	-.01410	-.01950	-.01570	
+55.0	-.03260	-.03270	-.02480	-.01900	-.01840	-.02260	-.01700	-.02780	-.01200	-.02150	-.02920	-.02310	-.02660	
+60.0	-.03860	-.03280	-.02210	-.02500	-.02780	-.02870	-.02330	-.02330	-.02360	-.02180	-.02080	-.02510	-.03840	
+70.0	-.03870	-.04100	-.03570	-.03060	-.00380	-.02130	.01650	-.00490	-.00210	-.03120	-.03360	-.03360	-.03190	
+80.0	-.03760	-.03940	-.03840	-.03280	-.03710	-.03840	-.03020	-.03420	-.03190	-.03290	-.03800	-.03690	-.03460	
+90.0	-.05360	-.04570	-.04000	-.03660	-.03480	-.03560	-.03600	-.03660	-.03340	-.03430	-.03890	-.04000	-.04500	

TABLE II. - Continued

(e) $\Delta C_{X, \delta_h=25^\circ}$

		BETA											
ALPHA	-40.0	-30.0	-20.0	-15.0	-10.0	- 5.0	0.0	+ 5.0	+10.0	+15.0	+20.0	+30.0	+40.0
-10.0	-.02430	-.03300	-.04150	-.04580	-.04910	-.05320	-.05810	-.05450	-.04770	-.04570	-.04190	-.03440	-.02690
- 5.0	-.03520	-.04110	-.04690	-.04990	-.05310	-.05360	-.05820	-.05640	-.05090	-.05210	-.05130	-.04960	-.04800
0.0	-.05100	-.05390	-.05690	-.05820	-.05280	-.05820	-.05780	-.06010	-.05510	-.05670	-.05240	-.04370	-.03490
+ 5.0	-.05370	-.05870	-.06380	-.06630	-.06620	-.06950	-.06440	-.06850	-.05870	-.06230	-.06460	-.06930	-.07410
+10.0	-.05380	-.05790	-.06200	-.06400	-.06210	-.07070	-.07580	-.07180	-.07550	-.06670	-.06740	-.06900	-.07060
+15.0	-.10010	-.08550	-.07090	-.06360	-.07750	-.07200	-.08250	-.08520	-.08170	-.07310	-.06270	-.04170	-.02090
+20.0	-.01960	-.04530	-.07120	-.08400	-.08450	-.09060	-.09800	-.10210	-.09080	-.09000	-.07970	-.05890	-.03820
+25.0	-.05420	-.06740	-.08070	-.08730	-.09610	-.10420	-.10950	-.11120	-.10530	-.09890	-.08860	-.06810	-.04780
+30.0	-.02290	-.04900	-.07500	-.08800	-.09940	-.10600	-.10730	-.10970	-.09910	-.09270	-.08920	-.08230	-.07550
+35.0	-.01850	-.02740	-.07580	-.08040	-.09710	-.10490	-.10640	-.09810	-.08800	-.07610	-.07180	-.08640	-.09410
+40.0	-.09680	-.06630	-.06980	-.07280	-.09290	-.09860	-.09390	-.09180	-.08750	-.07560	-.08100	-.06230	-.09040
+45.0	-.07890	-.08250	-.07570	-.07880	-.08440	-.09320	-.09080	-.08060	-.07970	-.07290	-.06640	-.07190	-.06880
+50.0	-.07060	-.07410	-.06710	-.07240	-.07050	-.08190	-.08090	-.07210	-.06850	-.06300	-.05960	-.06960	-.06140
+55.0	-.08140	-.08010	-.07660	-.06900	-.06660	-.07580	-.07160	-.07840	-.06130	-.06550	-.08000	-.07480	-.07580
+60.0	-.09460	-.08790	-.07330	-.07140	-.06220	-.07680	-.06870	-.06950	-.06880	-.06860	-.06970	-.07910	-.09900
+70.0	-.10400	-.10430	-.09140	-.08660	-.04410	-.05080	-.03840	-.02860	-.04060	-.08640	-.09380	-.09000	-.09640
+80.0	-.10840	-.10840	-.10640	-.09910	-.10060	-.10340	-.09940	-.03990	-.09790	-.10440	-.10770	-.09720	-.10240
+90.0	-.11960	-.10550	-.11130	-.10930	-.09990	-.10220	-.10370	-.10070	-.09730	-.10340	-.10940	-.09700	-.10990

TABLE II. - Continued

(f) $\Delta C_{X,lef}$

		BETA											
ALPHA	-40.0	-30.0	-20.0	-15.0	-10.0	- 5.0	0.0	+ 5.0	+10.0	+15.0	+20.0	+30.0	+40.0
-10.0	.05510	.06140	.06780	.07100	.08060	.07850	.07450	.07680	.07550	.07110	.06810	.06210	.05610
- 5.0	.04030	.04830	.05630	.06030	.06390	.06930	.06970	.06770	.06440	.05590	.05060	.04000	.02930
0.0	.03880	.03880	.03880	.03890	.04640	.04270	.04360	.04540	.04340	.03870	.03650	.03220	.02790
+ 5.0	-.03500	-.01420	.00700	.01750	.01500	.01160	.02450	.01440	.01490	.01580	.00790	-.00800	-.02410
+10.0	.00600	.00090	-.00410	-.00660	-.00560	-.01100	-.01280	-.01450	-.01300	-.01250	-.00980	-.00460	.00060
+15.0	-.05320	-.04580	-.03840	-.03470	-.04720	-.05360	-.06710	-.06450	-.05670	-.04630	-.03570	-.01440	.00680
+20.0	-.00590	-.03870	-.07170	-.08810	-.09810	-.10250	-.10280	-.10700	-.09910	-.09380	-.08320	-.06210	-.04110
+25.0	-.10650	-.10820	-.11010	-.11100	-.11440	-.11300	-.11130	-.11760	-.12420	-.12290	-.11400	-.09610	-.07840
+30.0	-.12440	-.11700	-.10960	-.10580	-.11610	-.11930	-.11870	-.12750	-.11960	-.12270	-.11220	-.09130	-.07050
+35.0	-.10030	-.08850	-.11600	-.11010	-.10540	-.11830	-.12340	-.11440	-.09770	-.09670	-.09050	-.10120	-.10500
+40.0	-.10420	-.10380	-.10010	-.10020	-.09630	-.10840	-.10850	-.10210	-.09790	-.08740	-.09550	-.09960	-.09920
+45.0	-.08420	-.09490	-.09110	-.08740	-.08800	-.10490	-.10230	-.08780	-.09210	-.08930	-.08320	-.08400	-.07420
+50.0	-.07370	-.08180	-.07560	-.07740	-.07600	-.09000	-.08770	-.07860	-.07490	-.07130	-.07390	-.07910	-.06670
+55.0	-.07950	-.08140	-.08270	-.07510	-.07490	-.08260	-.07520	-.08150	-.06990	-.07370	-.08460	-.07490	-.07310
+60.0	-.08250	-.07760	-.07390	-.07510	-.07110	-.07670	-.07220	-.07040	-.07150	-.07370	-.06970	-.07060	-.08270
+70.0	-.07290	-.07280	-.06570	-.07060	-.06310	-.07230	-.06730	-.06680	-.05950	-.06400	-.06510	-.07030	-.06520
+80.0	-.06610	-.06410	-.06260	-.05850	-.05560	-.05600	-.05260	-.05250	-.05290	-.05720	-.06130	-.06030	-.06400
+90.0	-.06960	-.06220	-.05810	-.05710	-.04920	-.05180	-.05210	-.04930	-.04910	-.05440	-.05760	-.05760	-.06290

TABLE II. - Concluded

(g) $\Delta C_{Xq, \text{lef}}$, $\Delta C_{X, \text{sb}}$, and C_{Xq}

α , deg	$\Delta C_{Xq, \text{lef}}$	$\Delta C_{X, \text{sb}}$	C_{Xq}
-10.0	-1.2200	-.0490	.9530
- 5.0	-1.6600	-.0498	1.5500
0.0	-1.6200	-.0500	1.9000
+ 5.0	-1.5800	-.0498	2.4600
+10.0	-1.9600	-.0493	2.9200
+15.0	-2.5100	-.0483	3.3000
+20.0	-2.0400	-.0470	2.7600
+25.0	-1.6400	-.0453	2.0500
+30.0	-.8240	-.0433	1.5000
+35.0	-.8170	-.0410	1.4900
+40.0	-1.1000	-.0383	1.8300
+45.0	-.5500	-.0354	1.2100
+50.0	0.0000	-.0322	1.3300
+55.0	0.0000	-.0287	1.6100
+60.0	0.0000	-.0250	.9100
+70.0	0.0000	-.0171	3.4300
+80.0	0.0000	-.0087	.6170
+90.0	0.0000	0.0000	.2730

TABLE III.- Z-AXIS FORCE COEFFICIENT DATA USED IN SIMULATION

[All data are for $\delta_{1ef} = 25^\circ$ unless otherwise indicated]

(a) C_z

		BETA												
ALPHA		-40.0	-30.0	-20.0	-15.0	-10.0	- 5.0	0.0	+ 5.0	+10.0	+15.0	+20.0	+30.0	+40.0
-10.0	.77790	.74200	.70610	.68810	.73160	.71950	.72070	.68260	.66210	.63240	.62000	.59500	.57010	
- 5.0	.55000	.49120	.43230	.40290	.38820	.39010	.41130	.37040	.33490	.27140	.30060	.35890	.41720	
0.0	.31170	.21030	.10900	.05830	.05220	.02090	.02630	.02030	.03770	-.02280	.01390	.08720	.16060	
+ 5.0	-.36190	-.33580	-.30960	-.29660	-.31430	-.36840	-.32390	-.35730	-.31930	-.31950	-.35150	-.41550	-.47940	
+10.0	-.45410	-.53270	-.61140	-.65070	-.66450	-.71080	-.73180	-.70840	-.69850	-.67990	-.66630	-.63920	-.61220	
+15.0	-.97290	-.96590	-.95900	-.95550	-1.03740	-1.06970	-1.12300	-1.06350	-1.01760	-.99950	-.95430	-.86390	-.77350	
+20.0	-.78780	-1.01990	-1.25210	-1.36810	-1.43800	-1.44850	-1.41160	-1.40460	-1.33650	-1.32060	-1.29960	-1.25780	-1.21600	
+25.0	-1.30650	-1.45220	-1.59790	-1.67080	-1.70760	-1.75550	-1.77360	-1.72100	-1.67680	-1.60490	-1.57170	-1.50540	-1.43910	
+30.0	-1.75500	-1.79340	-1.83180	-1.85100	-1.94680	-2.05790	-2.09190	-2.04050	-1.93810	-1.80810	-1.76440	-1.67690	-1.58950	
+35.0	-1.78320	-1.88980	-2.01670	-2.05370	-2.17250	-2.27260	-2.31340	-2.25590	-2.13380	-2.01540	-1.88030	-1.86080	-1.65170	
+40.0	-1.90350	-2.00720	-2.13440	-2.18280	-2.30620	-2.41940	-2.45460	-2.40330	-2.30660	-2.11940	-2.08640	-1.92980	-1.79100	
+45.0	-1.86900	-2.02380	-2.16590	-2.25420	-2.35070	-2.50450	-2.50270	-2.38520	-2.30640	-2.20000	-2.09620	-1.93690	-1.76550	
+50.0	-1.86060	-1.97790	-2.14480	-2.20660	-2.33510	-2.48980	-2.51180	-2.36850	-2.28090	-2.15260	-2.11870	-1.89950	-1.72290	
+55.0	-1.89400	-2.04080	-2.16660	-2.21910	-2.28160	-2.34870	-2.42930	-2.35680	-2.20910	-2.19190	-2.11500	-1.90050	-1.74350	
+60.0	-1.95650	-2.10930	-2.16530	-2.24000	-2.23900	-2.38290	-2.41530	-2.34280	-2.21170	-2.14260	-2.09190	-1.96130	-1.82690	
+70.0	-1.97540	-2.16310	-2.20650	-2.24630	-2.19870	-2.24580	-2.22680	-2.21100	-2.17090	-2.16260	-2.14440	-2.01090	-1.78170	
+80.0	-2.05370	-2.21950	-2.32660	-2.28350	-2.28540	-2.22150	-2.20900	-2.17480	-2.21240	-2.23470	-2.25830	-2.07760	-1.89510	
+90.0	-2.19280	-2.24020	-2.34800	-2.29020	-2.21240	-2.21780	-2.22050	-2.20500	-2.19620	-2.21910	-2.25690	-2.08680	-1.97670	

TABLE III.- Continued

(b) $\Delta C_Z, \delta_h = -25^\circ$

		BETA												
ALPHA		-40.0	-30.0	-20.0	-15.0	-10.0	- 5.0	0.0	+ 5.0	+10.0	+15.0	+20.0	+30.0	+40.0
-10.0	.03950	.08890	.13830	.16300	.15740	.20450	.19170	.22860	.24910	.20660	.18280	.13530	.08770	
- 5.0	.13910	.12490	.11080	.10370	.20050	.18650	.13810	.17600	.20940	.20500	.16490	.08480	.00470	
0.0	.17810	.18160	.18500	.18680	.18050	.17100	.12710	.17770	.13270	.19360	.17760	.14570	.11370	
+ 5.0	.30920	.27470	.24000	.22280	.22630	.25680	.18970	.21800	.13780	.15830	.14820	.12800	.10770	
+10.0	.13860	.16110	.18360	.19480	.21310	.22020	.22990	.24380	.21200	.19010	.18270	.16810	.15350	
+15.0	.48450	.37630	.26830	.21420	.27130	.24000	.30150	.26000	.20240	.25140	.21350	.13780	.06210	
+20.0	-.09160	.07350	.23870	.32130	.27790	.25040	.23680	.26130	.22780	.24820	.21760	.15640	.09530	
+25.0	.06200	.14790	.23380	.27680	.28030	.27720	.27440	.25170	.25760	.26550	.21550	.11550	.01560	
+30.0	.08560	.17250	.25940	.30290	.29670	.31960	.27760	.29560	.30230	.21470	.20850	.19620	.18390	
+35.0	-.12430	.03410	.21280	.27570	.31380	.34450	.31040	.31480	.24460	.23670	.20700	.39830	.40000	
+40.0	.40790	.21510	.27430	.33760	.33820	.39620	.40940	.36370	.36930	.24810	.37620	.17220	.38680	
+45.0	.28910	.21890	.19250	.24520	.28010	.38350	.40910	.34210	.35630	.28270	.15830	.15390	.30680	
+50.0	.16160	.21530	.22260	.19080	.28520	.39780	.36720	.24960	.23720	.11030	.24780	.20240	.14010	
+55.0	.13930	.20900	.26920	.24810	.23830	.20480	.24210	.31160	.18670	.24260	.26820	.18200	.10230	
+60.0	.14070	.23450	.20450	.28960	.19510	.28380	.29190	.19790	.19860	.18780	.23630	.18780	.22540	
+70.0	.15080	.16930	.14240	.18930	.11610	.21790	.18020	.17710	.16980	.16110	.16350	.13320	.07670	
+80.0	.09570	.10490	.17450	.15580	.17270	.13150	.18840	.17180	.14550	.10930	.16960	.12410	.07910	
+90.0	.22210	.16020	.17490	.12980	.10700	.14530	.16160	.14830	.10340	.06410	.14770	.09040	.15840	

TABLE III. - Continued

(c) $\Delta C_Z, \delta_h = -10^\circ$

		BETA											
ALPHA	-40.0	-30.0	-20.0	-15.0	-10.0	- 5.0	0.0	+ 5.0	+10.0	+15.0	+20.0	+30.0	+40.0
-10.0	-.05130	.01000	.07130	.10200	.07950	.11360	.08230	.12440	.07500	.06700	.10860	.19190	.27520
- 5.0	-.05910	.00560	.07050	.10290	.12430	.08200	.08270	.11090	.09480	.16430	.13540	.07760	.01970
0.0	.10540	.09160	.07770	.07080	.10700	.14560	.10040	.11760	-.00010	.18660	.06870	-.16690	-.40270
+ 5.0	.37960	.25500	.13030	.06810	.12580	.15030	.09180	.11870	.11310	.06940	.08980	.13080	.17160
+10.0	.32230	.23530	.14840	.10500	.06880	.11380	.11830	.09470	.06670	.08710	.08050	.06750	.05460
+15.0	.50780	.32950	.15130	.06210	.13250	.08000	.08680	.07260	.11520	.10410	.09630	.08060	.06490
+20.0	-.23600	-.07430	.08740	.16820	.16660	.09800	.10320	.09780	.04610	.11000	.14790	.22390	.29990
+25.0	-.12740	-.03040	.06650	.11510	.11910	.09190	.12670	.09620	.10350	.13470	.09770	.02390	-.05000
+30.0	.03320	.06140	.08950	.10360	.10480	.12720	.10340	.11880	.11360	.09280	.09780	.10780	.11800
+35.0	-.01880	.01690	.07290	.07440	.11590	.11150	.10290	.12100	.09550	.07870	.05230	.25030	.25860
+40.0	.37370	.11240	.15290	.17320	.15350	.18950	.15850	.16290	.17670	.14160	.25110	.12410	.34400
+45.0	.20960	.11300	.10220	.10120	.11350	.23830	.16400	.17390	.18930	.16760	.05400	.12670	.24170
+50.0	.09280	.10800	.13410	.11390	.13870	.22410	.22920	.14090	.11000	.06180	.16710	.13990	.08740
+55.0	.08760	.16570	.20730	.17690	.16200	.09810	.16390	.17350	.12730	.20510	.23320	.13090	.05820
+60.0	.13400	.14900	.16770	.23110	.17870	.20250	.15740	.18620	.12930	.19760	.14970	.11600	.20180
+70.0	.09690	.13760	.10190	.12890	.08980	.17470	.10720	.19350	.14160	.10720	.12260	.09880	.06130
+80.0	.02000	.12890	.12590	.10590	.11670	.11760	.08840	.07080	.07150	.08900	.13490	.10290	.04520
+90.0	.14400	.07270	.10560	.05970	.05380	.10260	.14210	.06370	.06990	.09850	.09070	.07350	.12720

TABLE III.- Continued

(d) $\Delta C_Z, \delta_h=10^\circ$

		BETA												
ALPHA		-40.0	-30.0	-20.0	-15.0	-10.0	- 5.0	0.0	+ 5.0	+10.0	+15.0	+20.0	+30.0	+40.0
-10.0		-.21930	-.15560	-.09180	-.05990	-.12670	-.12790	-.11140	-.09020	-.10590	-.06950	-.13690	-.27140	-.40600
- 5.0		-.34080	-.22800	-.11510	-.05860	-.06220	-.09140	-.12870	-.09490	-.09190	-.03930	-.10240	-.22860	-.35480
0.0		-.22100	-.17830	-.13570	-.11430	-.14260	-.08510	-.12700	-.08340	-.14250	-.09220	-.08690	-.07620	-.06550
+ 5.0		.21790	.08320	-.05160	-.11890	-.12720	-.07850	-.12100	-.12300	-.20180	-.16590	-.12790	-.05180	.02410
+10.0		.04670	-.02100	-.08860	-.12240	-.12760	-.12690	-.16960	-.14420	-.12930	-.13910	-.11590	-.06930	-.02260
+15.0		.12780	.02070	-.08630	-.13980	-.16090	-.10910	-.07230	-.16010	-.13350	-.15120	-.12700	-.07850	-.03010
+20.0		-.38570	-.24880	-.11180	-.04340	-.08300	-.10090	-.12660	-.13800	-.17430	-.11830	-.10050	-.06450	-.02850
+25.0		-.11280	-.09400	-.07510	-.06560	-.14450	-.12640	-.09960	-.14400	-.14400	-.08000	-.08630	-.09870	-.11110
+30.0		.05020	-.01150	-.07320	-.10400	-.09400	-.09060	-.11790	-.10540	-.11020	-.09590	-.06460	-.00210	.06050
+35.0		-.08820	-.08190	-.05530	-.06840	-.09950	-.14120	-.14840	-.13820	-.12130	-.07510	-.08570	.14400	.18400
+40.0		.26300	-.01590	.04760	.04340	-.00740	-.04040	-.06900	-.05640	-.01750	.01300	.08010	.02810	.24970
+45.0		.12250	.01570	.01590	-.00660	.03800	.03890	-.03290	.01980	.04460	.06170	.01020	-.00500	.17190
+50.0		.02780	-.02120	.01250	.03560	.02380	.09970	.06650	-.02650	.02080	-.06920	.05040	.01860	.04550
+55.0		.01440	.05200	.02630	.00680	.04330	-.00280	.02130	.09050	-.02750	.07420	.07420	.01840	-.00850
+60.0		.05670	.05710	.02960	.06780	.03140	.06880	.02270	.03110	-.00660	.02360	.04490	.05280	.11330
+70.0		.02740	.08870	.04300	.07500	-.05800	.02000	-.13370	-.03250	-.03850	.07570	.10370	.05650	.00260
+80.0		-.00280	.05500	.08280	.01600	.09710	.06950	.06430	.03330	.04710	.03610	.10790	.07230	.03060
+90.0		.14070	.08900	.11810	.07050	.03430	.05490	.08310	.07020	.07670	.02810	.11270	.08250	.12090

TABLE III. - Continued

(e) $\Delta C_Z, \delta_h=25^\circ$

		BETA												
ALPHA		-40.0	-30.0	-20.0	-15.0	-10.0	- 5.0	0.0	+ 5.0	+10.0	+15.0	+20.0	+30.0	+40.0
-10.0		-.47340	-.36330	-.25310	-.19800	-.21810	-.22550	-.24960	-.19600	-.21050	-.17480	-.23130	-.34400	-.45690
- 5.0		-.44850	-.34410	-.23960	-.18740	-.20010	-.22770	-.24130	-.19370	-.17860	-.12990	-.21980	-.39960	-.57930
0.0		-.17760	-.18270	-.18800	-.19050	-.18280	-.17940	-.20710	-.16650	-.20000	-.17750	-.18440	-.19790	-.21150
+ 5.0		-.01010	-.07000	-.13000	-.15990	-.19620	-.15340	-.19700	-.16780	-.22950	-.21330	-.13120	.03290	.19700
+10.0		.01270	-.07810	-.16870	-.21410	-.25400	-.22820	-.17940	-.21290	-.15880	-.20230	-.17690	-.12600	-.07490
+15.0		.44280	.17810	-.08650	-.21880	-.16360	-.21320	-.14550	-.17770	-.20530	-.17960	-.18360	-.19160	-.19960
+20.0		-.12450	-.11350	-.10250	-.09700	-.14800	-.17920	-.22350	-.18250	-.22670	-.13460	-.09990	-.03040	.03920
+25.0		-.07120	-.07840	-.08570	-.08930	-.14480	-.15300	-.15820	-.17490	-.17120	-.11440	-.10320	-.08060	-.05800
+30.0		-.19960	-.15470	-.10970	-.08720	-.10380	-.14530	-.16210	-.13260	-.15890	-.17180	-.08530	.08750	.26050
+35.0		.07710	.00910	-.03860	-.08890	-.10610	-.12090	-.11680	-.09680	-.14980	-.19910	-.09490	.18420	.27370
+40.0		.26120	.04140	.04230	.03900	.03000	-.01010	-.00810	-.02130	.00470	-.00940	.14810	-.00400	.26000
+45.0		.15610	.04640	.02320	.04030	.02080	.06350	.06440	.00320	.02550	.05460	-.04260	.03640	.17120
+50.0		.04900	-.03040	.00890	-.00110	-.00950	.10880	.06550	.01830	.03840	-.05820	.00180	.01170	.04820
+55.0		.04570	.02930	.04520	.00580	.01180	-.05200	.02130	.04810	-.04510	-.00070	.07350	.03490	.00510
+60.0		.08360	.07230	.02180	.04460	-.01460	.06490	.03450	-.01950	-.02990	-.00840	.02590	.03770	.17580
+70.0		.07550	.11640	.04780	.08200	-.05590	-.11130	-.12560	-.12540	-.06180	.05650	.10930	.05050	.04390
+80.0		.10360	.13400	.13010	.07680	.13380	.08300	.10490	-.13150	.09370	.07440	.13540	.08470	.12900
+90.0		.24150	.13890	.15000	.09800	.09130	.07990	.07150	.10990	.06620	.07300	.08980	.10890	.20090

TABLE III.- Continued

(f) $\Delta C_{Z,lef}$

		BETA											
ALPHA	-40.0	-30.0	-20.0	-15.0	-10.0	- 5.0	0.0	+ 5.0	+10.0	+15.0	+20.0	+30.0	+40.0
-10.0	.22200	.14910	.07620	.03990	.03490	.01800	-.01990	-.02880	.01580	.01390	-.01070	-.05970	-.10880
- 5.0	-.16500	-.10430	-.04350	-.01310	-.02730	-.04550	-.10300	-.09940	-.02390	.04360	-.01120	-.12060	-.23010
0.0	-.29960	-.20060	-.10170	-.05220	-.06630	-.03460	-.07110	-.10220	-.08750	-.04090	-.04930	-.06610	-.08300
+ 5.0	.39250	.20530	.01790	-.07560	-.04760	-.01880	-.10510	-.04510	-.08210	-.08870	-.01230	.14070	.29350
+10.0	.01630	-.01990	-.05600	-.07410	-.10280	-.04320	-.05780	-.07320	-.07030	-.09070	-.09020	-.08910	-.08790
+15.0	.09470	.01460	-.06540	-.10550	-.05830	-.04180	.00210	-.05430	-.07310	-.08390	-.13720	-.24390	-.35050
+20.0	-.17900	-.11240	-.04570	-.01240	.03670	.01940	-.00700	-.02430	-.08620	-.11080	-.07480	-.00280	.06920
+25.0	-.17790	-.06710	.04380	.09920	.10690	.07880	.07610	.01820	.02760	.00840	.03890	.09990	.16080
+30.0	.03220	.06870	.10520	.12350	.14920	.13880	.12230	.12420	.06070	.06500	.09090	.14260	.19440
+35.0	.16890	.13920	.12980	.09870	.09670	.13240	.12520	.11480	.00500	.05340	.05550	.31060	.37610
+40.0	.30770	.11500	.08860	.16850	.12220	.16180	.14670	.18410	.15610	.13290	.24120	.10300	.28210
+45.0	.15900	.15600	.04610	.13430	.12710	.18460	.17060	.09070	.14170	.14530	.06920	.09440	.20630
+50.0	.05550	.11310	.14950	.07230	.13020	.19560	.17390	.05880	.12200	.03070	.16910	.07360	.04050
+55.0	.03040	.08140	.15640	.12710	.15100	.09520	.08190	.12650	.04080	.14820	.18310	.05520	.00180
+60.0	.07140	.12840	.11490	.16360	.09140	.12050	.07100	.08570	.05980	.06290	.11300	.05350	.11990
+70.0	.05690	.07150	.05690	.08660	.07070	.11920	.08090	.10400	.07920	.04940	.08620	.06500	.02910
+80.0	.04490	.11400	.09060	.05990	.10950	.08120	.05110	.05380	.06000	.07140	.10620	.10730	.08850
+90.0	.15890	.12440	.09950	.04560	.06730	.07690	.10060	.09000	.05240	.07000	.10800	.11810	.14240

TABLE III.- Concluded

(g) C_{Zq} , $\Delta C_{Zq,lef}$, and $\Delta C_{Z,sb}$

α , deg	C_{Zq}	$\Delta C_{Zq,lef}$	$\Delta C_{Z,sb}$
-10.0	-23.9000	15.1000	.0087
- 5.0	-29.5000	3.7000	.0044
0.0	-29.5000	.6000	0.0000
+ 5.0	-30.5000	-1.3000	-.0044
+10.0	-31.3000	-.3000	-.0087
+15.0	-29.1000	-3.8000	-.0130
+20.0	-27.7000	-4.6000	-.0171
+25.0	-28.2000	-.2000	-.0212
+30.0	-29.0000	-2.7000	-.0250
+35.0	-29.8000	-3.5000	-.0287
+40.0	-38.3000	-1.3000	-.0322
+45.0	-35.3000	-.6500	-.0354
+50.0	-32.3000	0.0000	-.0383
+55.0	-27.2000	0.0000	-.0410
+60.0	-25.2000	0.0000	-.0433
+70.0	-23.7000	0.0000	-.0470
+80.0	-9.3500	0.0000	-.0493
+90.0	-2.1600	0.0000	-.0500

TABLE IV.- PITCHING-MOMENT COEFFICIENT DATA USED IN SIMULATION

[All data are for $\delta_{lef} = 25^\circ$ unless otherwise indicated](a) C_m

		BETA												
ALPHA		-40.0	-30.0	-20.0	-15.0	-10.0	- 5.0	0.0	+ 5.0	+10.0	+15.0	+20.0	+30.0	+40.0
-10.0		.12540	.07480	.02420	-.00110	-.03140	-.04520	-.04420	-.05030	-.03090	-.00810	.00880	.04250	.07630
- 5.0		.06830	.03630	.00430	-.01170	-.03190	-.04450	-.05100	-.04900	-.03830	-.01490	-.00850	.00420	.01690
0.0		-.00230	-.00980	-.01730	-.02110	-.03160	-.02750	-.02500	-.02930	-.03230	-.01980	-.01820	-.01490	-.01170
+ 5.0		-.03090	-.02540	-.01990	-.01710	-.02220	-.01660	-.01820	-.01800	-.02100	-.01750	-.01510	-.01030	-.00550
+10.0		-.02570	-.02420	-.02270	-.02200	-.02130	-.01680	-.01480	-.01440	-.01790	-.01730	-.00630	.01570	.03770
+15.0		-.06320	-.04790	-.03250	-.02480	-.02380	-.01870	-.00930	-.00980	-.01820	-.01980	-.00450	.02610	.05670
+20.0		-.13830	-.08990	-.04150	-.01730	-.01360	-.01010	-.01260	-.01060	-.01810	-.00420	.00610	.02680	.04740
+25.0		-.15960	-.09900	-.03840	-.00810	-.01400	-.01550	-.01220	-.01180	-.00830	-.02930	-.00100	.05550	.11210
+30.0		.07750	.04040	.00320	-.01530	-.01720	-.02010	-.01080	-.00540	.01580	.00910	.00440	-.00510	-.01460
+35.0		.30910	.19300	.04880	-.00990	-.02350	-.03670	-.02570	-.02270	.00140	-.00250	-.00550	.22770	.30090
+40.0		.25320	.19710	.03770	-.00980	-.00330	-.02970	-.04280	-.00550	-.00480	.00220	.01620	.22160	.28130
+45.0		.31030	.24710	.12830	.01190	.00050	.03220	.01520	-.01740	.02460	.03330	.15650	.27110	.33840
+50.0		.29380	.21650	.17250	.10110	.01690	.07360	.08040	.07280	.03960	.12290	.20840	.19290	.21590
+55.0		.15500	.06140	.10720	.14240	.03070	.05680	.07700	.03610	.05050	.11840	.13410	.02960	.08320
+60.0		.00250	-.05310	-.08760	-.06180	-.03710	.00870	.05910	.06640	.01150	-.00060	-.07990	-.05470	-.02590
+70.0		-.20060	-.27540	-.32340	-.29800	-.30540	-.26030	-.26610	-.28400	-.32720	-.31040	-.33290	-.30380	-.23300
+80.0		-.45360	-.47650	-.47210	-.45820	-.47250	-.44510	-.42200	-.45250	-.47710	-.45650	-.47690	-.47890	-.47520
+90.0		-.60570	-.60360	-.59740	-.58860	-.59780	-.58780	-.58490	-.59800	-.59750	-.60010	-.59120	-.59100	-.59160

TABLE IV.- Continued

(b) $\Delta C_{m, \delta_h} = -25^\circ$

		BETA												
At PHA		-40.0	-30.0	-20.0	-15.0	-10.0	- 5.0	0.0	+ 5.0	+10.0	+15.0	+20.0	+30.0	+40.0
-10.0	.09090	.12740	.16390	.18210	.20980	.22530	.24570	.23070	.21130	.19300	.18180	.15950	.13700	
- 5.0	.10060	.13770	.17490	.19350	.21620	.21580	.20710	.21910	.22290	.19850	.19700	.19420	.19130	
0.0	.16380	.17950	.19520	.20310	.20470	.19500	.19410	.19990	.21100	.20920	.20310	.19070	.17840	
+ 5.0	.22460	.21650	.20840	.20430	.20390	.19780	.21420	.20980	.20900	.21750	.21700	.21600	.21510	
+10.0	.22140	.22500	.22860	.23050	.22440	.22860	.23940	.23190	.22780	.23180	.23030	.22720	.22410	
+15.0	.19830	.22310	.24770	.26000	.26160	.25810	.25130	.25330	.26360	.26190	.24790	.21970	.19150	
+20.0	.24410	.25300	.26200	.26650	.27490	.26620	.25950	.26070	.27620	.26770	.24960	.21350	.17740	
+25.0	.18720	.21630	.24550	.26000	.27470	.26670	.26230	.26480	.27890	.24940	.24140	.22540	.20940	
+30.0	.05650	.13000	.20350	.24020	.26080	.27200	.26660	.26510	.23690	.19430	.20380	.22280	.24190	
+35.0	-.01840	.05250	.15140	.18750	.24140	.26380	.26830	.25270	.20690	.18950	.18460	-.06460	-.15370	
+40.0	.15500	.11240	.14490	.15350	.20360	.28630	.26990	.27300	.23530	.18930	.13070	.09550	.10720	
+45.0	-.04500	.15610	.03450	.14000	.18680	.19660	.21010	.23220	.16410	.14020	.05210	.13420	-.06500	
+50.0	-.08690	-.02460	.11510	.11060	.14430	.12290	.15710	.15630	.16190	.11720	.03380	.02160	.00880	
+55.0	-.02070	.06560	-.02720	.05140	.12710	.06280	.14510	.09620	.12810	.04450	-.02210	.07120	.05130	
+60.0	.05560	.09750	.11230	.07330	.08850	.04810	.08740	.07350	.05260	.06500	.06240	.11270	.01260	
+70.0	.06990	.08600	.10560	.10070	.11000	.08220	.09720	.10120	.12960	.10820	.11690	.09810	.11520	
+80.0	.12610	.12410	.12670	.11650	.14390	.14450	.12890	.14690	.15360	.12590	.13190	.12560	.12390	
+90.0	.14460	.12330	.11710	.11910	.11670	.12730	.14610	.11400	.12520	.12080	.10860	.11620	.13650	

TABLE IV.- Continued

(c) $\Delta C_{m, \delta_h} = -10^\circ$

		BETA												
ALPHA		-40.0	-30.0	-20.0	-15.0	-10.0	- 5.0	0.0	+ 5.0	+10.0	+15.0	+20.0	+30.0	+40.0
-10.0	.06350	.07560	.08770	.09380	.11110	.11630	.12170	.12610	.11790	.11020	.10500	.09480	.08440	
- 5.0	.06000	.07750	.09510	.10390	.11230	.11330	.11530	.11480	.11550	.10890	.10640	.10160	.09680	
0.0	.09070	.09730	.10390	.10720	.10660	.10870	.11200	.11030	.11330	.10650	.10570	.10410	.10250	
+ 5.0	.08370	.09410	.10460	.10970	.10800	.10460	.11090	.10620	.10850	.10610	.10590	.10540	.10500	
+10.0	.09000	.09840	.10680	.11110	.10690	.10390	.10320	.10240	.10190	.10780	.10050	.08590	.07120	
+15.0	.09250	.10010	.10750	.11130	.11420	.11180	.10670	.10440	.11090	.10920	.10570	.09870	.09170	
+20.0	.10230	.10820	.11420	.11710	.11450	.11630	.11570	.10830	.12430	.11230	.10210	.08170	.06140	
+25.0	.06930	.08420	.09920	.10670	.11690	.11300	.11330	.11070	.11840	.09330	.09490	.09820	.10140	
+30.0	-.02940	.01840	.06620	.09010	.10320	.11450	.11520	.10610	.06720	.05950	.05120	.03470	.01820	
+35.0	-.07940	-.04440	.01870	.03680	.08930	.10230	.10840	.09160	.06600	.04840	.04520	-.20020	-.28570	
+40.0	.09300	.02100	.03890	.05970	.08370	.11350	.12160	.10230	.09670	.05420	.03080	.02610	.00980	
+45.0	-.12840	.07280	.01900	.05850	.08250	.07290	.06120	.08850	.04280	.02670	-.00690	.04140	-.13590	
+50.0	-.18030	-.06730	.05370	.03630	.08530	.02900	.06970	.06470	.07070	.05270	.01940	-.00750	-.05660	
+55.0	-.07250	.00900	-.01990	.01500	.08360	.03820	.09400	.03900	.06810	-.00280	-.04620	.03710	-.01160	
+60.0	-.03010	.04620	.05580	.05120	.05500	.01200	.07060	.03140	.01160	-.05000	.09050	.05100	-.06920	
+70.0	.00290	.04100	.04710	.02690	.03490	-.00690	.00790	.02280	.03630	.03180	.04110	.04110	.00850	
+80.0	.00170	.05380	.02240	.03790	.05340	.05740	.04420	.04330	.06460	.03290	.05050	.06340	.05220	
+90.0	.07050	.06040	.04830	.05290	.05350	.04110	.04660	.03880	.04130	.04200	.03520	.03430	.04530	

TABLE IV.- Continued

(d) $\Delta C_{m, \delta_h=10^\circ}$

		BETA												
ALPHA		-40.0	-30.0	-20.0	-15.0	-10.0	- 5.0	0.0	+ 5.0	+10.0	+15.0	+20.0	+30.0	+40.0
-10.0		-.07910	-.08870	-.09820	-.10300	-.09840	-.10480	-.10330	-.09960	-.09390	-.09390	-.09350	-.09250	-.09160
- 5.0		-.13250	-.11620	-.09990	-.09170	-.10260	-.11060	-.10400	-.10380	-.10220	-.09760	-.09480	-.08910	-.08350
0.0		-.10840	-.10560	-.10290	-.10150	-.10570	-.11440	-.11430	-.11310	-.10580	-.10330	-.10000	-.09360	-.08710
+ 5.0		-.03950	-.07080	-.10210	-.11780	-.11490	-.11800	-.11310	-.11730	-.12130	-.12000	-.10960	-.08890	-.06810
+10.0		-.08870	-.09910	-.10960	-.11470	-.12380	-.12160	-.12160	-.12370	-.11800	-.11980	-.11430	-.10350	-.09260
+15.0		-.03180	-.06260	-.09350	-.10900	-.11570	-.11470	-.11850	-.11610	-.11760	-.10980	-.10010	-.08090	-.06170
+20.0		.03280	-.02010	-.07300	-.09940	-.11560	-.10890	-.09670	-.11440	-.12040	-.09350	-.07850	-.04870	-.01880
+25.0		.09720	.02440	-.04840	-.08480	-.10970	-.10590	-.10990	-.11030	-.10680	-.04820	-.05270	-.06170	-.07080
+30.0		.03330	-.01000	-.05310	-.07480	-.08510	-.09330	-.09320	-.09230	-.08640	-.06380	-.04270	-.00030	.04210
+35.0		.01500	-.02580	-.03850	-.05830	-.07040	-.07550	-.07570	-.06970	-.07140	-.05330	-.04430	-.26550	-.32670
+40.0		.00390	-.01550	-.04080	-.02070	-.04130	-.01740	-.01800	-.02900	-.01330	-.03310	-.04500	-.04270	-.05940
+45.0		-.19550	-.00470	-.05210	-.02190	.01050	-.01320	-.03650	.00110	-.03970	-.03460	-.08500	-.02130	-.19280
+50.0		-.22080	-.13280	-.00580	-.01840	.02970	-.03470	-.01820	-.01320	.01700	-.02220	-.04010	-.08740	-.11270
+55.0		-.13470	-.07590	-.05740	-.02390	.04020	-.04530	.00590	-.02650	.02030	-.02250	-.11030	-.04320	-.07700
+60.0		-.07120	-.02900	.00210	-.01160	-.00760	-.04020	-.01420	-.03170	-.04550	-.00990	-.00170	-.02750	-.10770
+70.0		-.05260	-.04050	-.03260	-.01590	.04500	.00080	.12330	.03720	.06540	-.02480	-.00280	-.02410	-.05640
+80.0		-.03230	-.01610	.00100	-.00810	-.00270	-.01160	-.00430	-.00510	.00420	-.01330	.00070	-.01960	-.01240
+90.0		.03310	.01640	.02570	-.00920	.01580	.01440	.01010	.00550	.02500	.00360	.00800	.00570	.01270

TABLE IV.- Continued

(e) $\Delta C_{m, \delta_h=25^\circ}$

		BETA												
ALPHA	-40.0	-30.0	-20.0	-15.0	-10.0	-5.0	0.0	+5.0	+10.0	+15.0	+20.0	+30.0	+40.0	
-10.0	-.21440	-.22100	-.22760	-.23090	-.23020	-.22960	-.23130	-.22140	-.21600	-.21820	-.21910	-.22060	-.22220	
-5.0	-.26790	-.24320	-.21850	-.20620	-.20650	-.20990	-.21680	-.20910	-.19450	-.20720	-.21510	-.23090	-.24670	
0.0	-.22560	-.21580	-.20590	-.20090	-.19630	-.20730	-.21150	-.20630	-.19660	-.20460	-.20190	-.19660	-.19120	
+5.0	-.05110	-.11410	-.17710	-.20860	-.21400	-.21780	-.21730	-.21860	-.20890	-.20530	-.18820	-.15390	-.11960	
+10.0	-.06380	-.11450	-.16530	-.19060	-.20870	-.22520	-.22350	-.21430	-.20220	-.18440	-.17620	-.15960	-.14310	
+15.0	.03290	-.04850	-.12990	-.17070	-.19520	-.19480	-.19520	-.19770	-.19790	-.16980	-.14360	-.09110	-.03860	
+20.0	.11530	.01020	-.09500	-.14760	-.16850	-.17920	-.19960	-.20300	-.18240	-.15080	-.10080	-.00100	.09900	
+25.0	.07520	-.00630	-.08780	-.12860	-.15050	-.16120	-.18760	-.16870	-.14930	-.12270	-.08340	-.00450	.07420	
+30.0	.18730	.00250	-.06220	-.12460	-.13150	-.13520	-.14320	-.14140	-.16710	-.12650	-.09180	-.02230	.04730	
+35.0	.07530	-.00500	-.05710	-.09660	-.08960	-.08750	-.08530	-.08560	-.13710	-.08960	-.08220	-.30660	-.37100	
+40.0	-.08450	-.07810	-.04850	-.05070	-.07920	-.01730	-.00960	-.02330	-.01790	-.04030	-.06590	-.08030	-.10200	
+45.0	-.20810	-.00840	-.11200	-.04260	-.04090	-.02240	-.02130	.00520	-.03160	-.04150	-.11830	-.04370	-.21220	
+50.0	-.22960	-.16890	-.04000	-.05480	.00450	-.05200	-.04080	-.02780	-.01990	-.03300	-.07330	-.11470	-.13610	
+55.0	-.16120	-.09980	-.09540	-.06180	.01110	-.06120	-.01910	-.05520	-.01580	-.05040	-.14600	-.07650	-.08550	
+60.0	-.10680	-.05750	-.01010	-.03230	.02610	-.05520	-.01700	-.03770	-.06200	-.00990	.00040	-.04920	-.14940	
+70.0	-.12300	-.05740	-.00920	-.00790	.04790	.02970	.09130	.13570	.07860	-.01490	-.01180	-.00900	-.11060	
+80.0	.01660	.02650	.01170	.01520	.02170	.00180	-.00380	.08910	.02280	-.00910	.00400	.03280	.04060	
+90.0	.10900	.08990	.02080	.02950	.03930	.02510	.02980	.03620	.04190	.02480	.00520	.07470	.09510	

TABLE IV.- Continued

(f) $\Delta C_{m,lef}$

		BETA											
ALPHA	-40.0	-30.0	-20.0	-15.0	-10.0	- 5.0	0.0	+ 5.0	+10.0	+15.0	+20.0	+30.0	+40.0
-10.0	.01360	.01040	.00710	.00550	.00470	.00670	.01680	.02530	.01580	.01920	.01460	.00530	-.00400
- 5.0	-.00960	.00510	.01980	.02720	.03960	.04550	.05040	.05330	.04760	.03410	.03310	.03120	.02930
0.0	.00840	.02300	.03760	.04490	.04250	.03560	.03230	.03890	.04540	.04610	.04230	.03460	.02700
+ 5.0	.01390	.02290	.03200	.03640	.03630	.02880	.03460	.03030	.03710	.03610	.03850	.04330	.04820
+10.0	.01770	.02400	.03220	.03330	.03820	.03910	.04240	.04010	.03600	.03160	.02110	0.00000	-.02110
+15.0	-.03570	-.00970	.01620	.02920	.04600	.06700	.06930	.06340	.04470	.03240	.02090	-.00200	-.02500
+20.0	.01280	.00700	.00130	-.00160	.01720	.04080	.04820	.03950	.02540	.00110	.00050	-.00090	-.00210
+25.0	-.05120	-.03540	-.01960	-.01160	.00050	.00560	.01690	.00530	.00450	-.00970	-.02690	-.06130	-.09590
+30.0	-.04640	-.03810	-.02980	-.02570	-.03270	-.03250	-.02530	-.04150	-.03080	-.03660	-.03680	-.03710	-.03750
+35.0	.02590	-.00570	-.00930	-.02450	-.04030	-.03900	-.04340	-.04200	-.01540	-.02440	-.01590	-.23810	-.30020
+40.0	-.05320	.00630	-.01550	-.00910	.00120	.01560	.01680	.00540	.00440	-.01200	-.02630	-.01290	-.07610
+45.0	-.15640	.03360	-.07040	.01770	.00060	.02480	.01060	.02810	-.02300	-.01040	-.09100	.01160	-.17160
+50.0	-.18060	-.12190	.01030	-.01020	.01960	-.02300	.00210	.00600	.02130	.01780	-.07660	-.05130	-.09670
+55.0	-.11780	-.04750	-.05830	-.03350	.04230	-.05940	.01650	-.02730	.01510	-.05340	-.10330	-.03280	-.06370
+60.0	-.06050	-.00510	.02260	-.00750	.01230	-.00480	-.00090	-.00620	-.02030	-.02780	-.01990	-.00580	-.09280
+70.0	-.03340	-.02530	-.01190	-.02850	-.01470	-.05870	-.00300	-.02410	.00420	-.00540	.00350	-.01980	-.02100
+80.0	.00750	.01620	.02310	.00900	.01740	.00400	.00230	.01140	.01640	.00080	.01820	.00360	.01330
+90.0	.03360	.02310	.02150	.01520	.03730	.02180	.02600	.02760	.02780	.01280	.01020	.02410	.02020

TABLE IV.- Continued

(g) $C_{m,1}$

		BETA												
ALPHA	-40.0	-30.0	-20.0	-15.0	-10.0	- 5.0	0.0	+ 5.0	+10.0	+15.0	+20.0	+30.0	+40.0	
-10.0	.12540	.07480	.02420	-.00110	-.03140	-.04520	-.04420	-.05230	-.03090	-.00810	.00880	.04250	.07630	
- 5.0	.06830	.03630	.00430	-.01170	-.03100	-.04450	-.05100	-.04920	-.03830	-.01490	-.00850	.00420	.01690	
0.0	-.00230	-.00980	-.01730	-.02110	-.03160	-.02750	-.02500	-.02930	-.03230	-.01980	-.01820	-.01490	-.01170	
+ 5.0	-.03090	-.02540	-.01990	-.01710	-.02220	-.01660	-.01820	-.01800	-.02100	-.01750	-.01510	-.01030	-.00550	
+10.0	-.02570	-.02420	-.02270	-.02200	-.02130	-.01680	-.01480	-.01440	-.01790	-.01730	-.00630	.01570	.03770	
+15.0	-.06320	-.04790	-.03250	-.02480	-.02380	-.01870	-.00930	-.00980	-.01820	-.01980	-.00450	.02610	.05670	
+20.0	-.13830	-.08990	-.04150	-.01730	-.01360	-.01010	-.01260	-.01260	-.01810	-.00420	.00610	.02680	.04740	
+25.0	-.15960	-.09900	-.03840	-.00810	-.01400	-.01550	-.01220	-.01180	-.00830	-.02930	-.00100	.05550	.11210	
+30.0	.07750	.04040	.00320	-.01530	-.01720	-.02010	-.01080	-.00540	.01580	.00910	.00440	-.00510	-.01460	
+35.0	.30910	.19300	.04880	-.00990	-.02350	-.03670	-.02570	-.02270	.00140	-.00250	-.00550	.22770	.30090	
+40.0	.25320	.19710	.03770	-.00980	-.00330	-.02970	-.04280	-.00550	-.00480	.00220	.01620	.22160	.28130	
+45.0	.25630	.19310	.07430	-.04210	-.05350	-.02180	-.03880	-.07140	-.02940	-.02070	.10250	.21710	.28440	
+50.0	.18380	.10650	.06250	-.00890	-.09310	-.03640	-.02960	-.03720	-.07040	.01290	.09840	.08290	.10590	
+55.0	.03300	-.06060	-.01480	-.02040	-.09130	-.06520	-.04500	-.08590	-.07150	-.00360	.01210	-.09240	-.03880	
+60.0	-.11750	-.17310	-.20760	-.18180	-.15710	-.11130	-.06090	-.05360	-.10850	-.12060	-.19990	-.17470	-.14590	
+70.0	-.20060	-.27540	-.32340	-.29800	-.30540	-.26030	-.26610	-.28400	-.32720	-.31040	-.33290	-.30380	-.23300	
+80.0	-.45360	-.47650	-.47210	-.45820	-.47250	-.44510	-.42200	-.45250	-.47710	-.45650	-.47690	-.47890	-.47520	
+90.0	-.60570	-.60360	-.59740	-.58860	-.59780	-.58780	-.58490	-.59800	-.59750	-.60010	-.59120	-.59100	-.59160	

TABLE IV.- Continued

(h) $C_{m,2}$

		BETA											
ALPHA	-40.0	-30.0	-20.0	-15.0	-10.0	- 5.0	0.0	+ 5.0	+10.0	+15.0	+20.0	+30.0	+40.0
-10.0	.12540	.07480	.02420	-.00110	-.03140	-.04520	-.04420	-.05030	-.03090	-.00810	.00880	.04250	.07630
- 5.0	.06830	.03630	.00430	-.01170	-.03190	-.04450	-.05100	-.04900	-.03830	-.01490	-.00850	.00420	.01690
0.0	-.00230	-.00980	-.01730	-.02110	-.03160	-.02750	-.02500	-.02930	-.03230	-.01980	-.01820	-.01490	-.01170
+ 5.0	-.03090	-.02540	-.01990	-.01710	-.02220	-.01660	-.01820	-.01800	-.02100	-.01750	-.01510	-.01030	-.00550
+10.0	-.02570	-.02420	-.02270	-.02200	-.02130	-.01680	-.01480	-.01440	-.01790	-.01730	-.00630	.01570	.03770
+15.0	-.03630	-.04790	-.03250	-.02480	-.02380	-.01870	-.00930	-.00980	-.01820	-.01980	-.00450	.02610	.05670
+20.0	-.13830	-.08990	-.04150	-.01730	-.01360	-.01010	-.01260	-.01060	-.01810	-.00420	.00610	.02680	.04740
+25.0	-.15960	-.09900	-.03840	-.00810	-.01400	-.01550	-.01220	-.01180	-.00830	-.02930	-.00100	.05550	.11210
+30.0	.07750	.04040	.00320	-.01530	-.01720	-.02010	-.01080	-.00540	.01580	.00910	.00440	-.00510	-.01460
+35.0	.30910	.19300	.04880	-.00990	-.02350	-.03670	-.02570	-.02270	.00140	-.00250	-.00550	.22770	.30090
+40.0	.25320	.19710	.03770	-.00980	-.00330	-.02970	-.04280	-.00550	-.00480	.00220	.01620	.22160	.28130
+45.0	.22530	.16210	.04330	-.07310	-.08450	-.05280	-.06980	-.10240	-.06040	-.05170	.07150	.18610	.25340
+50.0	.12380	.04650	.00250	-.06890	-.15310	-.09640	-.08960	-.09720	-.13040	-.04710	-.03840	.02290	.04590
+55.0	-.04200	-.13560	-.08980	-.05460	-.16630	-.14020	-.12000	-.16090	-.14650	-.07860	-.06290	-.16740	-.11380
+60.0	-.21750	-.27310	-.30760	-.28180	-.25710	-.21130	-.16090	-.15360	-.20850	-.22060	-.29990	-.27470	-.24590
+70.0	-.20060	.27540	-.32340	-.29800	-.30540	-.26030	-.26610	-.28400	-.32720	-.31040	-.33290	-.30380	-.23300
+80.0	-.45360	-.47650	-.47210	-.45820	-.47250	-.44510	-.42200	-.45250	-.47710	-.45650	-.47690	-.47890	-.47520
+90.0	-.60570	-.60360	-.59740	-.58860	-.59780	-.58780	-.58490	-.59800	-.59750	-.60010	-.59120	-.59100	-.59160

TABLE IV.- Concluded

(i) C_{mq} and $\Delta C_{mq,lef}$

α , deg	C_{mq}	$\Delta C_{mq,lef}$
-10.0	-6.8400	-.3670
- 5.0	-3.4200	2.8800
0.0	-5.4800	.2500
+ 5.0	-5.4500	.2700
+10.0	-6.0200	-.2100
+15.0	-6.7000	.3600
+20.0	-5.6900	-1.2600
+25.0	-6.6300	-2.5100
+30.0	-7.9700	-1.6600
+35.0	-9.3800	-1.7200
+40.0	-11.2000	-1.2000
+45.0	-13.3000	-.6000
+50.0	-13.4000	0.0000
+55.0	-7.1000	0.0000
+60.0	-7.7300	0.0000
+70.0	6.8200	0.0000
+80.0	-5.6000	0.0000
+90.0	-4.0400	0.0000

TABLE V.- Y-AXIS FORCE COEFFICIENT DATA USED IN SIMULATION

[All data are for $\delta_{lef} = 25^\circ$ unless otherwise indicated]

(a) C_Y

ALPHA	BETA												
	-40.0	-30.0	-20.0	-15.0	-10.0	- 5.0	0.0	+ 5.0	+10.0	+15.0	+20.0	+30.0	+40.0
-10.0	.73650	.55080	.36510	.27230	.18680	.07260	-.00170	-.07250	-.17260	-.27720	-.35630	-.51460	-.67280
- 5.0	.75640	.58440	.41230	.32630	.21250	.10510	-.00410	-.10030	-.21560	-.31800	-.41860	-.61980	-.82100
0.0	.86330	.65710	.45090	.34780	.22780	.11180	-.00380	-.10510	-.23600	-.33980	-.44680	-.66090	-.87500
+ 5.0	.92810	.69860	.46910	.35430	.23940	.11530	-.00070	-.10440	-.22270	-.35680	-.46060	-.66840	-.87610
+10.0	.91420	.69660	.47900	.37020	.25790	.11760	.00810	-.09720	-.23790	-.35140	-.44850	-.64260	-.83680
+15.0	.76670	.60670	.44670	.36670	.24680	.11940	-.00240	-.09690	-.23340	-.35360	-.39010	-.46320	-.53630
+20.0	.79480	.60070	.40660	.30950	.21440	.10740	.00560	-.09080	-.21920	-.26700	-.29410	-.34840	-.40270
+25.0	.74870	.55050	.35240	.25330	.21310	.11470	.00100	-.10140	-.18670	-.16160	-.25000	-.42680	-.60360
+30.0	.35470	.30910	.26350	.24070	.18700	.11580	.01310	-.07060	-.10760	-.13710	-.24340	-.45620	-.66890
+35.0	.60510	.35210	.20900	.15130	.14350	.10910	.03670	-.01900	-.03520	-.15050	-.26610	-.32450	-.59010
+40.0	.58090	.35860	.17890	.09470	.02670	.11260	.03610	-.05110	-.17710	-.21060	-.18650	-.35310	-.53820
+45.0	.50740	.32860	.15370	.07810	.01020	.02230	-.04520	-.18580	-.18120	-.09010	-.15790	-.30390	-.45160
+50.0	.43300	.30110	.19570	.14490	.07860	.06720	-.00450	-.08590	-.09770	-.16010	-.18940	-.31110	-.43890
+55.0	.45260	.31030	.19190	.14670	.12530	.08430	.00570	-.05840	-.13990	-.18700	-.21700	-.33140	-.45430
+60.0	.42150	.31750	.20110	.17320	.11770	.08680	-.00410	-.09870	-.14030	-.17220	-.23800	-.34550	-.44220
+70.0	.46320	.34150	.23700	.18450	.12100	.07450	-.00500	-.07600	-.13520	-.20160	-.25260	-.36590	-.47860
+80.0	.52620	.37730	.23250	.18040	.11610	.06220	-.00470	-.07220	-.12960	-.20000	-.25190	-.38930	-.53670
+90.0	.57550	.38870	.22710	.16020	.10740	.05650	-.01330	-.07330	-.12390	-.18560	-.25390	-.39980	-.58340

TABLE V. - Continued

(b) $\Delta C_Y, \delta_a=20^\circ$

ALPHA	BETA												
	-40.0	-30.0	-20.0	-15.0	-10.0	- 5.0	0.0	+ 5.0	+10.0	+15.0	+20.0	+30.0	+40.0
-10.0	-.02615	-.01610	-.00610	-.00110	.01085	.01010	.01110	.00885	.01390	-.00540	-.02120	-.05270	-.08420
- 5.0	-.04405	-.02910	-.01415	-.00665	.01620	.01730	.01590	.01105	.02560	-.00345	-.01720	-.04465	-.07210
0.0	-.04055	-.02690	-.01320	-.00635	.02365	.01750	.01635	.01520	.01310	-.00135	-.02415	-.06980	-.11540
+ 5.0	-.06590	-.03945	-.01300	.00020	.01820	.02135	.01265	.01545	.00925	-.00685	-.01420	-.02890	-.04365
+10.0	-.13685	-.07900	-.02110	.00785	.01065	.01630	.00205	.01460	.01285	-.00525	-.04105	-.11255	-.18410
+15.0	-.13000	-.07975	-.02960	-.00450	.02160	.01860	.01535	.01145	.00735	-.00095	-.04745	-.14050	-.23350
+20.0	-.04125	-.03085	-.02045	-.01525	.00035	.00415	-.00190	.00240	-.00710	-.02350	-.02810	-.03735	-.04655
+25.0	-.05050	-.03475	-.01910	-.01125	-.00630	-.00440	-.01135	-.00590	-.01350	-.00580	-.01805	-.04265	-.06730
+30.0	-.02980	-.02160	-.01340	-.00925	-.01100	-.01015	-.00725	-.00800	-.01385	-.00825	-.01095	-.01640	-.02180
+35.0	-.11335	-.07715	-.04095	-.02285	-.02450	-.01270	-.01030	-.00980	-.01740	-.02375	-.02135	-.01655	-.01180
+40.0	-.02330	-.03445	-.02810	-.01815	-.00775	-.01690	-.01555	-.01185	-.02165	-.02535	-.05200	-.04800	-.03115
+45.0	-.00755	-.02665	-.02975	-.03340	-.01535	-.02725	-.02225	-.02535	-.02905	-.03580	-.03235	-.02995	-.01225
+50.0	.00155	-.00740	-.03235	-.04585	-.03395	-.03760	-.04415	-.03895	-.02465	-.03515	-.02415	-.01090	-.00705
+55.0	.00860	-.00280	-.01500	-.02535	-.04355	-.04475	-.03715	-.03715	-.03595	-.02175	-.01175	-.00920	-.01595
+60.0	-.00295	-.01085	-.01290	-.01420	-.02550	-.03050	-.04185	-.02650	-.02235	-.02540	-.01460	-.01550	-.00480
+70.0	.00165	-.00490	-.01855	-.02145	-.02065	-.04165	-.04175	-.03460	-.02775	-.02475	-.02215	-.00965	-.00710
+80.0	-.00195	-.00095	-.01390	-.01855	-.01300	-.01010	-.00130	-.01165	-.01440	-.01805	-.02235	-.00620	-.00460
+90.0	-.00350	.00510	-.01310	-.01555	-.00830	.00040	-.00415	-.00380	-.00380	-.01065	-.00240	.00095	-.00020

TABLE V. - Continued

(c) $\Delta C_{Y, \delta_a=20^\circ, \text{lef}}$

		BETA													
ALPHA		-40.0	-30.0	-20.0	-15.0	-10.0	- 5.0	0.0	+ 5.0	+10.0	+15.0	+20.0	+30.0	+40.0	
-10.0		-.05860	-.03695	-.01525	-.00435	.00390	.00290	.00575	-.00200	-.00835	-.00200	-.00065	.00205	.00470	
- 5.0		-.07245	-.04090	-.00935	.00635	.00345	-.00040	-.00385	.00875	-.01200	-.01135	-.00365	.01170	.02700	
0.0		-.05390	-.03240	-.01100	-.00030	-.01015	-.00215	-.00770	-.00555	-.00025	-.00245	-.00225	-.00190	-.00155	
+ 5.0		-.06575	-.04025	-.01470	-.00190	-.00540	-.00890	-.00720	.00485	.00255	.00195	-.01475	-.04825	-.08165	
+10.0		-.00985	-.00950	-.00920	-.00905	-.00410	-.01095	.00035	-.00340	-.01310	-.00115	.00675	.02230	.03790	
+15.0		.01505	.01075	.00650	.00435	-.01220	-.01130	-.02550	-.00005	-.00060	.00220	.03680	.10620	.17550	
+20.0		.07160	.04440	.01720	.00360	.00405	.00160	.00560	.00900	.01290	.02110	.01650	.00735	-.00180	
+25.0		-.00300	.00035	.00385	.00555	.01270	.00770	.01260	.00870	.01385	.00395	.01460	.03615	.05770	
+30.0		-.09215	-.05590	-.01960	-.00150	.00025	.00770	.00400	.00550	.00855	-.00710	.00595	.03210	.05820	
+35.0		.08690	.04725	.00755	-.01230	.00320	-.00410	-.00925	-.01125	-.01490	-.00180	-.00590	-.01405	-.02215	
+40.0		-.00175	.00335	-.00205	-.00955	-.01140	-.01020	-.01360	-.01085	-.00020	-.00820	.06225	.01430	-.00735	
+45.0		-.00900	.00850	-.00235	-.00810	-.00850	-.00520	-.01620	-.00475	-.01535	-.00035	-.00315	.00560	-.00160	
+50.0		-.01345	-.00240	-.00135	.00740	-.00545	-.00585	.00360	-.01045	-.01380	-.00315	.00665	-.00175	.01020	
+55.0		-.00255	-.00935	-.00855	.00085	.00375	.01405	.00295	-.00625	-.00550	-.00930	-.00985	-.00050	.01635	
+60.0		-.00370	.00160	-.01330	-.00725	.00070	.00100	-.00165	-.00620	-.00770	-.00360	-.00930	-.00045	.00045	
+70.0		-.00640	-.03445	-.00130	.00770	-.00655	.00165	-.00195	-.00335	.00090	-.00130	-.00240	.00035	.00440	
+80.0		-.01385	-.00955	-.00475	.00570	-.00275	-.01115	-.00980	-.00470	-.00315	-.00400	-.00020	.00055	-.00925	
+90.0		-.01080	-.00990	-.00335	.00485	.00340	-.00450	-.00050	-.00615	-.00200	-.00285	-.00830	-.00630	-.01035	

TABLE V.- Continued

(d) $\Delta C_{Y, \delta_D=5^\circ}$

		BETA													
ALPHA		-40.0	-30.0	-20.0	-15.0	-10.0	- 5.0	0.0	+ 5.0	+10.0	+15.0	+20.0	+30.0	+40.0	
-10.0	.01655	.01085	.00510	.00225	.01045	.00840	.01210	.01200	.00600	.01050	.00050	-.01970	-.03980		
- 5.0	-.03150	-.01655	-.00155	.00595	.00705	.00490	.00230	.00435	.01490	.00050	.00765	.02190	.03620		
0.0	-.01000	-.00570	-.00145	.00070	.00375	.00370	.01290	.00835	.00515	.00705	.00780	.00930	.01085		
+ 5.0	-.06930	-.03815	-.00695	.00865	.00860	.01115	.01175	.00470	-.00230	.00470	.00610	.00895	.01180		
+10.0	-.00035	.00190	.00420	.00530	.01040	.01570	.01500	.01005	.00885	.01490	.00685	-.00930	-.02545		
+15.0	-.05635	-.03060	-.00490	.00800	.01385	.01105	.00940	.01380	.01190	.00010	-.00610	-.01850	-.03090		
+20.0	-.00020	.00240	.00510	.00645	-.00170	.00400	.00785	.01430	.01170	.00715	.00165	-.00930	-.02020		
+25.0	.00700	.00430	.00155	.00025	.00455	.00780	.00745	.01195	.00650	.00700	-.00015	-.01450	-.02880		
+30.0	-.03695	-.02440	-.01195	-.00565	-.00105	.00795	.01590	.00605	.00055	-.00490	-.01765	-.04300	-.06840		
+35.0	-.01780	-.01255	-.00735	-.00475	-.00210	.00315	.00585	.00025	-.00025	-.00515	-.00415	-.00235	-.00045		
+40.0	.00785	-.00060	-.00045	-.00440	-.01730	.00445	.00235	-.00130	-.00290	-.00710	-.00710	.00460	-.01235		
+45.0	-.00600	-.00845	-.01090	-.00870	-.00795	.00025	.00340	-.00310	-.00075	-.00295	-.00555	-.01385	-.02020		
+50.0	-.03125	-.00435	-.00690	-.00485	-.01045	-.01585	-.01050	-.01045	.00095	-.00915	-.00425	-.01185	.00265		
+55.0	-.00500	-.01400	-.01520	-.01230	-.01190	-.01320	-.01605	-.01380	-.00830	-.00505	-.01495	-.01145	-.00510		
+60.0	.00080	-.01650	-.01445	-.01060	.00160	-.00395	-.02250	-.00780	-.00105	-.00265	-.00910	-.01215	.00435		
+70.0	.00010	-.00835	-.01290	-.00620	-.00365	-.00570	-.01075	.00080	-.00115	-.00495	-.01265	-.01390	-.00840		
+80.0	-.01030	-.00925	-.00465	-.01005	-.00250	-.00580	-.00745	-.00585	-.00360	-.00915	-.00915	-.00600	-.01055		
+90.0	-.00695	-.00590	-.00140	-.00205	.00120	-.00030	.00300	-.00045	-.00340	-.00475	-.00500	.00225	-.01085		

TABLE V.- Continued

(e) $\Delta C_{Y, \delta_r=30^\circ}$

		BETA												
		-40.0	-30.0	-20.0	-15.0	-10.0	- 5.0	0.0	+ 5.0	+10.0	+15.0	+20.0	+30.0	+40.0
ALPHA														
-10.0		.03275	.05120	.06970	.07890	.09390	.10680	.09710	.10770	.08690	.07480	.05225	.00710	-.03800
- 5.0		-.01910	.02305	.06525	.08630	.09895	.11120	.10205	.10265	.08725	.07825	.05795	.01730	-.02335
0.0		.00940	.03895	.06850	.08330	.09710	.10860	.10090	.09920	.09490	.08080	.06660	.03810	.00970
+ 5.0		.01465	.04250	.07035	.08425	.10200	.10605	.10195	.09330	.08190	.07755	.06145	.02905	-.00330
+10.0		.02510	.04920	.07335	.08540	.10005	.11110	.09645	.09955	.10060	.08345	.04750	-.02445	-.09640
+15.0		.01810	.04150	.06485	.07655	.09705	.10815	.10950	.11025	.10080	.07035	.04835	.00425	-.03980
+20.0		.06580	.05990	.05400	.05110	.08330	.10260	.10240	.10600	.08220	.04230	.05340	.07550	.09770
+25.0		.01120	.02595	.04065	.04805	.07735	.11150	.10290	.10425	.07180	.03965	.04865	.06665	.08470
+30.0		.05715	.05480	.05250	.05135	.04750	.09695	.10485	.09120	.05275	.04190	.03660	.02605	.01550
+35.0		-.00960	.01075	.03105	.04125	.06040	.09150	.09230	.06810	.05905	.02170	.03110	.04990	.06865
+40.0		.02815	.03335	.02770	.03260	.04560	.05760	.07595	.05745	.04475	.03085	.04335	.02405	.05330
+45.0		.03795	.00235	-.00215	.01430	.03300	.03890	.03910	.03055	.03015	.01300	.01965	.01430	.03095
+50.0		.02500	.00610	.00490	.01155	.01905	.01535	.01620	.01470	.00610	.00675	.01025	.00540	.00280
+55.0		.00620	.00175	.00705	.00790	.01450	.00855	.00420	.01020	.00815	.00170	.01835	.00380	.00560
+60.0		.01155	.00625	.01075	.00855	.00575	.00475	.00575	.01140	.00985	.00555	.00725	.00425	.00635
+70.0		.00135	.00575	.00030	.00770	.00720	-.00130	.01310	.00075	.01020	.00410	.00500	.00805	.00225
+80.0		.00890	.00665	.00655	.01120	.00555	.00950	.01175	.01330	.01075	.00735	.00320	.00395	.00810
+90.0		.01220	.01035	.00930	.01195	.01545	.00580	.01390	.00645	.00935	.01235	.00515	.00670	.00575

TABLE V, - Concluded

(f) C_{Yp} , $\Delta C_{Yp,lef}$, C_{Yr} , and $\Delta C_{Yr,lef}$

α , deg	C_{Yp}	$\Delta C_{Yp,lef}$	C_{Yr}	$\Delta C_{Yr,lef}$
-10.0	.0233	-.1410	1.4400	-.5580
- 5.0	-.1770	.0690	1.0500	-.1980
0.0	.0055	-.1970	.9810	-.1070
+ 5.0	.0679	.0601	.9390	.0270
+10.0	.3100	-.1210	.9990	-.0850
+15.0	.2340	-.0520	.9810	-.0460
+20.0	.3440	.0750	.8190	.3310
+25.0	.3620	.1060	.4830	.2150
+30.0	.6110	-.0770	.5900	.4200
+35.0	.5290	-.6420	1.2100	-.0600
+40.0	.2980	-.2550	-.4930	-.5740
+45.0	-2.2700	-.1280	-1.0400	-.1870
+50.0	.9710	0.0000	-1.2100	0.0000
+55.0	1.0200	0.0000	-1.5800	0.0000
+60.0	2.9000	0.0000	-1.3700	0.0000
+70.0	.4510	0.0000	-.0259	0.0000
+80.0	-.2940	0.0000	-.1270	0.0000
+90.0	-.2610	0.0000	.1930	0.0000

TABLE VI. - YAWING-MOMENT COEFFICIENT DATA USED IN SIMULATION

[All data are for $\delta_{lef} = 25^\circ$ unless otherwise indicated]

(a) C_n

		BETA												
ALPHA		-40.0	-30.0	-20.0	-15.0	-10.0	- 5.0	0.0	+ 5.0	+10.0	+15.0	+20.0	+30.0	+40.0
-10.0	-10.0	-.10580	-.08500	-.06410	-.05360	-.03890	-.01300	.00140	.01770	.03840	.05770	.06680	.08490	.10300
- 5.0	- 5.0	-.13070	-.10430	-.07790	-.06480	-.04370	-.01870	.00210	.02100	.04680	.06550	.08150	.11340	.14530
0.0	0.0	-.15740	-.12210	-.08670	-.06900	-.04880	-.02160	.00100	.02160	.05190	.06890	.08730	.12400	.16070
+ 5.0	+ 5.0	-.16720	-.12880	-.09030	-.07100	-.05260	-.02500	-.00050	.02210	.04850	.07030	.08710	.12050	.15390
+10.0	+10.0	-.15690	-.12450	-.09200	-.07580	-.05860	-.02800	-.00340	.02040	.05160	.06950	.08880	.12730	.16580
+15.0	+15.0	-.08280	-.08080	-.07890	-.07790	-.05800	-.02800	-.00180	.01800	.04850	.07370	.07820	.08710	.09600
+20.0	+20.0	-.09040	-.07590	-.06130	-.05400	-.04400	-.02160	-.00410	.01240	.04020	.05060	.06220	.08520	.10830
+25.0	+25.0	-.10370	-.07140	-.03900	-.02290	-.03360	-.02050	-.00250	.01550	.03470	.00770	.03350	.08510	.13670
+30.0	+30.0	-.19270	-.10760	-.02240	.02020	.00230	.00150	.00670	.01720	-.01630	.00250	.00790	.01880	.02970
+35.0	+35.0	-.09180	-.04000	-.01760	.02840	.04900	.03400	.02210	.00070	-.02820	-.04890	-.06130	.03820	.06800
+40.0	+40.0	-.07720	-.03610	.01470	.02870	.04420	.03240	.01130	-.02260	-.06360	-.08720	-.03700	.02680	.05610
+45.0	+45.0	-.04680	-.00260	.01190	.03820	.03470	.01380	-.01170	-.05650	-.06350	-.04770	-.00820	.00400	.02620
+50.0	+50.0	-.03040	-.02030	-.01060	.00400	.01990	.01060	-.00310	-.02140	-.01830	-.00310	.01120	.01580	.01710
+55.0	+55.0	-.02690	-.00900	-.02120	-.02930	.00570	.00320	-.00320	-.00340	.00410	.00560	.00790	-.00650	.01920
+60.0	+60.0	-.02030	.00350	.00200	-.00970	-.02860	-.00900	.00250	-.01010	.01040	.00640	-.01200	-.01620	.00730
+70.0	+70.0	.00580	.02250	.02190	.01660	.00840	-.00650	-.00090	-.00170	-.00920	-.01210	-.01630	-.02260	-.01150
+80.0	+80.0	-.02430	.01080	.01770	.00990	.00970	.00360	-.00050	-.00290	-.00720	-.00700	-.01490	-.01290	.02310
+90.0	+90.0	-.05130	-.01370	.00780	.00600	.00200	.00190	.00160	.00050	-.00090	.00030	-.00450	.00890	.04810

TABLE VI. - Continued

(b) $\Delta C_{n, \delta_h} = -25^\circ$

		BETA												
ALPHA		-40.0	-30.0	-20.0	-15.0	-10.0	- 5.0	0.0	+ 5.0	+10.0	+15.0	+20.0	+30.0	+40.0
-10.0	.00430	.00410	.00380	.00360	.00410	.00060	.00070	-.00370	-.02440	-.00120	-.00110	-.00080	-.00050	
- 5.0	-.01200	-.00620	-.00050	.00250	.00470	.00200	-.00070	-.00060	-.00030	.00080	.00200	.00450	.00700	
0.0	-.01070	-.00500	.00060	.00340	.00440	.00210	-.00070	.00020	-.00240	.00060	.00030	-.00010	-.00040	
+ 5.0	-.00450	-.00060	.00320	.00510	.00270	.00430	-.00060	-.00070	.00110	-.00380	-.00110	.00450	.01000	
+10.0	.00410	.00550	.00690	.00760	.00730	.00050	.00070	.00230	-.00370	-.00510	-.00140	.00630	.01400	
+15.0	-.02340	-.01100	.00160	.00780	.00390	.00430	.00220	.00150	-.00290	-.00910	.00260	.02600	.04950	
+20.0	-.00300	-.00020	.00250	.00390	.00830	.00410	.00150	-.00120	-.01020	-.01090	-.00280	.01370	.03010	
+25.0	.02400	.01760	.01110	.00800	.01140	.00810	0.00000	-.00640	-.01190	-.00330	.00060	.00830	.01610	
+30.0	.03080	.02260	.01440	.01030	.02050	.01020	.00010	-.01460	-.01340	-.00910	-.01030	-.01280	-.01540	
+35.0	-.14860	-.08770	.00260	.01300	.01300	.00480	-.00650	-.01640	-.02170	-.01100	-.01600	-.15020	-.21480	
+40.0	.02910	.00150	0.00000	-.00060	.00460	-.00880	-.01190	-.00680	-.00190	-.00020	-.06300	-.00940	-.01290	
+45.0	-.01480	-.00760	.03230	.01040	.00860	-.00140	.00510	.02310	.00190	-.03880	-.03530	.00240	.02400	
+50.0	-.01950	.00440	-.00240	.00410	.00760	.00760	.00110	-.00370	-.02290	-.01080	-.00270	-.00630	.02680	
+55.0	-.00300	.00430	.02050	.00510	-.01740	.00350	.00270	-.00900	-.00220	.00020	-.01850	-.00630	.01090	
+60.0	-.01360	.01580	.00480	.01100	.02700	.00990	-.00250	-.00820	-.02270	-.01320	-.00990	-.00690	-.01390	
+70.0	-.01240	-.00320	-.00390	-.00010	.00150	.00820	.00060	-.00100	-.00300	-.00660	-.00210	.00320	.01860	
+80.0	.00090	-.00030	-.00960	-.00820	-.00470	-.00030	-.00130	-.00440	.00080	.00420	.00680	.00050	-.00520	
+90.0	.02330	.00770	-.00430	-.00260	.00230	-.00020	-.00050	-.00560	-.00520	.00110	.00340	-.01190	-.02280	

TABLE VI. - Continued

(c) $\Delta C_{n, \delta_h=25^\circ}$

		BETA												
ALPHA		-40.0	-30.0	-20.0	-15.0	-10.0	- 5.0	0.0	+ 5.0	+10.0	+15.0	+20.0	+30.0	+40.0
-10.0	.03440	.02130	.00810	.00140	.00400	-.00030	.00080	.00240	.00430	-.00020	-.00530	-.01540	-.02560	
- 5.0	.01740	.01110	.00480	.00170	-.00040	-.00080	.00050	.00270	.00300	.00370	-.00410	-.01970	-.03530	
0.0	.01970	.01220	.00470	.00090	-.00400	-.00340	-.00100	.00310	.00440	.00400	-.00250	-.01560	-.02860	
+ 5.0	.02470	.01520	.00550	.00070	-.00230	-.00170	.00100	.00190	.00520	.00070	-.00280	-.00970	-.01650	
+10.0	.00810	.00670	.00530	.00470	.00400	.00270	.00140	.00380	.00230	.00120	-.00360	-.01320	-.02280	
+15.0	.01260	.00870	.00490	.00300	.00270	.00080	-.00070	.00440	.00390	-.00050	-.00630	-.01780	-.02930	
+20.0	.03980	.02320	.00640	-.00200	.00010	-.00170	-.00120	.00410	-.00210	.00310	-.00530	-.02200	-.03880	
+25.0	.05650	.03180	.00690	-.00540	-.00070	-.00190	-.00160	.00270	.00440	.00980	.00020	-.01910	-.03840	
+30.0	.03920	.02300	.00670	-.00150	.00030	-.00020	.00150	-.00490	-.00220	.00250	-.00790	-.02860	-.04940	
+35.0	-.07700	-.05090	.00460	-.00240	.00500	.00190	.00590	.00440	-.00760	.00470	-.01420	-.17630	-.26880	
+40.0	.04040	.03710	-.00940	-.01060	-.00780	-.01810	-.01160	-.00500	.00190	.00620	-.05320	-.01060	-.03120	
+45.0	.01100	-.01480	.01330	-.00660	.00060	-.00260	.00860	.02470	-.00990	-.03160	-.03030	.01100	-.00370	
+50.0	.00510	.01140	-.00290	.00070	.00620	.01110	.00060	-.00370	-.01100	.00500	.00600	-.00990	-.00620	
+55.0	.01000	.00710	.00580	-.00680	-.02880	.00520	-.00170	-.00840	-.00030	.01730	-.00860	-.00590	-.01330	
+60.0	.01430	.01550	-.00430	.00300	-.00930	.00030	-.00170	.00270	-.00710	.00670	.00130	-.00710	-.03400	
+70.0	-.02360	-.01430	-.00360	-.00050	-.00140	.00770	-.00060	-.00970	.00090	-.00370	-.00510	.01230	.02780	
+80.0	-.03300	-.02340	-.00920	-.00350	-.00650	-.00100	-.00130	-.00350	.00270	.00050	.00500	.01380	.02880	
+90.0	-.01800	-.01010	-.00720	-.00440	-.00290	-.00280	-.00380	.00010	.00020	.00300	.00050	.00530	.02070	

TABLE VI. - Continued

(d) $\Delta C_{n,lef}$

ALPHA	BETA												
	-40.0	-30.0	-20.0	-15.0	-10.0	- 5.0	0.0	+ 5.0	+10.0	+15.0	+20.0	+30.0	+40.0
-10.0	-.01250	-.01060	-.00890	-.00800	-.01050	-.00910	-.00050	.00680	.01060	.01050	.01160	.01400	.01630
- 5.0	-.00600	-.00450	-.00290	-.00200	-.00560	-.00240	-.00120	.00420	.00520	.00420	.00390	.00330	.00280
0.0	.01190	.00680	.00160	-.00110	-.00200	-.00010	-.00090	.00070	-.00040	.00200	.00070	-.00170	-.00410
+ 5.0	-.00030	.00080	.00170	.00210	.00330	.00120	.00030	-.00050	.00140	-.00050	.00230	.00810	.01390
+10.0	.00030	.00220	.00400	.00490	.00410	.00310	.00210	.00200	-.00120	-.00100	-.00220	-.00450	-.00680
+15.0	-.01460	-.00620	.00230	.00650	.00360	-.00040	.00050	.00200	.00240	-.00540	.00320	.02040	.03760
+20.0	.02390	.02330	.02250	.02210	.00240	-.00020	-.00010	.00090	-.00430	-.02340	-.02690	-.03370	-.04070
+25.0	.04540	.03720	.02880	.02470	.02900	.00730	.00040	-.00670	-.03510	-.00450	-.01110	-.02410	-.03710
+30.0	-.00610	.00300	.01200	.01650	.03040	.00990	.00250	-.02180	-.02300	-.00040	-.03500	-.10420	-.17340
+35.0	-.05680	-.03730	.01150	.00120	-.00500	0.00000	-.00560	-.00770	-.02400	.00270	-.00610	-.14810	-.22030
+40.0	.02300	.02450	.00040	-.00440	-.01620	-.01610	-.01400	-.01020	.01300	.01470	-.05050	-.02830	-.02150
+45.0	.01890	-.01870	.01010	-.01240	-.00620	-.00560	.00620	.02140	.00340	-.02310	-.03290	.00990	-.00410
+50.0	.00890	.00680	-.01050	-.00710	-.00130	.00610	-.00200	-.00350	.00070	.00890	-.00100	-.00440	-.00560
+55.0	.00470	.00210	.00500	-.00540	-.03290	-.00360	.00070	-.00870	-.00240	.00170	-.00790	-.00510	-.00990
+60.0	.00260	.01380	-.00280	-.00980	-.00030	-.00850	.00240	-.00290	-.01100	-.01160	.00160	-.00600	-.02660
+70.0	-.00780	-.00270	-.00310	-.00640	-.00250	.00550	-.00480	-.00310	.00310	0.00000	-.00280	.00070	.00830
+80.0	-.00340	-.00140	-.00390	-.00370	-.00330	-.00360	.00010	-.00150	.00050	.00040	-.00040	.00540	.00170
+90.0	-.00250	-.00250	-.00480	-.00290	-.00150	-.00230	-.00050	-.00310	-.00100	.00080	.00240	.00520	.00010

TABLE VI. - Continued

(e) $\Delta C_n, \delta_a=20^\circ$

		BETA												
ALPHA		-40.0	-30.0	-20.0	-15.0	-10.0	- 5.0	0.0	+ 5.0	+10.0	+15.0	+20.0	+30.0	+40.0
-10.0	.02470	.01335	.00205	-.00355	-.00835	-.00750	-.00640	-.00725	-.00795	-.00130	.00425	.01530	.02630	
- 5.0	.02110	.01235	.00360	-.00075	-.00860	-.00955	-.00950	-.00845	-.01015	-.00035	.00515	.01610	.02710	
0.0	.02050	.01140	.00230	-.00225	-.01115	-.01025	-.00935	-.00940	-.00865	-.00180	.00570	.02080	.03585	
+ 5.0	.02525	.01400	.00270	-.00290	-.00895	-.01035	-.00795	-.00870	-.00605	-.00045	.00490	.01560	.02625	
+10.0	.03920	.02225	.00525	-.00325	-.00615	-.00845	-.00465	-.00775	-.00615	-.00065	.01055	.03290	.05525	
+15.0	.04625	.02790	.00960	.00040	-.00835	-.00860	-.00685	-.00630	-.00470	.00090	.01440	.04130	.06825	
+20.0	.02195	.01610	.01025	.00735	.00125	-.00010	.00300	.00115	.00335	.00785	.00665	.00425	.00190	
+25.0	.00890	.00845	.00805	.00780	.00750	.00560	.00705	.00510	.00640	-.00485	-.00030	.00885	.01805	
+30.0	-.00040	.00170	.00370	.00480	.00390	.00500	.00635	.00605	.00725	-.00335	-.00865	-.01925	-.02985	
+35.0	.03035	.01975	.00915	.00385	-.00005	.00405	.00330	.00165	.00290	-.00165	.00185	.00885	.01580	
+40.0	.01020	.01025	.00465	.00430	.00315	.00370	.00295	.00375	-.00270	.00275	-.02005	.00970	.00830	
+45.0	.00335	.00480	.00990	.01140	.00405	.00465	.00390	.00760	.00340	.00535	.01315	.00900	.00490	
+50.0	.00020	.00335	.01120	.01255	.00710	.00885	.00285	.00775	.02065	.00590	.01185	.00280	.00290	
+55.0	.00050	.00160	.00550	.00905	.01235	.01120	.01000	.01230	.01230	.00975	.00670	.00215	.00190	
+60.0	.00160	.00575	.00625	.00755	.00525	.01800	.01690	.01925	.01090	.01240	.01020	.00625	-.00035	
+70.0	.00535	.00840	.01130	.01260	.01385	.02435	.02305	.01870	.01700	.01375	.01230	.00675	.00680	
+80.0	.00845	.00530	.01165	.01290	.01045	.00835	.00735	.00895	.01185	.01255	.01085	.00780	.00905	
+90.0	.00870	.00490	.01080	.01380	.01080	.00830	.00780	.01030	.01055	.01155	.01020	.00485	.00840	

TABLE VI. - Continued.

(f) $\Delta C_n, \delta_a=20^\circ, \text{lef}$

		BETA													
ALPHA		-40.0	-30.0	-20.0	-15.0	-10.0	- 5.0	0.0	+ 5.0	+10.0	+15.0	+20.0	+30.0	+40.0	
-10.0		.00545	.00415	.00285	.00215	-.00085	-.00145	-.00330	-.00050	.00150	.00165	.00120	.00035	-.00050	
- 5.0		.01370	.00785	.00200	-.00090	-.00145	-.00095	.00040	-.00245	.00215	.00110	.00115	.00130	.00150	
0.0		.01030	.00680	.00330	.00155	.00285	.00100	.00240	.00120	.00065	.00155	.00200	.00290	.00385	
+ 5.0		.01040	.00670	.00310	.00120	.00195	.00285	.00215	-.00025	.00010	.00065	.00325	.00855	.01385	
+10.0		.00595	.00460	.00325	.00260	.00235	.00360	.00150	.00260	.00410	.00135	-.00065	-.00450	-.00840	
+15.0		-.01420	-.00810	-.00205	.00100	.00425	.00505	.00780	.00240	.00165	-.00065	-.00865	-.02460	-.04060	
+20.0		-.03915	-.02535	-.01160	-.00480	-.00530	-.00390	-.00455	-.00570	-.00665	-.00870	-.00750	-.00505	-.00255	
+25.0		-.01140	-.01050	-.00960	-.00915	-.01395	-.00930	-.00900	-.00770	-.01080	-.00005	-.00400	-.01200	-.01995	
+30.0		.03510	.01880	.00260	-.00560	-.00505	-.00765	-.00720	-.00780	-.00670	.00305	.01250	.03135	.05030	
+35.0		-.01870	-.01045	-.00215	.00200	-.00010	-.00440	-.00545	-.00175	.00330	.00765	.00300	-.00620	-.01535	
+40.0		-.00045	-.00560	-.00235	.00010	.00090	-.00115	-.00285	-.00035	.00390	.00200	.04315	-.00045	.00280	
+45.0		-.00110	-.00210	-.00440	-.00150	.00230	-.00045	.00030	-.00090	-.00080	.00130	-.00290	-.00710	-.00375	
+50.0		.00345	-.00090	-.00290	.00015	.00205	-.00080	.00555	.00035	-.01310	.00090	-.00525	.00050	-.00405	
+55.0		-.00295	-.00030	-.00165	0.00000	.00040	.00515	.00300	-.00180	-.00295	.00640	.00035	.00400	-.00180	
+60.0		-.00045	-.00130	.00220	-.00165	.00120	-.00825	.00250	-.00065	.00330	.00105	-.00205	-.00060	-.00130	
+70.0		-.00210	-.00150	-.00090	-.00050	-.00025	-.00275	.00080	.00150	-.00205	-.00160	-.00095	.00055	-.00255	
+80.0		-.00105	.00045	-.00115	0.00000	.00045	.00210	.00250	0.00000	-.00075	.00025	-.00075	-.00210	.00015	
+90.0		.00195	.00100	-.00190	-.00145	-.00010	.00095	.00055	-.00160	-.00020	0.00000	0.00000	.00360	.00130	

TABLE VI. - Continued

(g) $\Delta C_{n, \delta_D=5^\circ}$

		BETA												
ALPHA		-40.0	-30.0	-20.0	-15.0	-10.0	- 5.0	0.0	+ 5.0	+10.0	+15.0	+20.0	+30.0	+40.0
-10.0	-	.00115	.00270	.00430	.00595	.00665	.00580	.00700	.00670	.00635	.00605	.00400	.00010	.00425
- 5.0	.	.00730	.00235	-.00265	-.00510	-.00580	-.00560	-.00500	-.00520	-.00670	-.00405	-.00405	-.00395	-.00385
0.0	.	.00180	-.00030	-.00245	-.00350	-.00450	-.00490	-.00660	-.00565	-.00415	-.00495	-.00345	-.00045	.00255
+ 5.0	.	.01130	.00470	-.00180	-.00515	-.00550	-.00600	-.00630	-.00495	-.00365	-.00445	-.00400	-.00315	-.00230
+10.0	.	.00110	-.00140	-.00385	-.00505	-.00600	-.00730	-.00685	-.00570	-.00565	-.00615	-.00425	-.00040	.00335
+15.0	.	.00810	.00300	-.00205	-.00465	-.00705	-.00580	-.00485	-.00655	-.00555	-.00235	0.00000	.00465	.00925
+20.0	.	.00610	.00200	-.00215	-.00420	-.00205	-.00360	-.00365	-.00540	-.00520	-.00320	-.00165	.00165	.00455
+25.0	.	.00055	-.00015	-.00080	-.00110	-.00335	-.00380	-.00280	-.00350	-.00150	-.00325	.00005	.00655	.01310
+30.0	-	.01085	-.00420	.00245	.00580	-.00050	-.00175	-.00170	-.00200	.00095	.00455	-.00230	-.01595	-.02955
+35.0	.	.01225	.00680	.00135	-.00135	.00240	.00105	.00050	.00420	.00105	-.00535	.00450	.02420	.04390
+40.0	-	.00630	.00335	.00245	.00105	.00280	.00545	.00315	.00700	.00775	.00230	.00250	.00125	.00320
+45.0	.	.00385	.00225	.00515	.00665	.00400	.00480	.00540	.00645	.00650	.00615	.00440	.00680	.00505
+50.0	.	.00735	.00285	.00615	.00535	.00855	.00695	.00630	.00890	.01235	.00825	.00575	.00455	.00295
+55.0	.	.00140	.00705	.00625	.00680	.00565	.00680	.00925	.00680	.00745	.00590	.00655	.00745	.00195
+60.0	.	.00315	.00650	.00570	.00495	.00745	.00765	.01450	.00965	.00470	.00380	.00485	.00585	.00570
+70.0	.	.00190	.00460	.00760	.00565	.00460	.00360	.00620	.00715	.00460	.00650	.00605	.00680	.00640
+80.0	.	.00575	.00830	.00490	.00530	.00400	.00430	.00515	.00475	.00495	.00585	.00580	.00715	.00565
+90.0	.	.00735	.00425	.00370	.00405	.00475	.00430	.00410	.00405	.00450	.00400	.00175	.00580	.00730

TABLE VI. - Continued

(h) $\Delta C_{n, \delta_T=30^\circ}$

		BETA												
ALPHA		-40.0	-30.0	-27.0	-15.0	-10.0	- 5.0	0.0	+ 5.0	+10.0	+15.0	+20.0	+30.0	+40.0
-10.0	-0.00995	-0.02030	-0.03065	-0.03585	-0.04415	-0.04975	-0.04780	-0.04990	-0.04215	-0.03530	-0.02795	-0.01330	0.00135	
- 5.0	0.00455	-0.01295	-0.03045	-0.03915	-0.04530	-0.05055	-0.04765	-0.04835	-0.04170	-0.03625	-0.02935	-0.01555	-0.00180	
0.0	-0.00340	-0.01725	-0.03105	-0.03800	-0.04585	-0.04990	-0.04680	-0.04710	-0.04325	-0.03710	-0.03005	-0.01585	-0.00175	
+ 5.0	-0.01145	-0.02180	-0.03215	-0.03730	-0.04570	-0.04910	-0.04750	-0.04605	-0.04205	-0.03710	-0.03025	-0.01645	-0.00260	
+10.0	-0.00940	-0.02050	-0.03165	-0.03730	-0.04490	-0.05045	-0.04650	-0.04715	-0.04385	-0.03895	-0.02655	-0.00170	0.02310	
+15.0	0.01005	-0.00820	-0.02645	-0.03555	-0.04460	-0.05010	-0.04960	-0.05045	-0.04345	-0.03330	-0.02160	0.00170	0.02495	
+20.0	-0.02370	-0.02325	-0.02275	-0.02250	-0.03765	-0.04860	-0.04785	-0.04915	-0.03955	-0.02090	-0.02335	-0.02820	-0.03305	
+25.0	-0.01135	-0.01455	-0.01775	-0.01935	-0.03280	-0.04970	-0.04860	-0.04880	-0.03340	-0.01600	-0.02210	-0.03435	-0.04660	
+30.0	-0.00480	-0.00950	-0.01415	-0.01650	-0.01885	-0.04255	-0.05000	-0.04280	-0.01845	-0.01850	-0.01125	0.00325	0.01775	
+35.0	-0.01570	-0.01265	-0.00950	-0.00795	-0.02190	-0.03655	-0.04115	-0.02840	-0.02700	-0.01795	-0.00835	0.01080	0.02995	
+40.0	-0.01230	-0.01225	-0.00480	-0.00780	-0.02260	-0.02455	-0.03650	-0.02800	-0.01810	-0.01290	0.02110	-0.01010	-0.01825	
+45.0	-0.01660	-0.00320	-0.00755	-0.00070	-0.01430	-0.01790	-0.01800	-0.01080	-0.01205	-0.01015	0.00580	-0.00405	-0.01395	
+50.0	-0.00900	-0.00120	-0.00490	-0.00170	-0.00470	-0.00655	-0.00585	-0.00275	-0.00595	-0.00365	-0.00410	-0.00165	-0.00385	
+55.0	-0.00290	-0.00025	-0.00910	-0.00115	-0.00145	-0.00410	-0.00425	-0.00330	-0.00280	-0.00460	-0.00450	-0.00190	-0.00190	
+60.0	-0.00365	0.00090	-0.00170	-0.00130	-0.00335	0.00055	-0.00165	-0.00380	-0.00250	-0.00425	-0.00475	-0.00180	-0.00370	
+70.0	-0.00135	-0.00495	-0.00210	-0.00260	-0.00155	-0.00130	-0.00520	0.00000	-0.00305	-0.00115	-0.00285	-0.00250	-0.00255	
+80.0	-0.00360	-0.00265	-0.00180	-0.00320	-0.00425	-0.00470	-0.00525	-0.00455	-0.00555	-0.00310	-0.00275	-0.00255	-0.00580	
+90.0	-0.00145	-0.00435	-0.00330	-0.00280	-0.00325	-0.00370	-0.00495	-0.00325	-0.00220	-0.00345	-0.00235	-0.00385	-0.00305	

TABLE VI. - Concluded

(i) C_{np} , $\Delta C_{np,lef}$, C_{nr} , and $\Delta C_{nr,lef}$

α , deg	C_{np}	$\Delta C_{np,lef}$	C_{nr}	$\Delta C_{nr,lef}$
-10.0	-.0006	.0615	-.5170	.1370
- 5.0	.0424	.0091	-.4610	.0980
0.0	-.0075	.0610	-.4140	.0370
+ 5.0	-.0214	.0129	-.3970	.0160
+10.0	-.0744	.0439	-.3730	.0070
+15.0	-.0997	.0512	-.3630	.0140
+20.0	-.0726	-.0294	-.4780	-.1030
+25.0	-.0621	.0017	-.5820	-.0980
+30.0	.0184	.0584	-.7200	-.3100
+35.0	.1580	.2110	-.6370	-.4370
+40.0	-.0671	.3920	-1.0200	.1670
+45.0	-.3040	.1960	-.0762	.0840
+50.0	.4370	0.0000	-.5410	0.0000
+55.0	.1590	0.0000	-.1850	0.0000
+60.0	.5250	0.0000	-.1900	0.0000
+70.0	-.1110	0.0000	-.2800	0.0000
+80.0	.0895	0.0000	-.0311	0.0000
+90.0	.0559	0.0000	-.1310	0.0000

TABLE VII. - Continued

(c) $\Delta C_{L, \delta_H=25^\circ}$

		BETA												
ALPHA		-40.0	-30.0	-20.0	-15.0	-10.0	- 5.0	0.0	+ 5.0	+10.0	+15.0	+20.0	+30.0	+40.0
-10.0		-.00850	-.00230	.00390	.00690	.00220	.00040	-.00180	-.01150	-.01570	-.01360	-.01830	-.02770	-.03700
- 5.0		.01430	.00870	.00310	.00020	.00130	.00010	.00170	-.00950	-.00730	-.01080	-.01450	-.02190	-.02920
0.0		.00290	.00310	.00320	.00330	.00240	.00200	.00510	-.00410	-.00630	-.00410	-.00830	-.01670	-.02510
+ 5.0		.01180	.00750	.00310	.00090	.00010	.00100	.00110	-.00170	-.00750	-.00330	-.00090	.00390	.00880
+10.0		.02700	.01730	.00760	.00280	.00100	.00010	-.00210	.00360	.00410	.00110	.00070	-.00010	-.00100
+15.0		.01890	.01210	.00530	.00200	.00300	.00050	.00050	.00990	.00830	.00460	.00290	-.00050	-.00390
+20.0		-.00210	-.00230	-.00240	-.00250	.00100	.00080	-.00140	.00600	.00430	.00410	.00460	.00550	.00630
+25.0		-.03040	-.01900	-.00760	-.00180	-.00650	-.00670	.00140	.00990	.00630	.00290	.00660	.01400	.02140
+30.0		.00760	.00390	.00030	-.00160	-.01010	-.00500	.00040	.01150	.01140	.00620	.01590	.03520	.05450
+35.0		-.04390	-.01300	.00320	.00740	-.00850	.00180	.00150	.00410	.01580	-.00620	.00540	.02950	.07050
+40.0		-.01770	-.00040	.00430	.00170	-.00050	.00320	-.00420	-.01110	.00050	.00240	-.01410	.00280	.00090
+45.0		.03460	-.01060	.00220	.00640	.00420	.00400	.00270	-.00930	-.00480	-.01130	-.00910	-.00050	-.04230
+50.0		.03100	.02420	-.00100	.00140	.00300	0.00000	-.00150	-.00050	-.00510	-.00090	-.01370	-.00910	-.01950
+55.0		.00090	.00100	.00010	0.00000	-.00760	.00600	.00840	-.00110	.00530	-.00300	-.00440	.00050	.00930
+60.0		-.00360	-.00200	.00150	-.00430	-.00160	.00040	-.00060	-.00390	-.00290	.00350	.00270	0.00000	.00430
+70.0		.00530	.00590	-.00110	.00100	-.00430	-.00060	.00170	-.00180	.00280	.00160	-.00100	-.00650	-.00790
+80.0		.00330	-.00180	-.00150	.00110	-.00190	.00270	.00100	.00530	.00020	-.00100	.00230	.00180	0.00000
+90.0		-.01830	-.00980	-.00230	-.00050	-.00120	.00130	.00060	-.00140	.00100	.00020	.00170	.01100	.00640

TABLE VII.- Continued

(d) $\Delta C_{l,lef}$

		BETA												
ALPHA		-40.0	-30.0	-20.0	-15.0	-10.0	- 5.0	0.0	+ 5.0	+10.0	+15.0	+20.0	+30.0	+40.0
-10.0		-.02250	-.01600	-.00940	-.00620	-.00870	-.00460	-.00170	-.00890	-.00500	-.00080	-.00460	-.01240	-.02000
- 5.0		-.01320	-.01230	-.01130	-.01100	-.00930	-.00810	.00290	-.00480	.00380	-.00180	.00150	.00810	.01470
0.0		.02230	.01050	.00260	-.00430	-.00080	-.00230	-.00020	-.00490	-.00310	-.00190	-.00700	-.01730	-.02760
+ 5.0		.01830	.01320	.00810	.00550	.00350	.00480	-.00010	-.00320	-.00730	-.00560	-.00450	-.00230	-.00010
+10.0		.01910	.01300	.00680	.00380	.00150	.00120	-.00170	.00400	.00170	.00600	-.00100	-.01480	-.02870
+15.0		-.01000	-.00880	-.00760	-.00700	-.00580	-.00450	-.00120	.01150	.01260	.00850	.01750	.03550	.05350
+20.0		.00570	-.01690	-.03950	-.05080	-.03420	-.01740	-.00150	.01780	.02920	.04260	.04600	.05280	.05950
+25.0		-.02530	-.03160	-.03790	-.04100	-.03030	-.01350	.00130	.01520	.03910	.05410	.04700	.03300	.01900
+30.0		-.11100	-.06950	-.02790	-.00710	-.01800	-.01010	.00220	.01570	.01520	.02120	.03540	.06400	.09250
+35.0		-.11360	-.05680	-.01460	.00250	.01290	.00820	-.00050	-.00500	.01520	-.00930	-.00480	.00490	.03150
+40.0		-.02050	-.02730	-.00860	-.01150	-.00100	.01170	-.00040	-.02030	-.01190	-.00700	-.01660	.02100	.00900
+45.0		.00080	-.00900	-.00370	-.00430	-.00110	.00720	.01130	-.00590	-.01080	-.01240	-.00150	.00120	-.01430
+50.0		.00670	.00480	-.00020	.00040	.00130	.00030	-.00080	.00120	.00070	.00160	-.01480	.00620	.00140
+55.0		-.00760	-.01080	-.00360	0.00000	-.00660	.00240	.00850	-.00230	.00440	-.00370	-.00180	.00990	.01550
+60.0		-.00740	-.01040	-.00140	-.00550	-.00390	-.00090	0.00000	-.00070	.00040	.00520	.00320	.00610	.01020
+70.0		-.00220	-.00390	-.00260	.00050	-.00060	-.00380	.00120	.00140	-.00060	.00020	.00030	.00030	-.00070
+80.0		-.00770	-.00850	-.00400	.00180	-.00200	0.00000	.00070	.00250	.00030	-.00050	.00270	-.00160	.00280
+90.0		-.01160	-.00670	-.00180	-.00090	.00360	.00010	-.00030	-.00150	-.00180	-.00080	.00090	-.00010	.00430

TABLE VII. - Continued

(e) $\Delta C_{l, \delta_a=20^\circ}$

ALPHA	BETA													
	-40.0	-30.0	-20.0	-15.0	-10.0	- 5.0	0.0	+ 5.0	+10.0	+15.0	+20.0	+30.0	+40.0	
-10.0	-.01915	-.02575	-.03235	-.03565	-.03170	-.03085	-.02865	-.02885	-.03060	-.03500	-.03325	-.02985	-.02635	
- 5.0	-.03150	-.03250	-.03350	-.03400	-.03245	-.03395	-.03620	-.03660	-.03510	-.03550	-.03425	-.03185	-.02935	
0.0	-.02770	-.03220	-.03680	-.03905	-.03970	-.04095	-.04120	-.03985	-.04125	-.04125	-.03715	-.02885	-.02055	
+ 5.0	-.05340	-.04830	-.04315	-.04060	-.04130	-.04225	-.04685	-.04055	-.04050	-.04015	-.04170	-.04480	-.04790	
+10.0	-.05110	-.04585	-.04065	-.03800	-.04130	-.04265	-.04535	-.04360	-.04180	-.03765	-.04060	-.04655	-.05250	
+15.0	-.00760	-.02110	-.03460	-.04135	-.04200	-.04360	-.04750	-.04425	-.04125	-.04010	-.03455	-.02355	-.01260	
+20.0	-.00410	-.01740	-.03075	-.03740	-.03845	-.03790	-.03685	-.03745	-.03705	-.03565	-.03515	-.03415	-.03315	
+25.0	-.03365	-.03090	-.02820	-.02685	-.03040	-.03140	-.03405	-.03290	-.03195	-.02515	-.02405	-.02185	-.01970	
+30.0	.02530	.00725	-.01085	-.01990	-.01975	-.02405	-.02535	-.02510	-.01945	-.01315	-.00730	.00440	.01610	
+35.0	-.05610	-.03720	-.01835	-.00895	-.00855	-.01520	-.01745	-.01365	-.01130	-.00860	-.01065	-.01490	-.01905	
+40.0	-.01945	-.01260	-.01130	-.01085	-.01120	-.01040	-.01360	-.00855	-.00630	-.00710	-.01250	-.01870	-.01600	
+45.0	-.00865	-.00645	-.01015	-.01070	-.00910	-.01135	-.00905	-.00900	-.00840	-.00935	-.00950	-.00835	-.00880	
+50.0	-.00465	-.01150	-.00555	-.01005	-.00970	-.00890	-.00950	-.01075	-.00650	-.01080	-.01135	-.00965	-.00780	
+55.0	-.00580	-.00720	-.00780	-.00820	-.00865	-.00870	-.00890	-.00915	-.01000	-.00880	-.00690	-.00765	-.01065	
+60.0	-.00965	-.00750	-.00715	-.00660	-.00850	-.00850	-.00840	-.00815	-.00825	-.00815	-.00635	-.00620	-.00975	
+70.0	-.00790	-.00195	-.00360	-.00595	-.00945	-.01300	-.01150	-.01265	-.01255	-.00730	-.00430	-.00345	-.00770	
+80.0	-.00445	-.00430	-.00300	-.00450	-.00445	-.00390	-.00180	-.00390	-.00420	-.00425	-.00420	-.00635	-.00565	
+90.0	-.00200	.00060	-.00185	-.00155	-.00290	-.00155	-.00230	-.00095	-.00165	-.00225	-.00160	-.00015	-.00390	

TABLE VII.- Continued

(f) $\Delta C_{l, \delta_a=20^\circ, \text{lef}}$

		BETA												
		-40.0	-30.0	-20.0	-15.0	-10.0	- 5.0	0.0	+ 5.0	+10.0	+15.0	+20.0	+30.0	+40.0
ALPHA														
-10.0		-.02355	-.01590	-.00830	-.00445	-.00590	-.00830	-.01030	-.01145	-.00895	-.00555	-.00740	-.01120	-.01500
- 5.0		-.00885	-.01050	-.01210	-.01290	-.01195	-.01375	-.00780	-.00840	-.01115	-.01420	-.01155	-.00620	-.00090
0.0		-.00965	-.00860	-.00740	-.00685	-.00330	-.00420	-.00415	-.00650	-.00505	-.00390	-.00575	-.00955	-.01345
+ 5.0		.01485	.00785	.00085	-.00265	-.00120	.00035	.00220	-.00375	-.00340	-.00215	.00055	.00595	.01135
+10.0		.00650	.00350	.00055	-.00105	.00280	.00160	.00125	.00390	.00165	.00080	-.00110	-.00485	-.00860
+15.0		-.02330	-.01180	-.00035	.00540	.00605	.00755	.01175	.00785	.00505	.00685	.00125	-.00990	-.02095
+20.0		-.00220	.00265	.00755	.01000	.01335	.01335	.01385	.01405	.01285	.00855	.01050	.01445	.01830
+25.0		-.00470	.00340	.01155	.01560	.01650	.01375	.01460	.01415	.01770	.01130	.01160	.01225	.01290
+30.0		-.06110	-.03250	-.00385	.01050	.00845	.00960	.00890	.01150	.00625	.00285	-.00600	-.02385	-.04165
+35.0		.01050	.00570	.00095	-.00140	-.00090	.00395	.00535	.00345	-.00355	-.00410	-.00170	.00320	.00805
+40.0		.00665	.00085	.00030	-.00050	-.00115	-.00040	.00120	-.00270	-.00155	-.00400	.00775	.00675	-.00015
+45.0		-.00200	-.00015	-.00075	-.00135	.00005	.00115	-.00100	.00040	.00145	.00025	-.00165	-.00295	-.00205
+50.0		-.00630	-.00050	-.00540	-.00030	-.00085	-.00025	-.00150	.00195	-.00385	-.00075	.00230	-.00275	.00085
+55.0		-.00230	-.00160	.00040	.00010	.00030	.00085	.00170	-.00090	-.00060	.00030	-.00155	-.00110	.00075
+60.0		.00185	.00145	-.00075	-.00065	.00070	-.00050	-.00135	-.00025	-.00030	-.00105	-.00135	-.00090	.00295
+70.0		.00085	-.00105	-.00155	.00155	.00485	.00180	.00185	.00110	.00465	.00190	-.00095	.00105	.00140
+80.0		-.00040	.00005	.00075	.00185	.00080	.00095	-.00095	.00070	.00145	.00050	.00145	.00280	.00020
+90.0		-.00230	-.00110	-.00075	.00110	.00070	0.00000	-.00025	-.00125	-.00145	.00035	-.00015	-.00015	-.00190

TABLE VII. - Continued

(g) $\Delta C_{l, \delta_D=5^\circ}$

		BETA													
		-40.0	-30.0	-20.0	-15.0	-10.0	- 5.0	0.0	+ 5.0	+10.0	+15.0	+20.0	+30.0	+40.0	
ALPHA															
-10.0		-.01070	-.00850	-.00620	-.00510	-.00445	-.00660	-.00565	-.00455	-.00730	-.00440	-.00475	-.00545	-.00610	
- 5.0		-.00625	-.00605	-.00585	-.00575	-.00525	-.00565	-.00605	-.00740	-.00480	-.00590	-.00700	-.00910	-.01120	
0.0		-.00065	-.00315	-.00560	-.00685	-.00630	-.00700	-.00630	-.00435	-.00510	-.00675	-.00605	-.00485	-.00355	
+ 5.0		-.01205	-.00930	-.00660	-.00525	-.00690	-.00380	-.00605	-.00545	-.00740	-.00565	-.00710	-.01000	-.01290	
+10.0		-.01760	-.01335	-.00910	-.00700	-.00665	-.00420	-.00625	-.00625	-.00715	-.00535	-.00825	-.01405	-.01990	
+15.0		-.00695	-.00670	-.00655	-.00640	-.00825	-.00555	-.00525	-.00685	-.00570	-.00535	-.00600	-.00725	-.00850	
+20.0		.00175	-.00185	-.00550	-.00725	-.00595	-.00585	-.00565	-.00510	-.00530	-.00525	-.00460	-.00340	-.00225	
+25.0		.00115	-.00125	-.00365	-.00490	-.00625	-.00535	-.00590	-.00475	-.00555	-.00130	-.00330	-.00735	-.01130	
+30.0		.02845	.01365	-.00120	-.00855	-.00660	-.00720	-.00550	-.00580	-.00650	-.00255	.00315	.01455	.02590	
+35.0		-.00405	-.00275	-.00140	-.00070	-.00560	-.00745	-.00800	-.00850	-.00465	.00150	-.00230	-.00985	-.01740	
+40.0		.01205	.00150	0.00000	-.00135	-.00105	-.00540	-.00540	-.00810	-.00385	-.00160	-.00290	.00120	-.00445	
+45.0		0.00000	-.00095	-.00090	.00010	-.00095	-.00225	-.00220	.00025	-.00005	.00020	-.00110	-.00250	-.00260	
+50.0		-.00565	.00125	-.00045	-.00130	-.00015	-.00075	-.00110	-.00270	-.00050	-.00140	-.00065	.00015	.00085	
+55.0		.00005	-.00210	.00015	-.00115	-.00240	-.00260	-.00275	-.00285	-.00290	-.00425	-.00250	-.00060	-.00075	
+60.0		-.00070	-.00170	-.00210	-.00155	-.00195	-.00195	-.00260	-.00195	-.00145	-.00195	-.00170	-.00180	.00045	
+70.0		-.00115	.00105	-.00205	-.00250	-.00215	-.00345	-.00455	-.00570	-.00600	-.00250	-.00210	-.00070	-.00375	
+80.0		-.00430	-.00625	-.00100	-.00145	-.00055	-.00055	-.00170	-.00220	-.00105	-.00070	-.00165	-.00420	-.00470	
+90.0		-.00695	-.00220	.00050	.00040	.00085	.00015	-.00030	.00045	-.00085	-.00090	-.00110	-.00080	-.00855	

TABLE VII. - Continued

(h) $\Delta C_L, \delta_r=30^\circ$

		BETA												
ALPHA		-40.0	-30.0	-20.0	-15.0	-10.0	- 5.0	0.0	+ 5.0	+10.0	+15.0	+20.0	+30.0	+40.0
-10.0	.00240	.00660	.01080	.01290	.01590	.01840	.01725	.01885	.01460	.01125	.00865	.00350	-.00165	
- 5.0	-.00070	.00485	.01035	.01315	.01490	.01860	.01800	.01800	.01480	.01055	.00800	.00290	-.00220	
0.0	-.00655	.00055	.00760	.01110	.01375	.01605	.01905	.01585	.01360	.01075	.00975	.00770	.00565	
+ 5.0	-.00290	.00330	.00950	.01260	.01535	.01580	.01505	.01410	.01265	.01030	.00865	.00545	.00225	
+10.0	.00010	.00440	.00880	.01100	.01370	.01570	.01455	.01645	.01450	.00805	.00865	.00985	.01105	
+15.0	.00170	.00410	.00660	.00780	.01155	.01550	.01430	.01495	.01390	.00995	.00540	-.00360	-.01265	
+20.0	.00370	.00495	.00625	.00685	.01000	.01280	.01365	.01365	.00910	.00490	.00530	.00605	.00680	
+25.0	.00030	.00190	.00345	.00425	.00665	.01400	.01300	.01225	.00600	.00335	.00530	.00920	.01310	
+30.0	.02625	.01560	.00505	-.00025	.00075	.00910	.01245	.00830	.00095	.00455	.00325	.00055	-.00210	
+35.0	.01320	.00835	.00350	.00110	.00600	.00760	.01065	.00600	.00965	.00465	.00150	-.00480	-.01110	
+40.0	-.00485	.00385	.00315	.00515	.00790	.00600	.01025	.00720	.00785	.00580	.00435	.00350	.01245	
+45.0	.00300	.00145	.00035	.00545	.00470	.00490	.00515	.00215	.00245	.00300	.00305	.00075	.00080	
+50.0	.00220	-.00070	-.00065	.00185	.00225	.00030	.00160	.00120	.00260	.00140	.00360	-.00065	-.00300	
+55.0	-.00040	.00080	.00060	.00155	.00175	.00090	.00065	.00185	-.00030	.00110	.00130	.00185	.00125	
+60.0	.00215	.00065	.00125	.00100	.00135	.00145	.00095	.00080	.00060	.00035	.00015	.00005	.00150	
+70.0	.00025	.00040	-.00050	.00075	.00150	-.00030	.00270	.00025	.00145	.00040	-.00085	.00040	.00065	
+80.0	.00100	.00025	.00015	.00120	-.00010	.00065	.00025	.00150	.00045	.00015	-.00085	-.00020	.00280	
+90.0	.00190	.00110	-.00025	.00115	.00255	.00005	-.00005	.00140	.00210	.00025	-.00095	.00070	-.00075	

TABLE VII. - Concluded

(i) C_{lp} , $\Delta C_{lp,lef}$, C_{lr} , and $\Delta C_{lr,lef}$

α , deg	C_{lp}	$\Delta C_{lp,lef}$	C_{lr}	$\Delta C_{lr,lef}$
-10.0	-.3660	.0060	-.1550	.0290
- 5.0	-.3770	.0180	-.2010	.1750
0.0	-.3450	-.1000	-.0024	.0665
+ 5.0	-.4340	.0200	.0880	.0360
+10.0	-.4080	.0580	.2050	.0070
+15.0	-.3880	.0870	.2200	.0660
+20.0	-.3290	.0270	.3190	.2010
+25.0	-.2940	-.0560	.4370	.0060
+30.0	-.3170	-.0820	.6800	-.0680
+35.0	-.9010	.3620	.1000	-.5370
+40.0	-.0568	.1940	.4470	-.7870
+45.0	.5940	.0970	-.3300	-.3940
+50.0	-.0218	0.0000	-.0680	0.0000
+55.0	-.2160	0.0000	.1180	0.0000
+60.0	-.2500	0.0000	.0802	0.0000
+70.0	-.2130	0.0000	.0529	0.0000
+80.0	-.2330	0.0000	.0868	0.0000
+90.0	-.2030	0.0000	-.0183	0.0000

TABLE VIII.- THRUST VALUES USED IN SIMULATION

(a) SI Units

Mach number	Thrust in N at altitude in m of -								
	0	1524	3048	4572	6096	7620	9144	10 668	12 192
T_{idle}									
0.0	4 537	3 777	3 123	2 562	2 086	1 686	1 348	1 072	841
.1	3 736	3 109	2 571	2 108	1 717	1 388	1 112	881	694
.2	3 114	2 589	2 140	1 757	1 432	1 157	925	734	578
.3	2 313	1 926	1 592	1 308	1 063	859	689	547	431
.4	1 157	961	796	654	534	431	343	271	214
.5	0	0	0	0	0	0	0	0	0
.6	↓	↓	↓	↓	↓	↓	↓	↓	↓
.7	↓	↓	↓	↓	↓	↓	↓	↓	↓
.8	↓	↓	↓	↓	↓	↓	↓	↓	↓
.9	↓	↓	↓	↓	↓	↓	↓	↓	↓
1.0	↓	↓	↓	↓	↓	↓	↓	↓	↓
T_{mil}									
0.0	46 715	38 873	32 134	26 373	21 485	17 357	13 901	11 023	8 318
.1	46 715	39 362	32 886	27 281	22 455	18 331	14 830	11 881	9 021
.2	47 178	40 069	33 802	28 299	23 504	19 354	15 791	12 753	9 742
.3	49 148	41 884	35 439	29 759	24 790	20 471	16 743	13 558	10 395
.4	50 612	43 357	36 871	31 106	26 026	21 583	17 726	14 412	11 089
.5	52 578	45 132	38 455	32 503	27 241	22 628	18 616	15 155	11 694
.6	54 713	47 044	40 145	33 984	28 522	23 722	19 541	15 925	12 317
.7	55 923	48 348	41 466	35 270	29 732	24 834	20 533	16 801	13 042
.8	56 207	49 028	42 396	36 333	30 844	25 929	21 569	17 748	13 834
.9	57 208	50 349	43 895	37 894	32 392	27 397	22 922	18 958	14 830
1.0	57 867	51 524	45 381	39 540	34 073	29 038	24 456	20 351	15 969
T_{max}									
0.0	79 178	65 883	54 460	44 705	36 413	29 421	23 558	18 682	14 096
.1	82 096	69 054	57 693	47 858	39 393	32 161	26 018	20 840	15 831
.2	85 464	72 595	61 234	51 266	42 578	35 061	28 607	23 104	17 646
.3	92 038	78 435	66 367	55 732	46 422	38 330	31 356	25 390	19 465
.4	97 896	83 867	71 314	60 171	50 345	41 747	34 291	27 877	21 449
.5	105 365	90 446	77 061	65 135	54 597	45 350	37 307	30 372	23 433
.6	113 274	97 398	83 115	70 357	59 050	49 113	40 452	32 975	25 497
.7	119 751	103 532	88 795	75 522	63 667	53 174	43 971	35 973	27 926
.8	124 354	108 470	93 795	80 379	68 240	57 364	47 721	39 260	30 604
.9	130 911	115 222	100 445	86 718	74 121	62 693	52 453	43 379	33 940
1.0	136 480	121 521	107 033	93 252	80 362	68 480	57 680	48 001	37 659

TABLE VIII.- Concluded

(b) U.S. Customary Units

Mach number	Thrust in lb at altitude in ft of -								
	0	5000	10 000	15 000	20 000	25 000	30 000	35 000	40 000
T_{idle}									
0.0	1 020	849	702	576	469	379	303	241	189
.1	840	699	578	474	386	312	250	198	156
.2	700	582	481	395	322	260	208	165	130
.3	520	433	358	294	239	193	155	123	97
.4	260	216	179	147	120	97	77	61	48
.5	0	0	0	0	0	0	0	0	0
.6	↓	↓	↓	↓	↓	↓	↓	↓	↓
.7	↓	↓	↓	↓	↓	↓	↓	↓	↓
.8	↓	↓	↓	↓	↓	↓	↓	↓	↓
.9	↓	↓	↓	↓	↓	↓	↓	↓	↓
1.0	↓	↓	↓	↓	↓	↓	↓	↓	↓
T_{mil}									
0.0	10 502	8 739	7 224	5 929	4 830	3 902	3 125	2 478	1870
.1	10 502	8 849	7 393	6 133	5 048	4 121	3 334	2 671	2028
.2	10 606	9 008	7 599	6 362	5 284	4 351	3 550	2 867	2190
.3	11 049	9 416	7 967	6 690	5 573	4 602	3 764	3 048	2337
.4	11 378	9 747	8 289	6 993	5 851	4 852	3 985	3 240	2493
.5	11 820	10 146	8 645	7 307	6 124	5 087	4 185	3 407	2629
.6	12 300	10 576	9 025	7 640	6 412	5 333	4 393	3 580	2769
.7	12 572	10 869	9 322	7 929	6 684	5 583	4 616	3 777	2932
.8	12 636	11 022	9 531	8 168	6 934	5 829	4 849	3 990	3110
.9	12 861	11 319	9 868	8 519	7 282	6 159	5 153	4 262	3334
1.0	13 009	11 583	10 202	8 889	7 660	6 528	5 498	4 575	3590
T_{max}									
0.0	17 800	14 811	12 243	10 050	8 186	6 614	5 296	4 200	3169
.1	18 456	15 524	12 970	10 759	8 856	7 230	5 849	4 685	3559
.2	19 213	16 320	13 766	11 525	9 572	7 882	6 431	5 194	3967
.3	20 691	17 633	14 920	12 529	10 436	8 617	7 049	5 708	4376
.4	22 008	18 854	16 032	13 527	11 318	9 385	7 709	6 267	4822
.5	23 687	20 333	17 324	14 643	12 274	10 195	8 387	6 828	5268
.6	25 465	21 896	18 685	15 817	13 275	11 041	9 094	7 413	5732
.7	26 921	23 275	19 962	16 978	14 313	11 954	9 885	8 087	6278
.8	27 956	24 385	21 086	18 070	15 341	12 896	10 728	8 826	6880
.9	29 430	25 903	22 581	19 495	16 663	14 094	11 792	9 752	7630
1.0	30 682	27 319	24 062	20 964	18 066	15 395	12 967	10 791	8466

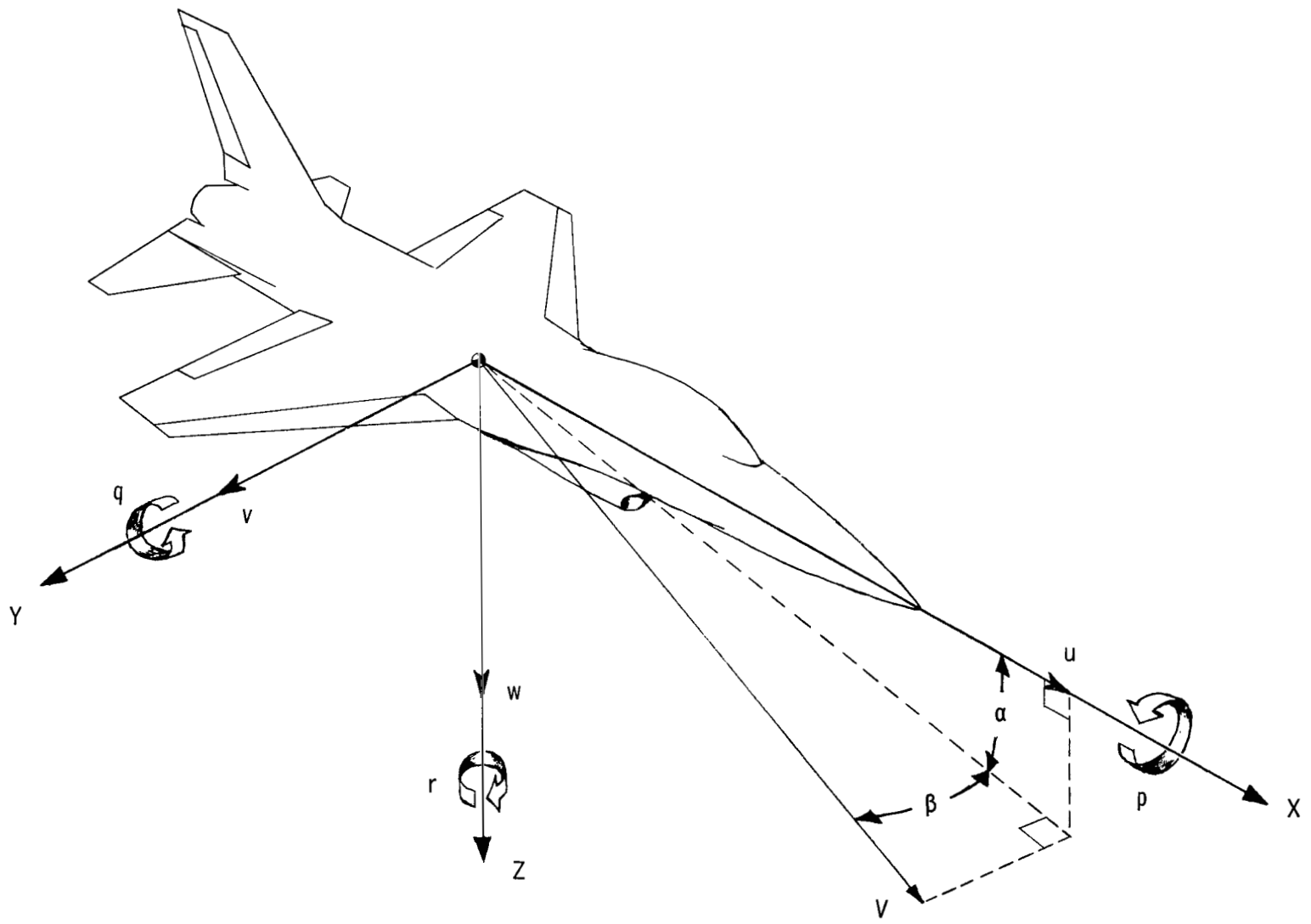


Figure 1.- The body system of axes.

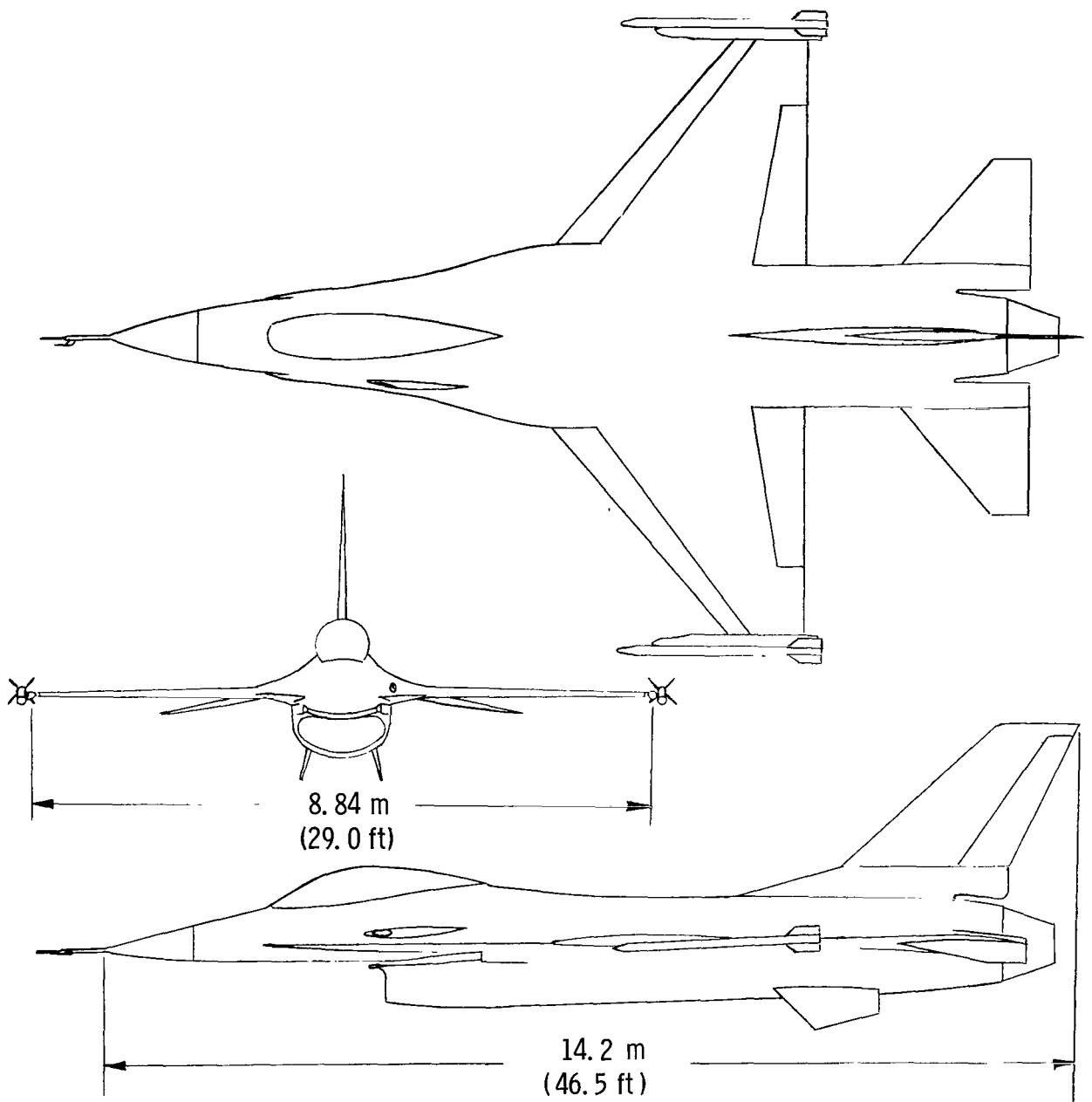
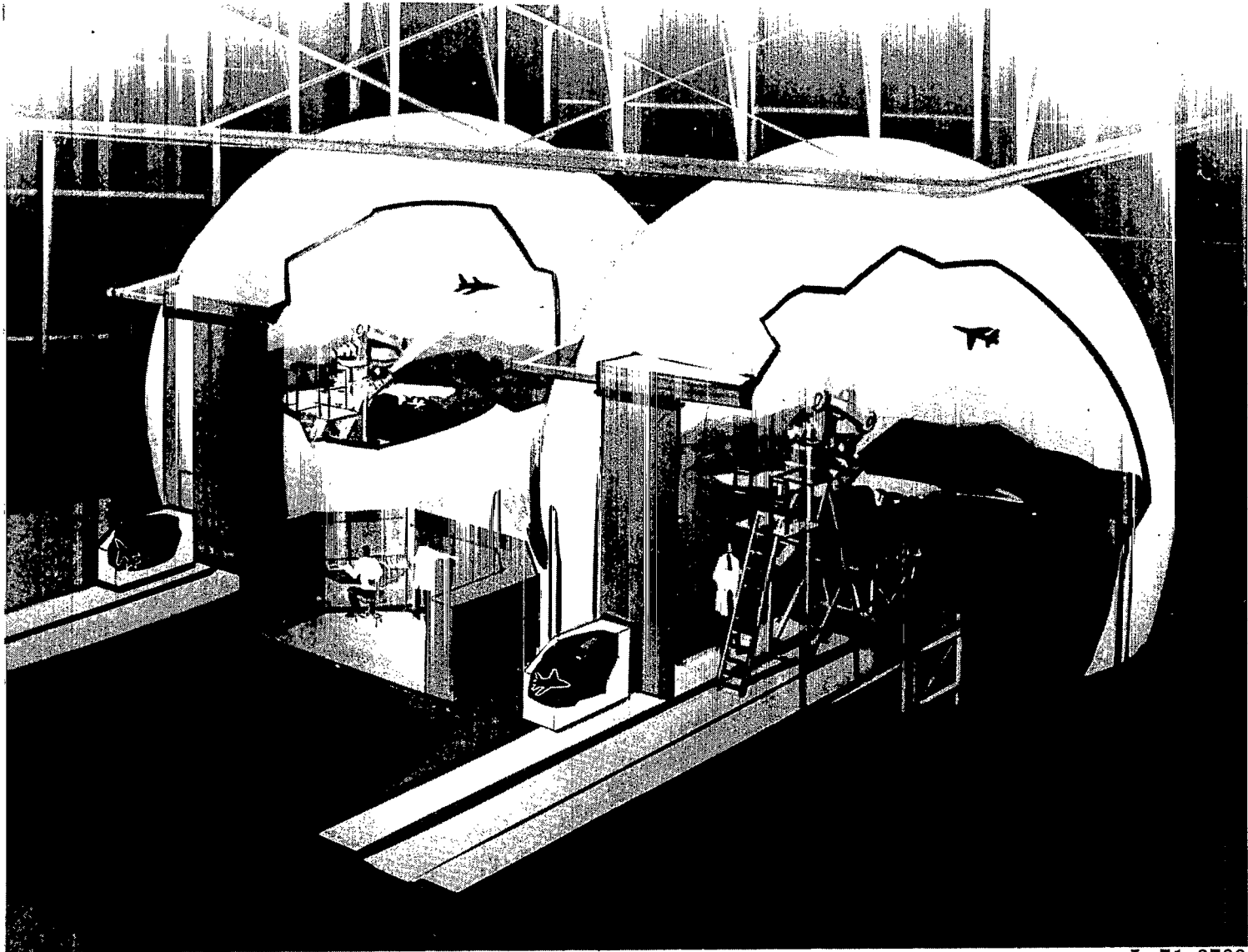
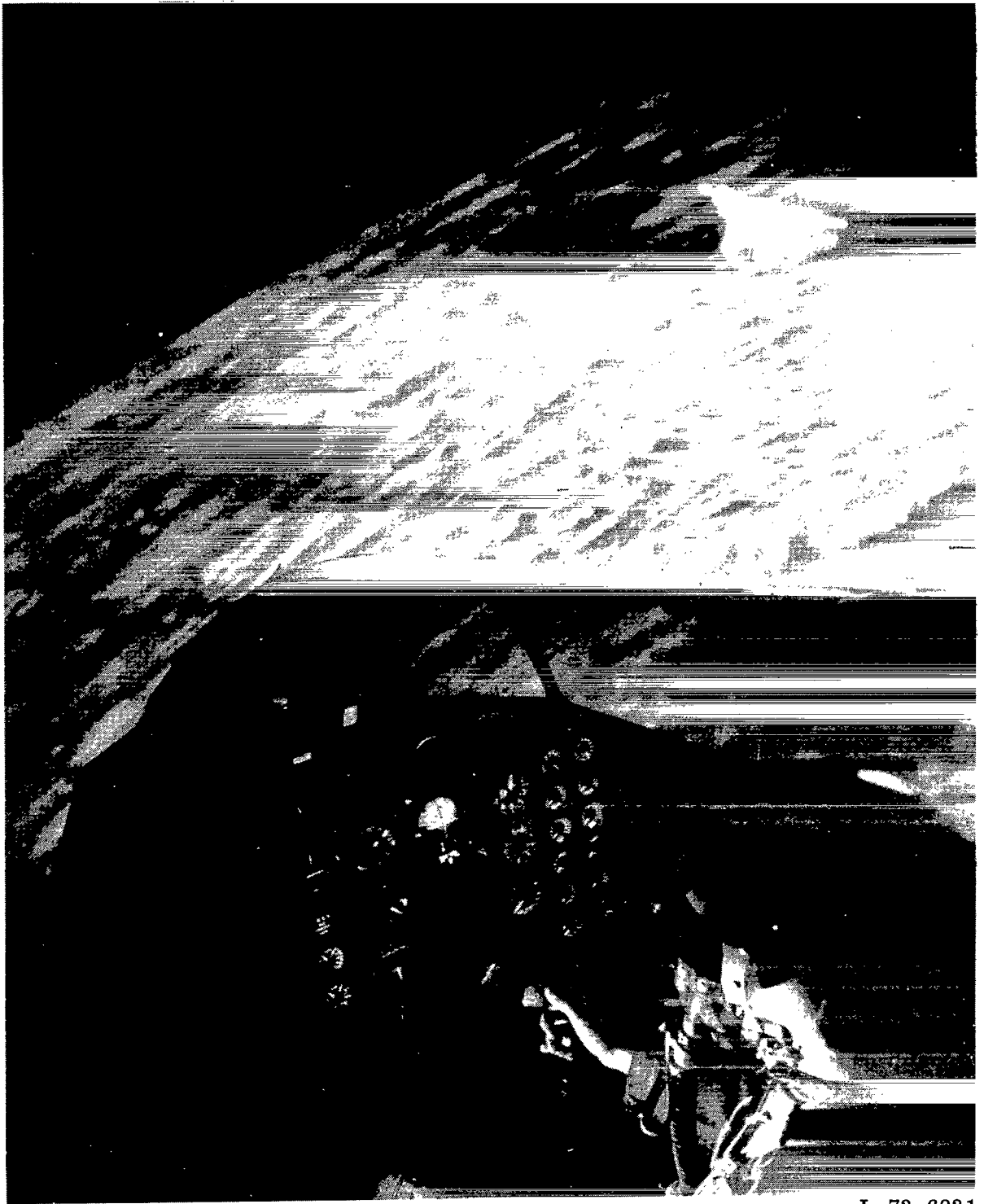


Figure 2. - Three-view sketch of airplane configuration.



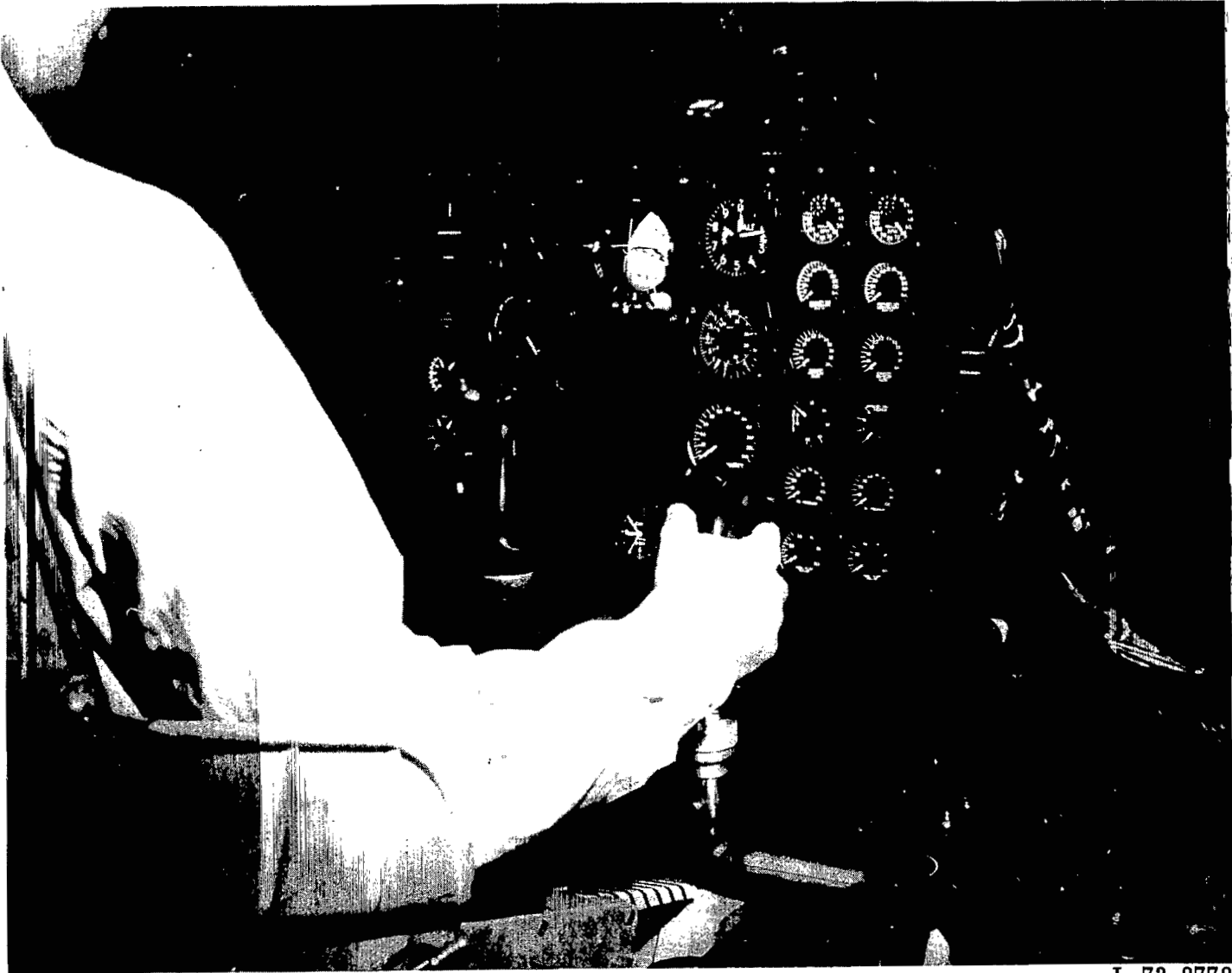
L-71-8700

Figure 3.- General arrangement of the Langley differential maneuvering simulator (DMS) facility.



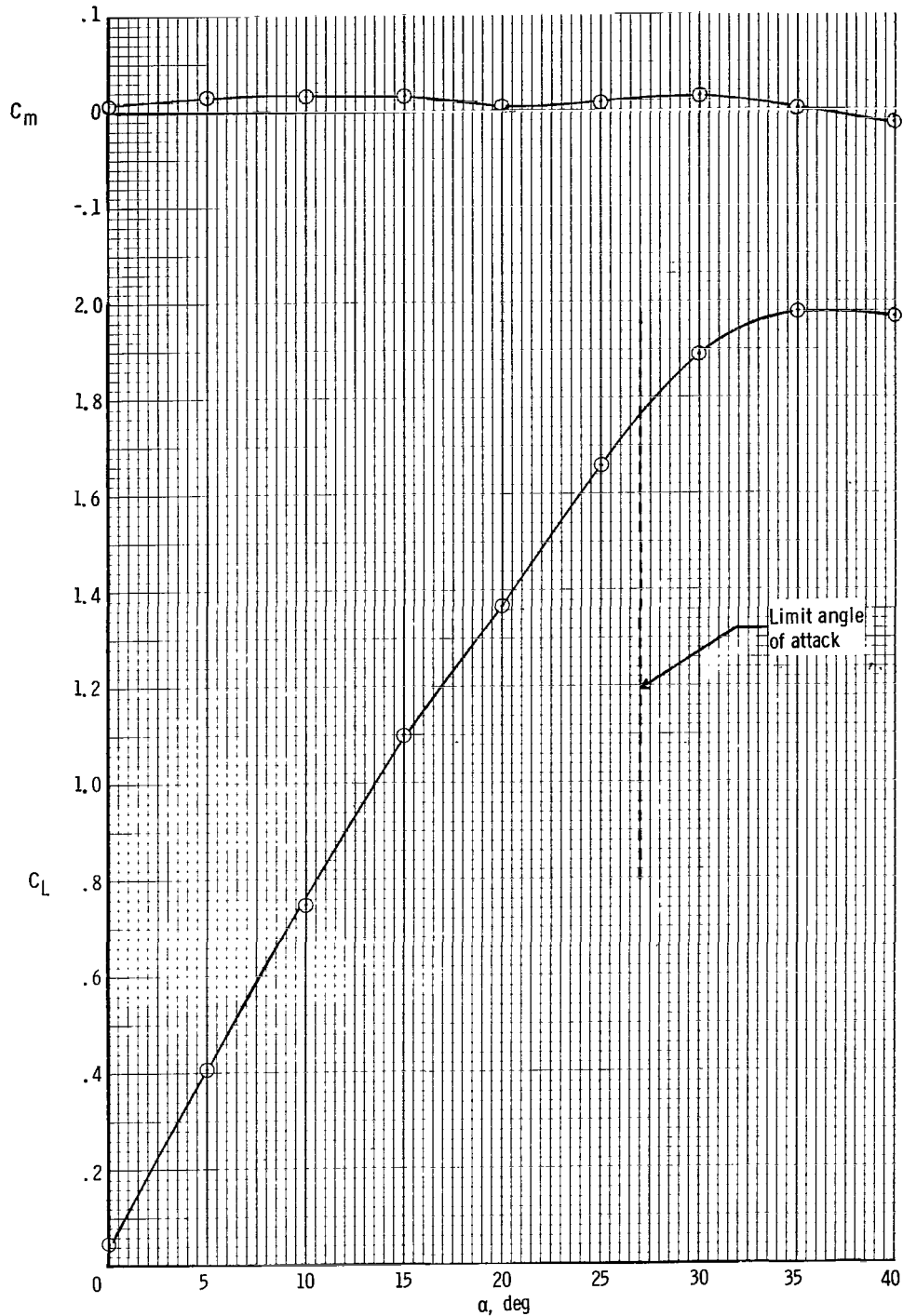
L-73-6831

Figure 4.- View of cockpit and visual display within one sphere of DMS.



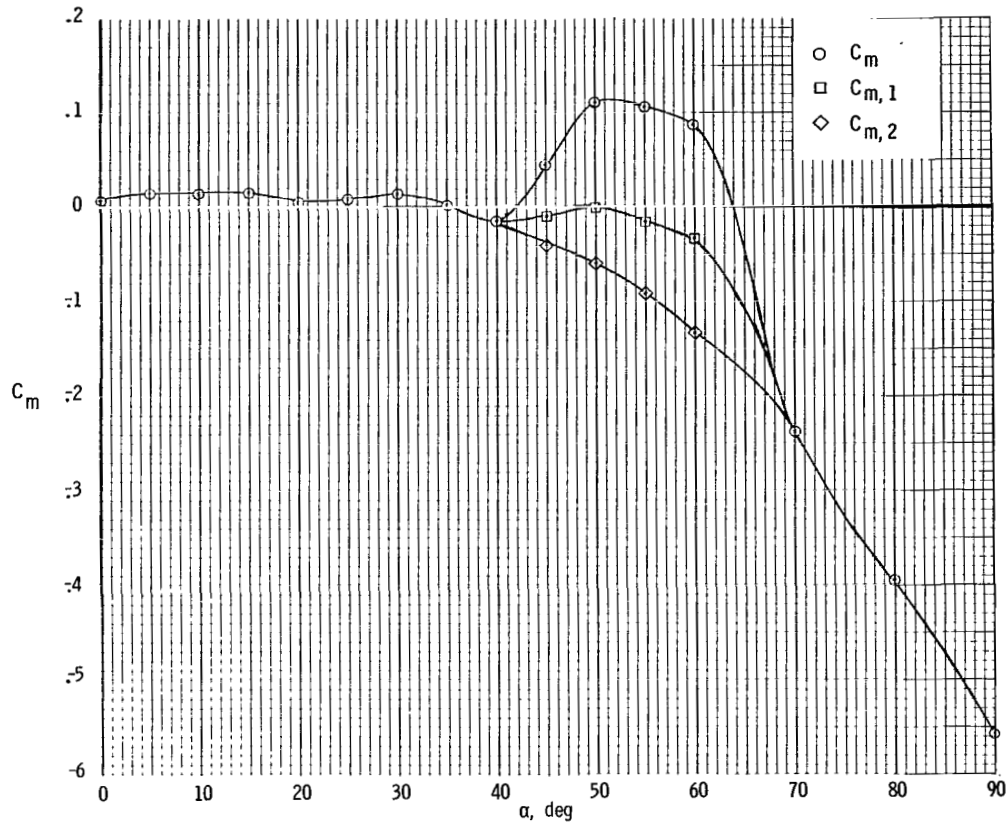
L-73-8778

Figure 5.- View of side-stick installation in simulator cockpit.

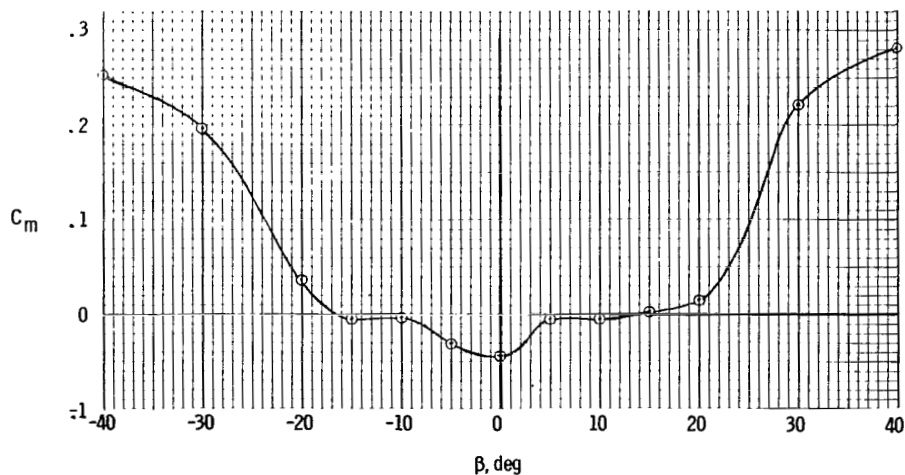


(a) Variation of basic airframe pitching moment and lift with angle of attack for scheduled leading-edge flap deflections; $\delta_h = 0^\circ$; center of gravity at $0.352\bar{c}$.

Figure 6. - Longitudinal characteristics of configuration.

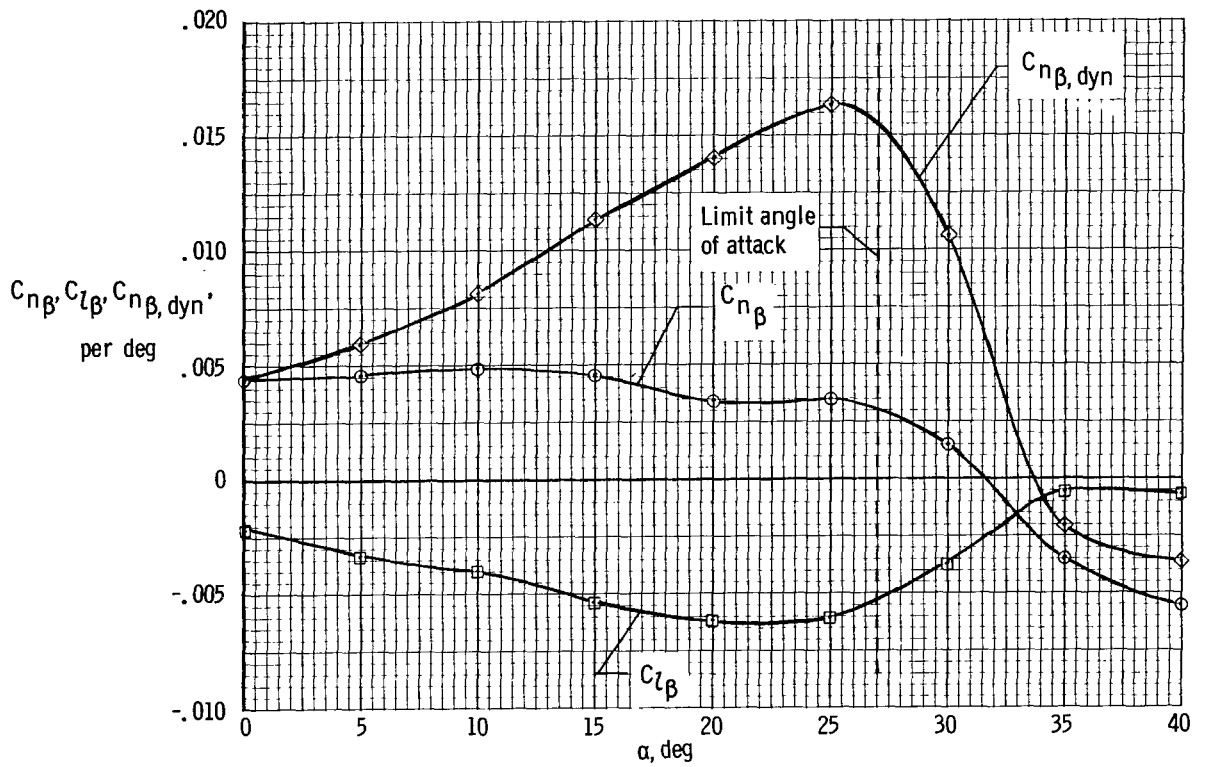


(b) Variation of pitching-moment curves with angle of attack for scheduled leading-edge flap deflections; $\delta_h = 0^\circ$; center of gravity at $0.352\bar{c}$.



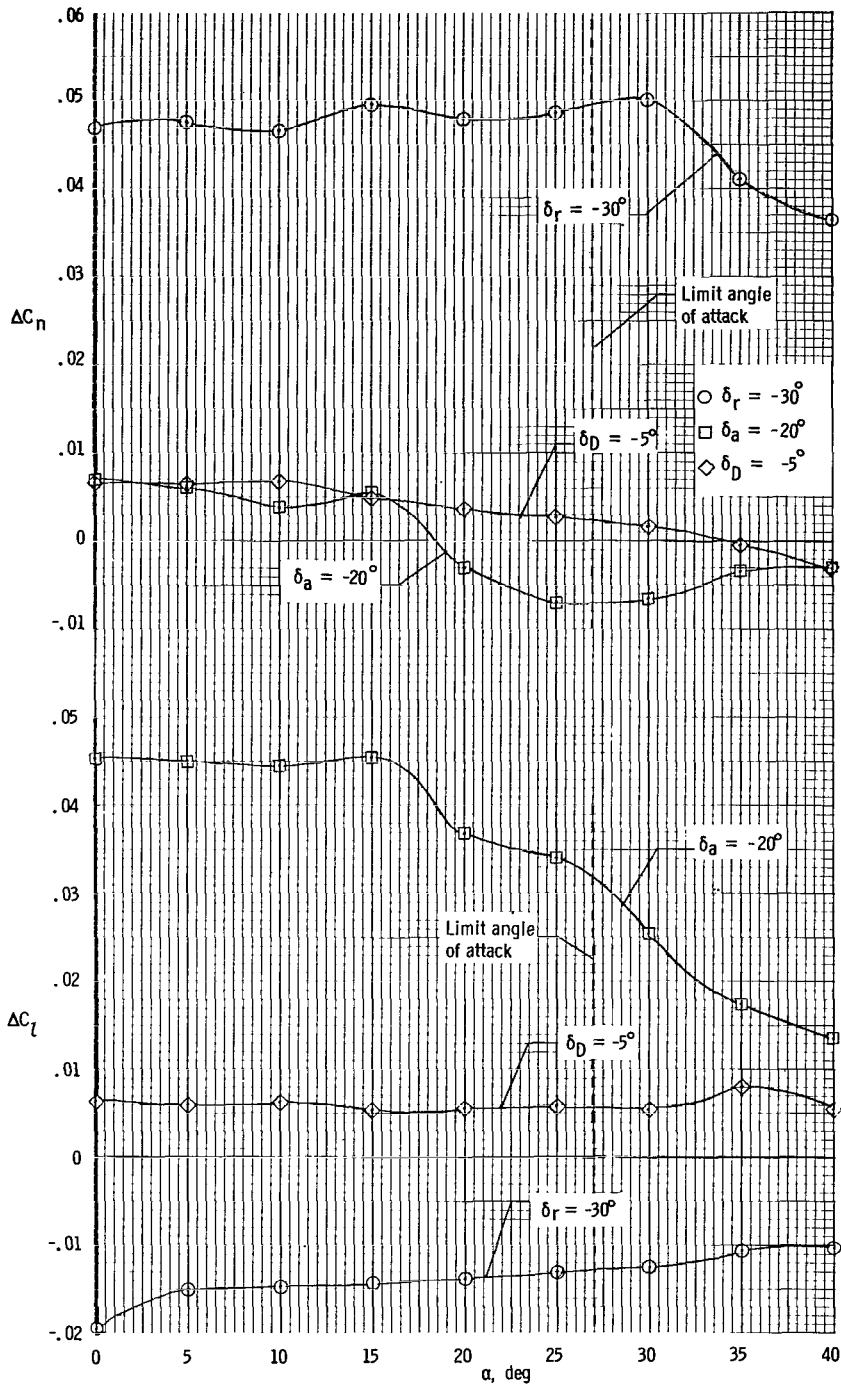
(c) Variation of pitching moment with sideslip for basic configuration at $\alpha = 40^\circ$ for leading-edge flap deflected 25° ; $\delta_h = 0^\circ$; center of gravity at $0.34\bar{c}$.

Figure 6.- Concluded.



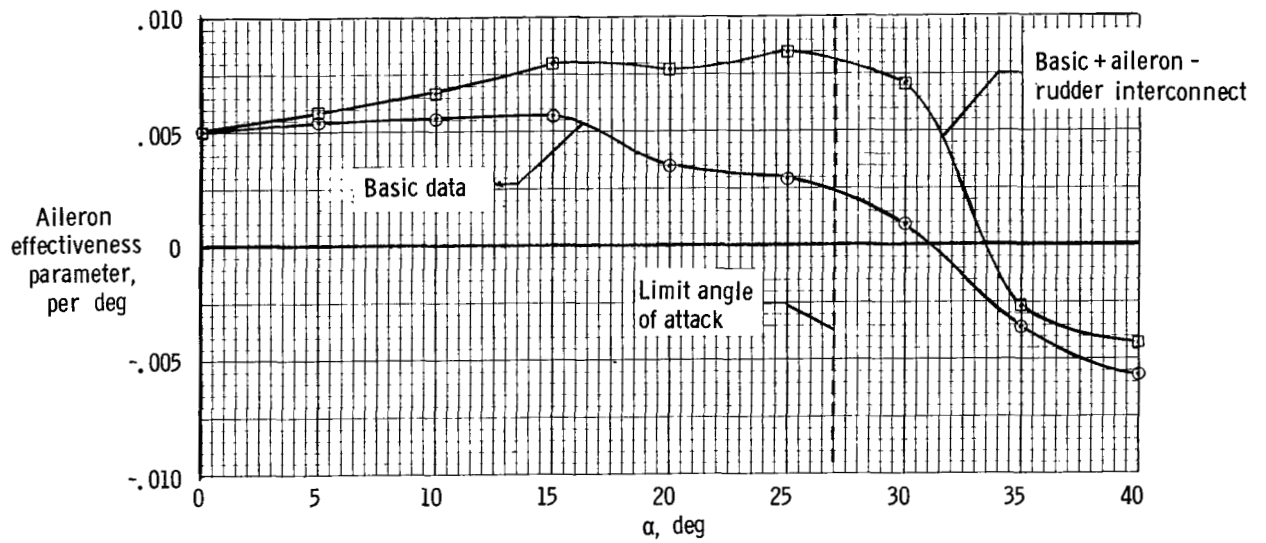
(a) Static stability characteristics.

Figure 7.- Variation of lateral-directional stability and control characteristics of basic configuration with angle of attack for scheduled leading-edge flap deflections; $\delta_h = 0^\circ$.



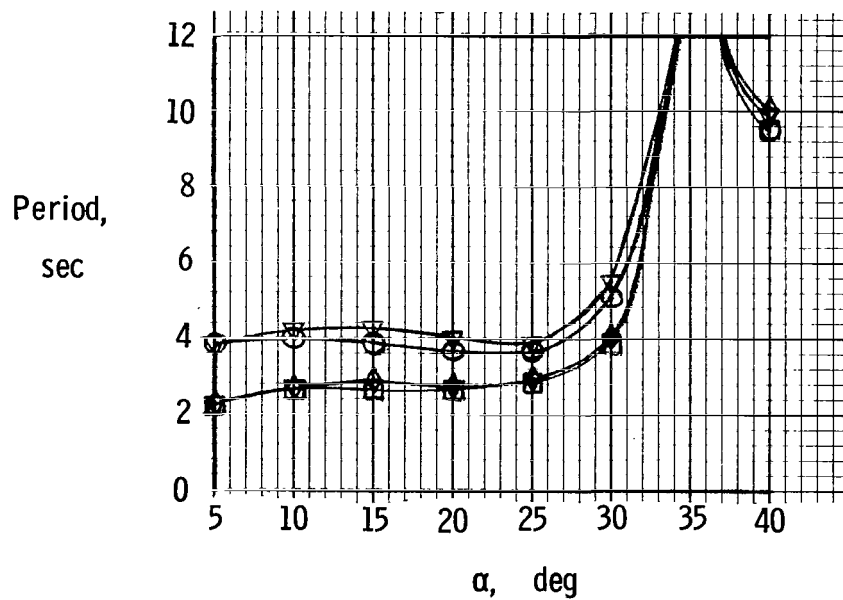
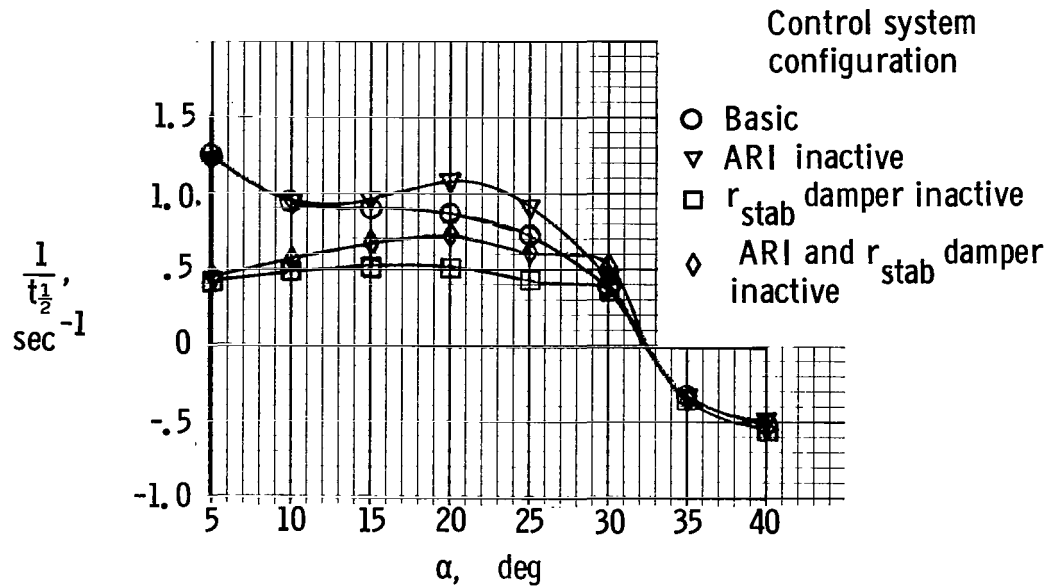
(b) Moment increments due to full deflection of lateral-directional controls.

Figure 7.- Continued.



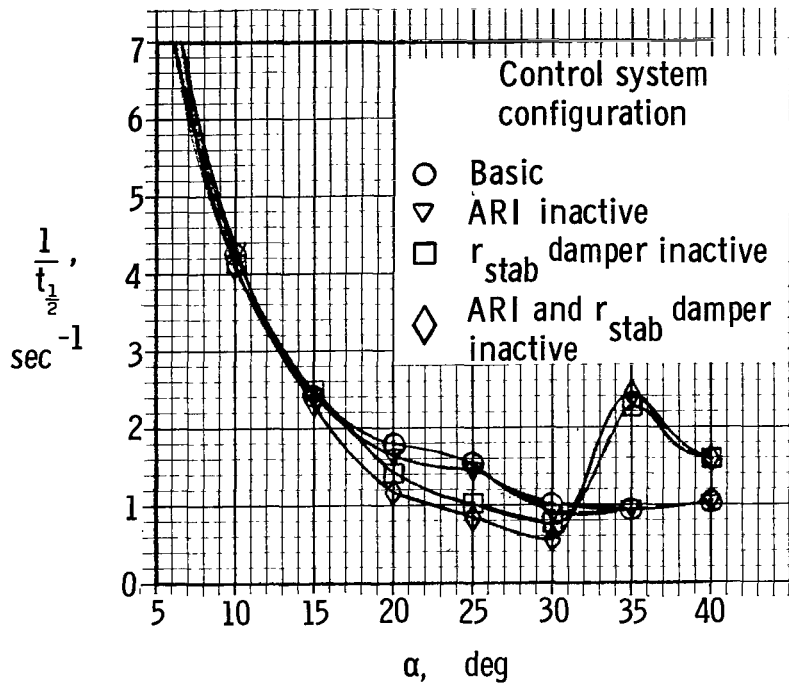
(c) Effect of aileron-rudder interconnect on aileron effectiveness parameter (effects of ailerons and differential tail included).

Figure 7. - Concluded.

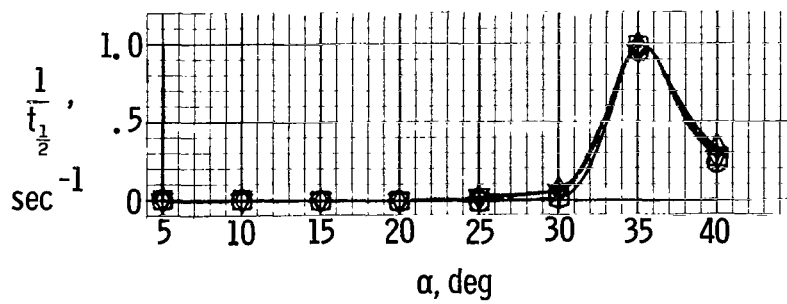


(a) Dutch roll mode.

Figure 8.- Variation of airplane dynamic lateral-directional stability with angle of attack for various augmentation configurations. $h = 6096 \text{ m (20 000 ft)}$; velocity for $1g$, level flight.



(b) Roll mode.



(c) Spiral mode.

Figure 8.- Concluded.

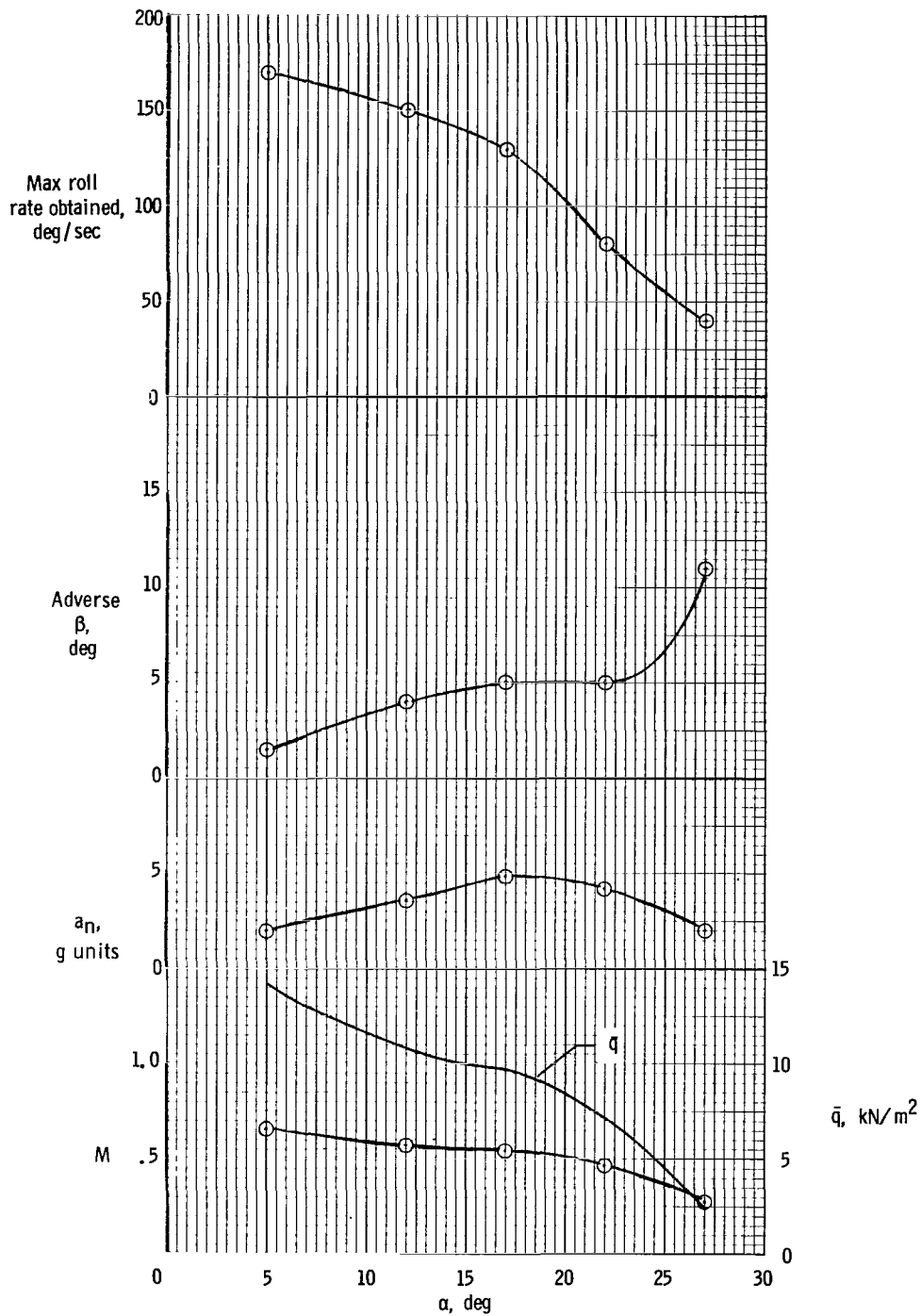
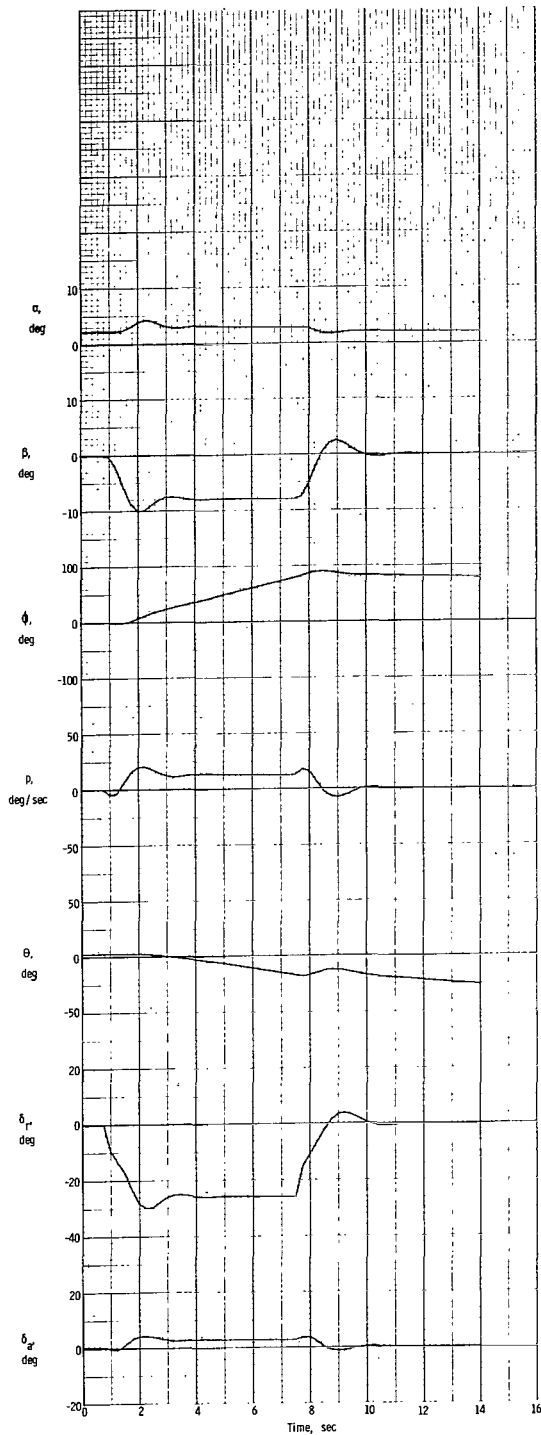
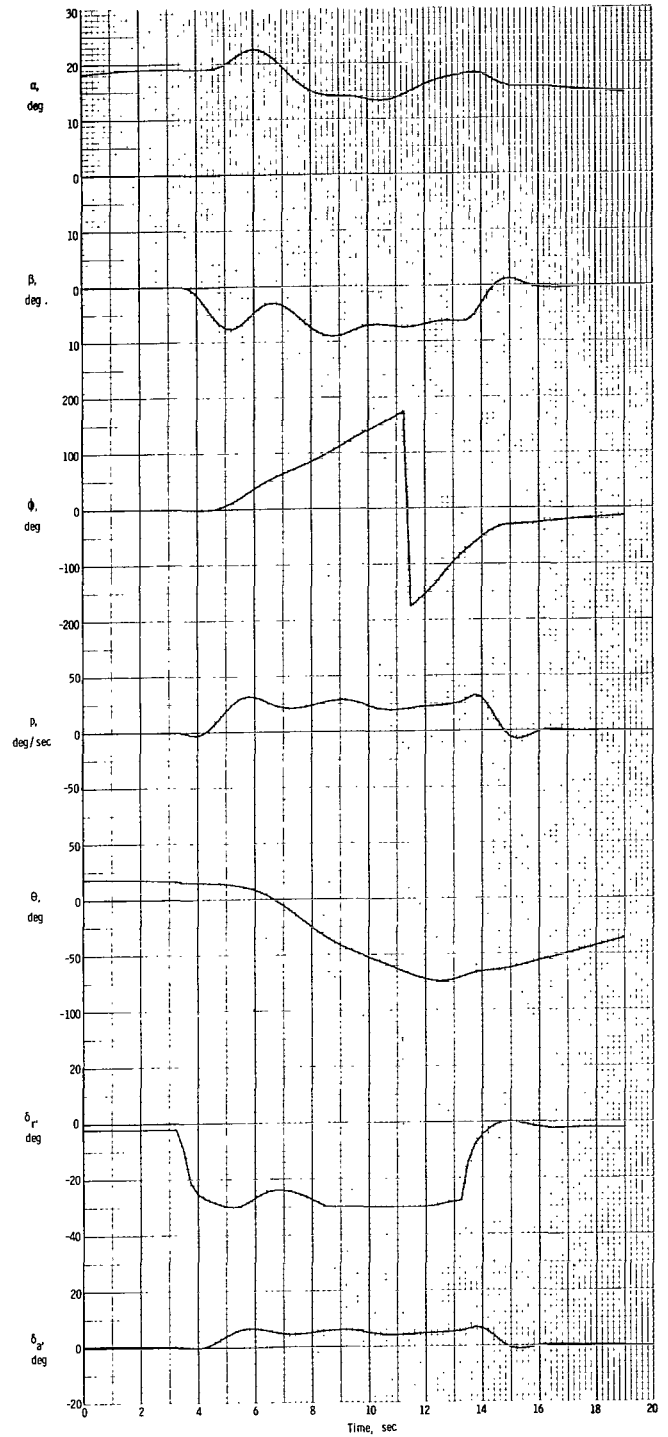


Figure 9.- Roll performance obtained with basic configuration at $h = 6096 \text{ m}$ (20 000 ft) with maximum roll control used to reverse bank angle.



(a) Initial $\alpha = 3^\circ$; $M \approx 0.6$.



(b) Initial $\alpha = 18^\circ$; $M \approx 0.24$.

Figure 10.- Simulated response of basic airplane to step rudder inputs in level flight at $h = 6096 \text{ m}$ ($20\,000 \text{ ft}$).

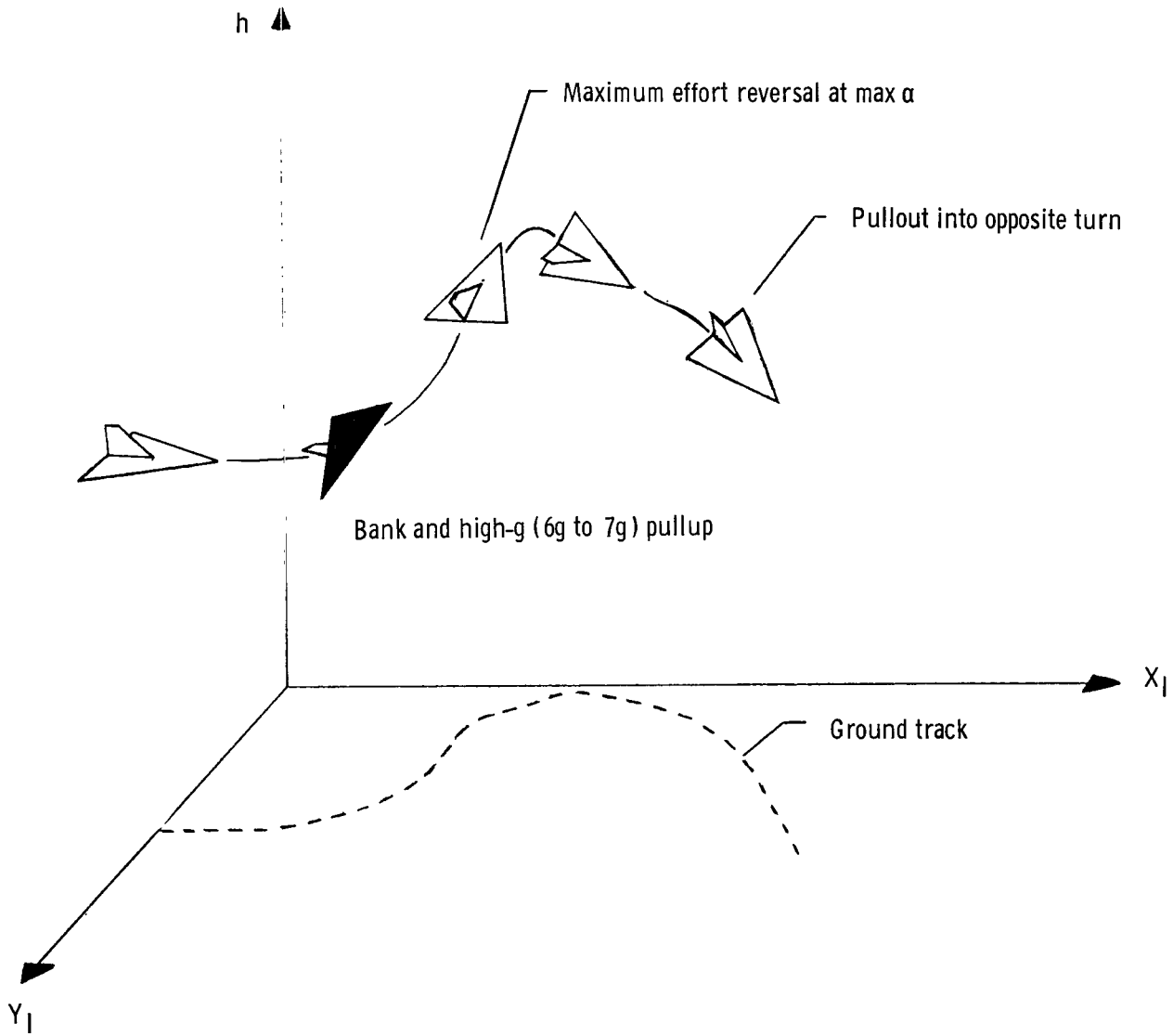


Figure 11.- Sketch of roll performance task.

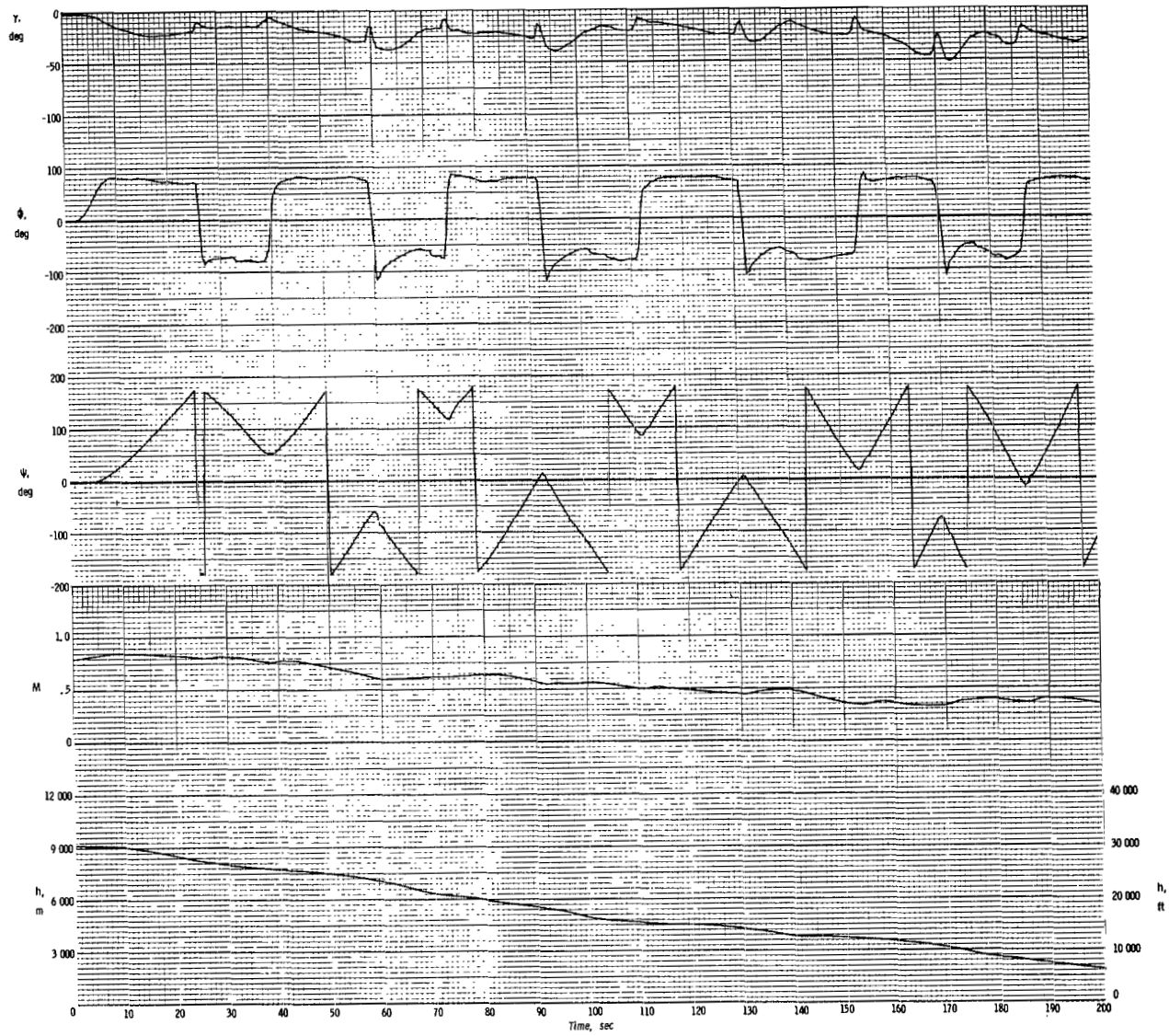
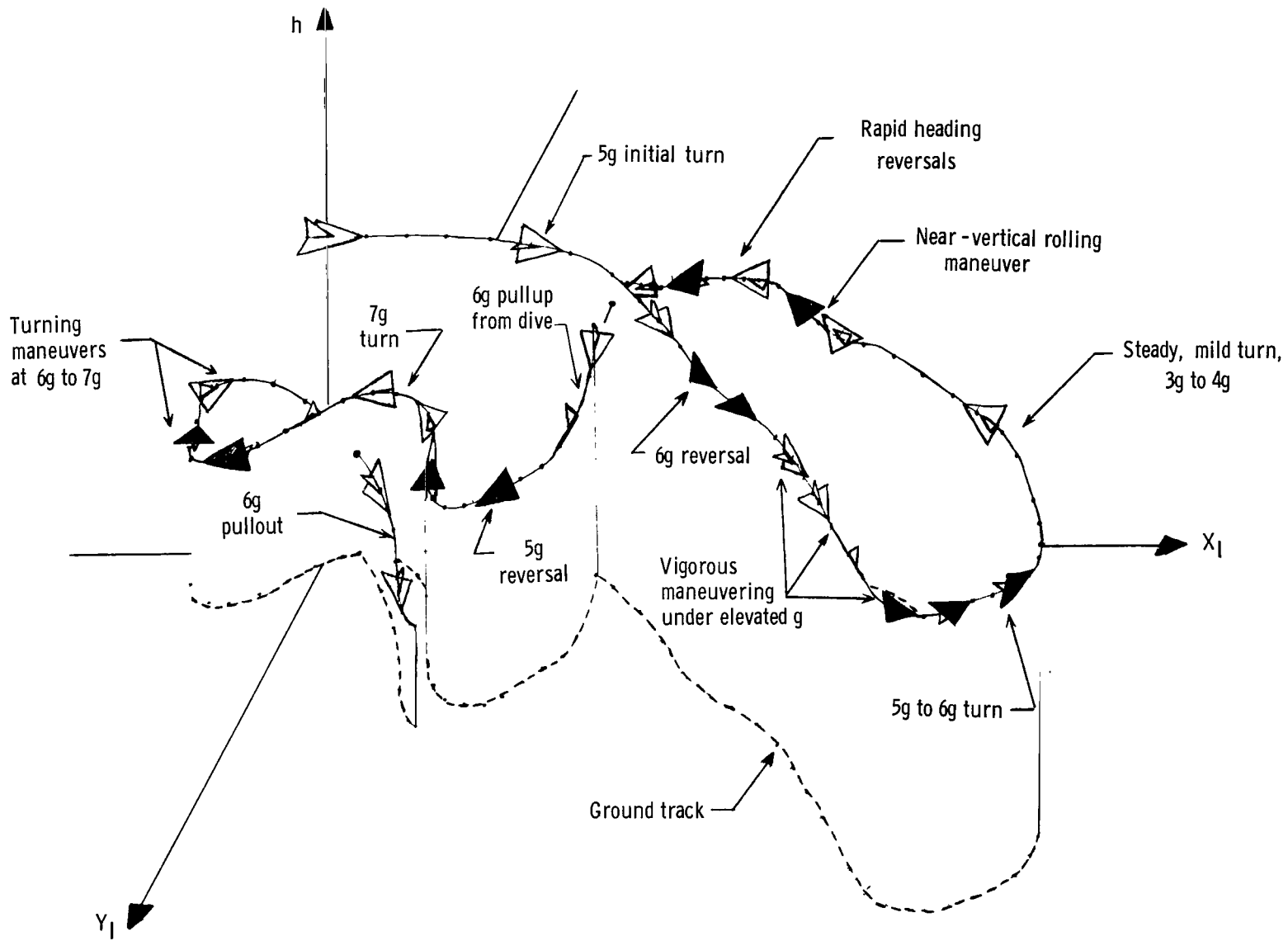
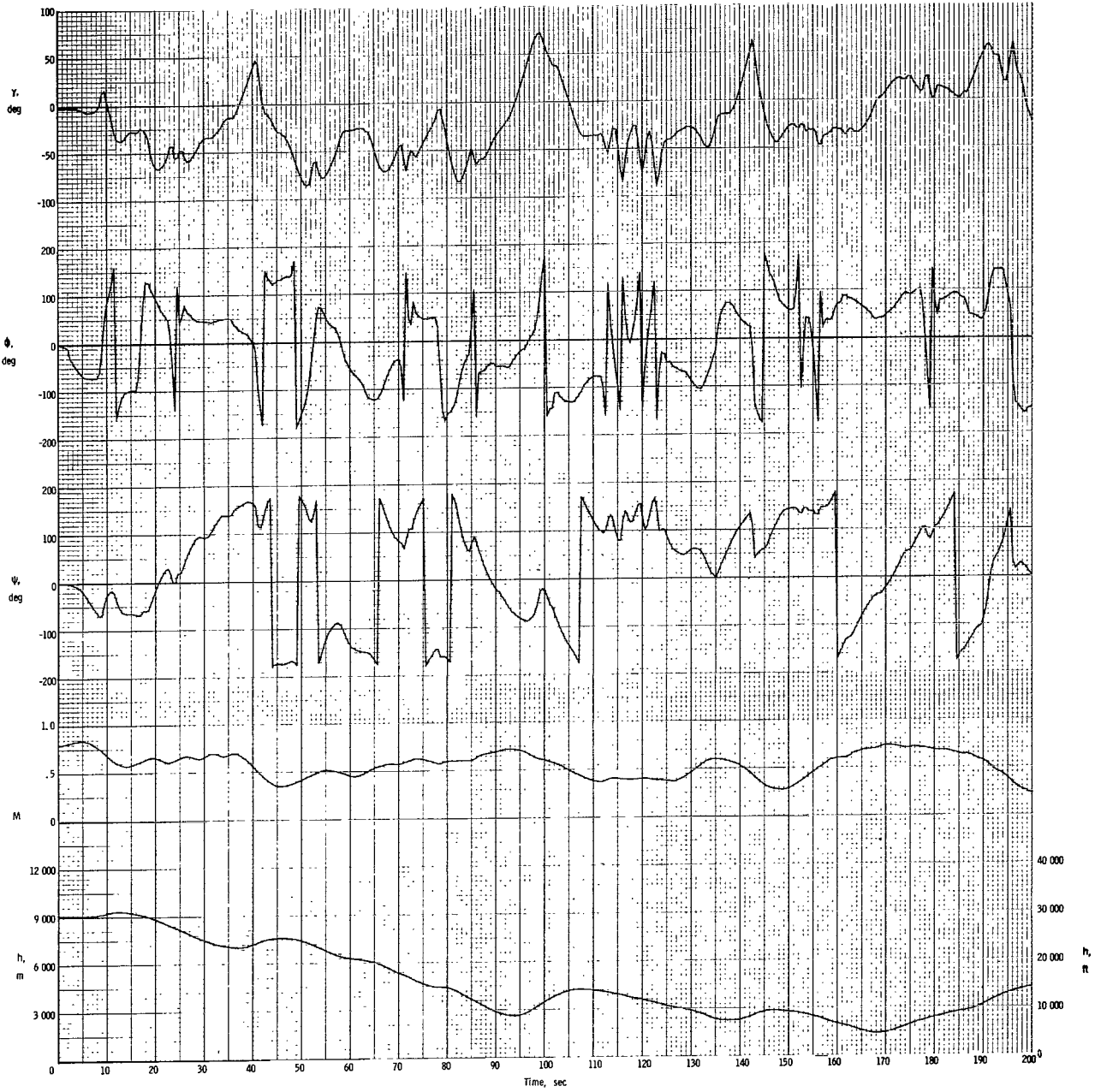


Figure 12.- Time history of target airplane flying bank-to-bank ACM task.



(a) Sketch of first half of task.

Figure 13.- Illustration of general ACM task.



(b) Time history of task.

Figure 13.- Concluded.

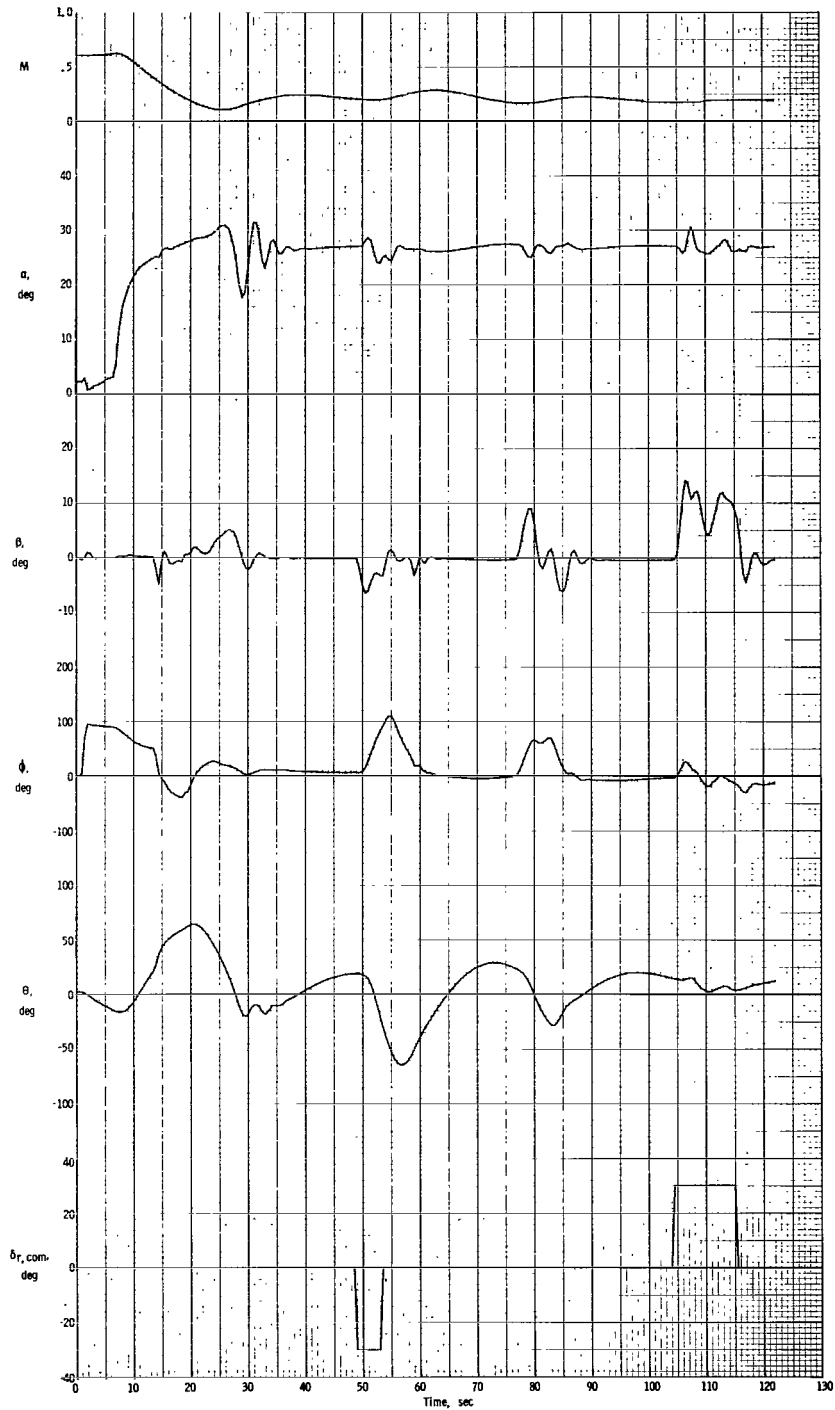


Figure 14.- Time history of controllability evaluation at maximum α for basic airplane.

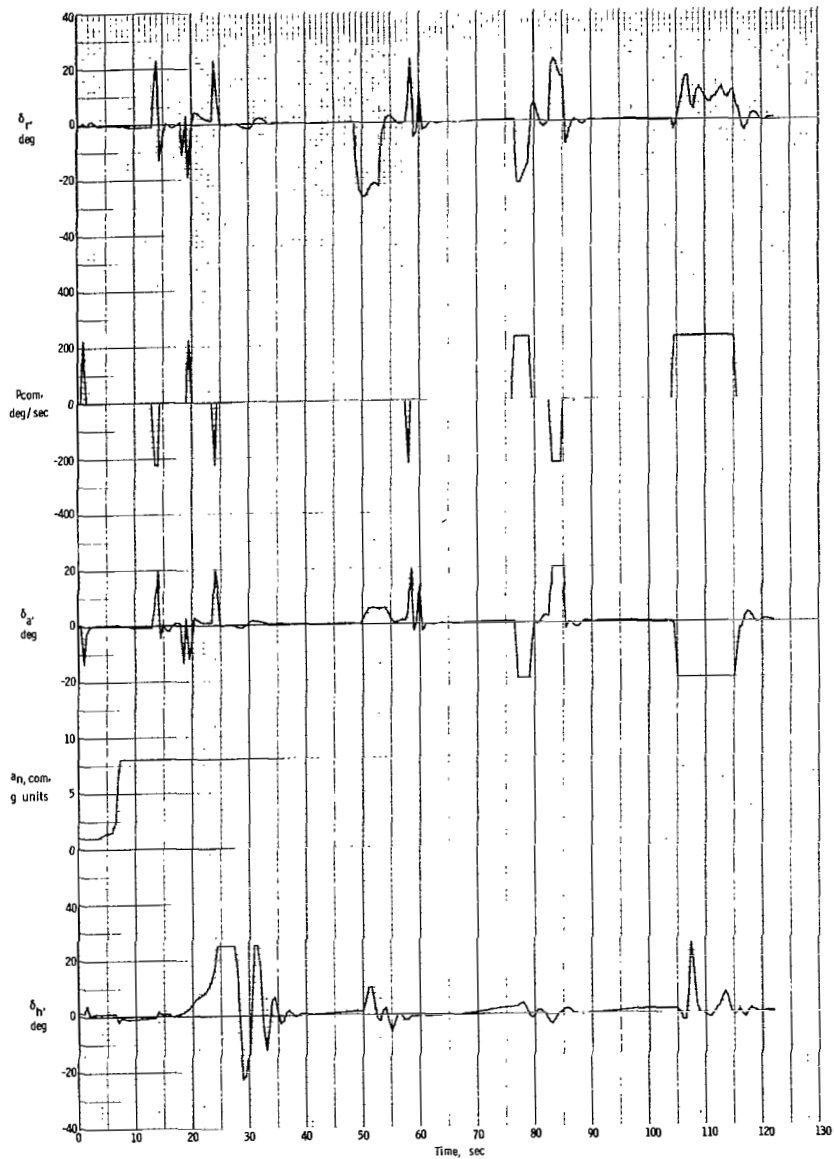


Figure 14. - Concluded.

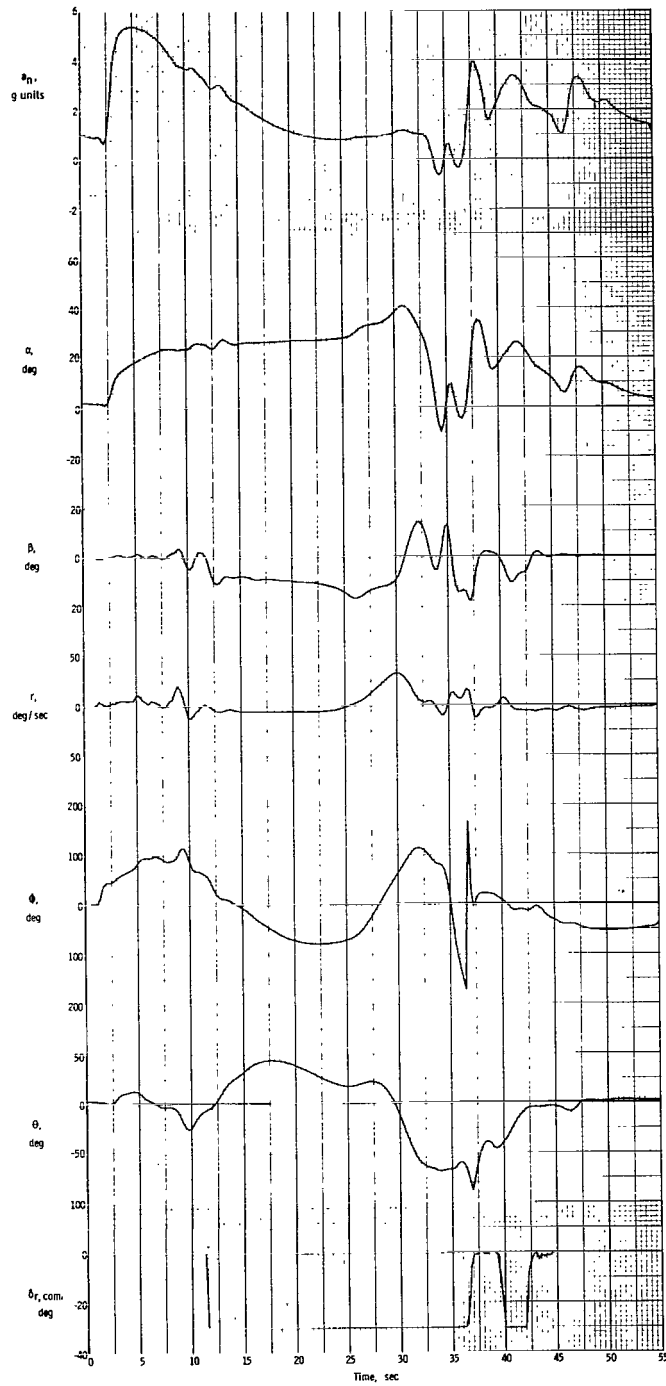


Figure 15.- Time history of motions resulting from full prospin controls during an accelerated stall.

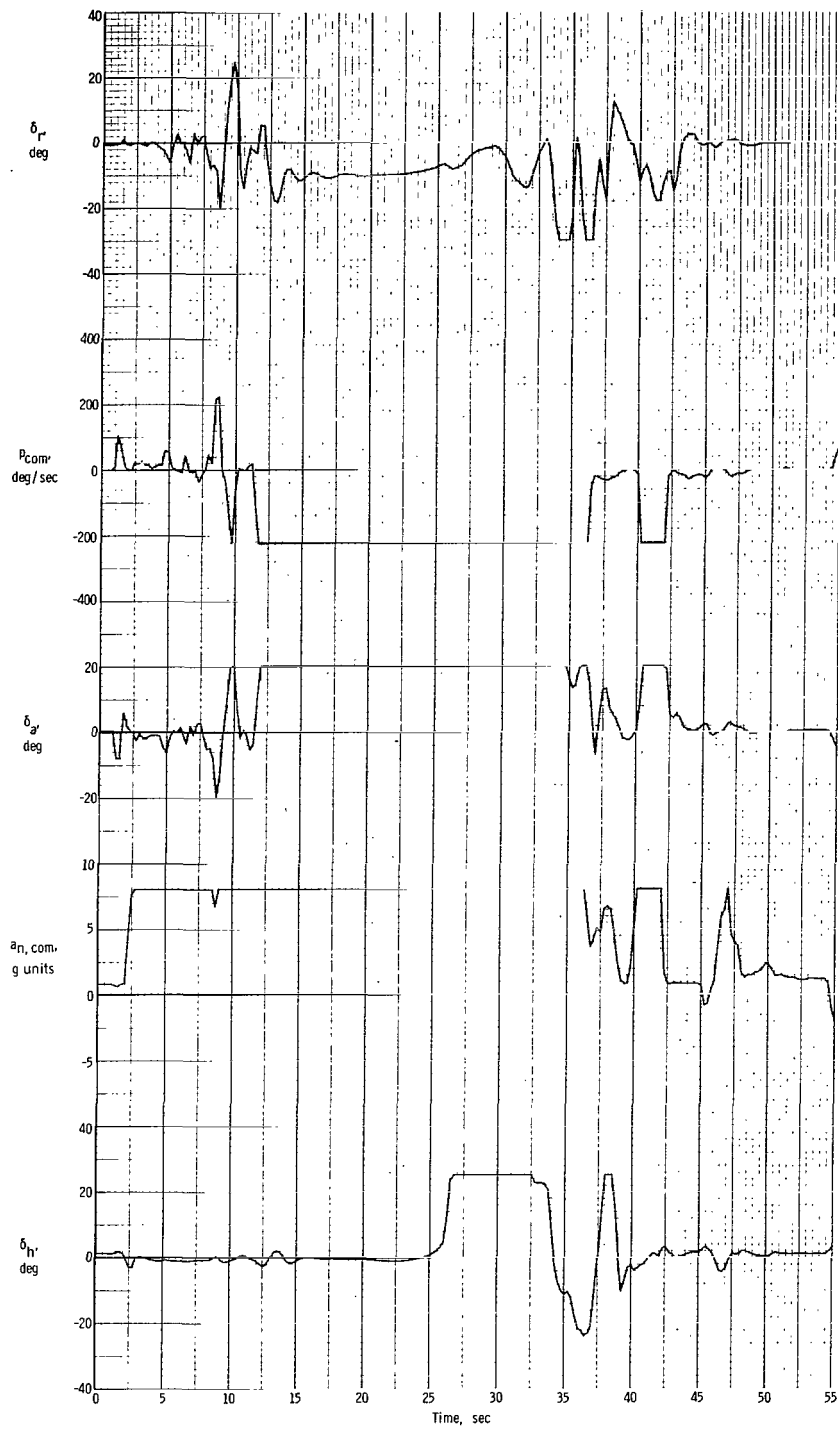


Figure 15.- Concluded.

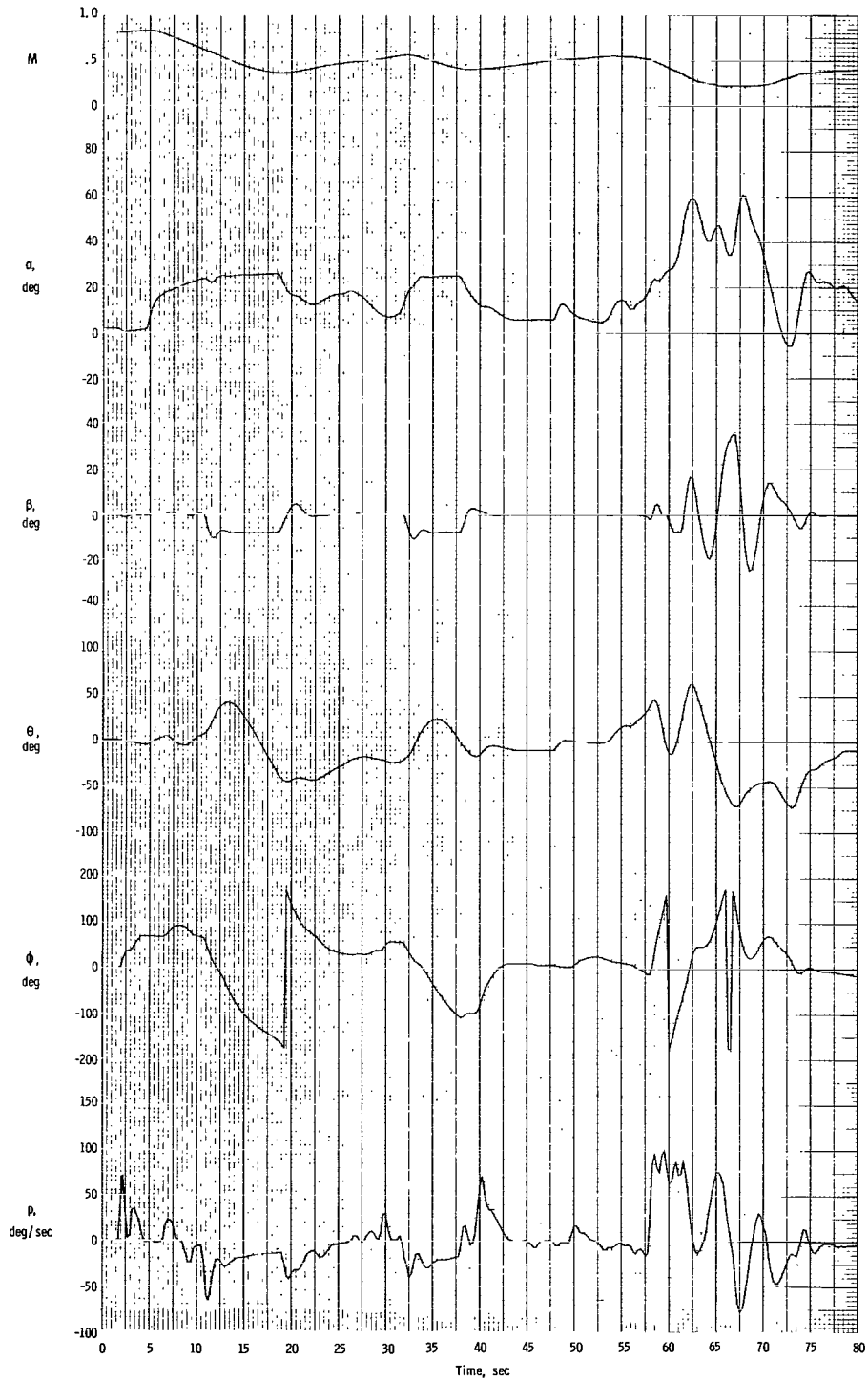


Figure 16.- Basic airplane motions in inertially coupled departure (maneuver starting near $t = 50$ sec).

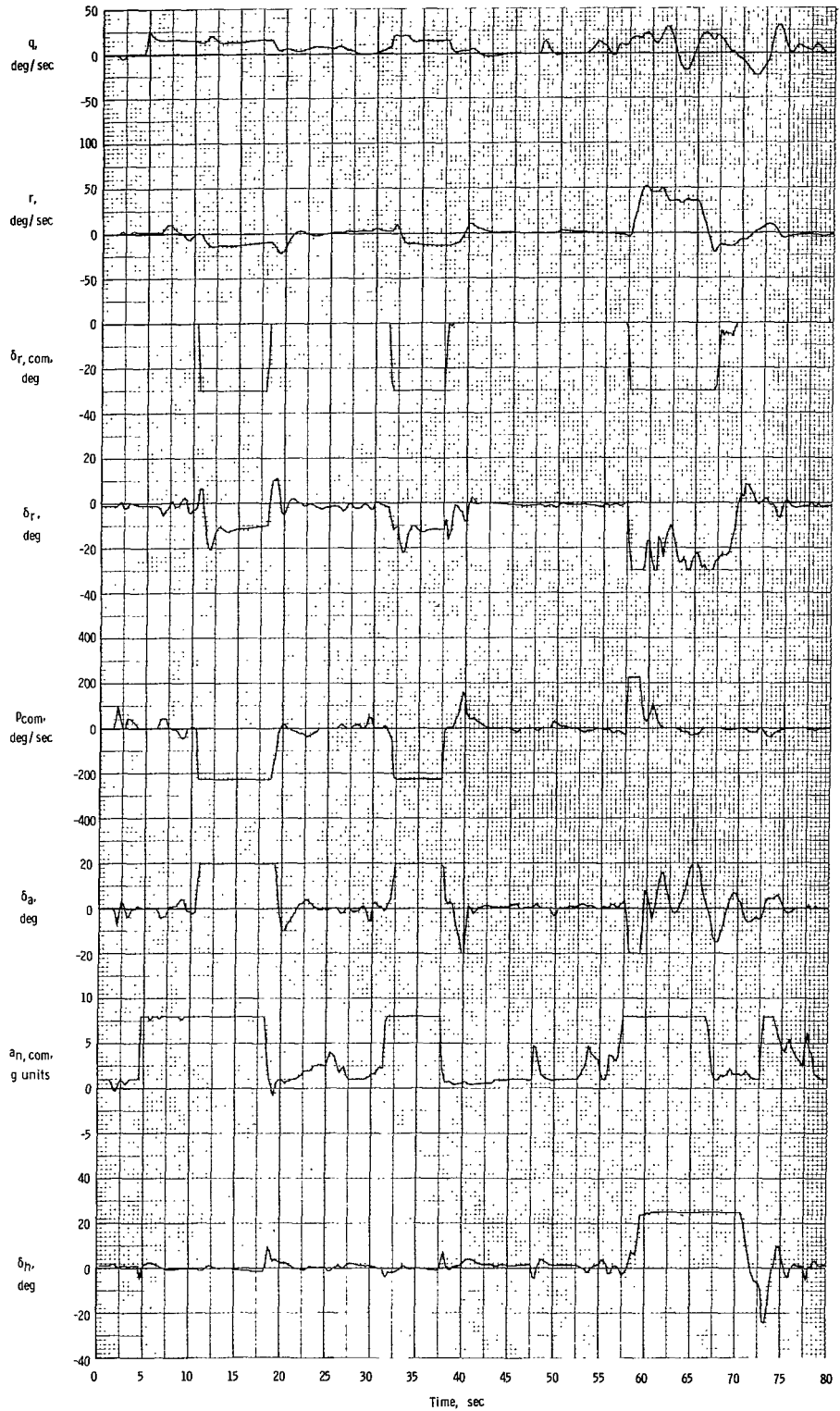


Figure 16. - Concluded.

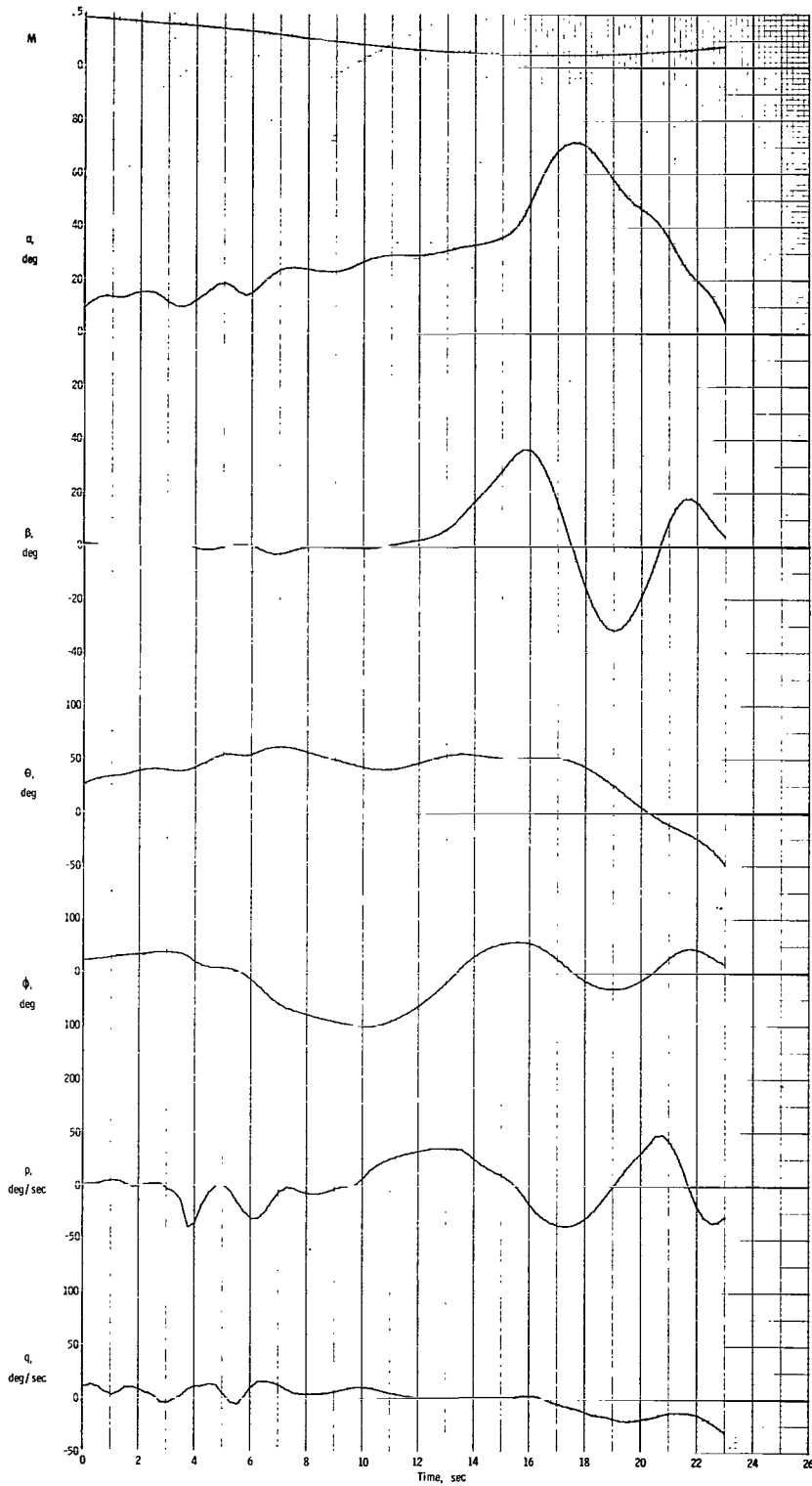


Figure 17.- Airplane motions resulting from aerodynamically coupled departure.

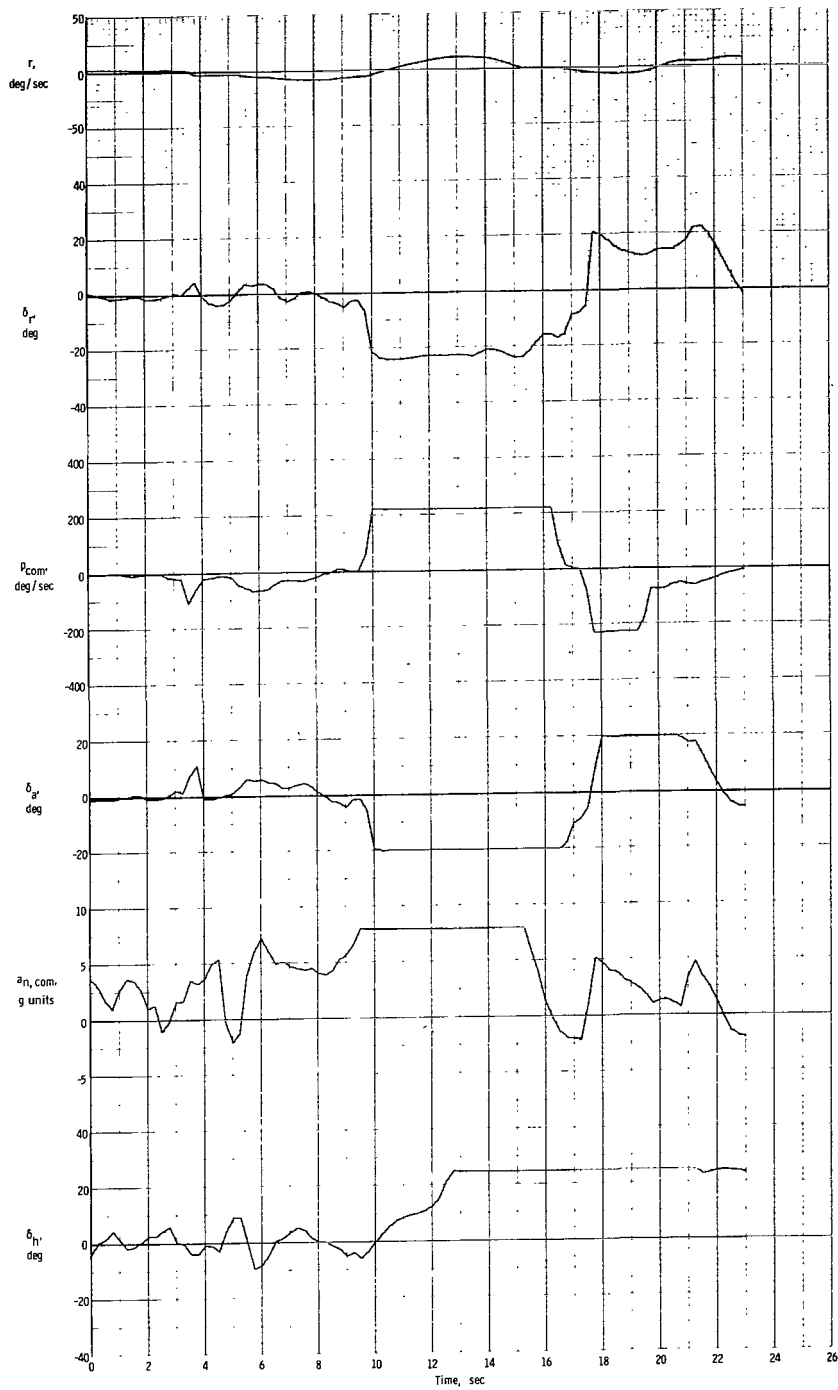


Figure 17.- Concluded.

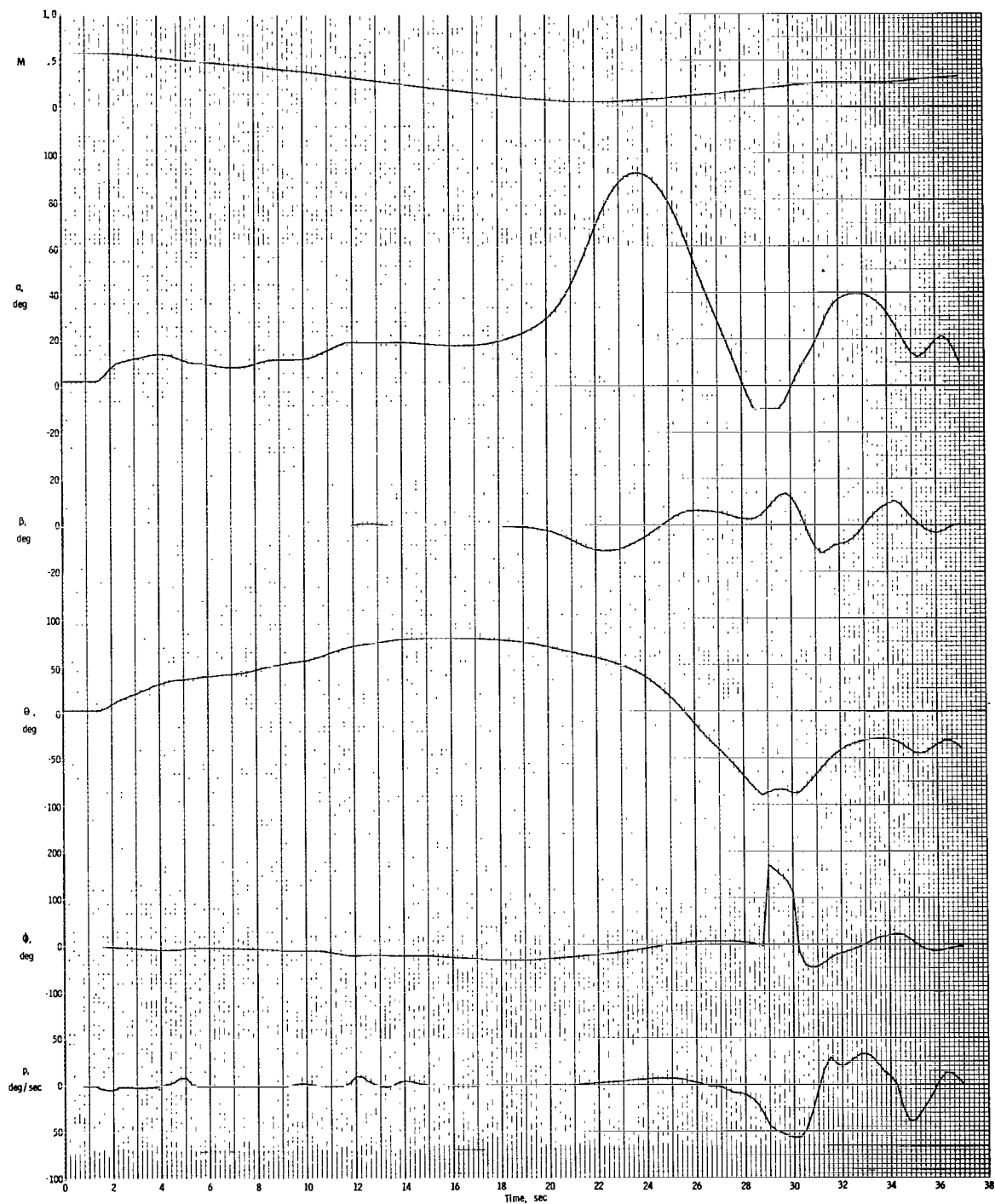


Figure 18.- Motions of airplane in vertical or hammerhead stall.



Figure 18.- Concluded.

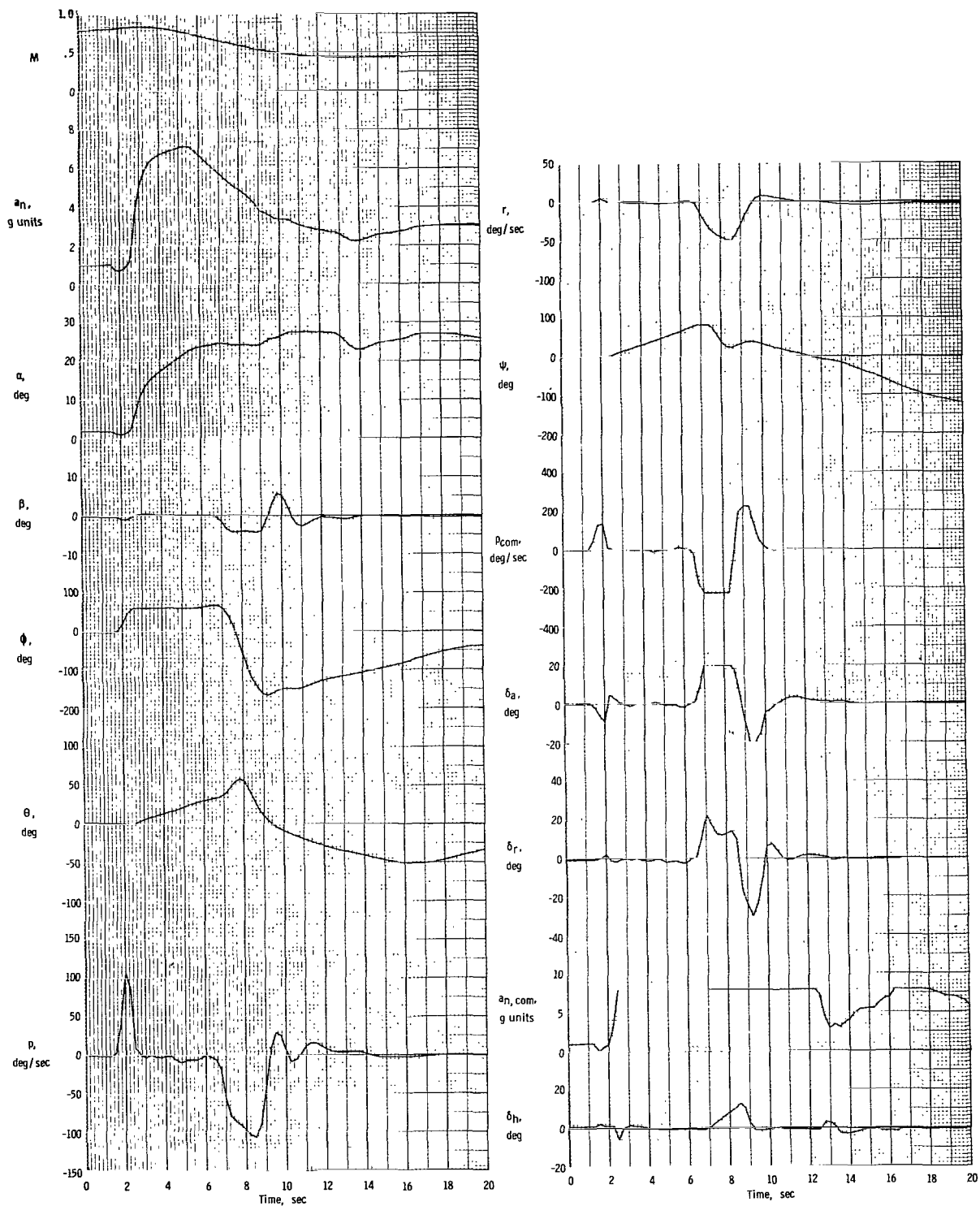


Figure 19. - Performance of airplane in roll-reversal task.

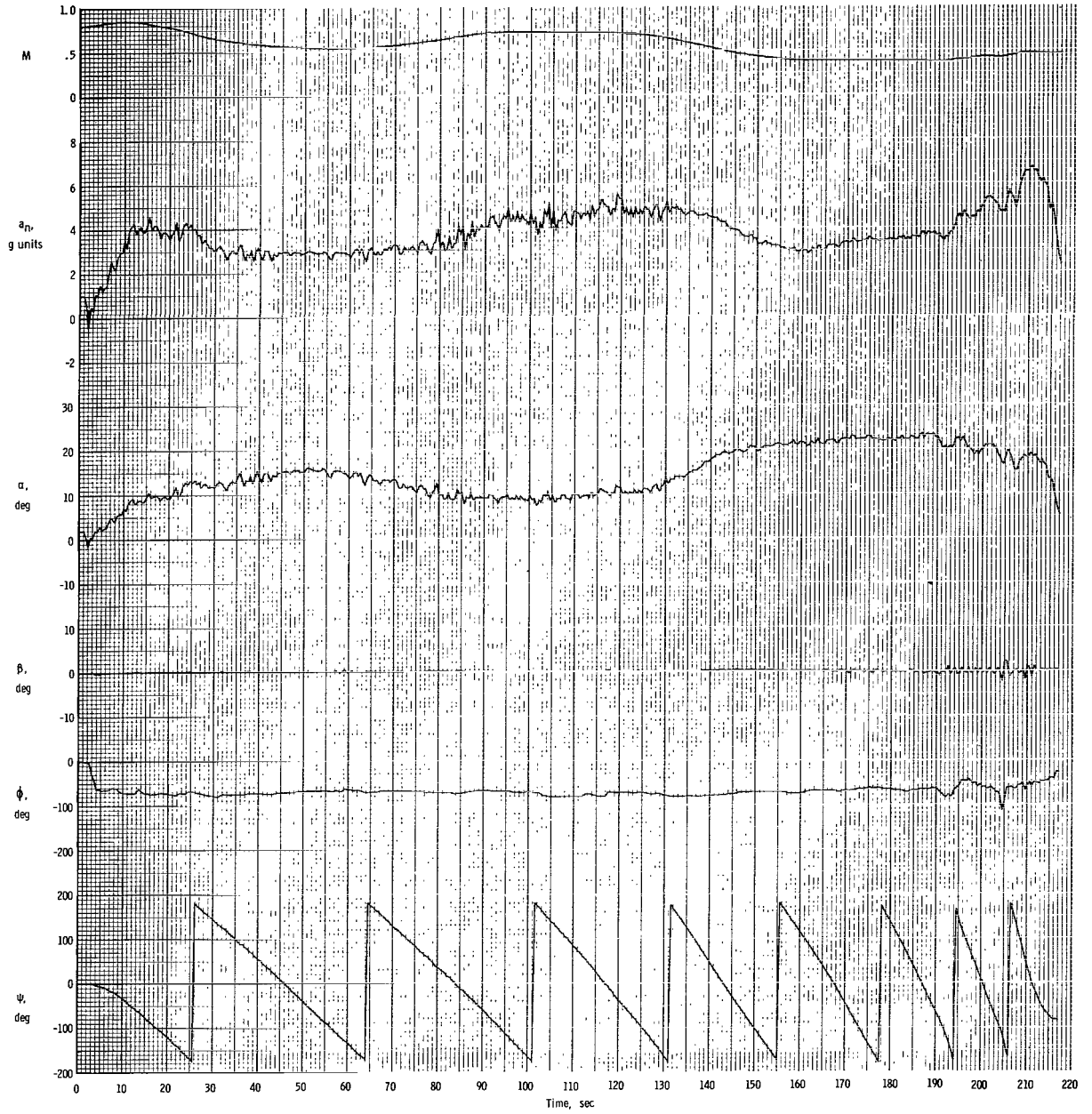


Figure 20.- Performance of airplane in steady tracking task.

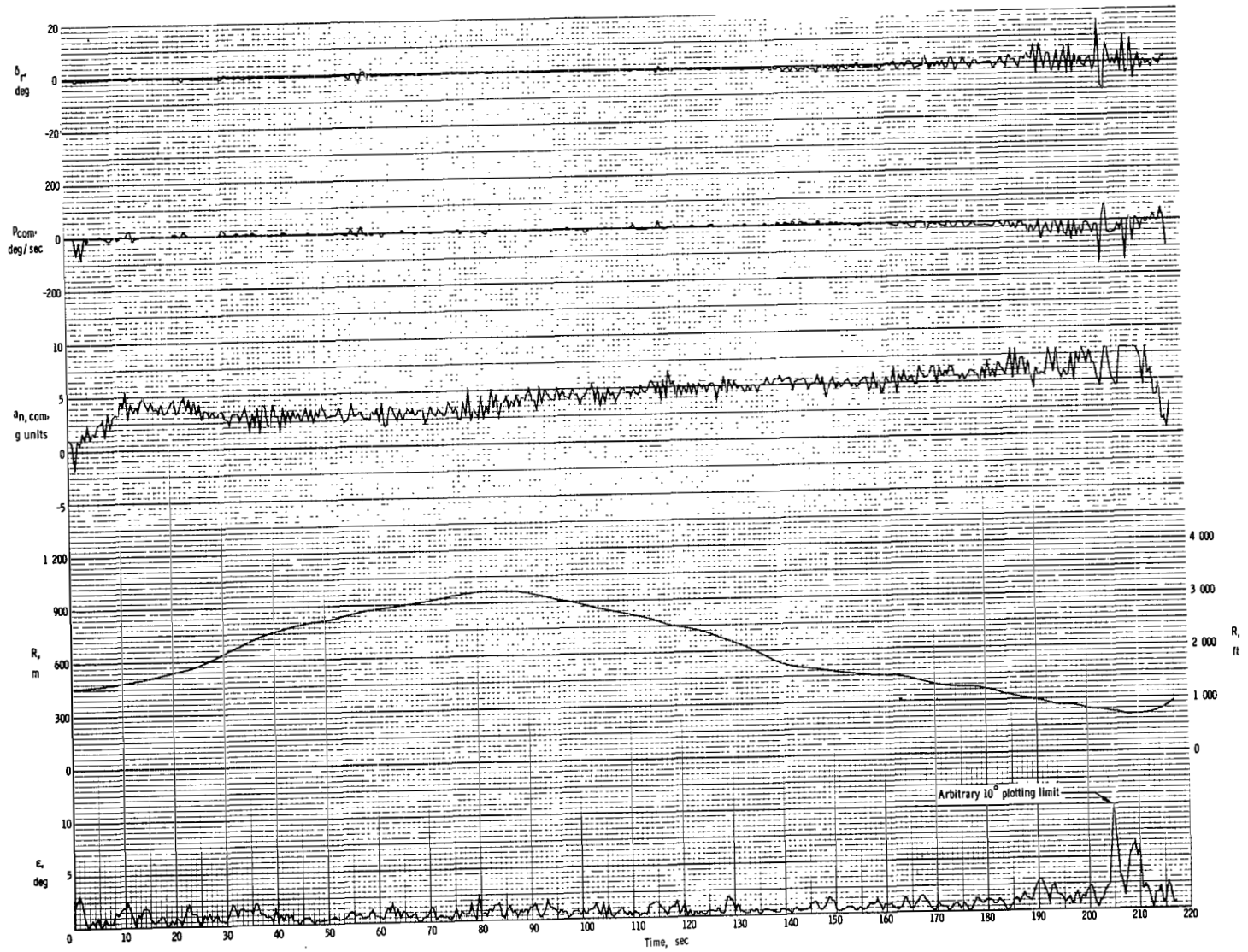
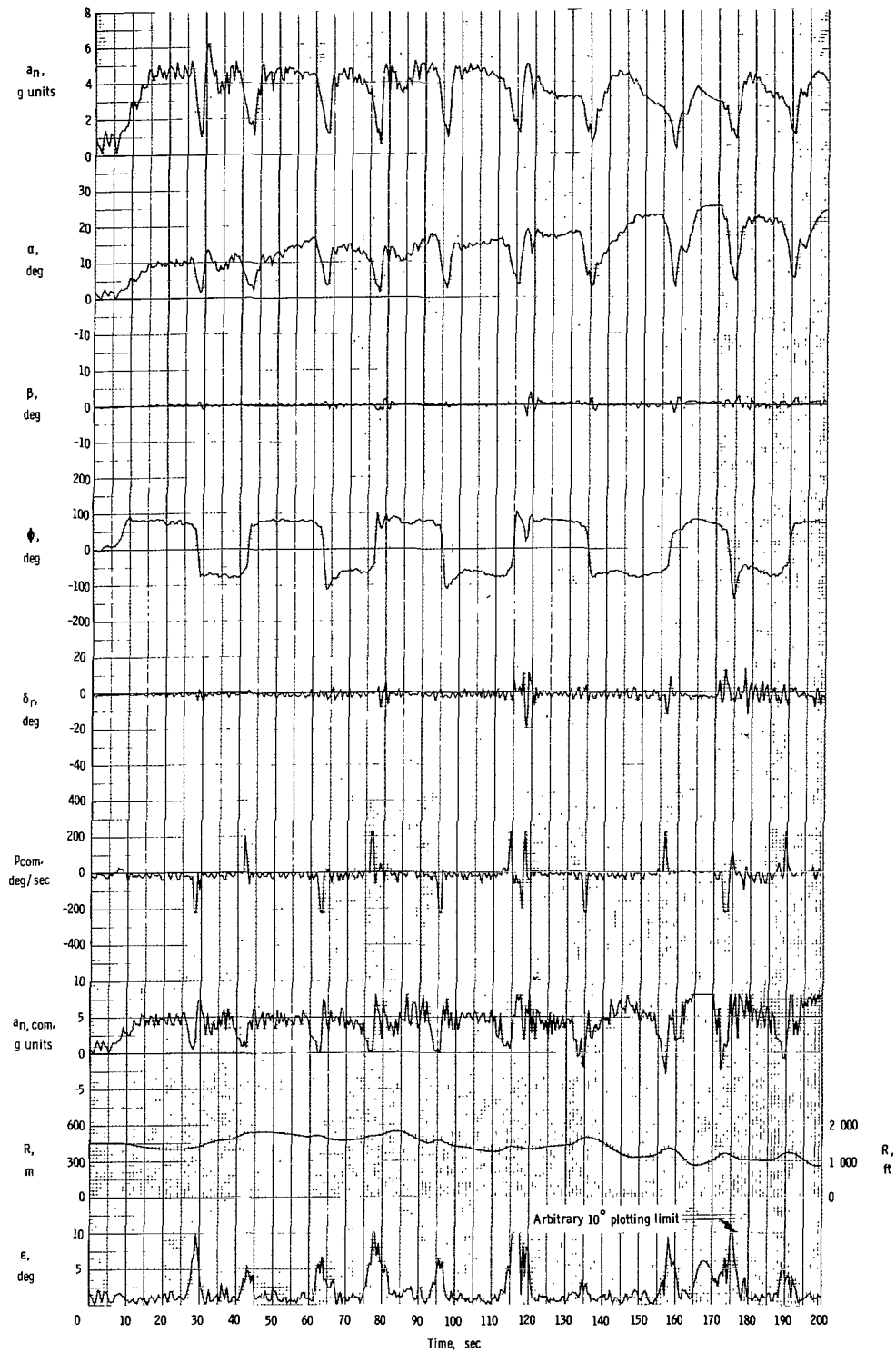


Figure 20.- Concluded.



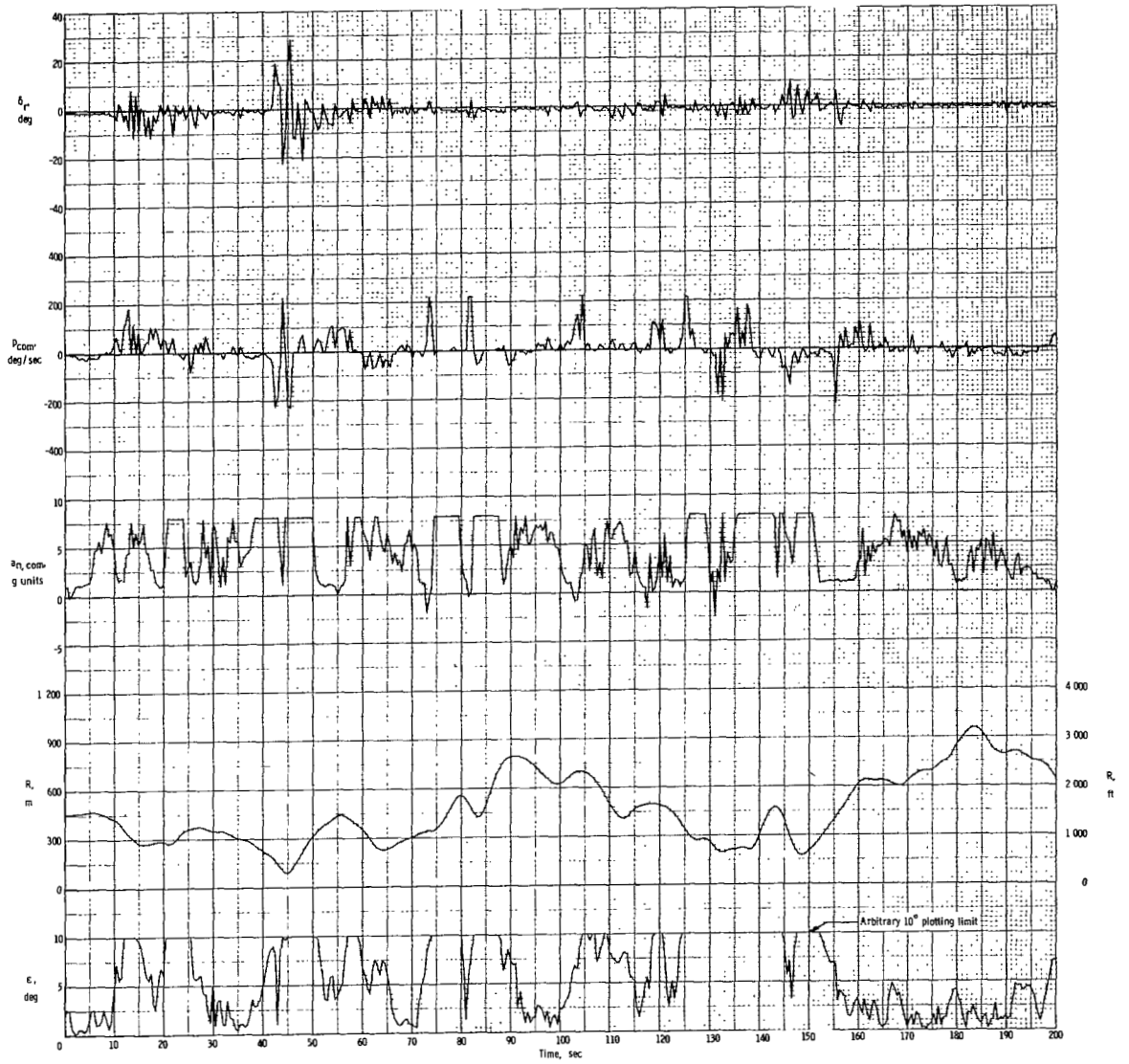
(a) Bank-to-bank task.

Figure 21.- Performance of airplane in ACM tasks.



(b) General ACM task.

Figure 21.- Continued.



(b) Concluded.

Figure 21.- Concluded.

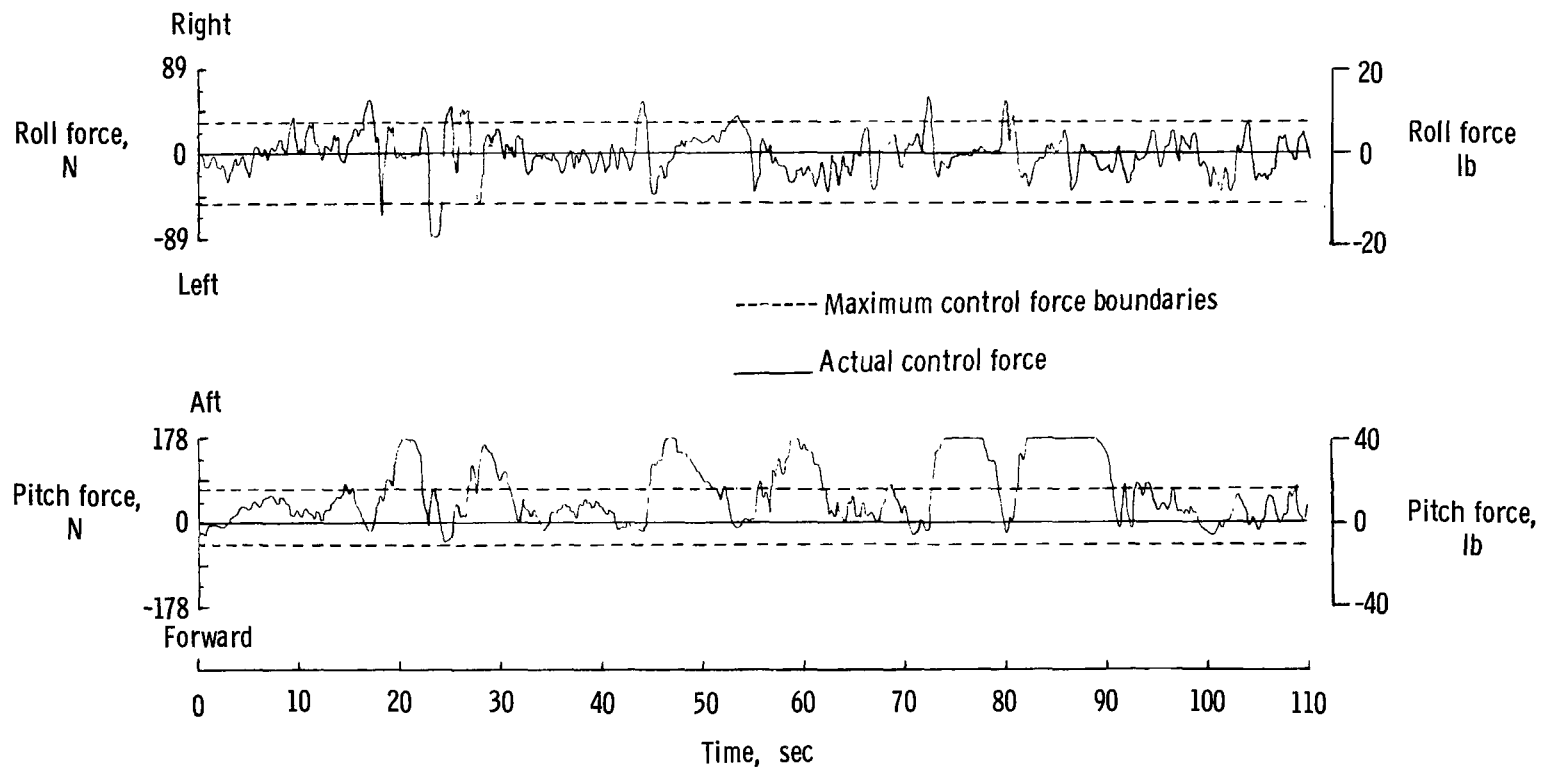


Figure 22.- Time history of pilot lateral and longitudinal control forces in ACM task compared with force levels for maximum commands.

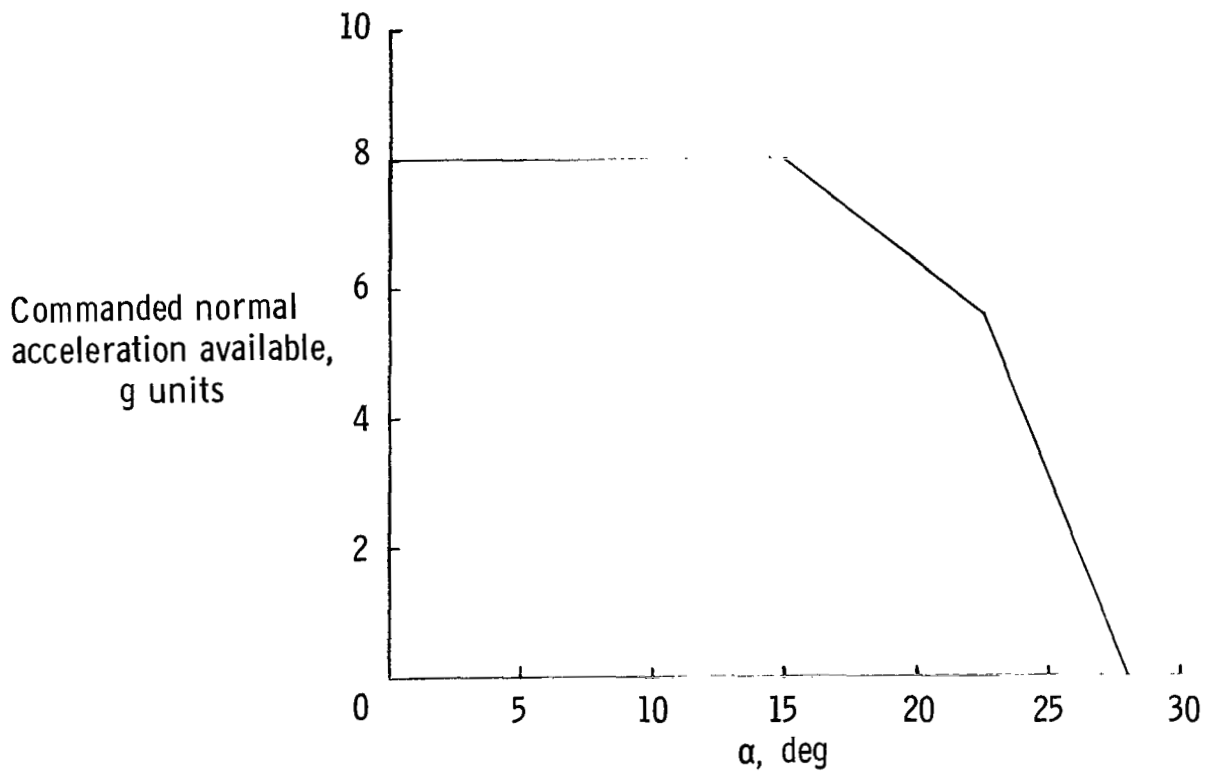


Figure 23.- Schedule of maximum available positive normal acceleration for angle-of-attack limiting (-4g negative normal acceleration command available).

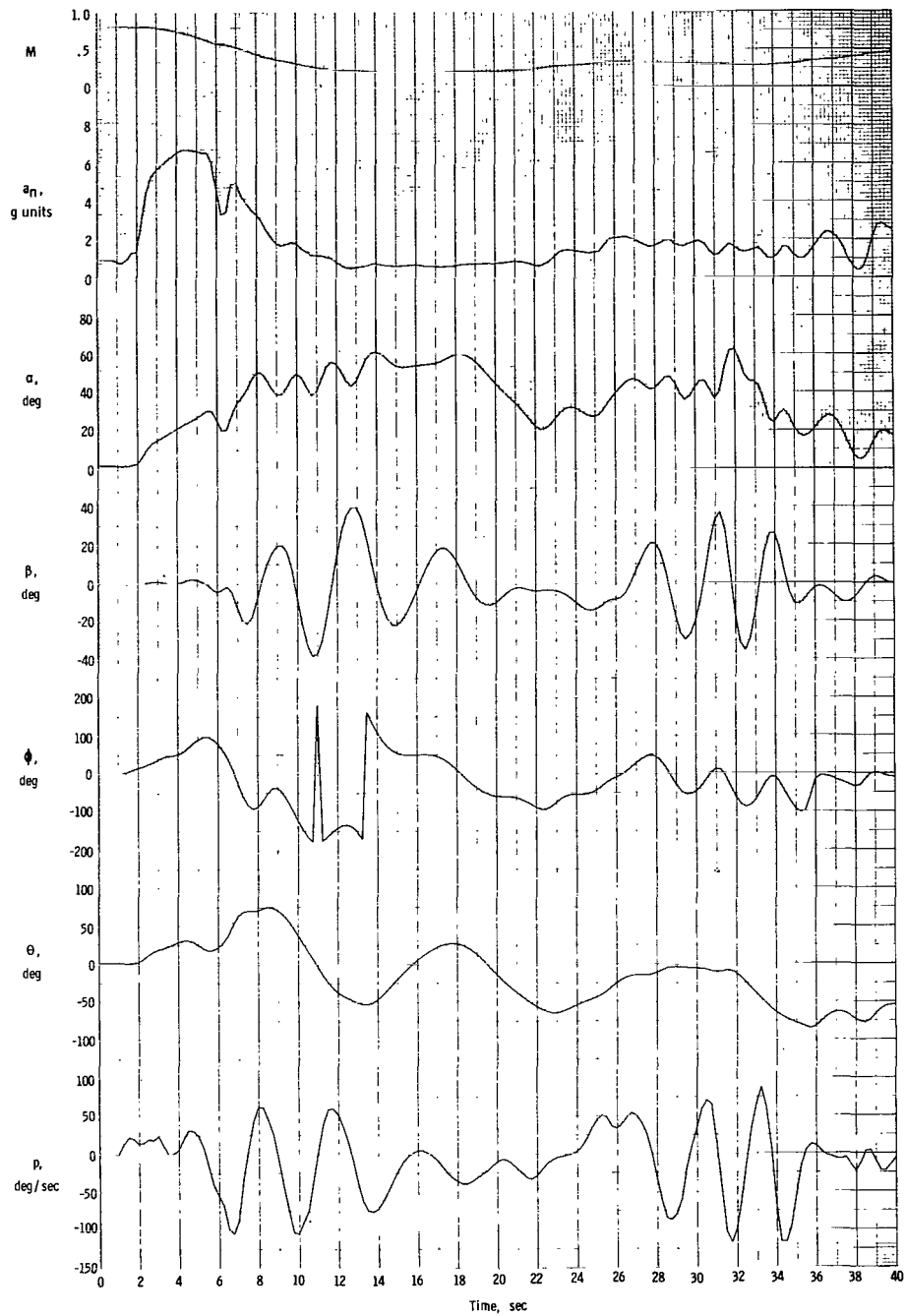


Figure 24.- Performance of airplane without angle-of-attack/normal-acceleration limiting (but with angle-of-attack overshoot prevention) in roll performance task.



Figure 24. - Concluded.

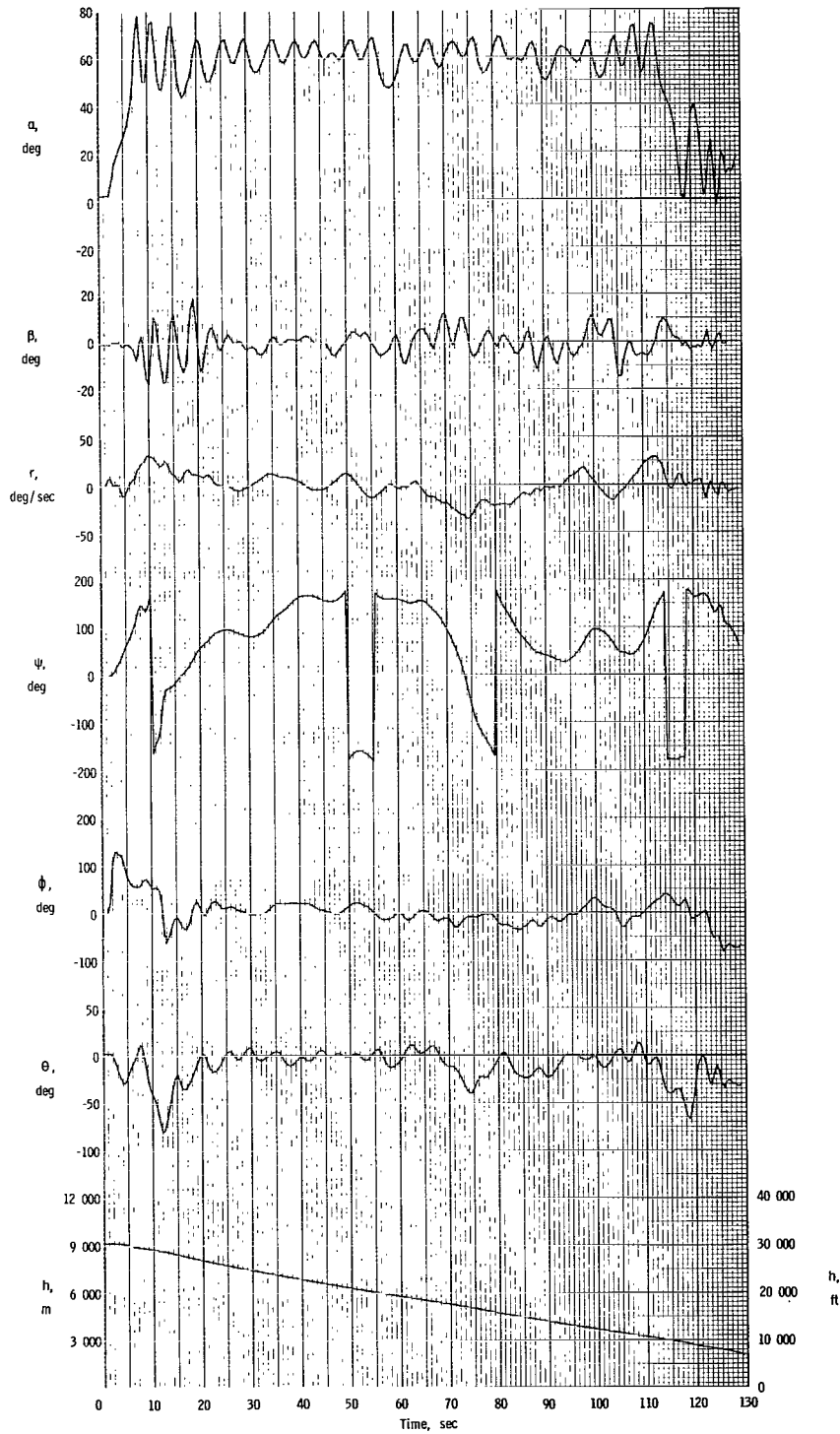


Figure 25.- Poststall recovery motions of airplane without angle-of-attack limiting feature for basic C_m curve (strong high-angle-of-attack trim point).

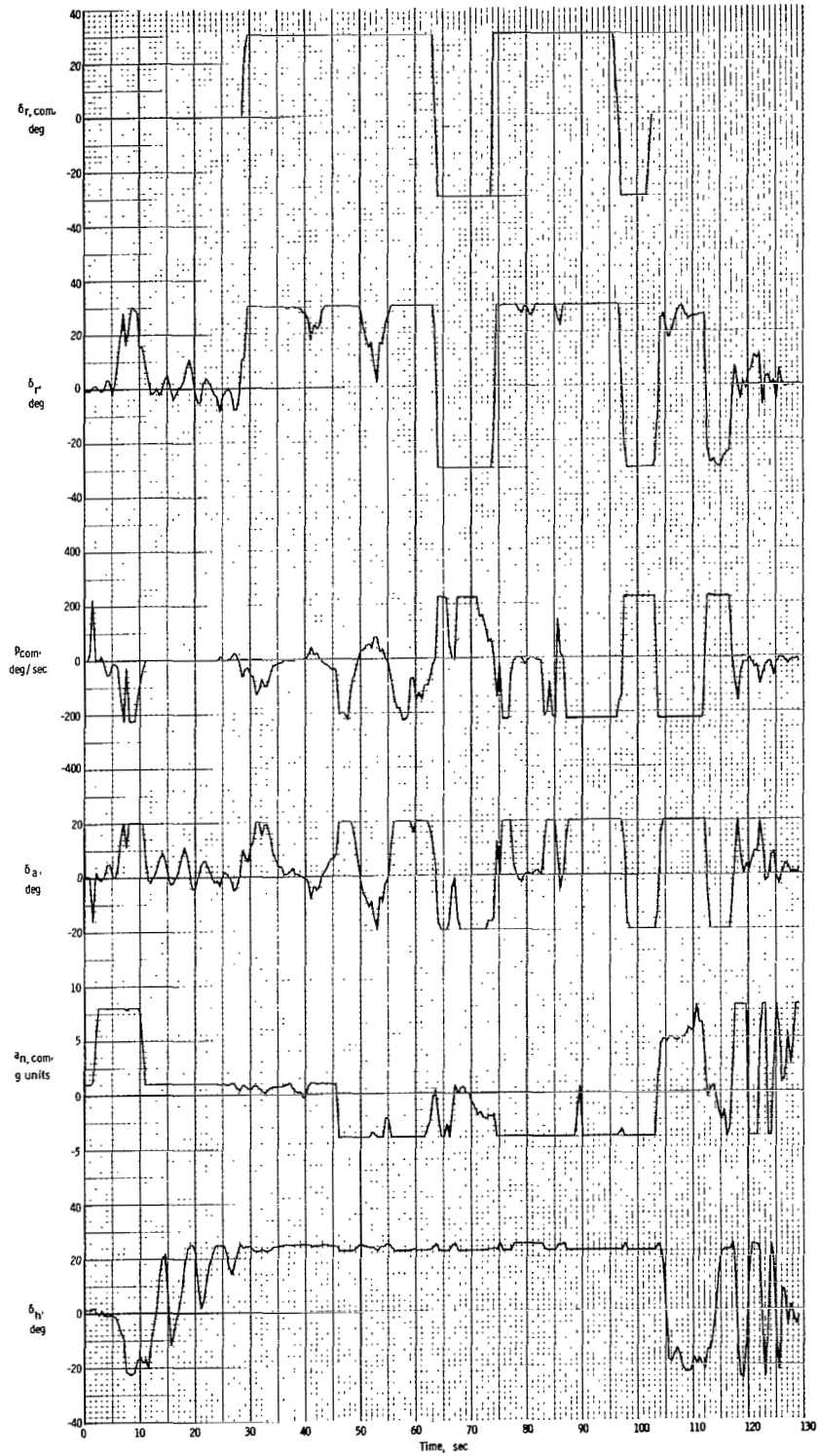


Figure 25. - Concluded.

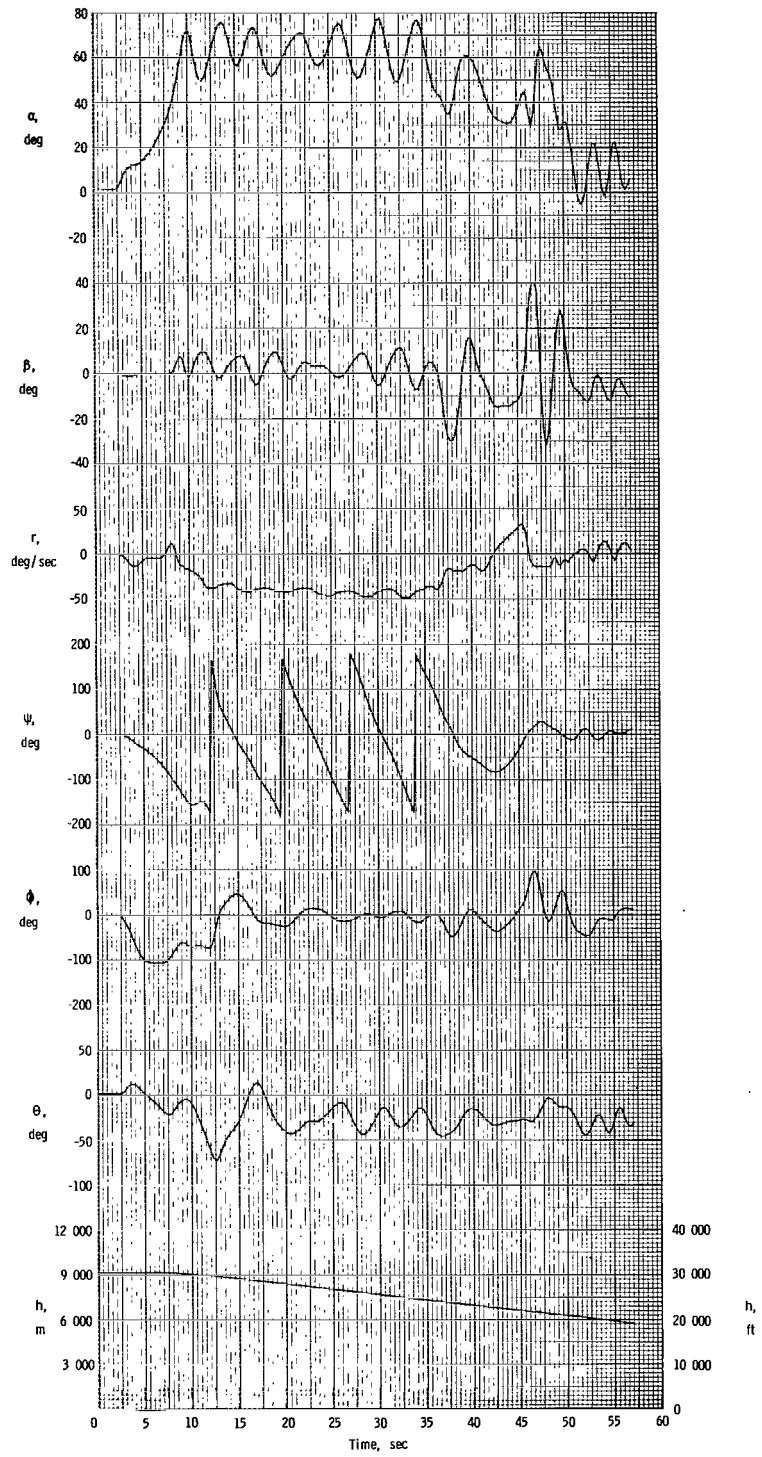


Figure 26.- Poststall recovery motions of airplane without angle-of-attack limiting for $C_{m,1}$ curve (mild high-angle-of-attack trim point).

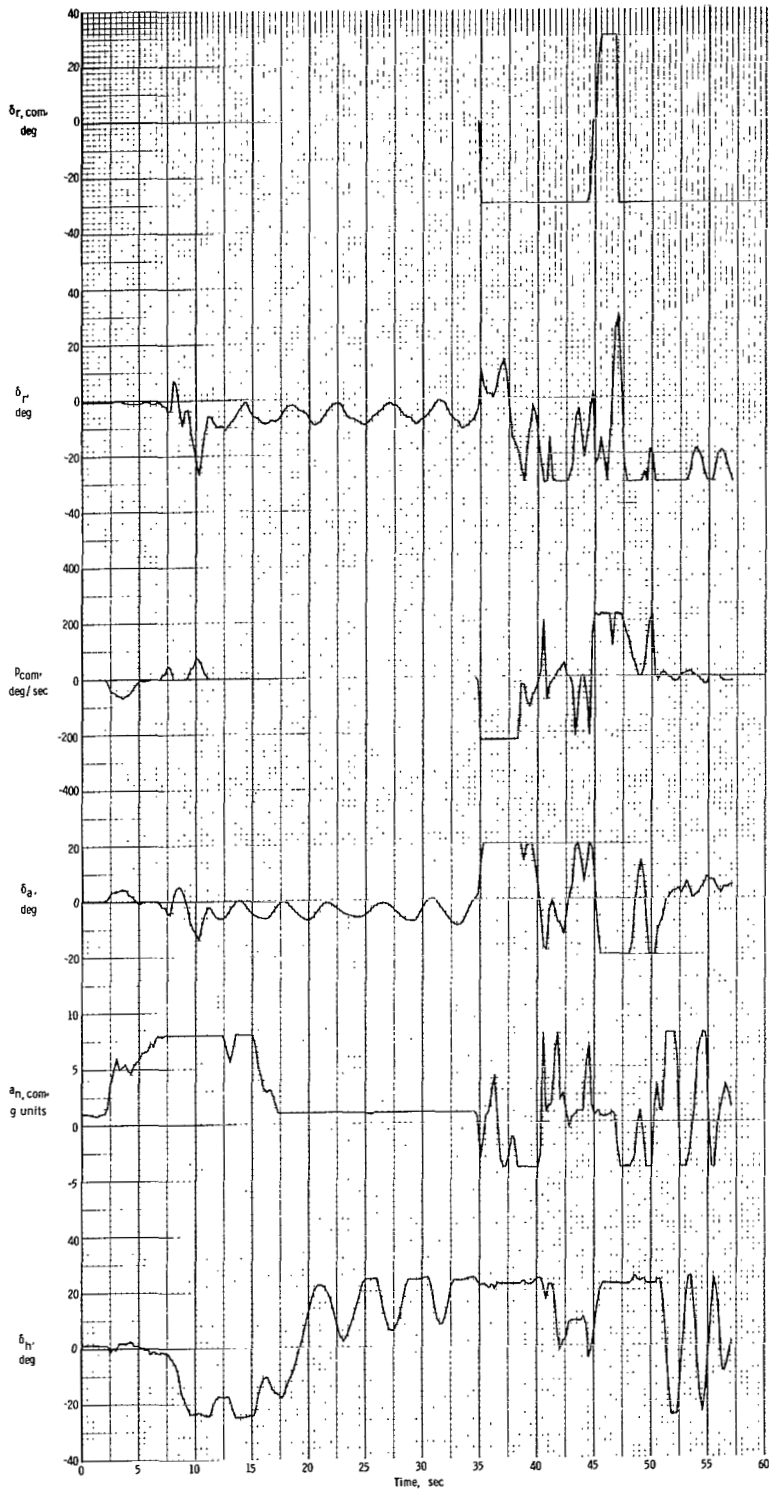


Figure 26. - Concluded.

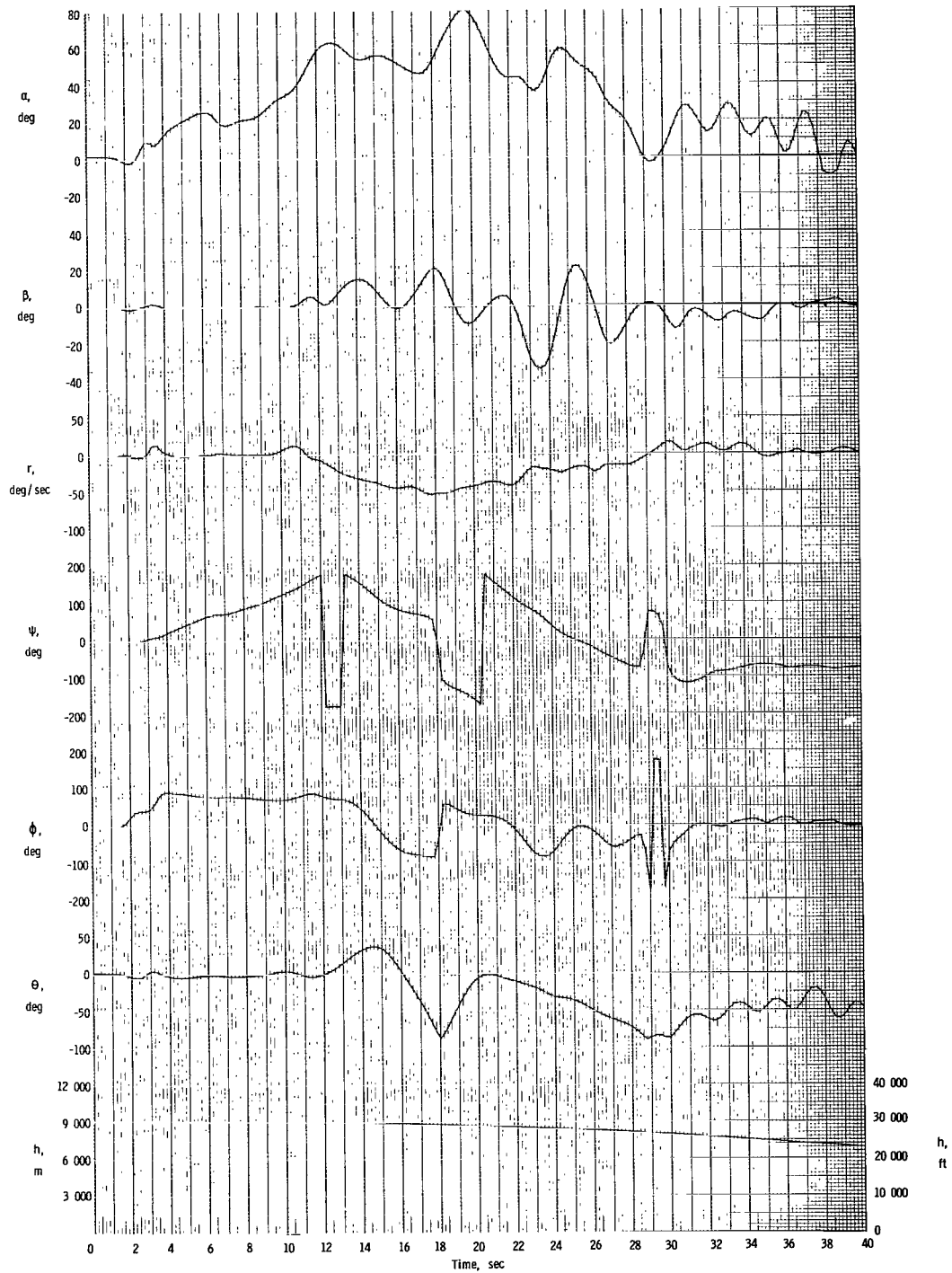


Figure 27.- Poststall recovery motions of airplane, without angle-of-attack limiting, for $C_{m,2}$ curve (conventional C_m curve).

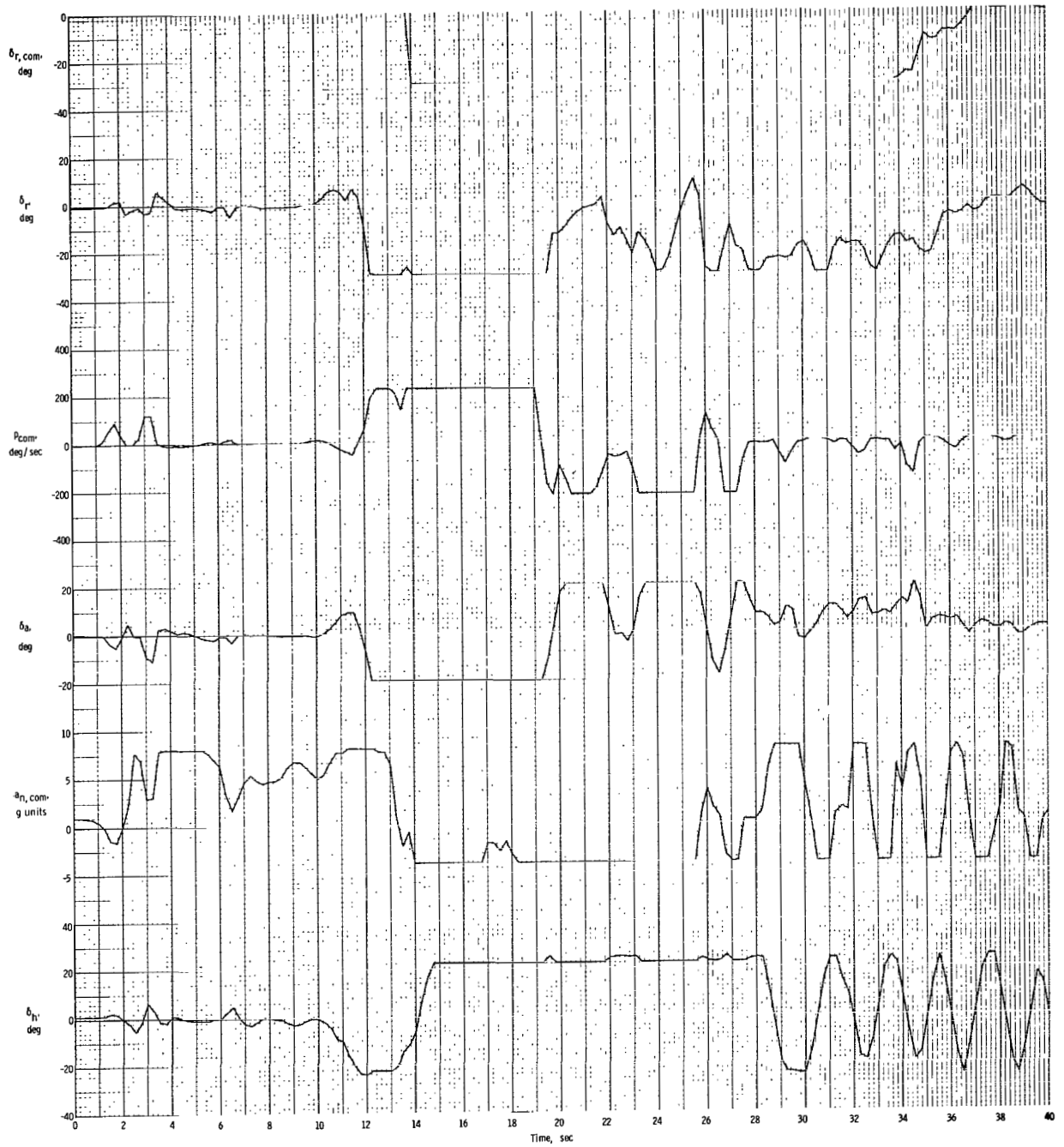


Figure 27.- Concluded.

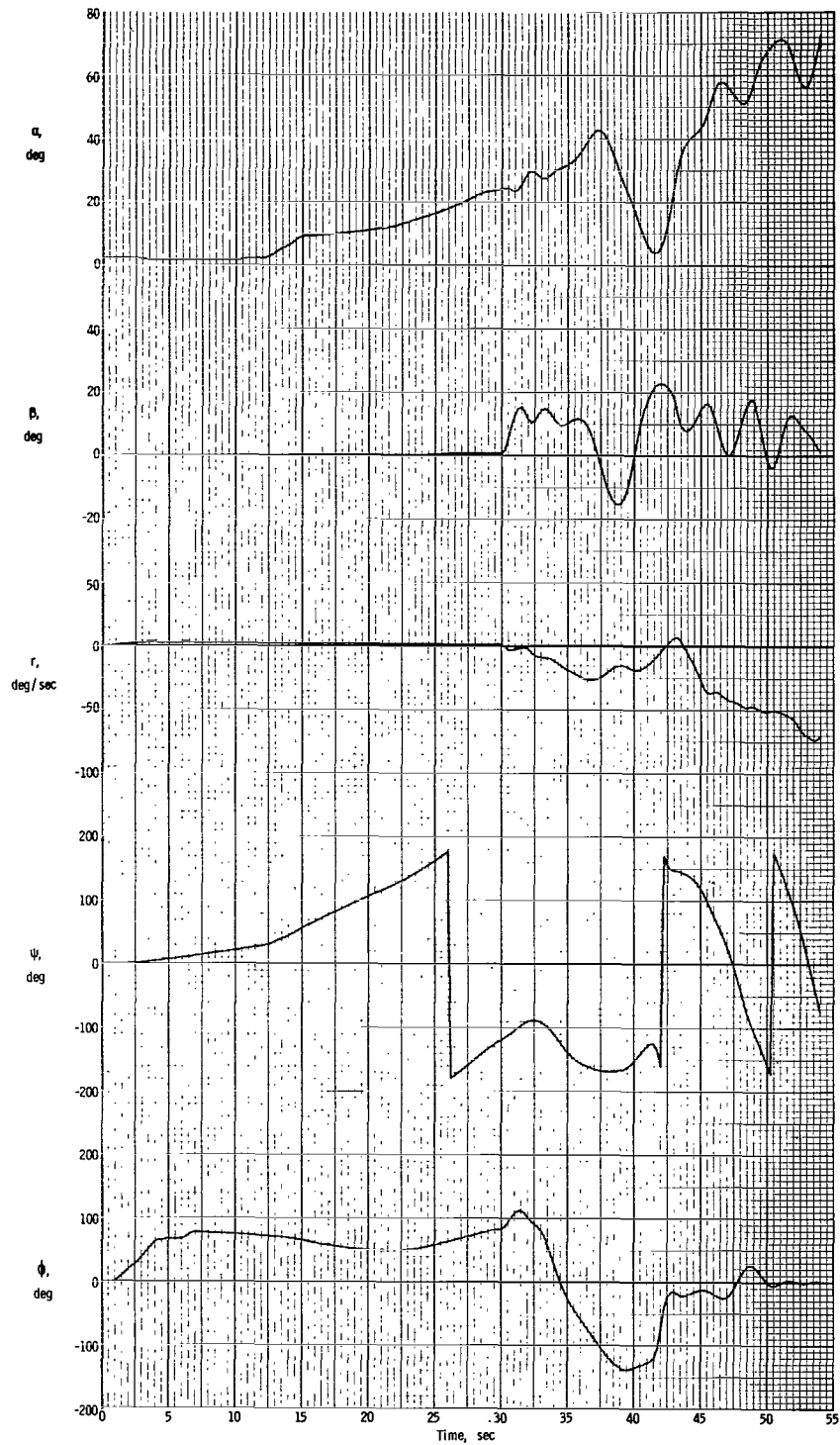


Figure 28.- Attempted spin entry in windup turn without ARI.

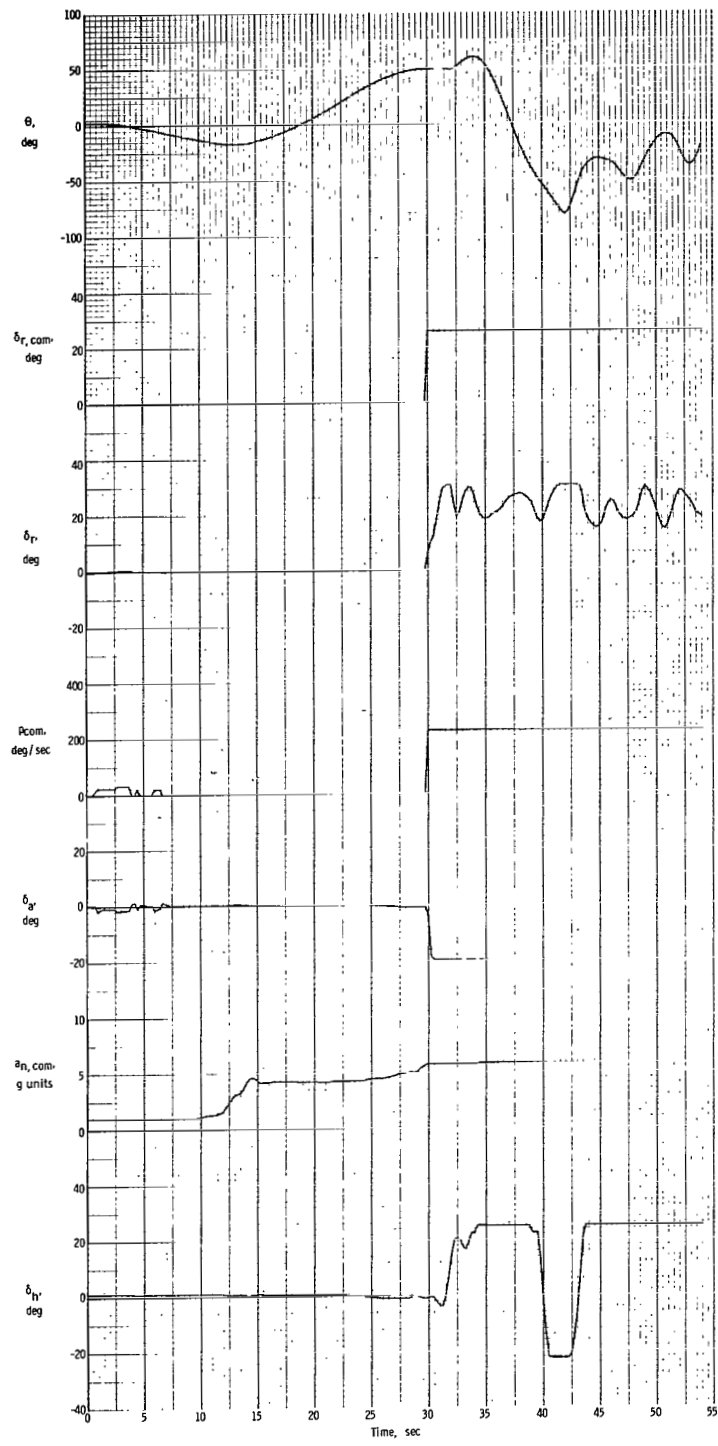


Figure 28.- Concluded.

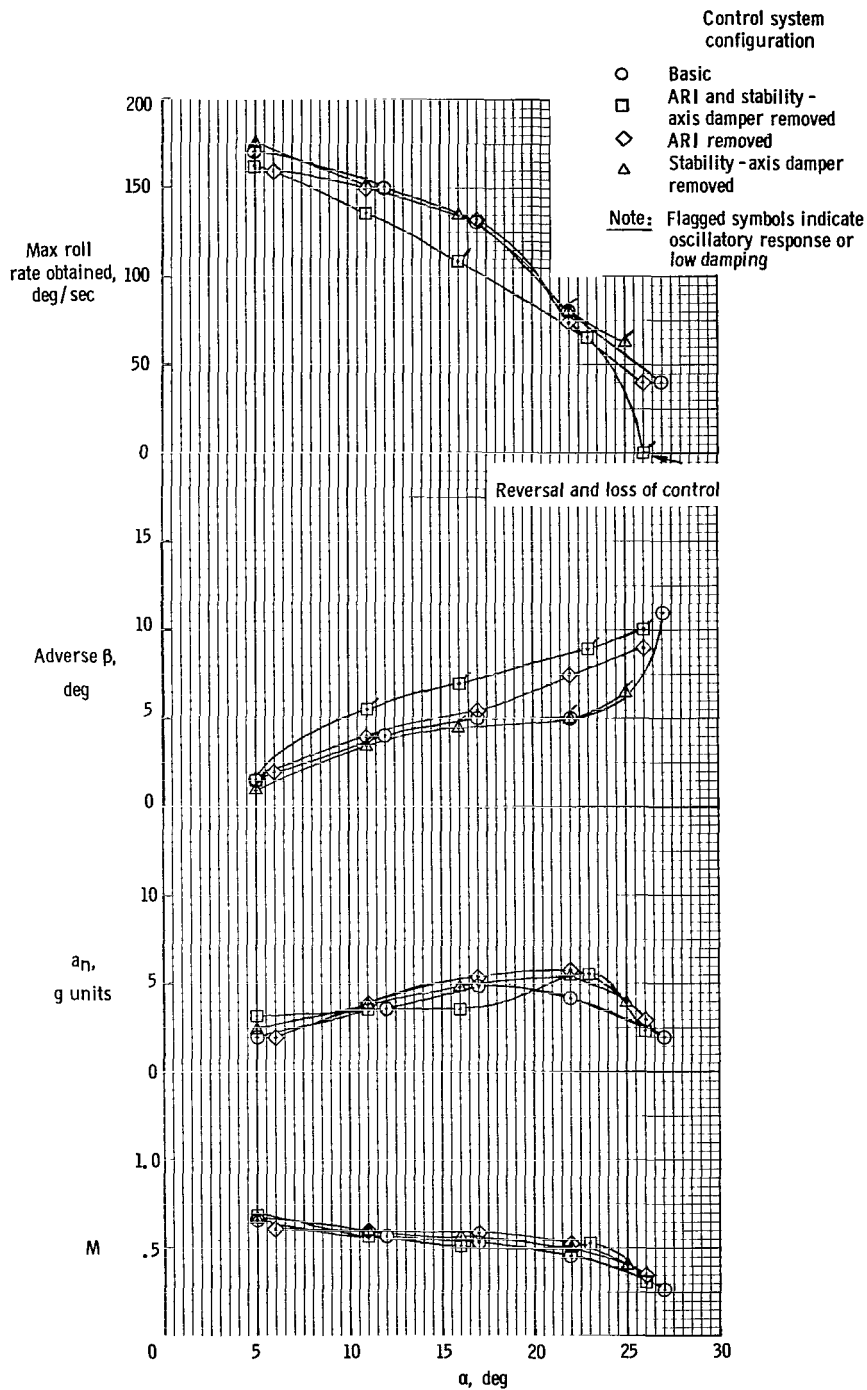


Figure 29.- Summary of roll performance obtained in maximum effort (full lateral control) bank-angle reversal as a function of angle of attack for roll initiation.

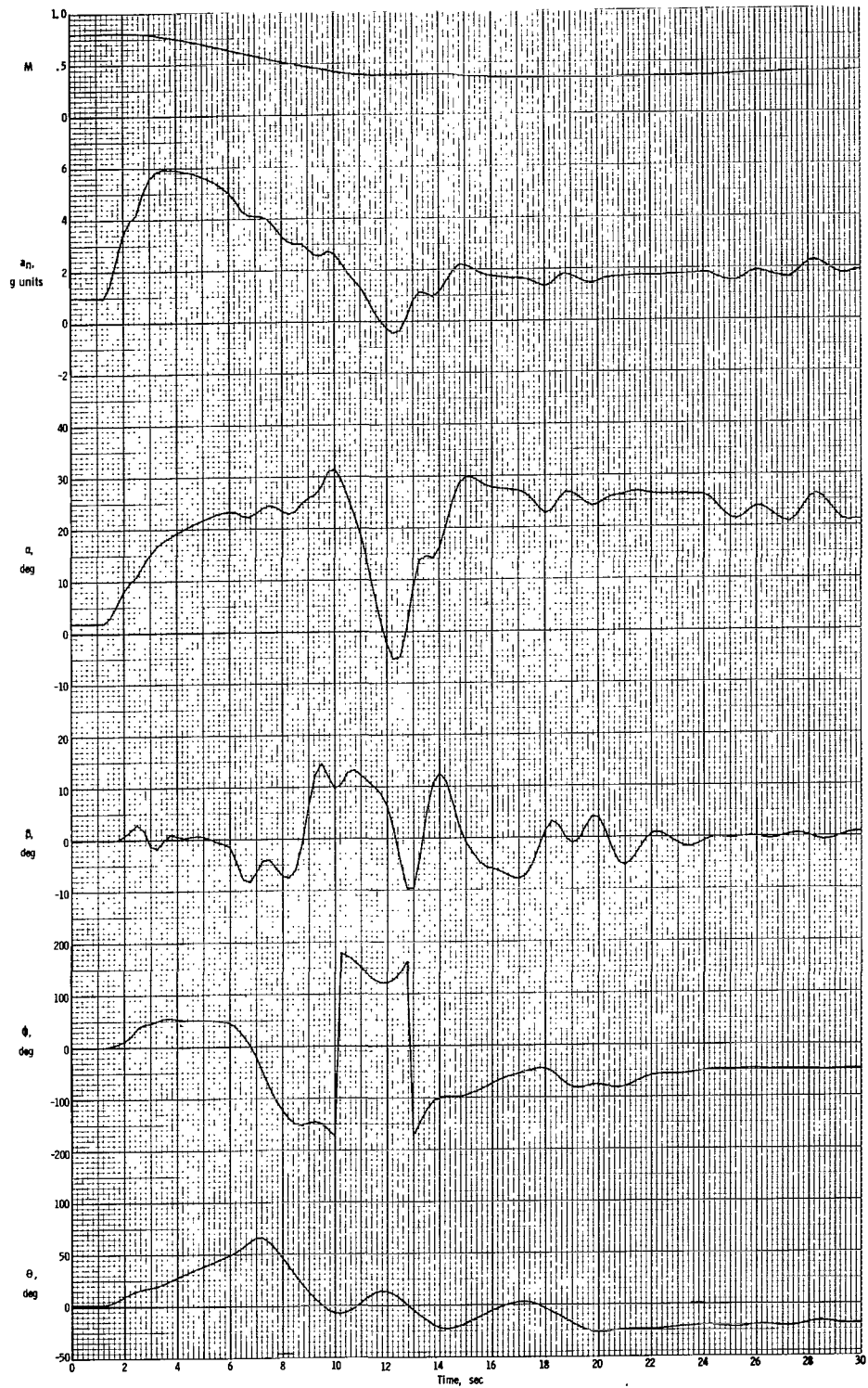


Figure 30.- Performance of airplane during roll performance task without ARI and stability-axis yaw damper.

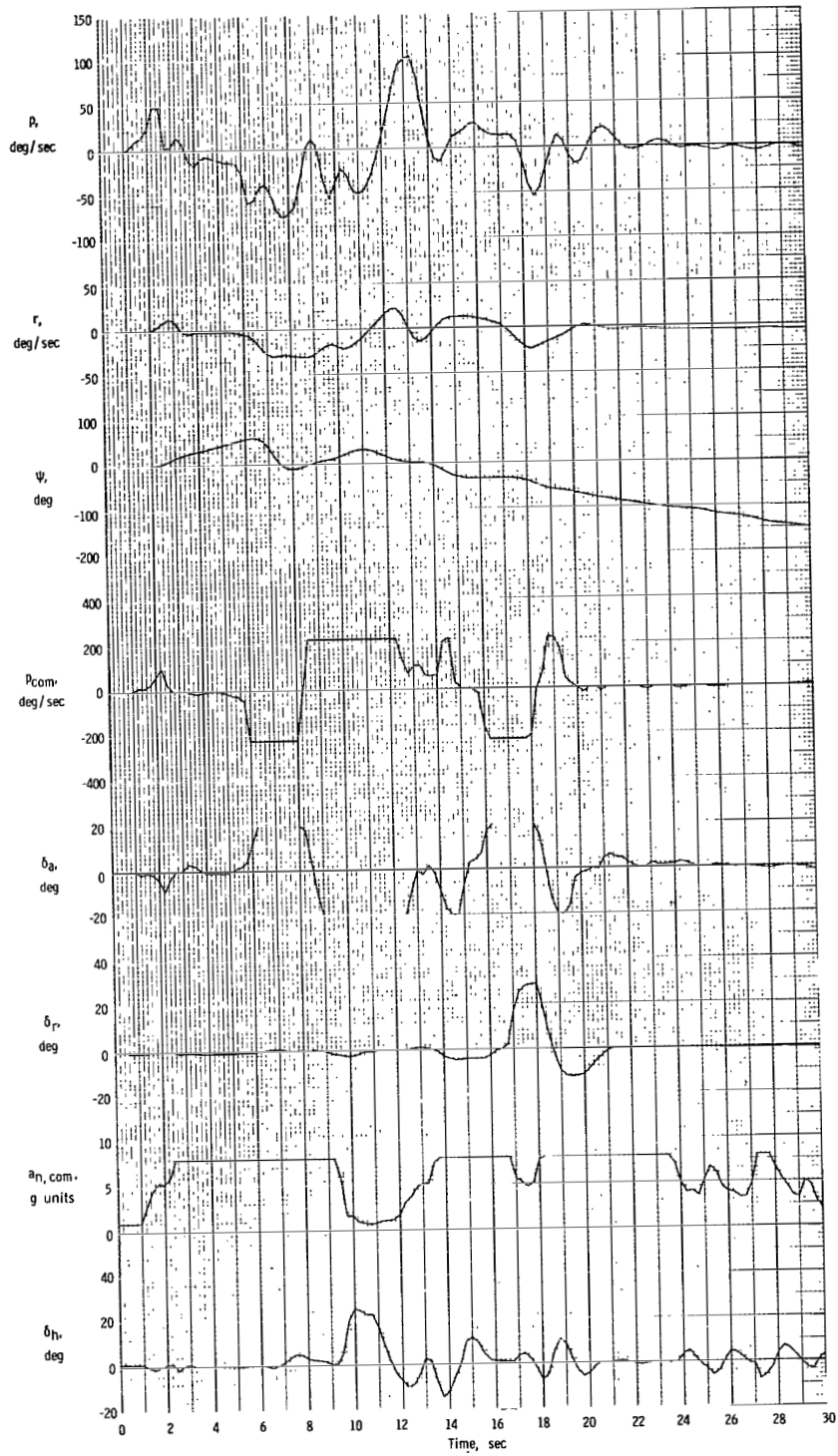


Figure 30.- Concluded.

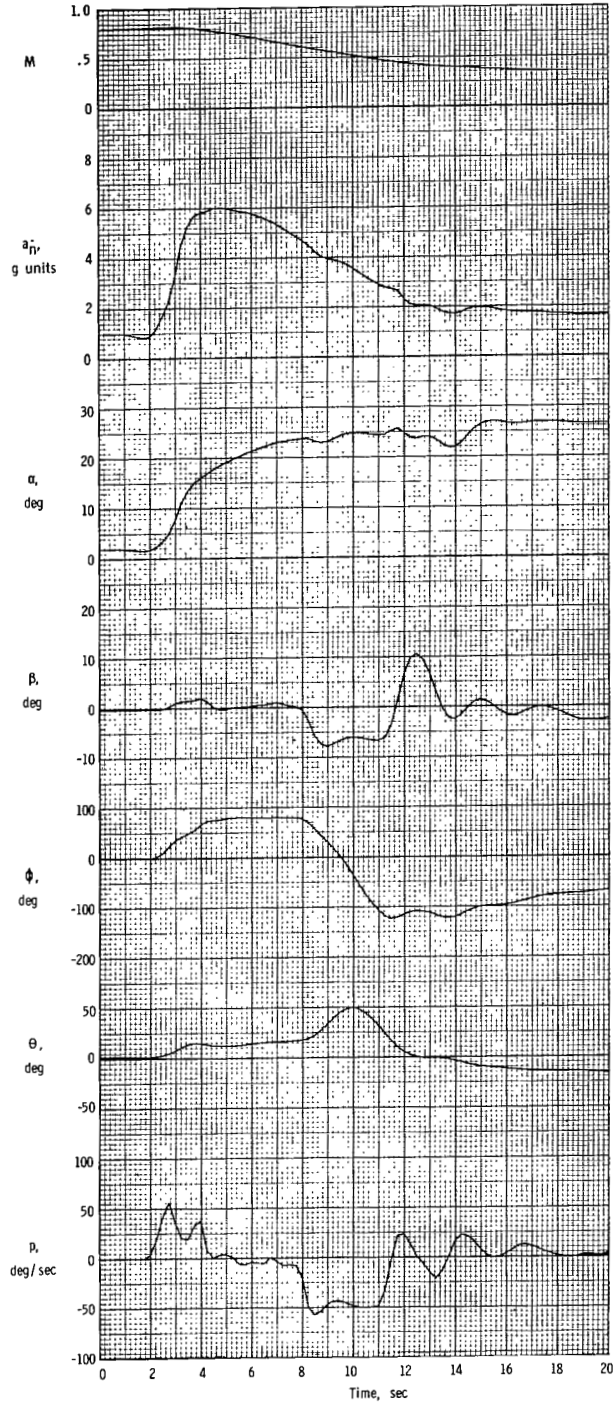


Figure 31.- Performance of airplane without ARI in roll performance task.

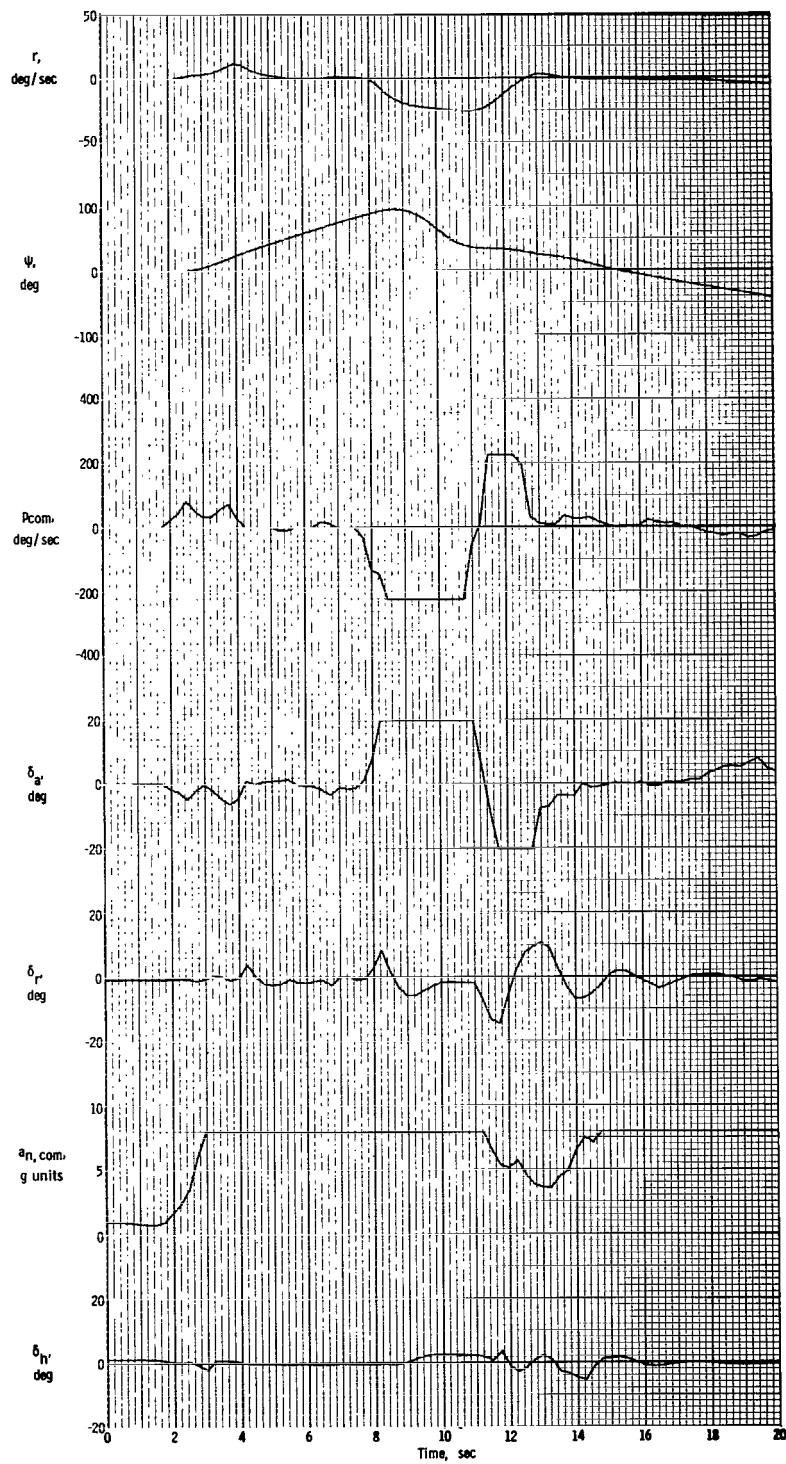


Figure 31. - Concluded.

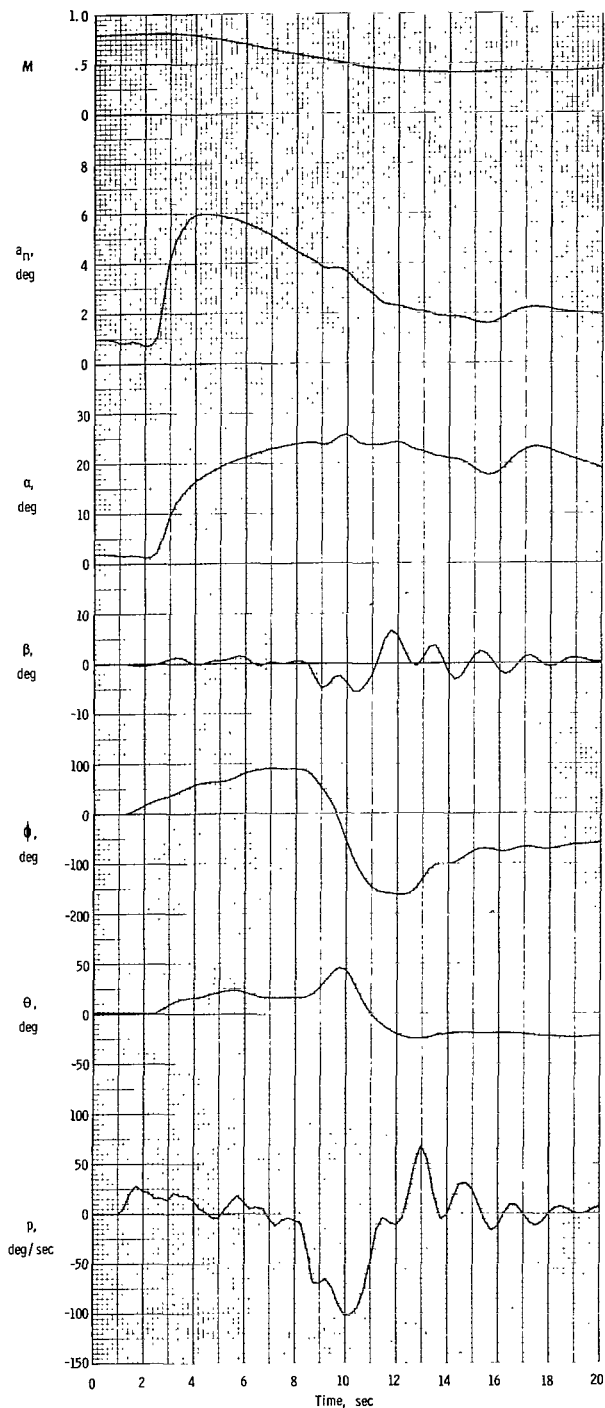


Figure 32.- Performance of airplane without stability-axis yaw damper in roll performance task.

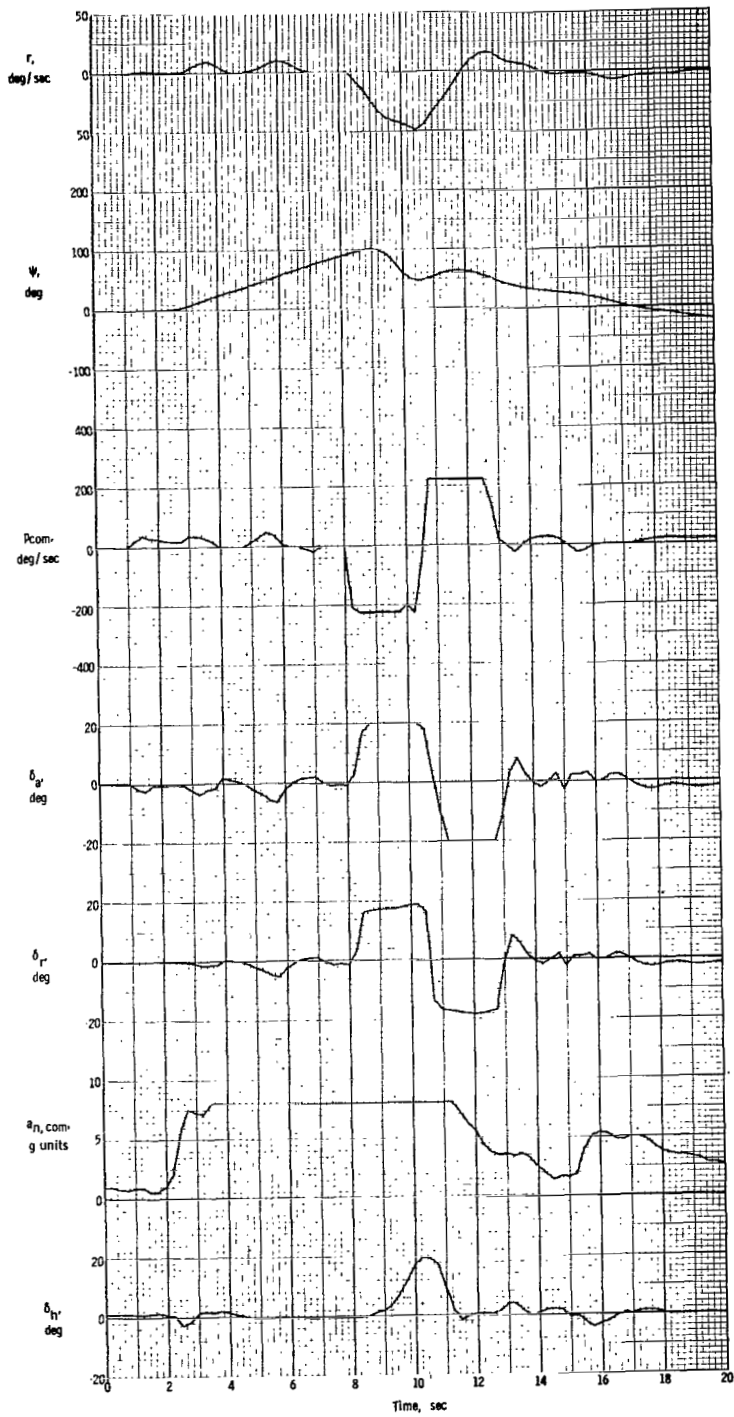
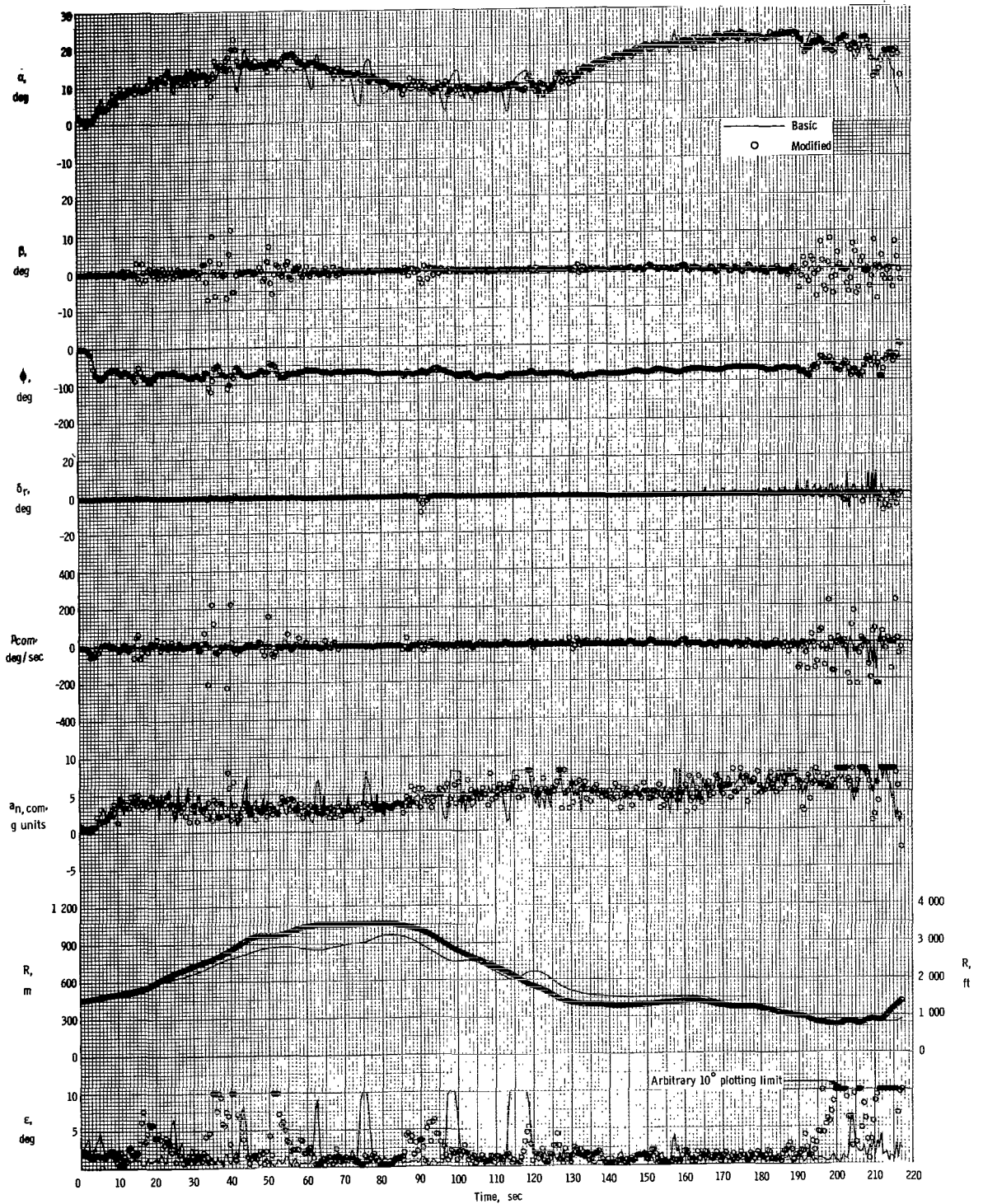
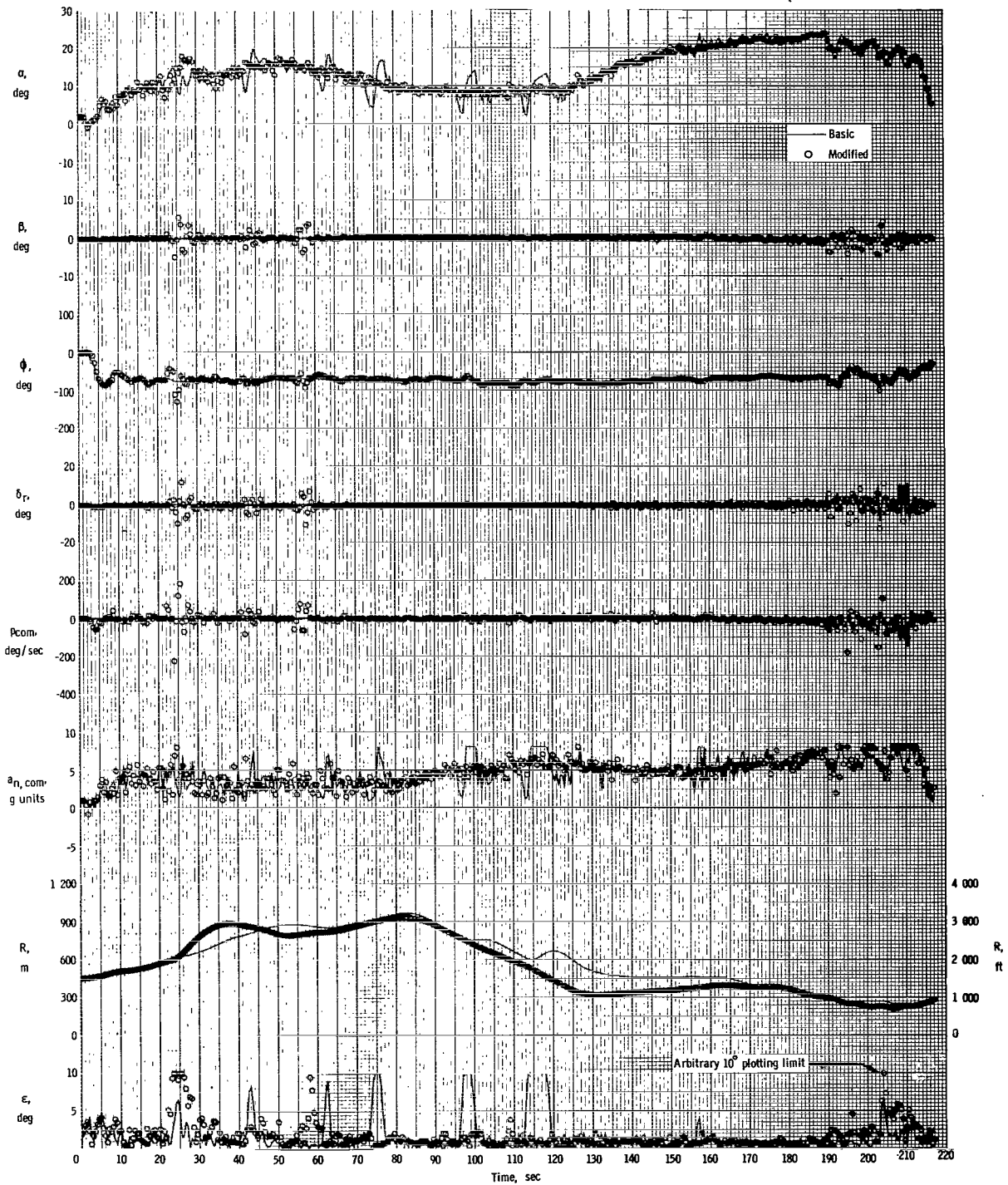


Figure 32.- Concluded.



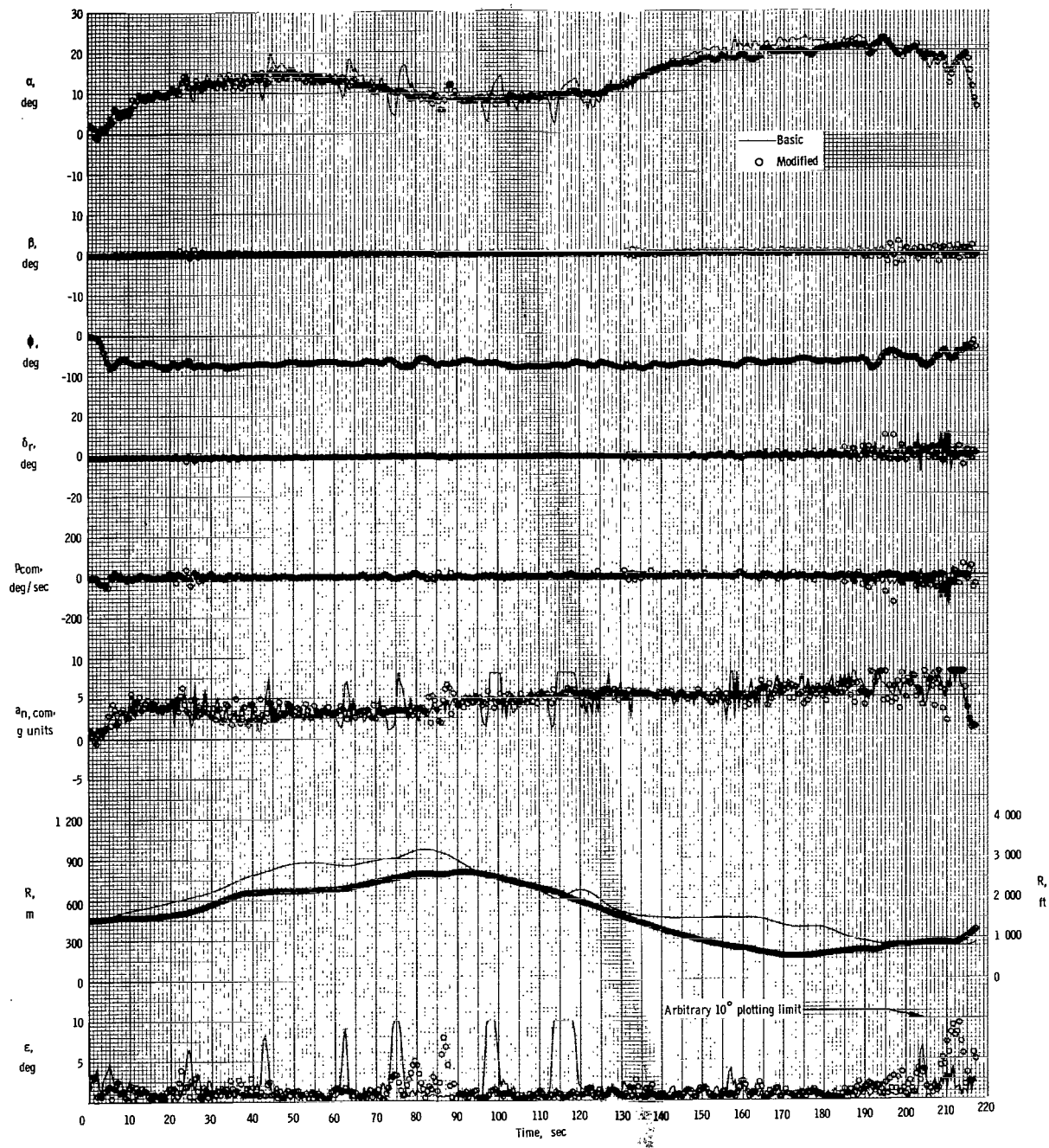
(a) Effect of removing both ARI and stability-axis yaw damper.

Figure 33.- Time-history comparisons of basic and modified configurations performing steady tracking tasks.



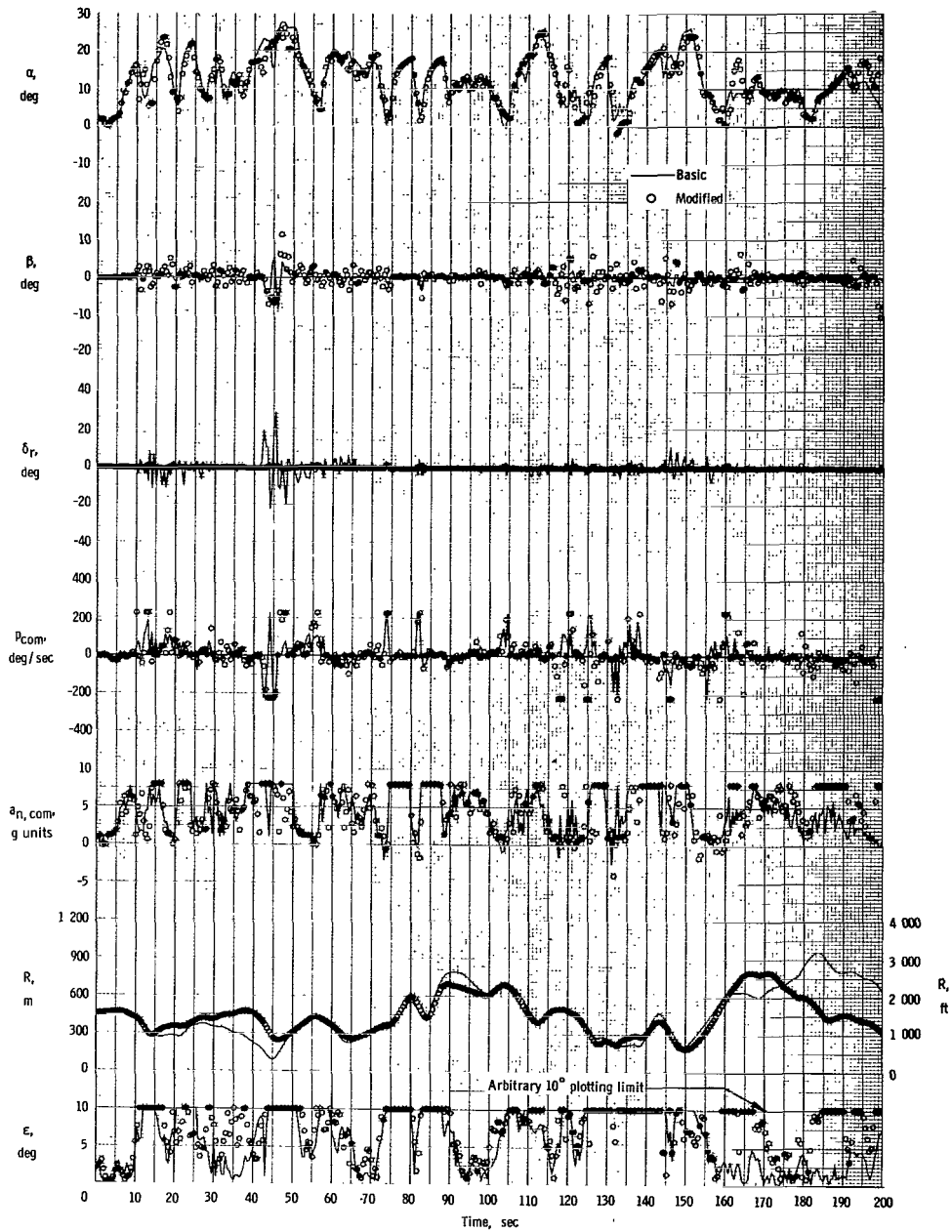
(b) Effect of removing only ARI.

Figure 33.- Continued.



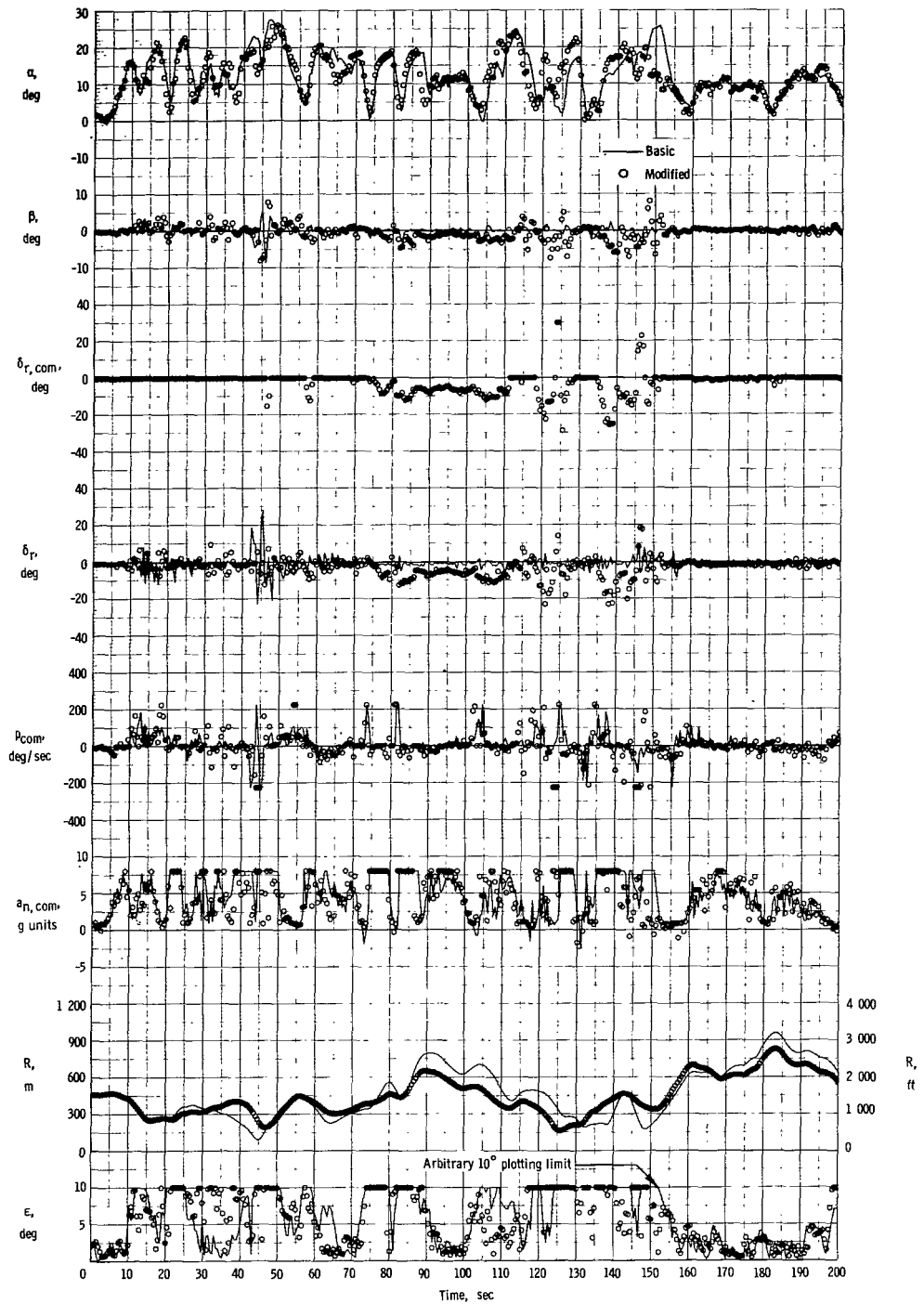
(c) Effect of removing only stability-axis yaw damper.

Figure 33.- Concluded



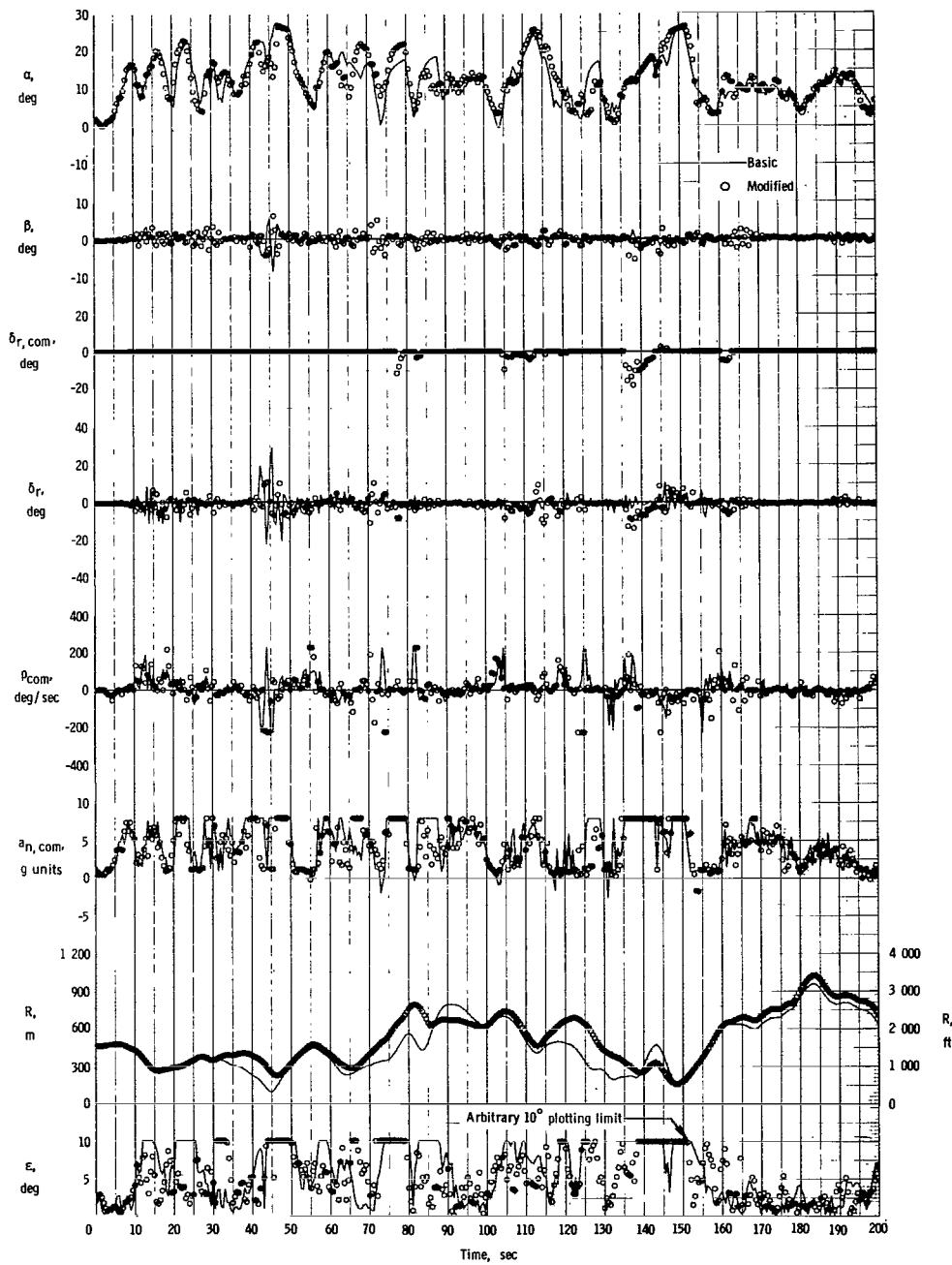
(a) Effect of removing both ARI and stability-axis yaw damper.

Figure 34.- Time-history comparisons of basic and modified airplane in general ACM task.



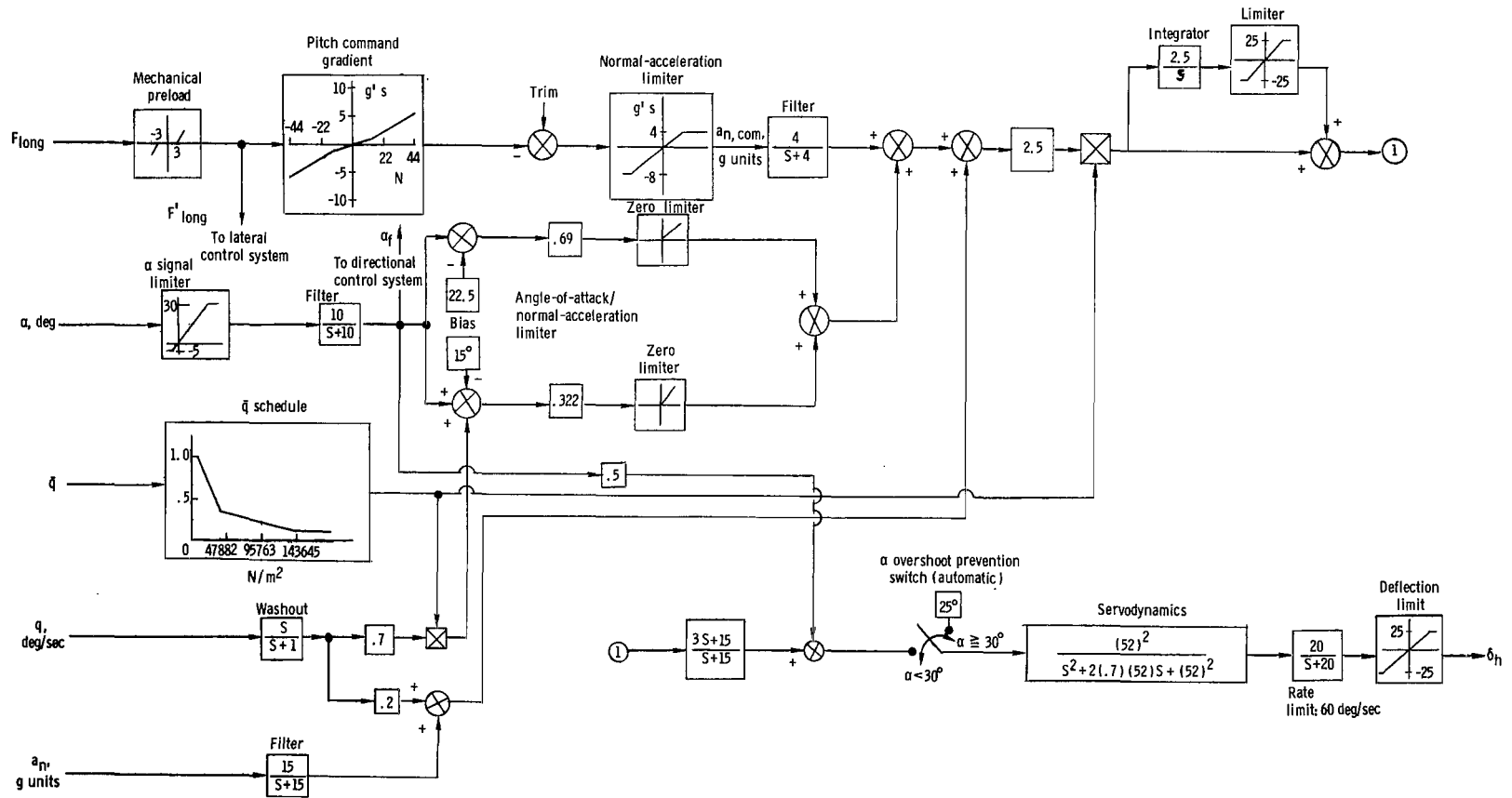
(b) Effect of removing only ARI.

Figure 34.- Continued.



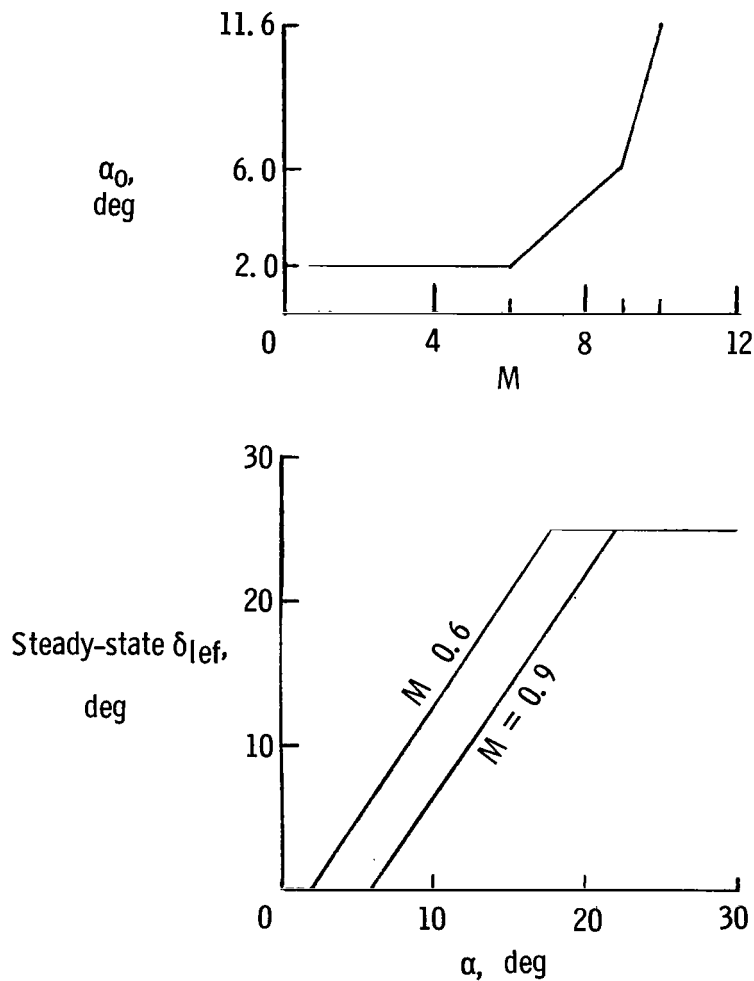
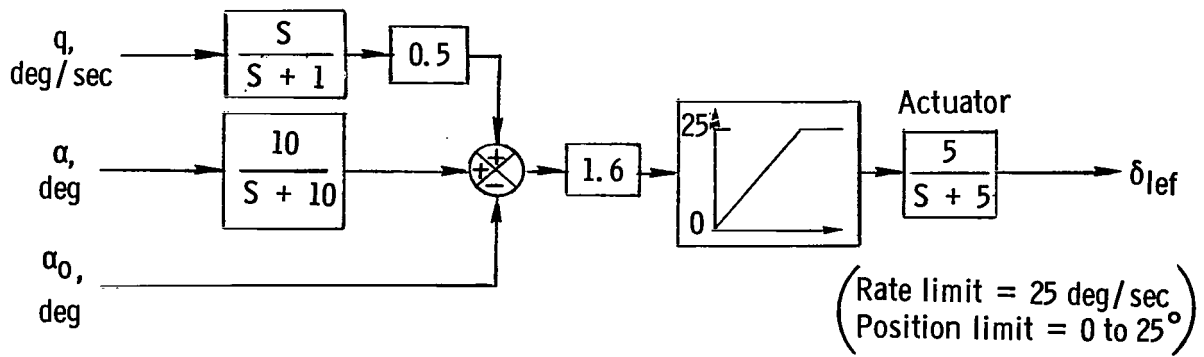
(c) Effect of removing only stability-axis yaw damper.

Figure 34. - Concluded.



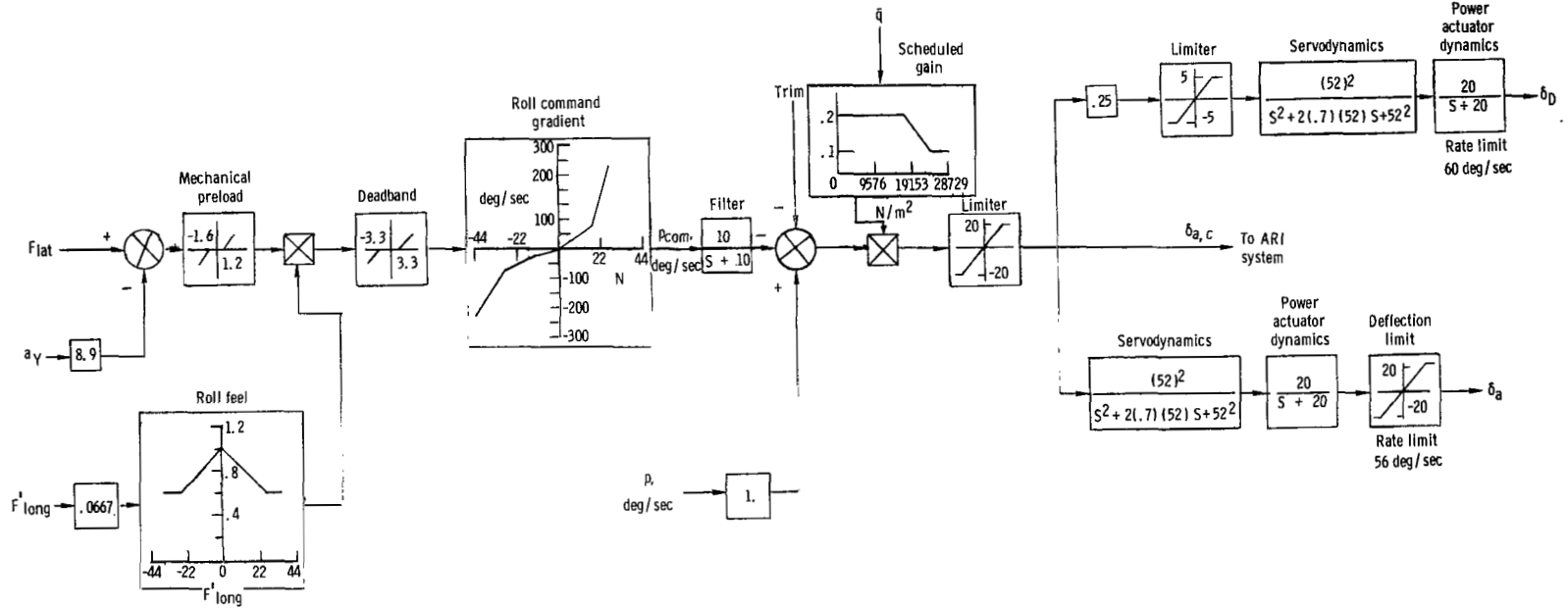
(a) Longitudinal control system diagram.

Figure 35.- Description of control system.



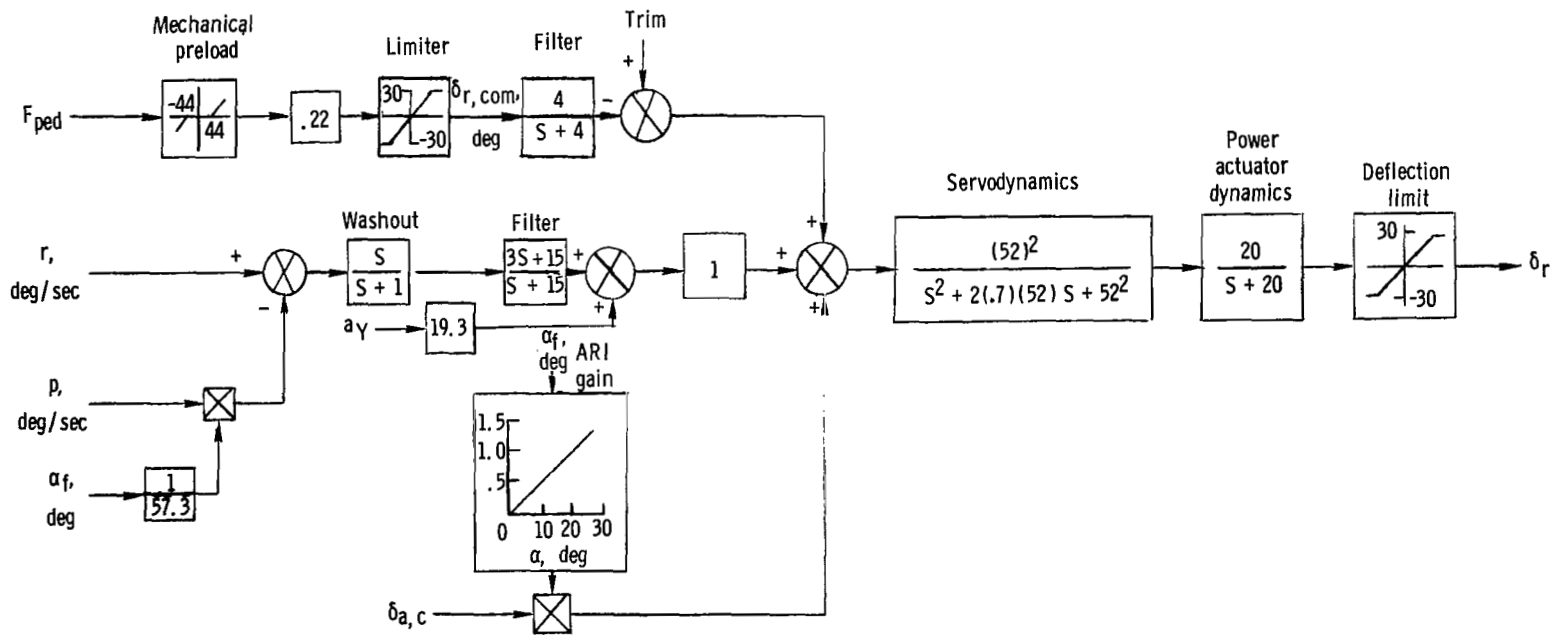
(b) Mathematical model for leading-edge flap actuation.

Figure 35.- Continued.



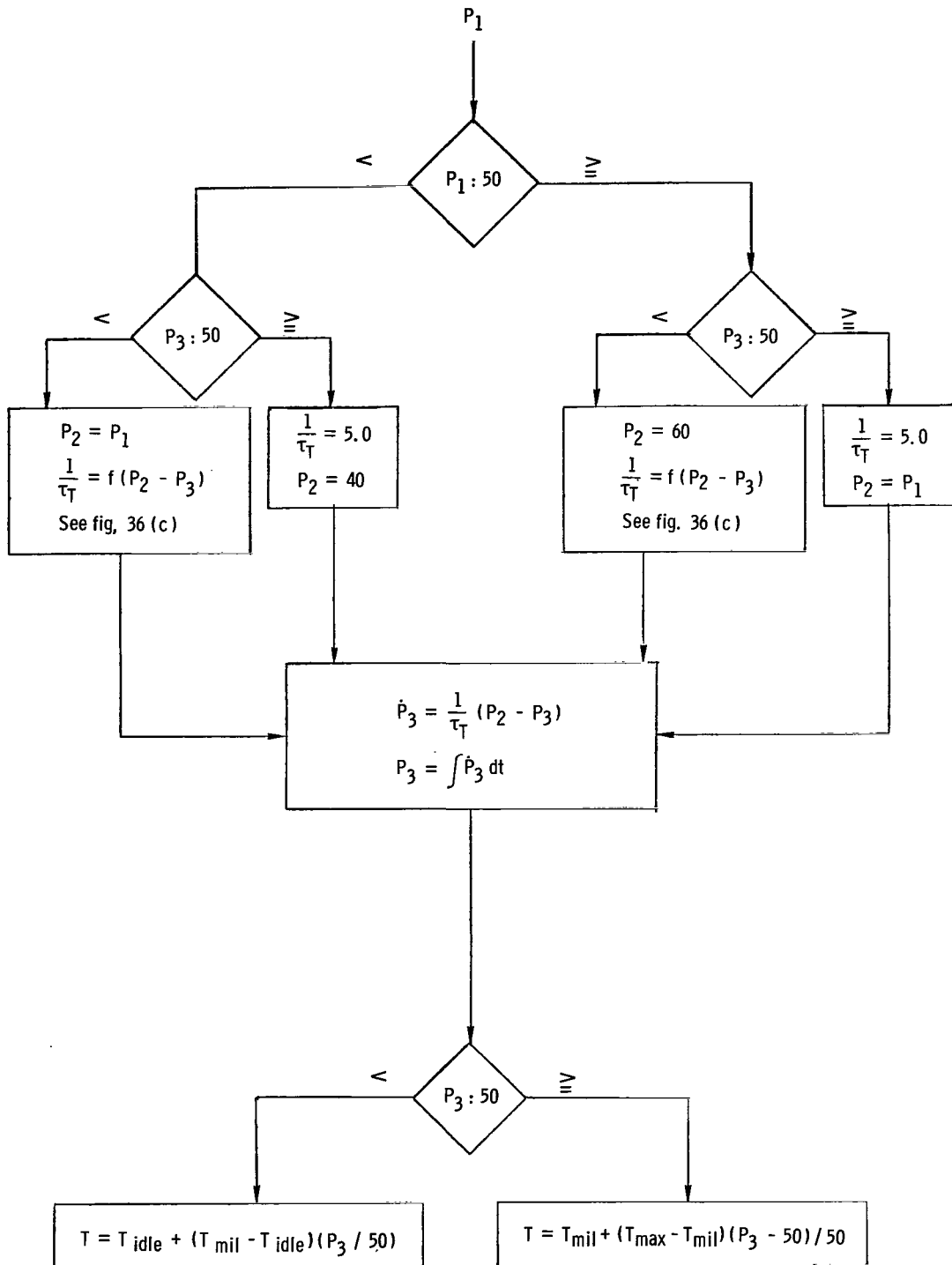
(c) Lateral control system diagram.

Figure 35.- Continued.



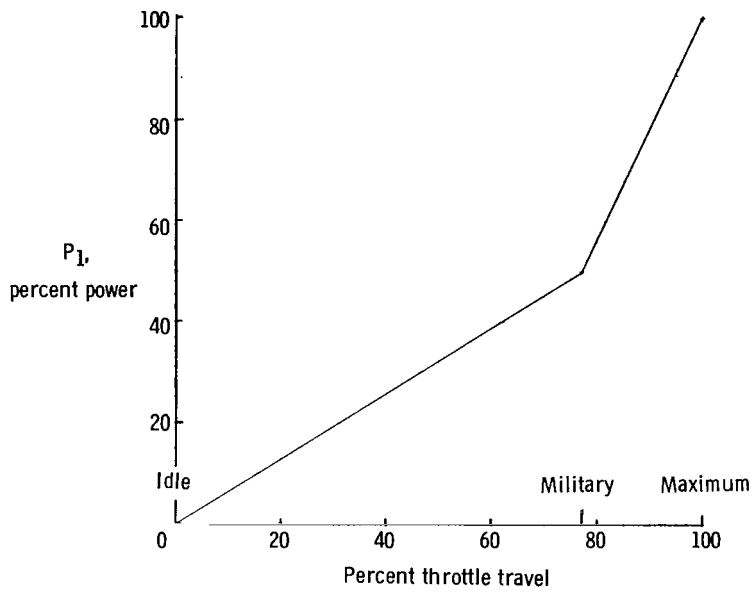
(d) Directional control system diagram.

Figure 35.- Concluded.

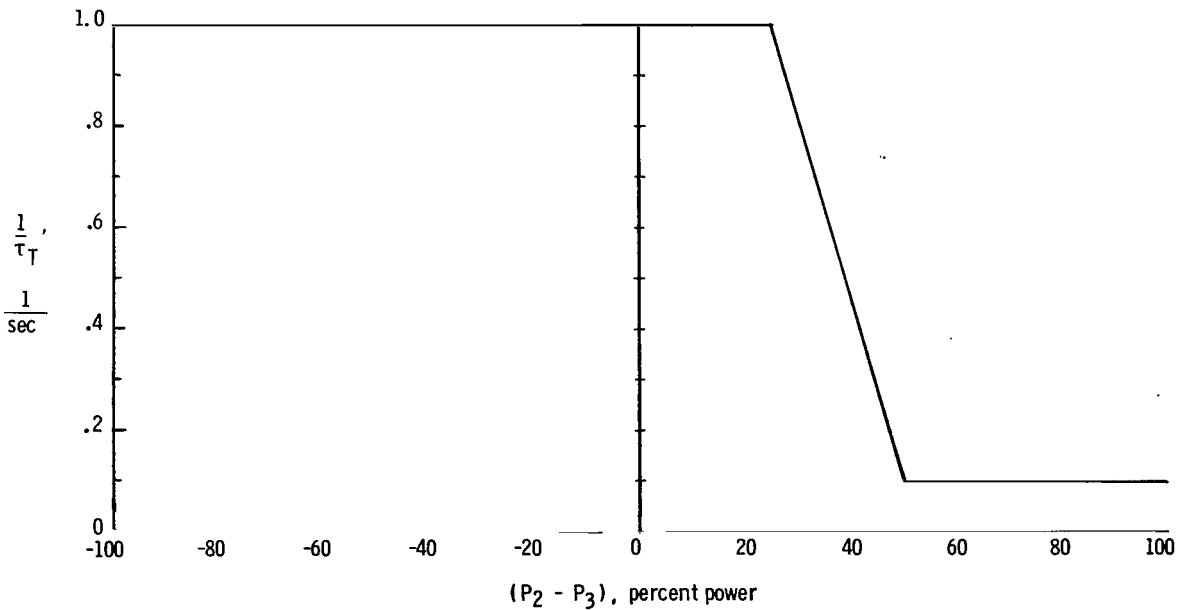


(a) Logic diagram for thrust dynamic model.

Figure 36. - Simulated powerplant characteristics.

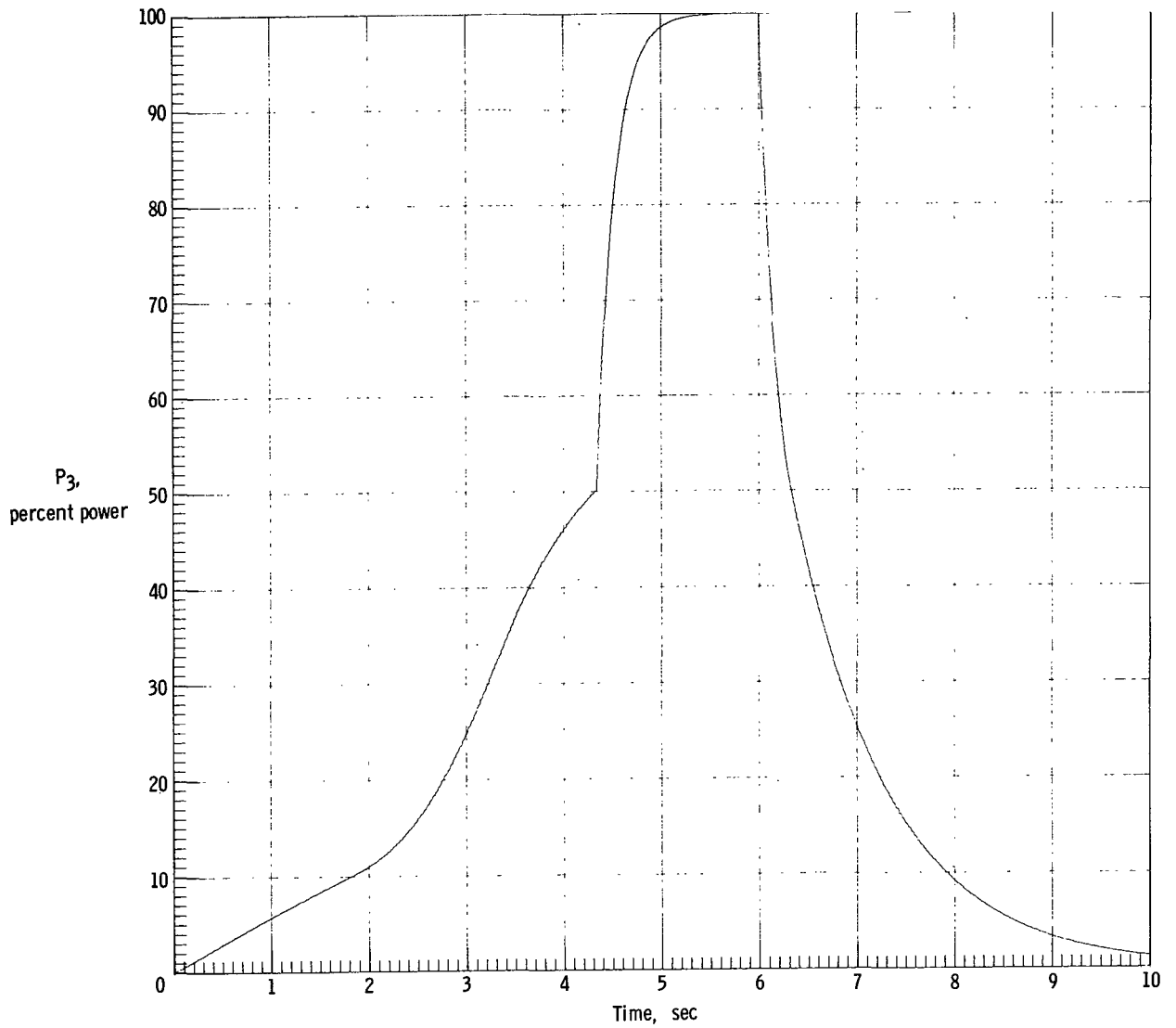


(b) Power variation with throttle position.



(c) Variation of inverse of thrust time constant with incremental power command.

Figure 36.- Continued.



(d) Power response to 100 percent step command ($P_1 = 100$) at $t = 0$ sec;
 step removed at $t = 6.0$ sec.

Figure 36.- Concluded.

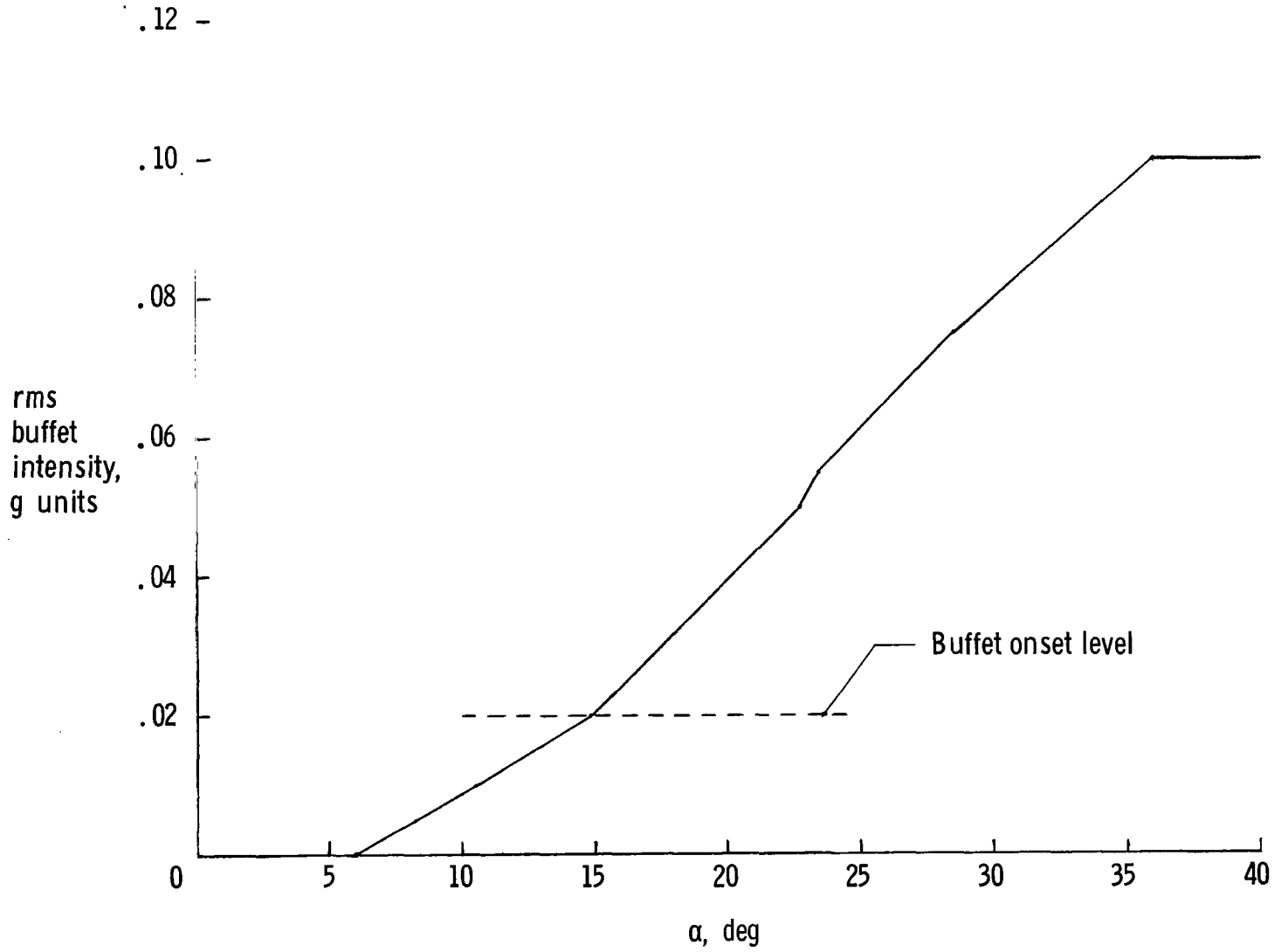


Figure 37. - Variation of buffet intensity with angle of attack.